

SEDIMENTOLOGY AND FOSSIL-FUEL
POTENTIAL OF THE UPPER
CARBONIFEROUS BARACHOIS
GROUP, WESTERN NEWFOUNDLAND

CENTRE FOR NEWFOUNDLAND STUDIES

**TOTAL OF 10 PAGES ONLY
MAY BE XEROXED**

(Without Author's Permission)

STEVEN MARK SOLOMON



National Library
of Canada

Bibliothèque nationale
du Canada

Canadian Theses Service

Services des thèses canadiennes

Ottawa, Canada
K1A 0N4

CANADIAN THESES

NOTICE

The quality of this microfiche is heavily dependent upon the quality of the original thesis submitted for microfilming. Every effort has been made to ensure the highest quality of reproduction possible.

If pages are missing, contact the university which granted the degree.

Some pages may have indistinct print especially if the original pages were typed with a poor typewriter ribbon or if the university sent us an inferior photocopy.

Previously copyrighted materials (journal articles, published tests, etc.) are not filmed.

Reproduction in full or in part of this film is governed by the Canadian Copyright Act, R.S.C. 1970, c. C-30.

**THIS DISSERTATION
HAS BEEN MICROFILMED
EXACTLY AS RECEIVED**

THÈSES CANADIENNES

AVIS

La qualité de cette microfiche dépend grandement de la qualité de la thèse soumise au microfilmage. Nous avons tout fait pour assurer une qualité supérieure de reproduction.

S'il manque des pages, veuillez communiquer avec l'université qui a conféré le grade.

La qualité d'impression de certaines pages peut laisser à désirer, surtout si les pages originales ont été dactylographiées à l'aide d'un ruban usé ou si l'université nous a fait parvenir une photocopie de qualité inférieure.

Les documents qui font déjà l'objet d'un droit d'auteur (articles de revue, examens publiés, etc.) ne sont pas microfilmés.

La reproduction, même partielle, de ce microfilm est soumise à la Loi canadienne sur le droit d'auteur, SRC 1970, c. C-30.

**LA THÈSE A ÉTÉ
MICROFILMÉE TELLE QUE
NOUS L'AVONS REÇUE**

Canada

SEDIMENTOLOGY AND FOSSIL-FUEL
POTENTIAL OF THE UPPER CARBONIFEROUS
BARACHOIS GROUP,
WESTERN NEWFOUNDLAND

Steven M. Solomon B.A.

A thesis submitted in partial fulfillment
of the requirements for the degree of
Master of Science

Department of Earth Sciences
Memorial University of Newfoundland

St. John's, Newfoundland

© June, 1986

Permission has been granted to the National Library of Canada to microfilm this thesis and to lend or sell copies of the film.

The author (copyright owner) has reserved other publication rights, and neither the thesis nor extensive extracts from it may be printed or otherwise reproduced without his/her written permission.

L'autorisation a été accordée à la Bibliothèque nationale du Canada de microfilmer cette thèse et de prêter ou de vendre des exemplaires du film.

L'auteur (titulaire du droit d'auteur) se réserve les autres droits de publication; ni la thèse ni de longs extraits de celle-ci ne doivent être imprimés ou autrement reproduits sans son autorisation écrite.

ISBN 0-315-33632-3

ABSTRACT

The coal-bearing Upper Carboniferous Barachois Group of western Newfoundland consists of the youngest known rocks in the St. George's Bay Lowlands. These lowlands are part of the Bay St. George Subbasin, which, in turn, is part of a network of Carboniferous depositional areas in eastern Canada. A detailed sedimentological study of the Barachois Group was undertaken as part of a more general study (involving geology and geophysics) to assess the fossil-fuel potential of the western Newfoundland Carboniferous subbasins.

Cores and exposures of the Barachois Group in the St. George's Bay Lowlands define a lower coarse unit and an upper fine unit. The coarse unit consists of alternating red-brown mudstone-dominated units and grey sandstone and conglomerate-dominated units. The fine unit consists of thick grey or red-brown mudstone-dominated units with interspersed sandstone units. Eleven facies (A to K) are recognized in the two units. The facies are organized into three facies associations and eight subassociations. Facies association I includes fluvial channel sandstones and conglomerates found in outcrops and the BSG61 core (subassociation IA) and channel and minor sheetflood deposits found in the FB2-76 core (subassociation IB). Facies association II comprises sandstones and mudstones

deposited in proximal crevasse channel and levee environments (subassociation IIA), in undifferentiated crevasse splay, levee, and floodplain environments (subassociation IIB), and by progradation of crevasse splay, levee, and delta environments (subassociation IIC). Facies association III includes mudstone-dominated subassociations which represent the deposits of floodplain lakes (subassociation IIIA), poorly-drained swamps (subassociation IIIB), and well-drained swamps (subassociation IIIC).

Sandstones of the Barachois Group are classified predominantly as arkose and subarkose, with up to 65% feldspar. The sandstones include a variety of authigenic minerals such as kaolinite, chlorite, illite, calcite, and silica. Sandstone mineralogy does not identify any distinctive provenance. Potential sources of the arkoses could have included several of the presently exposed igneous intrusive complexes in the Long Range Mountains located southeast, east, and north of the study area.

X-ray diffraction of the <2 micrometer fraction shows that mudstones contain illite, chlorite, kaolinite and mixed-layer clay minerals. Illite predominates in non-grey mudstone; chlorite is the most abundant clay mineral in grey mudstones. Variations in clay mineralogy are due to a combination of initial detrital mineralogy and relative stability of clay minerals through a variety of depositional and diagenetic environments.

Kerogen types in the Barachois Group are dominated by woody (type III) kerogen with lesser amounts of amorphous and herbaceous types. Thermal maturation indices and kerogen type indicate that mudstones have a fair gas potential, but potential reservoir rocks exhibit poor to fair porosity. Oil shales are lean and coals exhibit considerable variation both between and within seams in terms of ash and sulfur contents. Oil shales and coals appear to be of limited lateral extent and coals are commonly faulted.

ACKNOWLEDGEMENTS

In the course of this thesis many people have offered encouragement and helpful advice. In particular, fellow graduate students Jack Botsford, Paul Myrow and Russ Quick have lent an air of reality to graduate school. Co-supervisors Drs. R. Hyde and R. Hiscott are also acknowledged. Dr. S. Macko, Russ Quick and the geochemical laboratory of the Newfoundland Department of Mines and Energy all provided technical assistance and were instrumental in acquisition of geochemical data.

Palynological techniques and information were provided by Dr. E. Burden and Dr. C. Dewey furnished paleontological information. Jim Butler was an able and cheerful field assistant.

An N.S.E.R.C. Strategic Grant, a C.S.P.G. scholarship, and a Memorial University Bursary supported me and the research. My parents are thanked for their unflagging support (both spiritual and material). Finally, I would like to acknowledge the constant love and encouragement freely given by my wife, Sarah-Marie Loupe and son, Reuben.

TABLE OF CONTENTS

TITLE PAGE.....	i
ABSTRACT.....	ii
ACKNOWLEDGEMENTS.....	v
TABLE OF CONTENTS.....	vi
LIST OF TABLES.....	ix
LIST OF FIGURES.....	x
LIST OF PLATES.....	xi

CHAPTER 1 INTRODUCTION

Objectives and Rationale.....	1
Geological Setting.....	5
Basin History.....	6
Distribution of the Barachois Group....	7
Previous Work: Coal Evaluation.....	9
Previous Work: Stratigraphy, Age, and Sedimentology.....	11
Methods of Study.....	15

CHAPTER 2 STRUCTURE AND GENERAL DESCRIPTION OF BARACHOIS GROUP STRATA

Structure.....	18
General Description of BSG1 Core.....	19
General Description of FB2-76 Core.....	19
General Description of Middle Barachois Brook Exposures.....	20
Age and Correlation.....	22

CHAPTER 3 FACIES DESCRIPTIONS

Introduction.....	29
Facies A: Conglomerate.....	29
Facies B: Intraformational Mudclast Conglomerate.....	32
Facies C: Cross-stratified Sandstone..	34
Facies D: Parallel-laminated Sandstone.	38
Facies E: Structureless, Convolute, and Irregularly Laminated Sandstone....	40
Facies F: Cross-laminated Sandstone and Siltstone.....	44
Facies G: Interbedded Sandstone, Siltstone, and Mudstone.....	47
Facies H: Mudstone.....	50
Facies I: Sapropelic Mudstone/ Oil Shale.....	54
Facies J: Coal.....	57

Facies K: Ostracodal Micritic Limestone.....	60
--	----

CHAPTER 4 FACIES ASSOCIATIONS

Introduction.....	63
Facies Association I: Sandstone- and Conglomerate-dominated Deposits.....	63
Subassociation IA: Multistory and Single Story Deposits in Outcrops and BSG#1 Borehole.....	65
Subassociation IB: Multistory and Single Story Sandstone and Conglomerate Bodies in the FB2-76 Borehole.....	71
Subassociation IA: Interpretation.....	77
Subassociation IB: Interpretation.....	82
Interpretation of Facies Association I: Summary.....	87
Facies Association II: Mixed Sandstone, Siltstone and Mudstone Deposits.....	87
Subassociation IIA: Stacked Fining-Upward Deposits.....	88
Subassociation IIB: Heterogeneous Deposits.....	90
Subassociation IIC: Coarsening-Upward Deposits.....	96
Subassociation IIA: Interpretation.....	98
Subassociation IIB: Interpretation.....	101
Subassociation IIC: Interpretation.....	105
Interpretation of Facies Association II: Summary.....	107
Facies Association III: Mudstone-Dominated Deposits.....	108
Subassociation IIIA: Grey Mudstone-Dominated Sequences Including Sapropelic Beds.....	109
Subassociation IIIB: Grey Mudstone-Dominated Sequences With Common Coal or Carbonaceous Beds.....	110
Subassociation IIIC: Red-Brown Mudstone-Dominated Sequences.....	115
Subassociation IIIA: Interpretation.....	116
Subassociation IIIB: Interpretation.....	119
Subassociation IIIC: Interpretation.....	121
Implications of Calcium Carbonate Nodules.....	122
Interpretation of Facies Association III: Summary.....	126

CHAPTER 5 MARKOV CHAIN ANALYSIS

Background.....	128
Results and Interpretation: BSG#1.....	130
Results and Interpretation: FB2-76.....	133
Conclusions.....	134

CHAPTER 6 PETROGRAPHY

Introduction.....	136
Description of Framework Grains.....	141
Description of Matrix and Cement.....	144
Grain Size and Petrography.....	146
Interpretation.....	149
Summary of Petrographic	
Results and Conclusions,.....	152

CHAPTER 7 CLAY MINERALOGY

Sample Preparation.....	154
Mineral Identification.....	155
Quantification.....	161
Results.....	168
Interpretation.....	173
Summary and Conclusions.....	181

CHAPTER 8 ORGANIC GEOCHEMISTRY

Introduction.....	183
Methods.....	183
Results.....	188
Interpretation.....	193
Classification and Source of Organic	
Matter in the Barachois Group.....	193
Thermal Maturation.....	204
Quantity of Organic Matter.....	208
Source Rock Potential of the	
Barachois Group.....	208
Summary.....	213

CHAPTER 9 SYNTHESIS OF BARACHOIS GROUP DEPOSITION

Gross Trends in the Barachois Group....	214
Depositional contrasts between the	
Coarse and Fine Units.....	217
Mineralogical Contrasts Between the	
Coarse and Fine Units.....	219
Interpretation of Depositional Styles..	220

Controls on the Deposition of Organic-rich Facies.....	224
---	-----

CHAPTER 10 CONCLUSIONS

Conclusions.....	226
------------------	-----

REFERENCES.....	228
-----------------	-----

APPENDICES

A DETAILED SEDIMENTOLOGICAL SECTIONS.....	Back Pocket
B MARKOV CHAIN ANALYSIS PROGRAM.....	249

LIST OF TABLES

Table

1.1	Stratigraphy of the Bay St. George Subbasin.....	14
2.1	Miospores - BSG#1, 340.2 m.....	23
2.2	Miospores - Outcrop 38 (P13).....	24
2.3	Miospores - FB2-76, 278.6 m.....	25
2.4	Miospores - FB2-76, 774.4 m.....	26
3.1	Coal analyses.....	59
5.1	Markov chain analysis - BSG#1.....	131
5.2	Markov chain analysis - FB2-76.....	132
6.1	Petrographic data.....	137
6.2	Detrital modes.....	139
7.1	Proportions of clay minerals.....	165
7.2	X-ray diffraction - replicates.....	167
7.3	X-ray diffraction - with and without iron removal.....	167
8.1	Total organic carbon analyses.....	189
8.2	Organic geochemical analyses.....	190
8.3	Fischer Assay results.....	191
8.4	Rock-Eval pyrolysis results.....	191
8.5	Stable carbon isotope ratios.....	192
8.6	Rock-Eval assessment parameters.....	199
8.7	Indicators of kerogen source.....	203
8.8	Maturation parameters.....	205
8.9	Rock-Eval parameters - Source rock potential.....	212

LIST OF FIGURES (SHORT TITLES)

Figure

1.1	Distribution of Carboniferous strata....	2
1.2	Geomorphic subdivisions.....	3
1.3	Distribution of the Barachois Group....	4
1.4	Geological map of the Middle Barachois Brook area.....	8
1.5	Outcrop locations and paleocurrent directions along Middle Barachois Brook.....	Back Pocket
2.1	Diagrammatic cross-section along Middle Barachois Brook.....	Back Pocket
4.1	Legend for Stratigraphic Sections.....	64
4.2A	Subassociation IA: multistory sandstone.....	66
4.2B	Subassociation IA: single story sandstone.....	66
4.3	Subassociation IB: multistory sandstone.....	73
4.4	Subassociation IB: single story sandstone.....	75
4.5	Subassociations IIA, IIB, and IIIC.....	79
4.6	Subassociations IIB and IIIC.....	91
4.7	Subassociations IA, IIB and IIIA.....	92
4.8A	Subassociations IIC and IIIB.....	97
4.8B	Subassociations IIC and IIIA.....	97
4.9	Subassociations IIIB, IIIC, IIC, and IA.....	114
6.1	Sandstone petrography - QFL diagram....	140
6.2	Variations in feldspar proportions.....	145
7.1	X-ray diffractogram - sample P12.....	157
7.2	X-ray diffractogram - sample P9.....	157
7.3	X-ray diffractogram - sample F51.....	159
7.4	X-ray diffractogram - sample F35.....	162
7.5	Variations in clay mineral proportions.....	169
7.6	Triangular diagram -clay mineral proportions.....	170
7.7	Differences in clay mineral proportions based on colour and TOC....	171
7.8	Clay mineral proportions vs. TOC.....	174
8.1	Van Krevelen diagram.....	196
8.2	Hydrogen index vs. Oxygen index.....	200
8.3	Hydrogen index vs. Tmax.....	202
8.4	Stratigraphic relationships among the richest TOC samples.....	209
8.5	Source rock quality.....	211
9.1	Variations in maximum clast size.....	215

LIST OF PLATES

Plate	
3.1A	Facies A - stratified conglomerate.....30
3.1B	Facies A - massive conglomerate.....30
3.2	Facies C - intraformational conglomerate.....33
3.3	Facies C - cross-stratified sandstone.....35
3.4	Facies C - plan view.....36
3.5	Facies D - parallel-laminated sandstone.....39
3.6A	Facies E - massive sandstone.....42
3.6B	Facies E - convoluted sandstone.....42
3.7	Facies F - cross-laminated sandstone...45
3.8	Facies F - cross-laminated sandstone...46
3.9	Facies G - interbedded sandstone, siltstone and mudstone.....48
3.10	Facies G and facies H - field exposure.....51
3.11	Facies H - mudstone with nodules.....52
3.12	Facies H - Laminated mudstone.....53
3.13	Facies K - micrite.....61
4.1	Subassociation IA - multistory sandstone.....67
4.2	Subassociation IA - single story sandstone.....68
4.3	Subassociation IB - multistory sandstone.....74
4.4	Subassociation IB - single story sandstone.....76
4.5	Subassociation IIIB - Root cast.....94
4.6	Subassociation IIB - simple, unlined burrow (?) in massive sandstone.....95
4.7	Subassociation IIIB - calcium carbonate nodules.....111
4.8	Subassociation IIIB - <u>Stigmaria</u> cast and desiccation cracks.....112
4.9	Calcium carbonate nodules - slabbed....113
6.1	Fractured quartz grain.....142
6.2	Chlorite, kaolinite, and calcite grain replacement.....143
6.3	Pore-lining silica.....147
6.4	Calcite replacing albite.....148

CHAPTER 1 - INTRODUCTION

Objectives and Rationale

The Upper Carboniferous sedimentary rocks of Atlantic Canada contain important deposits of coal in Nova Scotia and New Brunswick (Macquebard, 1972). Strata equivalent to some of the older Westphalian A coals on the mainland are exposed in western Newfoundland, and are named the Barachois Group in the Bay St. George Subbasin and the Howley Formation in the Deer Lake Subbasin (Fig. 1.1). Both areas contain coal seams which were mined in the nineteenth century. In the St. George's Bay Lowlands (Fig. 1.2), this past-producing area is informally known as the St. George's Coalfield (Hayes, 1949).

A detailed study of the sedimentology of the Barachois Group in the St. George's Bay Lowlands (Fig. 1.3) is necessary to better understand the coal distribution, thickness, and quality. This study is part of a joint research effort involving the Department of Earth Sciences at Memorial University of Newfoundland and the Mineral Deposits Section of the Newfoundland Department of Mines and Energy. The overall aim of the project is to better assess the fossil fuel potential of the western Newfoundland Carboniferous basins. Specifically, the objectives of this thesis are: 1) to describe the facies and vertical sequences of the Barachois Group in the St. George's Bay Lowlands; 2)

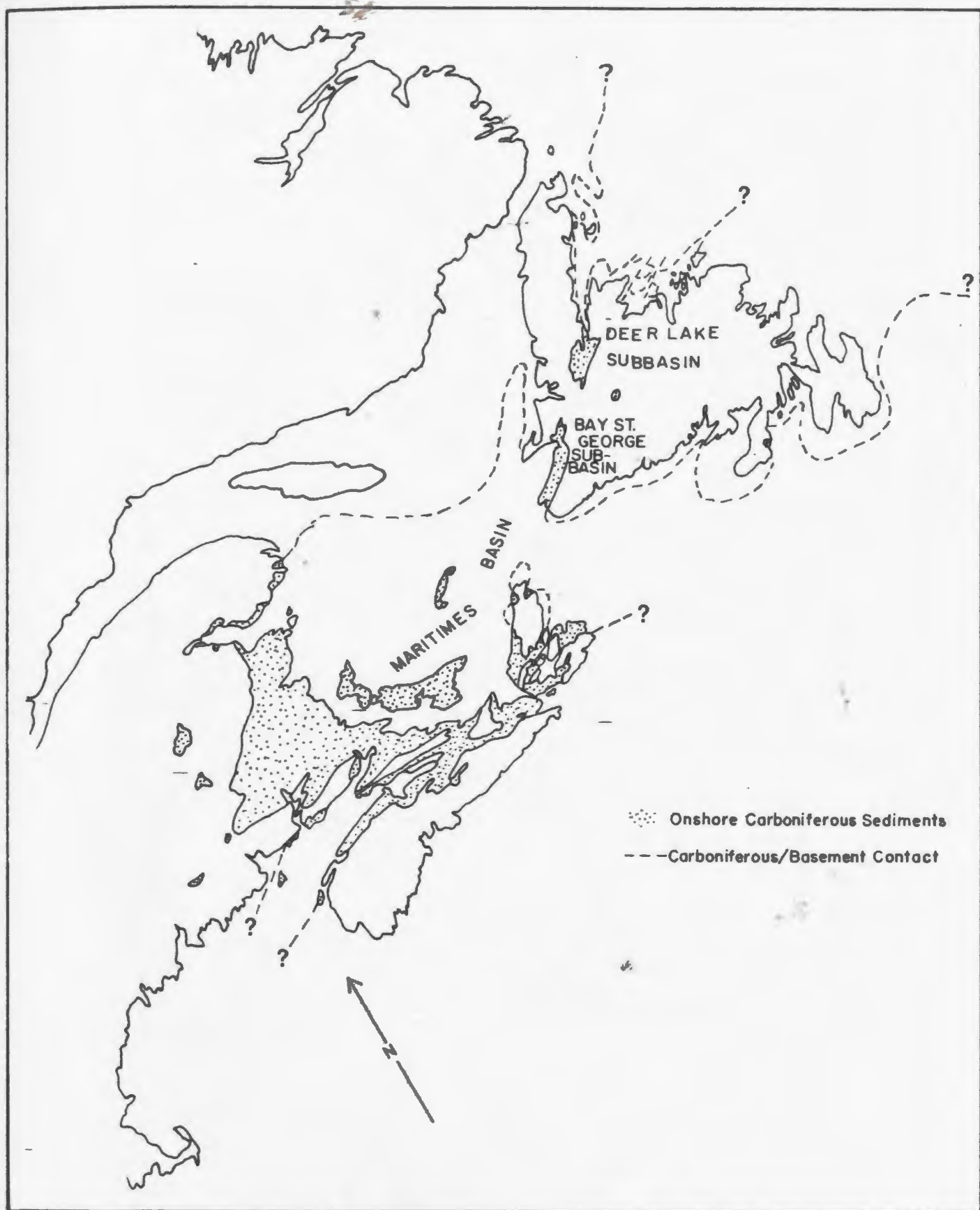


Figure 1.1: Distribution of Carboniferous Strata in the Maritimes Basin. After Knight, 1983.

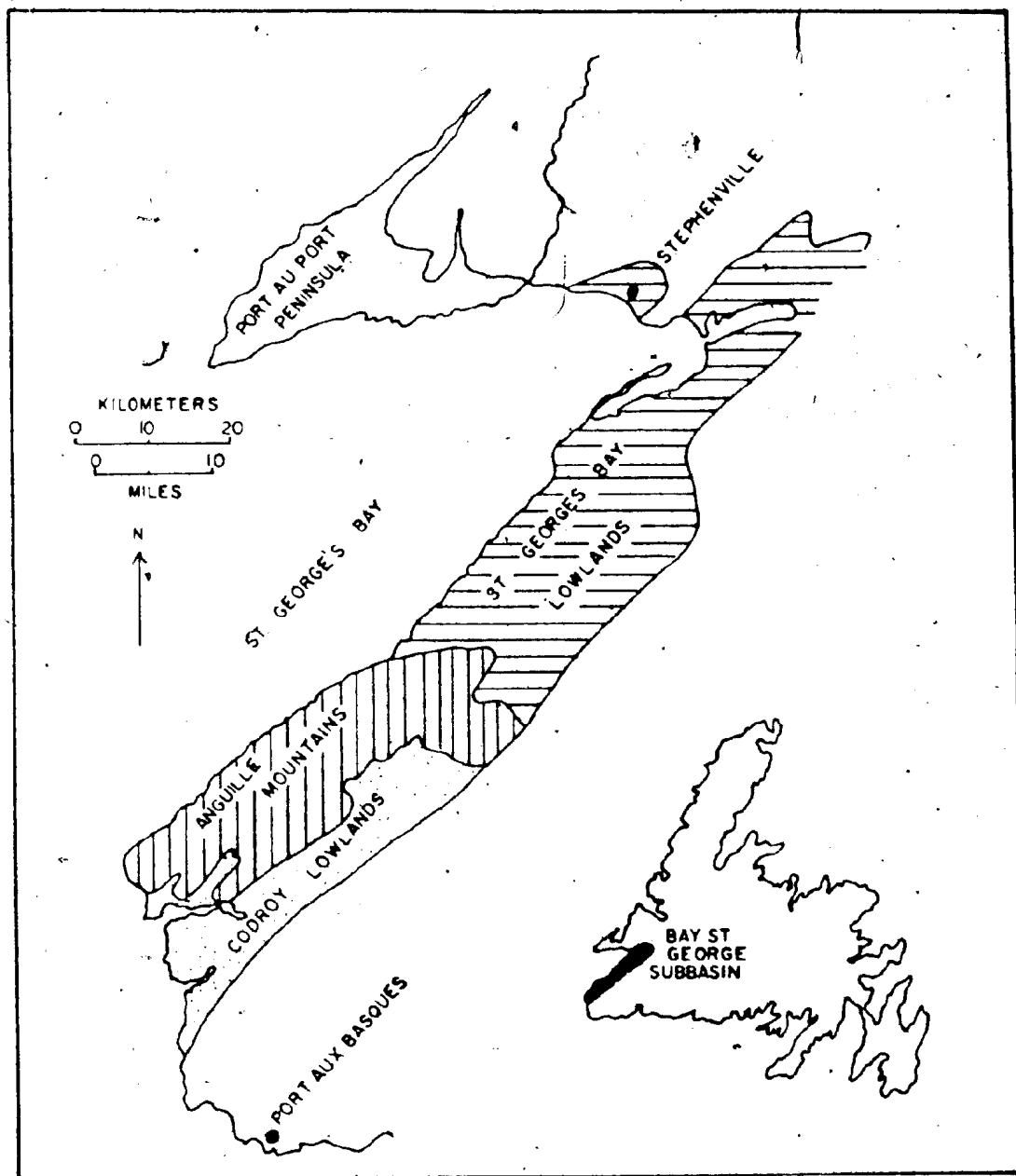


Figure 1.2: Geomorphic subdivisions of the Bay St. George Subbasin. After Knight, 1983.

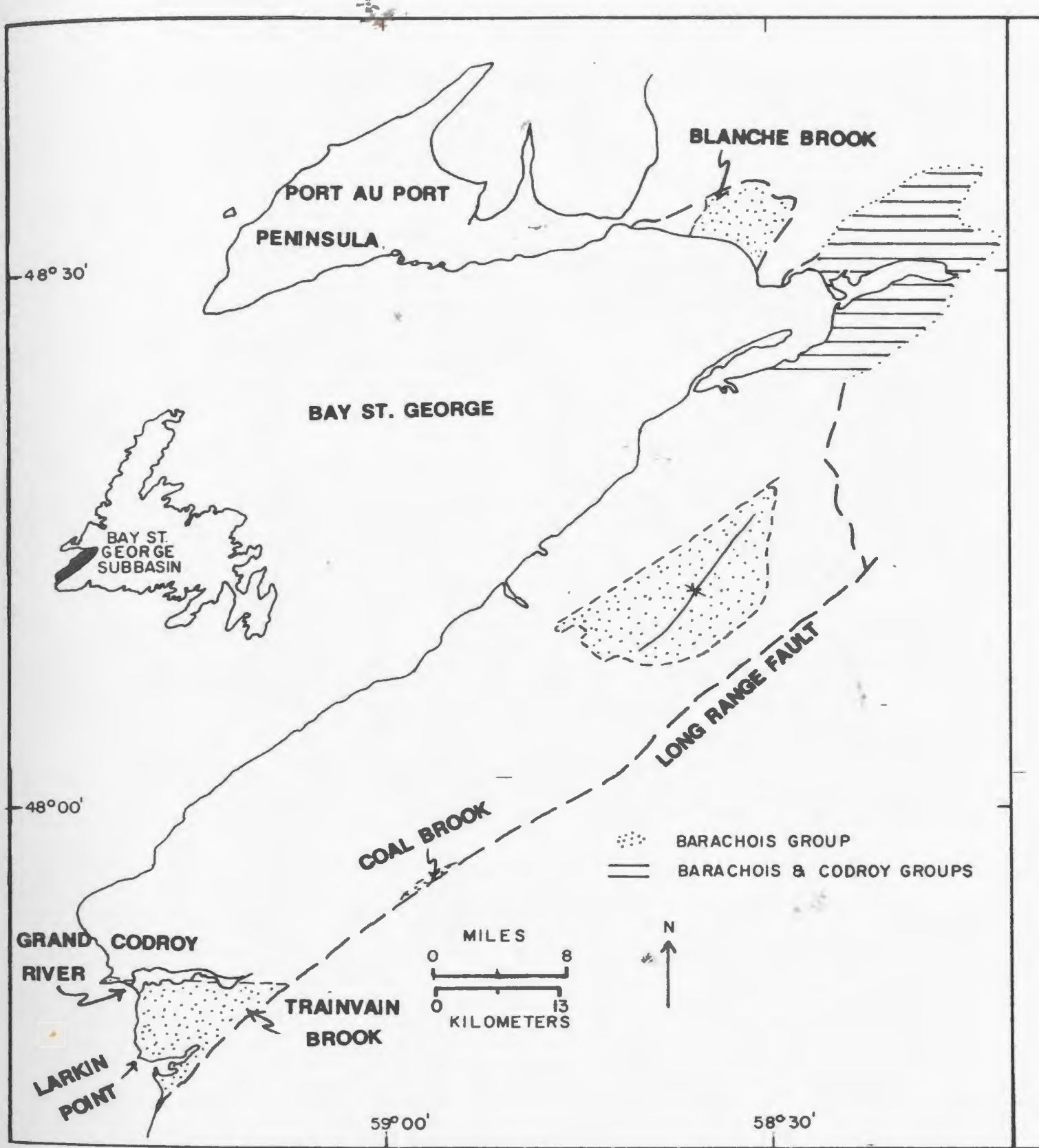


Figure 1.3: Distribution of the Barchois Group in the Bay St. George Subbasin. After Knight, 1983.

to reconstruct its environment of deposition; and 3) to evaluate its fossil fuel resource potential.

Geological Setting of the Barachois Group

The Bay St. George Subbasin is part of an extensive system of Carboniferous basins and highs collectively termed the Maritimes Basin (Williams, 1974; Knight, 1983) (see Fig. 1.1). Other names, such as Fundy Basin (Belt, 1964), Fundy geosyncline (Poole, 1967), Fundy epieugeosyncline (Hacquebard, 1972; Howie and Barss, 1975), and St. Lawrence basin (Geldsetzer, 1979) have been used for this feature. The name Maritimes Basin is preferred here for the same reasons given by Knight (1983); i.e., it is used in a geographical sense, which permits the inclusion of all the important features of the Carboniferous of the area, and does not allude to the presence or absence of deformation. The Maritimes Basin underlies much of Nova Scotia, New Brunswick and the Gulf of St. Lawrence, with sediment thickness reaching a maximum of about 9 km in the Gulf of St. Lawrence (Howie and Barss, 1975).

The Bay St. George Subbasin is presently bounded to the north by a variety of igneous, metamorphic, and sedimentary rocks. These include gneisses, granites, anorthosites, diabase dikes of Precambrian (Grenvillian) age, deep water Cambro-Ordovician siliciclastic rocks, carbonate rocks of the Cambro-Ordovician platform, allochthonous volcanic and

ophiolitic rocks, and greenschist grade metasedimentary rocks (Williams et al., 1972 and 1974). It is bounded to the southeast by dismembered ophiolites, metamorphic, volcanic, sedimentary, and intrusive rocks of the Dunnage and Gander Zones (Williams, 1978; Chorlton, 1984).

Basin History

The most recent and extensive geological survey of the Bay St. George Bay Subbasin is that of Knight (1983). The following basin history is summarized from his report. The Bay St. George Subbasin was probably produced by right-lateral strike-slip faulting which began sometime in the Devonian and continued at least until early or middle Visean time. The basin fill consists of three approximately 3000 meter-thick sequences of predominantly fluvial, lacustrine, and deltaic sediments. Marine strata are only present in the Codroy Group. The Anguille Group and the basal Codroy Group were deposited in a roughly 30 km wide graben, which widened to about 60 km by the time strike-slip motion ceased. Marine incursions which occurred in Visean time resulted in the deposition of salt and marginal marine deposits (Codroy Road Formation and the Jeffrey's Village Member), and were followed by renewed continental sedimentation that persisted through the deposition of the Barachois Group. Seismic evidence suggests that as much as 6 km of Codroy and Barachois Group sediments were deposited

in the region beneath St. George's Bay (Hobson and Overton, 1973). The Barachois Group contains the youngest known rocks in the basin. The rocks in the basin were deformed by renewed right-lateral strike-slip and vertical movements during the Late Pennsylvanian Maritime Disturbance (Poole, 1967; Knight, 1983).

Distribution of the Barachois Group and its Relationship to other Units

The major occurrences of the Barachois Group are located in the Codroy Lowlands (along the coast between Larkin Point and the mouth of the Grand Codroy River), (Fig. 1.3) and in the St. George's Lowlands (the undivided Barachois Group). The former location is the type section of the Searston Formation which was described in detail by Knight (1983). This thesis will focus on the less well known exposures in the St. George's Lowlands, including the St. George's Coalfield. Minor occurrences of the Barachois Group are found at Coal Brook and near Trainvain Brook in the Codroy Lowlands, and along Blanche Brook northwest of Stephenville (Fig. 1.3).

The Barachois Group in the St. George's Lowlands occupies a northeast-trending, doubly plunging syncline (Fig. 1.4). It is bounded to the west by the Crabbe's Brook Fault; to the south and southeast it conformably(?) overlies the Robinson's River Formation (Codroy Group), although

GEOLOGICAL MAP OF THE MIDDLE BARACHOIS BROOK AREA

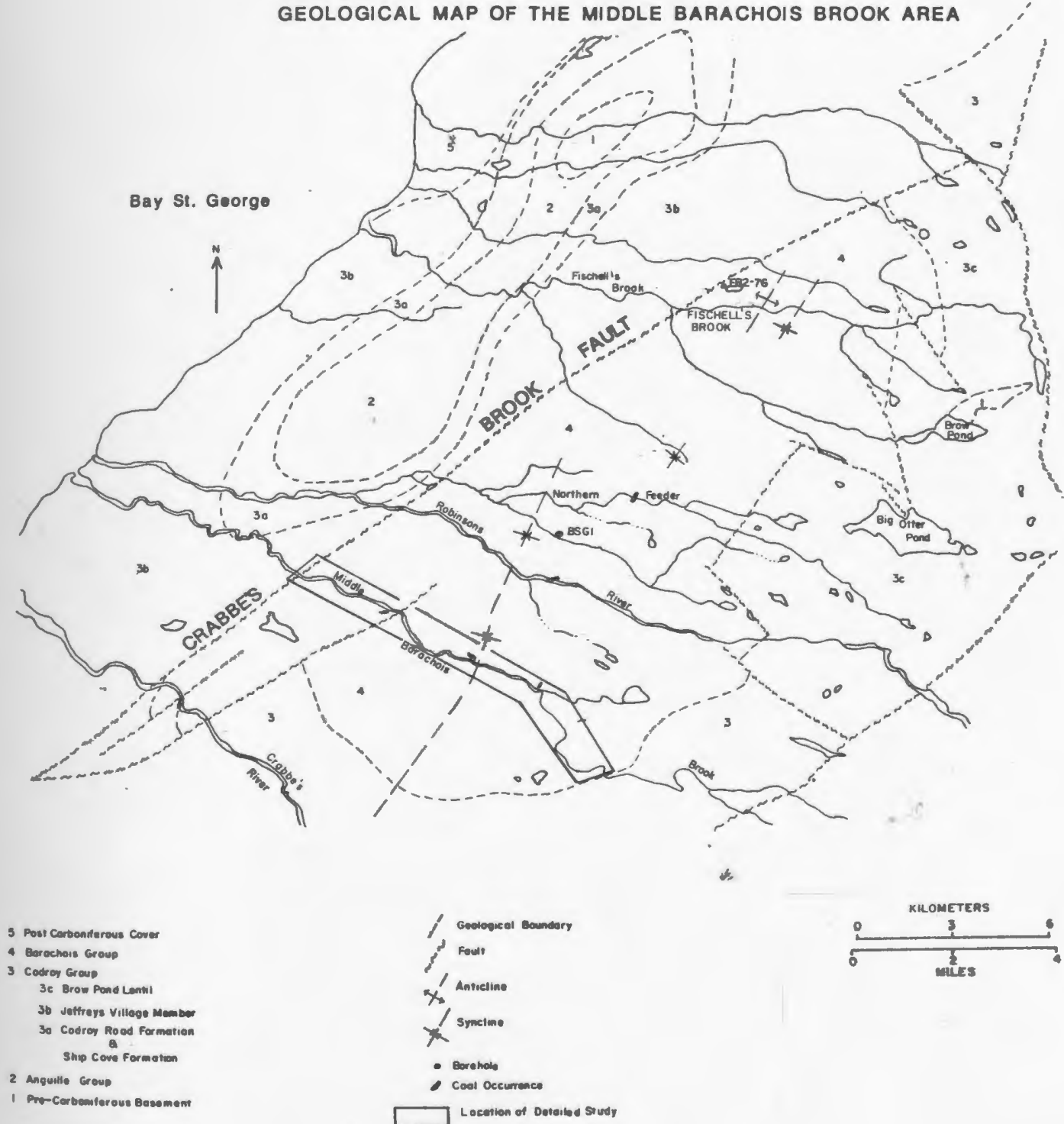


Figure 1.4: Geological map of the Middle Barachois Brook area. After Knight, 1983.

parts of the eastern boundary may be faulted. It is in conformable and/or fault contact with the Brow Pond Lentil (Codroy Group) to the north and northeast.

Previous Work: Coal Evaluation

The early studies of the Barachois Group were spurred by the presence of coal which, according to Baker (1927), was first reported in 1822 by W.E. Cormack. During the last quarter of the nineteenth century, several coal prospecting expeditions to the St. George's Coalfields were undertaken by the Geological Survey of Newfoundland (summarized in Howley, 1896). These surveys involved trenching and opening coal seams for distances up to about 400 m. A total of 12 coal seams were reported, nine of which were described as being thicker than 0.3 m. Published reports throughout the twentieth century record a gradual diminution of the coal prospects in western Newfoundland. Dowling (1920) estimated that the mineable coal reserves in the St. George's Coalfields are approximately 455,000 tonnes demonstrated and as much as 2,000,000 tonnes possible.

Baker (1927) produced the first geological map of the coalfields and supervised the drilling of eight closely spaced boreholes which were used to provide evidence for the economic potential of the coalfield. He was undaunted by the steep dips and by the lateral variability of the seams displayed in the cores and suggested that the gently dipping

strata to the east of the exposed seams probably contained considerable quantities of coal.

The exposed coal seams were described in detail by Bryan (1938), who concluded that although "considerable tonnage" of coal is present, extraction is neither practical nor economic, due to the variability of coal quality, the structural complexity of the strata, and the distance to markets. Based on the inability to correlate coal seams and the splitting of seams in eleven more diamond drill holes in the St. George's Coalfield (Summers, 1948), Hayes (1949) corroborated the findings of Bryan (1938). He suggested that in addition to the structural problems, the stable depositional conditions necessary for the formation of thick, continuous coals were not present during Barachois Group deposition.

Howse and Fleischman (1982) examined the coal-bearing outcrops along the Middle Barachois Brook and found evidence of only two seams. Electrical resistivity was used to map faults, although it was ineffective in tracing coal seams. Scintillometer readings were 2-3 times background in carbonaceous rocks and soils.

Knight (1979, 1983) summarized the history of the St. George's Coalfield exploration and the information contained in previous reports. Mapping by Fong (1976) and Knight (1983) has not led to a full understanding of the controlling structures and extent of the coal deposits, so

that Knight (1983) has advocated more detailed mapping, structural analysis and further core drilling to confirm the presence or absence of a mineable coalfield.

Previous work: Stratigraphy, Age, and Sedimentology

The stratigraphy of the Upper Carboniferous sedimentary rocks in the Bay St. George Subbasin is complicated by rapid lateral facies changes and diachronous boundaries (Knight, 1983). Particular difficulties noted by Knight (1983) are the definition of the Barachois Group/Codroy Group contact and lithostratigraphic definition in the upper part of the Codroy Group. These problems are compounded in the St. George's Bay Lowlands by poor exposure.

Early workers (Jukes, 1843; Murray, 1873; Howley, 1896, 1913; Baker, 1927; Bryan, 1938) reported the occurrence of Carboniferous rocks in the Bay St. George area, subdivided them into Mississippian Windsor strata and Pennsylvanian coal measures, and measured sections in the coalfields.

Hayes and Johnson (1938) described the general sedimentology and structure of the Carboniferous rocks, and proposed three series names, including the Barachois series of Late Carboniferous age. The contact between the Barachois Series and the underlying Codroy Series was found to be poorly defined. A Westphalian A age was obtained from the megafloreal remains in the coal measures. Bell (1948) followed the same nomenclature, but differentiated the

Searston Beds from the Barachois Series. The Searston Beds were dated as early Namurian based on megafloral remains, and it was suggested that they were transitional between the Codroy series and the Barachois Series. Baird and Cote (1964) redefined the series as groups.

Hacquebard et al. (1961) identified three biostratigraphic divisions based on palynomorph assemblages within the Barachois Group and suggested the use of the term "Howley Beds" to refer to strata of Westphalian A age which overlie the Searston Beds, but are older than the St. George's Lowland coals. The term has not found its way into common usage in this context. The Searston Beds were found to contain an early Namurian palynomorph assemblage which was equivalent to the Canso Group in Nova Scotia. Working in the same area, Utting (1966) provided additional palynological evidence for a Namurian A age for the Searston Beds and the Westphalian A age of the coal-bearing strata in the Codroy Lowlands. Spores from Barachois Group strata on Blanche Brook near Stephenville suggest a correlation with Middle Pictou Group strata (Westphalian C age) in Nova Scotia (Riley, 1962).

The type section of the Barachois Group was designated in the St. George's Coalfield by Belt (1969), who also described lithofacies assemblages, sedimentation patterns, and the tectonic framework for the Carboniferous rocks of eastern Canada (Belt, 1968, 1969). He included the Searston

Beds in the Barachois Group and suggested (as did Knight, 1983) that the source of the sediments in the Group as a whole lay somewhere southeast of the Long Range Fault. The St. George's Bay Lowlands were mapped by Fong (1975). He divided the Barachois Group into a lower sequence of coarse sandstones and conglomerates and an upper sequence of finer grained clastics with caliches and carbonate concretions. He also included the conglomeratic Brow Pond Lentil (Fig. 1.4) as part of the Barachois Group because it appears to overlie both Barachois and Codroy Group strata and because of the presence of Codroy Group pebbles. However, the Brow Pond Lentil was subsequently assigned to the Codroy Group by Knight (1983).

Knight (1983) mapped the sedimentary rocks of the Anguille Mountains and the Codroy Lowlands in the most detailed report to date. Table 1.1 illustrates Knight's (1983) stratigraphy of the St. George's Bay Subbasin and its correlation with European and American Stages. Most of Knight's (1983) work in the Barachois Group focused on (1) the well-exposed Searston Beds (which he elevated to formation status), and (2) on the Barachois Group within the Codroy Lowlands. The Searston Formation is at least 2500 m thick in the type section and was interpreted as the deposit of meandering rivers during a time when the climate was relatively humid. Previous authors (Hayes and Johnson, 1938; Utting, 1966; Belt, 1968, 1969) have noted the fluvial

Table 1.1: Carboniferous stratigraphy of the Bay St. George Subbasin. After Knight, 1983.

STRATIGRAPHY				STAGES	
HACQUEBARD #01, 1961	KNIGHT, 1983				
	CODROY LOWLANDS	ST. GEORGES BAY LOWLANDS	NOVA SCOTIA	EUROPE	N. AMERICA
COAL BEARING STRATA AT STEPHENVILLE	UPPER COAL BEARING BEDS ----- SEARSTON FORMATION	UNDIVIDED	PICTOU	C	PENNSYLVANIAN
			CUMBERLAND	B	
			RIVERSDALIAN	A	
			CANSOAN	NAMURIAN	
ST GEORGES COAL AREA HOWLEY BEDS SEARSTON BEDS	OVERFALL BROOK MEMBER		WINDSOR	VISEAN	MISSISSIPPIAN
	MOLlichIGNICK MEMBER	BROW POND LENTIL			
		HIGHLANDS MEMBER			
	JEFFREYS VILLAGE MEMBER				

character of the Barachois Group as well.

The previous investigations of the coal deposits of the St. George's Coalfields have concentrated on the area in the vicinity of Middle Barachois Brook (Fig. 1.4). The BSG#1 borehole was drilled and cored in 1983 along the axis of the coalfield as mapped by Baker (1927, his Fig. 1) in order to see if the coal seams exposed at Middle Barachois Brook are laterally continuous or if new seams could be encountered. The fact that only three thin (<5 cm) occurrences of coal were found in the core suggests that past pessimistic appraisals of the St. George's Coalfield are correct. These new data, along with the lack of detailed mapping of the Barachois Group in the St. George's Lowlands provided the impetus and direction for the study on which this thesis is based. Detailed sedimentological studies were required to interpret the depositional history of the Barachois Group in the St. George's Bay Lowlands and to evaluate the controls on the deposition of organic-rich sediments. This study, in conjunction with basinwide thermal maturation investigations and sedimentological research in other Carboniferous basins in Newfoundland (i.e. Deer lake Basin), will help to elucidate the tectonic history as well as the fossil fuel potential of the region.

Methods of Study

Facies and vertical facies sequences were described in

the field and in two continuously cored boreholes, one drilled in the centre of the basin as part of this project (BSG#1, 343 m) and one drilled in the northwestern corner as part of an exploration program for salt by Amax Exploration Inc. (FB2-76, 794 m) (see Fig. 1.4 for the location of boreholes). During the drilling of FB2-76, a fault was crossed resulting in the inadvertent coring of 522 m of possible Barachois Group sediments (Knight, 1983).

Exposure of the Barachois Group in the field is limited to river courses which flow perpendicular to the general strike of the beds. Unconsolidated Quaternary deposits (55 m thick in BSG#1) form the river banks and often obscures bedrock outcrops. Sections are best exposed along the Middle Barachois Brook and were measured with Jacob's staff, tape, or pace depending on the attitude and quality of the exposure and the water depth. The locations of outcrops which were measured or examined are shown in Figure 1.5. Outcrops became better exposed throughout the field season as water levels dropped. In general, sections are short, and coarser units are preferentially exposed. The sections provide a discontinuous view of the entire section from the faulted western margin and the conformable(?) eastern margin of the outcrop to the centre of the syncline.

There are no known marker beds in the Barachois Group, and megafossil remains are long-ranging, so there is no obvious basis for correlation of borehole and outcrop

sections. Palynological samples were collected, but detailed subdivision of the Barachois Group based on palynomorphs has not been undertaken as part of this study. Petrographical and clay mineralogical studies were undertaken in order to help elucidate the depositional history and to examine the possibility that differences in the amounts and/or types of minerals could aid in correlation.

Sections were subdivided into facies which were then grouped into associations. The facies associations were then interpreted in terms of their depositional environment. Stable carbon isotopic data obtained for some of the sediments provided additional clues as to their environment of deposition.

The assessment of fossil fuel (gas, oil, coal) potential is based on several types of data. Porosity estimates were made from well logs recorded in the BSG#1 borehole. The suitability of the shales as source rocks was evaluated by measuring their total organic carbon content and their extractable carbon content. General estimates of the quantities of coal and petroleum source rocks were made on the basis of their relative proportion in the vertical sections and predications of their lateral extent, based on inferred environments of deposition.

CHAPTER 2 - STRUCTURE AND GENERAL DESCRIPTION OF

BARACHOIS GROUP STRATA

Structure

A cross-section of the Barachois Group exposed along Middle Barachois Brook was constructed from data collected for this study (Fig. 2.1) and shows an overall synclinal structure. Gentler dips on the eastern limb of the syncline result in the exposure of considerably less vertical section than in the more steeply dipping western limb. The geometry of the synclinal structure suggests that the easternmost exposures are approximately equivalent (stratigraphically) to rocks exposed at outcrops 20-25 (Fig. 1.5).

Faults and small folds occur at several locations along Middle Barachois Brook. In most cases offset along the faults and the attitude of fault planes are unknown. In rare cases, centimeter-scale displacements on faults are observed (e.g. outcrop 92). Beds are commonly not traceable across the faults because of poor exposure.

There is, however, no evidence for large-scale fault movements within the Barachois Group, and this together with generally consistent facing directions suggest that the sections from the margins to the axis of the basinal syncline are arranged in a younging sequence. Small dip angles (10 to 40 degrees) throughout much of the section,

imply that vertical changes in lithology reflect changes due to basin location as well as temporal changes in deposition.

General Description of BSG#1 Core

The BSG#1 borehole was drilled and cored to a total depth of 343 m. Coring operations commenced after drilling 55 m of overburden. The BSG#1 core (Appendix A, Fig. 2) consists of approximately 4% conglomerate, 38% sandstone, and 58% mudstone. Grey and drab beds predominate, but reddish-brown beds become more common toward the top of the core. Thin (up to 5 cm) beds of dirty coal occur at 256.7 m, 250.0 m, and 220.1 m. Lean oil shales up to 1.5 m thick occur at 326 m, 256.5 m, 225 m, and 222 m. Oil shales contain a restricted fauna of fresh to brackish water ostracodes and gastropods (C. Dewey, pers. comm.).

Slickensided fault surfaces, calcite-filled fractures, and dips of 20 to 40 degrees from horizontal are common throughout the core.

General Description of FB2-76 Core

The FB2-76 borehole was drilled and cored to a total depth of 794.2 m. Coring commenced at 272 m following the discovery of gypsum in the drilled cuttings (AMAX, 1976). The FB2-76 core (Appendix A, Fig. 3) consists of 25% conglomerate, 36% sandstone, and 39% mudstone. The basal

56.5 m of the core are dominated by red and grey mudstones. At 737.5 m an abrupt transition to conglomerate-dominated sedimentation takes place. Apparent maximum clast (AMC) size varies throughout the core. AMC size decreases from 4.7 cm in the lower part of the core (737.5 m to 445 m) to 2.4 cm in the upper section (445 m to the top of the core). The coarsest clasts (up to 10 cm apparent long axis) occur in the interval 544 m to 525 m.

Coaly laminations and coal beds up to 2 cm thick occur at 778 m, 719.5 m, 715.3 m, and 629 m; coaly debris is most common in the lower half of the core. Calcified logs (up to about 12 cm in diameter) occur at 570.5 and 287.5 m.

Slickensided surfaces and calcite-filled fractures occur throughout the core; dips vary between 20 and 70 degrees from horizontal.

In general, the quality of the FB2-76 core is poor due to prolonged outdoor storage. Many of the shale units have been reduced to rubble as a result of freeze-thaw activity. Gypsum and halite-filled fractures were noted at 583-584 m by well-site personnel (AMAX, 1976). These minerals are no longer present. Lithostratigraphically, the occurrence of these minerals suggest a correlation with the Codroy Group

General Description of Middle Barachois Brook Strata

The stratigraphically lowest exposures along the Middle Barachois Brook are dominated by sequences of grey

conglomerate and sandstone which alternate with sequences of red-brown mudstone and sandstone. Stratigraphically higher exposures become progressively richer in mudstone, particularly grey mudstone. Coals and oil shales are confined to a zone between outcrops 21 and 51 (Fig. 1.5), although coalified woody debris is found in sandstones at all stratigraphic levels. With the exception of two exposures of ostracode-bearing limestone and two exposures of gastropod- and ostracode-bearing oil shales, the only known fossils present in the Barachois Group are plant remains and spores.

Two generalized paleoflow directions emerge from orientation measurements on cross-bedding. Flow was from the north in the stratigraphically lowest exposures (i.e. between outcrops 38 and 28 on the west limb and between outcrops 68 and 75 on the east limb of the syncline). Paleoflow was more variable, but generally northerly directed in the stratigraphically higher exposures (i.e. between outcrops 28 and 85).

Exposures along Middle Barachois Brook vary considerably in length and quality. Much of the outcrop is underwater (i.e. in the streambed). Measured sections illustrated in Appendix A range from less than 10 m (outcrop 10) in stratigraphic thickness up to almost 200 m (outcrop 13/14).

Age and Correlation

Since no marker beds are available with which to correlate sections, 45 samples of grey mudstones were collected and processed for palynomorphs. Although 35 samples yielded spores, only four were examined as part of this thesis. Species and genera identified from four samples are listed (along with their approximate ranges) in Tables 2.1 to 2.4. The youngest assemblage is found in the sample from 340.2 m in the BSG#1 borehole. The presence of Florinites pumicosis, F. similis, Punctatosporites species, Raistrickia saetosa, and Calamaspora cf. breviradiata indicate that it is probably Westphalian A in age (Clayton et al., 1977; Braman and Hills, 1977; Smith and Butterworth, 1967). Spore content (Hacquebard et al., 1961) and macrofloral evidence (Bell, 1948) indicate that the coal-bearing beds along the Middle Barachois Brook are also Westphalian A in age.

Most palynomorphs from a sample taken at 774.4 m from the FB2-76 core range from Visean to Namurian in age (e.g. Convolutispora ampla, Crassispora maculosa) (Smith and Butterworth, 1967). This sample probably represents the oldest assemblage examined.

Diverse palynomorph assemblages which contain common Westphalian-age spores are present in sample P13 from outcrop 38 (the stratigraphically lowest outcrop) and from 278.6 m in the FB2-76 core. Both of these samples are

TABLE 2.1: MIOSPORES FOUND IN BSG#1 340.2 m

Microreticulatisporites cf. M. microreticulatus
Knox 1950 (Namurian)
Raistrickia saetosa (Loose) Schopf, Wilson, and
Bentall 1944 (Westphalian A to B)
Calamaspora cf. breviradiata Kosanke 1950
(Westphalian A)
Radiizonates cf. R. striatus (Knox) Staplin, and
Jansonius 1964 (Westphalian A to B)
Anaplanasporites globulus Butterworth and Williams
emend. Smith and Butterworth 1967 (Namurian A)
Florinites pumicosis (Ibrahim)*Schopf, Wilson, and
Bentall 1944 (Westphalian A to D)
F. similis Kosanke 1950 (Westphalian A to D)
Lycospora pellucida (Wicher) Schopf, Wilson, and
Bentall 1944 (Visean to Westphalian D)
Punctatosporites minutus Ibrahim 1933 (Westphalian A)
Crassispora kosankei (Potonie and Kremp) Bharadwaj 1957
emend. Smith and Butterworth 1967 (Namurian to
Westphalian D)
Granulatisporites cf. G. minutus Potonie and Kremp 1955
(Westphalian A to C)
Cyclogranisporites multigranus emend. Smith and
Butterworth 1967 (Westphalian A to B)
Schopfiipollenites sp.
Stenzonotriletes sp.
Campotriletes sp.
Punctatasporites sp.
Dictyotriletes sp.
Punctatisporites sp.
Knoxisporites sp.
Apiculatisporis sp.
Verrucosisporites sp.
Lophotriletes sp.

TABLE 2.2: MIOSPORES FOUND IN OUTCROP 38 (P13)

- Dictyotrilletes bireticulatus (Ibrahim) emend. Smith and Butterworth 1967 (Westphalian A to C)
- Lycospora noctuina Butterworth and Williams 1958 (Visean to Westphalian D)
- Cyclogranisporites cf. minutus Bharadwaj 1957 (Namurian A to Westphalian D)
- Lycospora pusilla (Ibrahim) Schopf, Wilson, and Bentall 1944 (Visean to Westphalian D)
- Crassispora kosankei (Potonie and Kremp) Bharadwaj 1957 emend. Smith and Butterworth 1967 (Namurian to Westphalian D)
- Savitrisorites nux Butterworth and Williams emend. Smith and Butterworth 1967 (Namurian A to Westphalian)
- Knoxisorites cf. K. cinctus (Waltz) Butterworth and Williams 1958 (Namurian A)
- Laevigatosporites cf. L. vulgaris Ibrahim 1933 (Westphalian B?)
- ?Convolutispora florida Hoffmeister, Staplin, and Malloy 1955 (Visean)
- Verrucosisporites cf. V. cerosus (Hoffmeister, Staplin, and Malloy) Butterworth and Williams 1958 (Visean to Namurian)
- Calamaspora sp.

TABLE 2.3: MIOSPORES FOUND IN FB2-76: 278.6 m

<u>Granulatisporites granifatus</u>	Ibrahim 1933 (Visean to Westphalian C)
<u>Lycospora pusilla</u>	(Ibrahim) Schopf, Wilson and Bentall 1944 (Visean to Westphalian D)
<u>Cyclogranisporites minutus</u>	Bharadwaj 1957 (Namurian to Westphalian D)
<u>Verrucosisporites cerosus</u>	(Hoffmeister, Staplin, and Malloy) Butterworth and Williams 1958 (Visean to Namurian)
? <u>Stenzonotriletes bracteolus</u>	Butterworth and Williams comb. nov. Smith and Butterworth 1967 (Visean to Namurian)
<u>Savitrissporites nux</u>	Butterworth and Williams emend. Smith and Butterworth 1967 (Visean to Namurian A)
<u>Lophotriletes commissuralis</u>	(Kosanke) Potonie and Kremp 1955 (Namurian to Westphalian D)
<u>Apiculatisporis latigranifer</u>	(Loose) Potonie and Kremp 1955 (Westphalian)
<u>Waltzisporea polita</u>	Hoffmeister, Staplin and Malloy comb. nov. Smith and Butterworth 1967 (Visean to Namurian)
<u>Florinites cf. F. junior</u>	(broken) Potonie and Kremp 1955 (Westphalian)
<u>Raistrickia fulva</u>	Artuz 1957 (Westphalian)
<u>Lycospora pellucida</u>	(Wicher) Schopf, Wilson, and Bentall 1944 (Visean to Westphalian D)
<u>L. noctuina</u>	Butterworth and Williams 1958 (Visean to Westphalian D)
<u>Microreticulatisporites cf. M. nobilis</u>	(Wicher) Knox 1955 (Westphalian)
<u>Converrucosisporites armatus</u>	Dybova and Jachowicz emend. Smith and Butterworth 1967 (Westphalian A)
<u>Knoxisporites cf. K. triradiatus</u>	Hoffmeister, Staplin, and Malloy 1955 (Visean to Namurian)
<u>Endosporites ornatus</u>	Wilson and Goe 1940 (Westphalian?)
<u>Pustulatisporites cf. P. papillosus</u>	(Knox) Potonie and Kremp 1955 (Namurian A)
? <u>Krauselisporites</u>	sp.
<u>Cirratriradiates</u>	sp.
<u>Dictyotriletes</u>	sp.
<u>Puntatosporites</u>	sp.
? <u>Laevigatosporites</u>	sp.

TABLE 2.4: MIOSPORES FOUND IN FB2-76: 774.4 m

Convolutispora ampla Hoffmeister, Staplin and
Malloy 1955 (Visean to Namurian)
Densosporites cf. D. pseudoannulatus Butterworth and
Williams 1958 (Visean to Namurian)
Pustulatisporites cf. P. papillosus (Knox) Potonie and
Kremp 1955 (Namurian A)
Punctatisporites arearius Butterworth and Williams 1958
(Namurian)
Granulatisporites granulatus Ibrahim 1933
(Visean to Westphalian C)
Lycospora pusilla (Ibrahim) Schopf, Wilson and Bentall 1944
(Visean to Westphalian D)
Crassispora maculosa (Knox) Sullivan 1964
(Visean to Namurian)
Convolutispora cf. C. venusta Hoffmeister, Staplin and
Malloy 1955
Microreticulatisporites microreticulatus Knox 1950
(Namurian)
Verrucosisporites sp.
Convolutispora sp.

Namurian to Westphalian in age although they contain few palynomorphs in common. These two samples may be intermediate in age between the lower part of the FB2-76 core and the BSG#1 core.

In the Maritime provinces of Canada, European Stages are used with rock-stratigraphic units as illustrated in chapter 1 (Table 1.1). Based on palynological evidence, the apparently youngest sample (Westphalian-age) (BSG#1, 340.2 m) is equivalent to the Riversdale Group of the Maritimes; the other three samples are probably equivalent to Cansoan strata (Knight, 1983; Hacquebard et al., 1961).

Lists of generic miospore assemblages provided by Hacquebard et al. (1961), and Utting (1965) for the Maritime provinces of Canada and for Barachois Group strata in the Codroy Lowlands respectively, are similar to generic assemblage lists presented in Tables 2.1 to 2.4. According to the biostratigraphic zonation developed by Hacquebard et al. (1961), strata from which the samples were taken are assigned an age between the Namurian A and the Westphalian A.

Based on miospore assemblages, the rocks in the FB2-76 borehole appear to be equivalent in age to the ~~oldest~~ units of the Searston Formation (i.e. earliest Namurian). Knight, 1983). This information corroborates Knight's (1983) suggestion that the strata in the FB2-76 borehole be included in the Barachois Group. The presence of

evaporite-filled fractures in the core (as mentioned earlier) may be due to the proximity of the borehole to the Crabbe's Brook Fault and associated thick salt structures as opposed to being evidence in favor of inclusion in the underlying Codroy Group. For the purposes of this study, the rocks in the FB2-76 borehole are included in the Barachois Group. Further elucidation of the stratigraphy in the Barachois Group awaits more detailed palynological biostratigraphic information.

CHAPTER 3 - FACIES DESCRIPTIONS

Introduction

In this section, 11 facies (Facies A to K) are described from the cores and the outcrops. Each facies is illustrated by a photograph. Detailed lithological logs are provided in Appendix A.

Facies A: Conglomerate

DESCRIPTION. This facies is characterized by stratified, structureless and in rare cases trough cross-stratified conglomerate (Plate 3.1). Individual clasts are generally <2 cm (maximum of 10 cm) in size (measured along the apparent long axis), imbricated, and moderately well rounded to subangular. Clasts are usually well sorted and they are set in a medium to very coarse sand matrix. Both matrix and grain supported-conglomerate occur. Pebble lithologies include, microlitic and porphyritic volcanics, chert, quartz-muscovite and sericite schists, granite, and quartz.

Intraformational mudstone and limestone clasts are present locally. Conglomerates may contain coalified (field sections) or calcified (FB2-76) plant remains to 25 cm in diameter. Thin (<5 cm) beds of mudstone with sharp contacts occur within this facies. Massive conglomerates are rare in



3.1A



3.1B

Plate 3.1A: Facies A - stratified conglomerate.

FB2-76 borehole, 706.1 m.

Plate 3.1B: Facies A - massive conglomerate with a cross-section through a calcified log at the top of the core. FB2-76 borehole, 632.4 m.

the field sections, but they are common in the cores. Cross-stratification in conglomerates is only recognizable in the field sections where trough cross-sets are generally less than 0.5 m thick. In the field sections and in the BSG #1 borehole, rocks assigned to this facies are grey in colour and account for 0 to 15% of the section. In the FB2-76 borehole, rocks assigned to facies A are either red or grey and account for 23% of the section.

PROCESS INTERPRETATION. The lack of muddy and silty matrix in the rocks comprising facies A suggests that these deposits formed in relatively high velocity flows in which fines were winnowed out by the current. The absence of vertical clasts, clasts which project above the beds, and the general imbrication of clasts suggests that debris flows were not responsible for depositing the stratified and massive conglomerates (Rust and Koster, 1984). Lag deposits are indicated by the presence of basal scoured surfaces and mudclasts. Cross-stratified conglomerate is formed as scour-fill or by the migration of gravel bars with developed slipfaces (Rust, 1975). The abrupt upward gradation to finer grain size and the presence of muddy drapes indicate that flow generally waned rapidly rather than gradually.

The structureless or massive gravels in the cored intervals may only appear structureless on the scale at which they were examined. The core is 50 to 90 mm in diameter, so that maximum clast sizes approach the core

diameter, making it difficult to discern sedimentary structures. The fact that massive gravels are rare in the field sections suggest that stratification may be more common in the core than is apparent.

Facies B: Intraformational mudclast conglomerate.

DESCRIPTION. Rocks comprising facies B are present in both the outcrop and in the cores. These deposits consist of a mixture of locally-derived red or grey mudclasts and extraformational pebbles in a matrix of fine to coarse sand (Plate 3.2). The mudclasts range in size from less than 1 cm to 10 cm and form approximately 20-50% of the facies. Clasts are either rounded or preserved as 1-2 cm long, thin (several mm thick) flakes. Facies B rocks may be cross-stratified, horizontally stratified, or massive.

Facies B is rarely more than 10 cm thick. An exception is in the interval 344-348.4 m in the FB2-76 core. Thicker beds and beds with more well rounded clasts tend to be associated with pebbles (2-3 cm in diameter) and coarse sand. Facies B never comprises more than 5% of a section.

PROCESS INTERPRETATION. This facies is probably the product of deposition in erosive scours of locally derived, unlithified, but cohesive, muddy material. It is likely that more well-rounded clasts were transported as bedload. Flume experiments (Smith, 1972a) suggest that such intraformational clasts could not survive transport of more



Plate 3.2: Facies B - Intraformational conglomerate made up of dark grey mudstone flakes in a medium to coarse sandstone matrix. BSG#1 borehole, 266.5 m.

than hundreds of meters. Thin flakes associated with finer sediments may have been transported in suspension.

Facies C: Cross-stratified sandstone.

DESCRIPTION. Facies C strata consist of centimeter to decimeter scale, trough cross-stratified, fine-grained to very coarse-grained sand and pebbly sand (Plate 3.3). This facies is gradational into facies A (cross-stratified conglomerate). Decimeter-scale cross-stratification is recognized in the cores by non-parallel strata which suggest converging cross-bed foresets. The differentiation between planar and trough cross-stratification depends upon three-dimensional exposures (Reineck and Singh, 1980, p.98). The lack of such exposure in the core and in most outcrops necessitates grouping all cross-bed types into one facies. In several field examples, trough cross-beds are exposed in plan view (see Plate 3.4).

Lenses of coarser or finer material are interspersed throughout facies C. The coarser lenses have erosive bases and gradational tops, and may contain intraformational mudclasts. The finer lenses have sharp bases and tops. Grey shale drapes (<5 cm thick) are present, but uncommon within facies C (e.g. BSG#1, 210 to 212.5 m and outcrop 62). Rare examples of planar tabular cross-strata (up to 0.5 m thick) occur at 106 m, 176 m, and 182 m in outcrop 14 and at 8 m at outcrop 51b in red or grey, medium- to coarse-grained

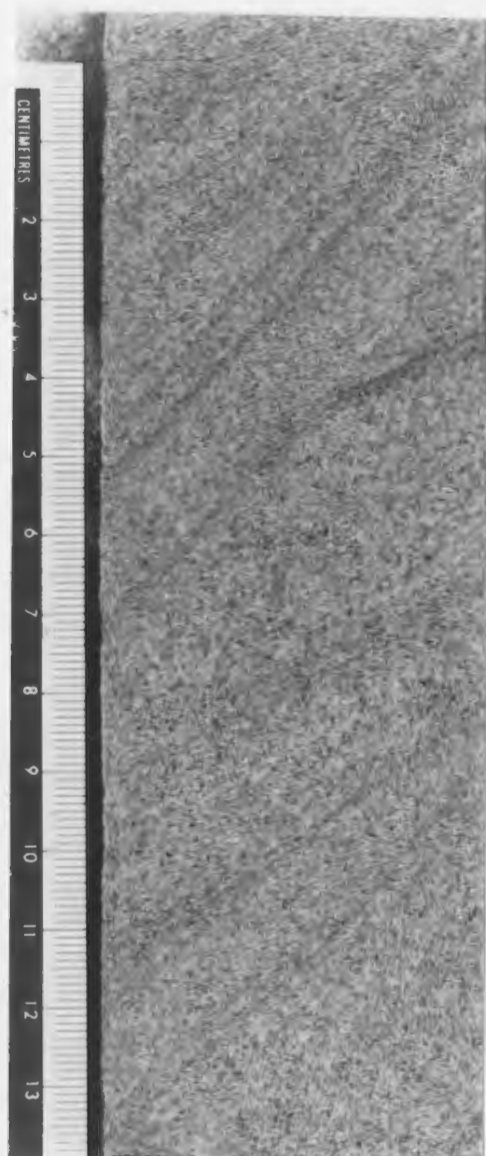


Plate 3.3: Facies C - cross-stratified sandstone.
FB2-76 borehole, 599 m.

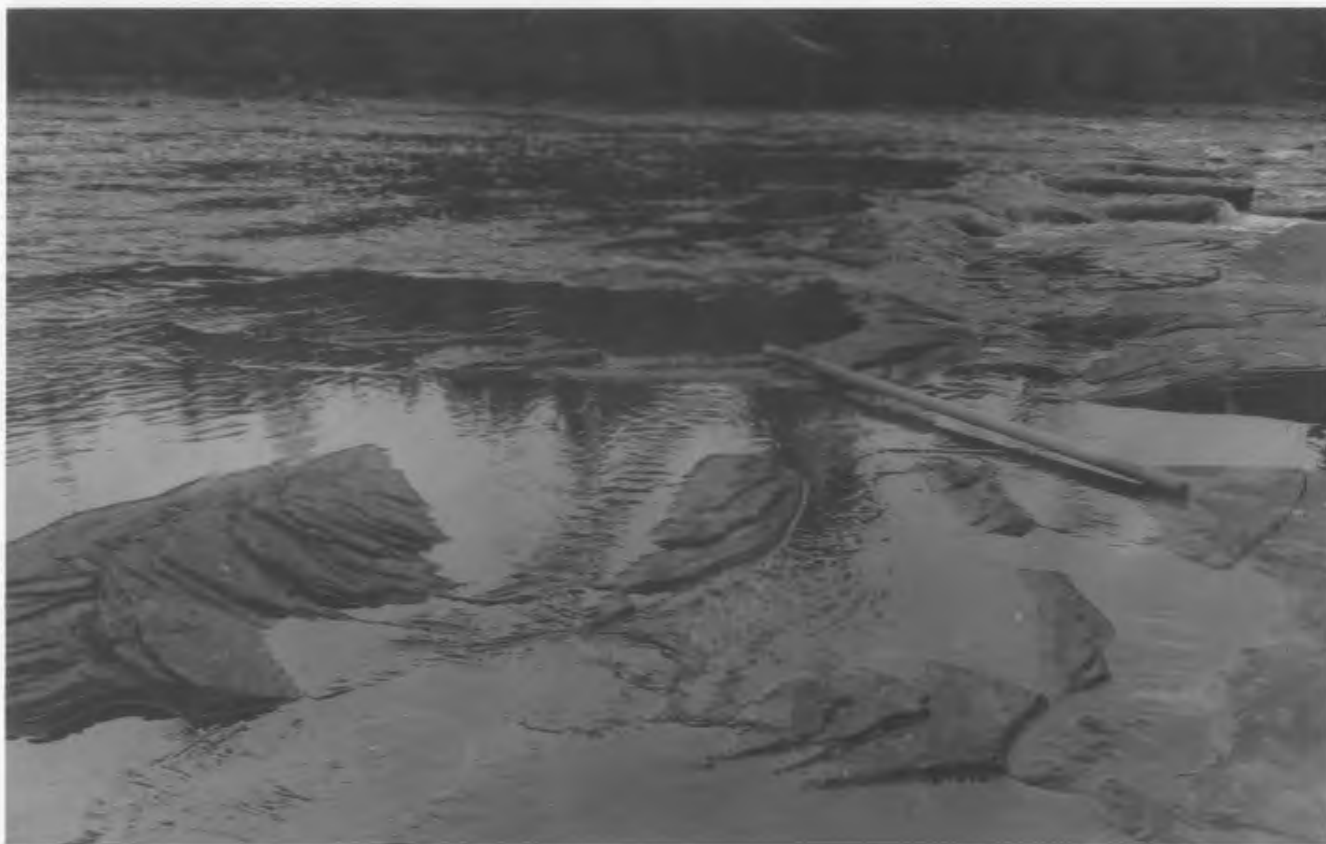


Plate 3.4: Facies C - trough cross-stratified sandstone in plan view (outcrop 69). The staff is 1.2 m long.

sandstones. Apparent dips of planar foreset laminae average about 20 degrees. Mudclasts occur at the base of one unit and hematitic plant remains are interspersed throughout another.

Coalified organic matter is common in facies C: it occurs as both discrete plant remains or as organic-rich laminations. Hematite-stained plant casts (Calamites and Stigmaria) occur in the vicinity of coal-bearing outcrops. Locally, within facies C, bedding is convoluted. At 176-178 m in BSG#1, beds of facies C are thinly interbedded with mudstones and contain convolute bedding.

Spherical, calcite-cemented concretions occur within facies C at several exposures. Cross-strata are continuous through the concretions. The concretions are similar to those described by other authors as "cannonball" concretions (Belt, 1965; Utting, 1966).

Facies C is common in both cores and in the field exposures. It accounts for 23% of the thickness of the FB2-76 core, 26.5% of the BSG#1 core, and between 6% and 49% (mean of 24%) of the field sections.

PROCESS INTERPRETATION. Cross-beds in facies C are formed by the migration of three-dimensional megaripples in the case of trough cross-stratification and by the migration of two-dimensional bedforms (i.e. sandwaves, transverse bars, or straight-crested megaripples) in the case of planar cross-stratification (Harms et al., 1982). Megaripples

(dunes) form at minimum mean flow velocities of about 40 cm/sec (Harms et al., 1982) for medium- to coarse-grained sand. The presence of finer and coarser deposits within the cross-stratified units indicates that current strength varied during the deposition of the unit, and, with the deposition of mudstone and organic-rich drapes, must have slackened considerably at times to allow deposition of suspended material to occur. Scour and fill were responsible for the coarser-grained interbeds, whereas a waning of current strength resulted in finer lenses being deposited. For the planar tabular units, deposition from avalanching bedload, with very little suspension load input, is indicated by the angular basal contact of the foreset laminae and the lack of fine grain sizes (Jopling, 1965). Convolute bedding may be due to penecontemporaneous deformation such as liquefaction.

Facies D: Parallel-laminated sandstone.

DESCRIPTION. Facies D ranges from very fine- to very coarse-grained and pebbly sands, but is most common in the very fine to medium sand sizes. Parallel lamination and parting lineation are the only visible sedimentary structures (Plate 3.5). The laminae are defined by grain size differences and micaceous layers in the sandstone. Mudstone rip-up clasts are locally present.

Units of facies D range from 0.2 to 2.0 m thick.



Plate 3.5: Facies D - parallel-laminated sandstone.
BSG#1 borehole, 156.6 m.

Parallel lamination in facies D occurs in both red and grey units. In most sections, facies D accounts for less than 2% of the total thickness, but reaches 9% in outcrops 15 and 51. In some cores, this facies is difficult to distinguish from facies C due to changes in stratal dip angles.

PROCESS INTERPRETATION. Facies D results from flow over a flat bed in either the upper or lower flow regime. For fine sand, flume studies show that parallel lamination forms only in the upper flow regime (mean flow velocities of at least 60 cm/sec for flow depths > 8 cm) (Harms et al., 1982). For grain sizes 0.45-0.55 mm (medium to coarse sand) flow velocities of about 1.1 m/sec. are required to form upper plane beds, regardless of flow depth (Harms et al., 1982). Horizontal lamination forms in silts and very fine sands which are deposited directly from suspension. Harms et al. (1982) suggest that lower flow regime plane beds will probably not result in substantial thicknesses of parallel-laminated deposits due to the low rate of transport of coarse grains (>0.7 mm) at low flow velocities. In cases where parting lineation is present, parallel lamination must have resulted from upper flow regime conditions (Harms et al., 1982).

Facies E: Structureless, convoluted and irregularly-laminated sandstone.

DESCRIPTION. Facies E consists of very fine- to coarse-grained red or grey sandstone with either no

discernible primary sedimentary structures (Plate 3.6A) or with convoluted or irregular laminations (Plate 3.6B). Structureless units of very fine- to medium-grained sandstone are less than 30 cm thick, and are interbedded with shales, mudstones, and ripple cross-laminated sandstones and siltstones with convolute laminations (BSG#1 260-263 m and Joe MacKay's Brook 0-4 m). In one case (BSG#1, 198 m), vertically elongate carbonate-cemented zones with coalified organic material in their cores are present.

Rare coarse-grained, structureless sandstone units are red or grey and attain a maximum thickness of 1 m. A single occurrence of massive, poorly sorted, coarse sandstone with a muddy hematite-rich matrix was noted at outcrop 51a (at 2 m; sample F78). Coarse-grained units in FB2-76 (542-543 m and 566-567 m) overlie shales and mudstones and underlie cross-stratified sands or gravels. In BSG#1, one coarse example of facies E lithology at 323.5 m to 324.5 m is faulted.

Convoluted and irregularly-laminated sandstones are common in the cores, but rarely observed in the outcrops. Irregularly-laminated sandstones are very fine- to coarse-grained, 20 cm to 70 cm thick and may contain disseminated organic material concentrated along bedding planes and abundant coaly material which disrupts



Plate 3.6A



Plate 3.6B

Plate 3.6A: Facies E - massive sandstone. BSG#1 borehole, 153.8 m.

Plate 3.6B: Facies E - convoluted sandstone. BSG#1 borehole, 254 m.

laminations. In some cases organic debris is not present and laminae have a churned appearance.

PROCESS INTERPRETATION. The lack of megascopic primary sedimentary structures in structureless sandstone and the disruption of primary sedimentary structures in irregularly-laminated sandstones may be the result of their complete or partial destruction by plant or animal bioturbation or liquefaction. Johnson (1984) and Gersib and McCabe (1981) both attribute the lack of structure in fine- to coarse-grained sandstones to both of these mechanisms. Alternatively, rapid sedimentation from high concentration flows may result in a lack of visible sedimentary structures (e.g. Lowe, 1982). In the finer-grained structureless sandstones, the elongate carbonate-rich zones with coalified cores are interpreted as root traces (Klappa, 1980). In these cases, phytoturbation is the probable explanation for the lack of sedimentary structure. Coaly traces in the irregularly-laminated sandstones strongly suggest that the disruption of primary sedimentary structures was caused by either interference with vegetation during deposition (Coleman and Gagliano, 1965) or by roots after deposition. Churning of the sediment where no evidence of plant activity is present may be due to animal activity. Where evidence for root structures in structureless sandstone is lacking, liquefaction, and/or rapid deposition may provide the best explanations for these sandstones. Distortion of

laminations in convoluted sandstones may be caused by liquefaction or dewatering (cf. Lowe, 1975). It is possible in some cases that the textural homogeneity of coarser units of structureless sandstone, or subsequent tectonic disturbances, make it difficult to discern the primary sedimentary structures.

Facies F: Cross-laminated sandstone and siltstone.

DESCRIPTION. Facies F consists of red or grey, cross-laminated, very fine- to fine-grained sandstone and siltstone (e.g., Plate 3.7, Plate 3.8). Where present, ripple form-sets are asymmetric. In some units, ripples climb with examples of both stoss-side erosion and preservation being present. In other units, ripples are draped by varying amounts of mica or muds and are flaser to lenticular bedded in part. Facies F may contain all or some of the following at any given occurrence: coalified rootlets and plant debris, greenish reduction spots, plant impressions and casts, calcium carbonate nodules, and evidence of bioturbation. No symmetrical or flat topped ripples were observed. The base of this facies is usually sharp and locally either scoured or gradational.

PROCESS INTERPRETATION. Facies F was probably formed by the migration of small current ripples; however, it is not possible to completely rule out its formation in some cases by migration of wave-current ripples (Harms, 1969).

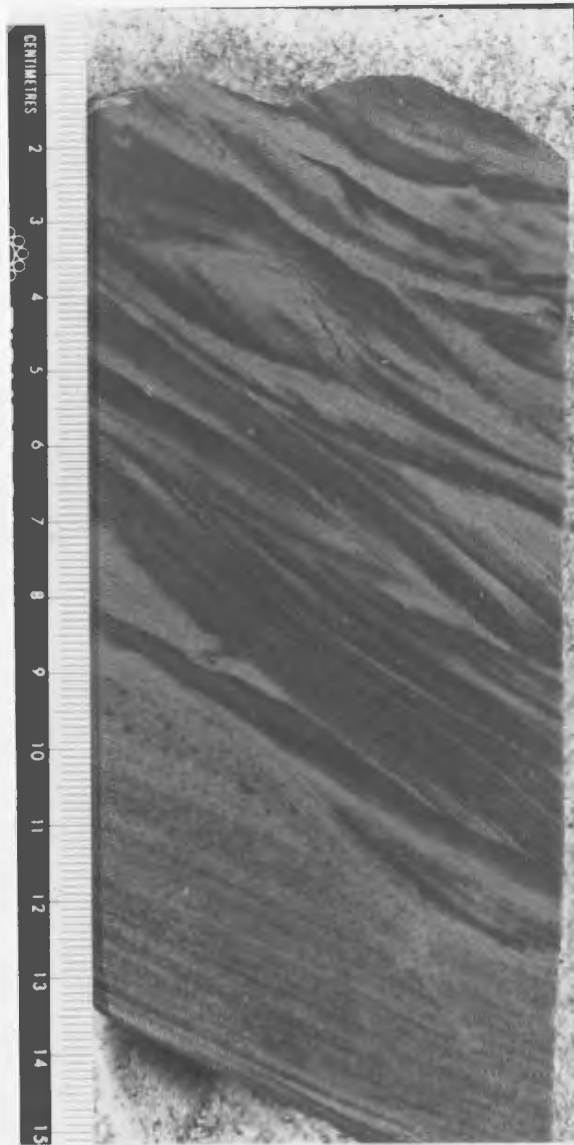


Plate 3.7: Cross-laminated sandstone (facies F) scoured into parallel-laminated sandstone (facies D). The hair-like subvertical lineation in the upper centre of the core is a coalified rootlet. BSG#1 borehole, 181.1 m.



Plate 3.8: Facies F - ripple cross-laminated sandstone
at outcrop 51b, 12 m. The book is 18 cm long.

Current ripples may form throughout a wide range of flow velocities, flow depths; and grain sizes. Climbing ripples indicate high rates of vertical deposition relative to the rate of downcurrent sediment transport (e.g. Harms et al., 1982).

Facies G: Interbedded sand, silt, and mudstone

DESCRIPTION. Facies G consists of red or grey, interbedded, cross-laminated, parallel-laminated, convoluted, or massive sandstone and laminated or massive mudstone (see Plate 3.9). In some cases climbing ripple cross-laminations occur, with examples of both stoss-side erosion and preservation being present. Sandstone beds exhibit scoured contacts with underlying mudstones, upper contacts of sandstones are commonly gradational. Laminations are several millimeters thick, while individual sandstone beds range from less than one centimeter to several tens of centimeters thick. Graded beds noted in the BSG#1 core are 1 to 2 cm thick and grade from coarse-grained or fine-grained, moderately-well sorted sandstone up to siltstone. One of these graded beds (BSG#1 241.8 m) is cross-laminated and contains abundant shale and siltstone clasts. Beds containing some of the following features were also observed: calcium carbonate nodules, plant impressions and casts (principally Stigmaria), coalified plant debris, rooted horizons, burrows (e.g. BSG#1 88.3 m) and soft-sediment deformation features (e.g. convolute laminae).



Plate 3.9: Facies G - Interbedded mudstone, siltstone and sandstone. In this case sandstone and mudstone are massive; micaceous siltstone is cross-laminated. BSG#1, 104.3 m.

Facies G accounts for 12% to 60% of the individual sections.

Plate 3.10 illustrates a field example of facies G. A hackly weathering shale is interbedded with centimeter-scale, silica-cemented, cross-laminated, very fine grained sandstone. As seen on bedding planes, the sandstone weathers into roughly rectangular blocks approximately 20 cm long and 10 cm wide.

PROCESS INTERPRETATION. The cross-laminated beds were probably deposited by current ripples, but as was the case for facies F, the possibility of wave rippling applies here as well. Currents of low velocity and competence are responsible for the deposition of the small-scale ripple cross-lamination seen in this facies. Relatively high rates of vertical deposition (relative to downcurrent transport rate) are indicated by the presence of climbing ripples. The laminated siltstones and mudstones represent slow deposition from suspension while the massive deposits may result from root bioturbation, water escape or a combination of the two. The lack of muddy matrix in the thin graded beds suggests that they are probably the deposits of waning, matrix-free currents rather than turbidity currents (Reineck and Singh, 1980, p.118).

The presence of Stigmaria casts, coalified rootlets, and calcium carbonate nodules suggests that, in some cases,

sediments represented by facies G formed a vegetated rudimentary soil.

Facies H: Mudstone

DESCRIPTION. Facies H consists of light to dark grey (N1 to N5), grey-brown (5YR to 10YR), or red (5R) to red-brown (10R) mudstone which may be fissile, massive or laminated (Plates 3.10, 3.11, and 3.12). Non-grey and grey colours may grade from one to the other (i.e. 172 m BSG#1); mottles of one colour can be present in the other. Laminations on a millimeter scale are present in organic-rich units and consist of bright or dull coaly bands. Calcium carbonate nodules and segregations generally less than 1 cm in diameter are common in both red and grey units, but pyrite is restricted to the dark grey zones. Carbonate nodules are commonly oblate and appear to bifurcate downward in some cases (Plate 3.11). At several locations (e.g., outcrop 38) they are cored with carbonaceous material. Larger calcium carbonate nodules are discussed in detail in the section on facies association III.

Dark grey units contain varying amounts of organic carbon, up to a maximum of 21% (sample F67 outcrop 2a). Carbonaceous shales (i.e. shales which contain the remains of higher plants and unidentified coaly debris) are common in the vicinity of coal seams and in the BSG#1 core. They



Plate 3.10: Facies G (interbedded mudstone and sandstone) overlying facies H (grey mudstone. Mudstones are soft, friable and rusty weathering. Sandstones are hard, siliceous, and cross-laminated. The staff is 1 m long. Outcrop #6.

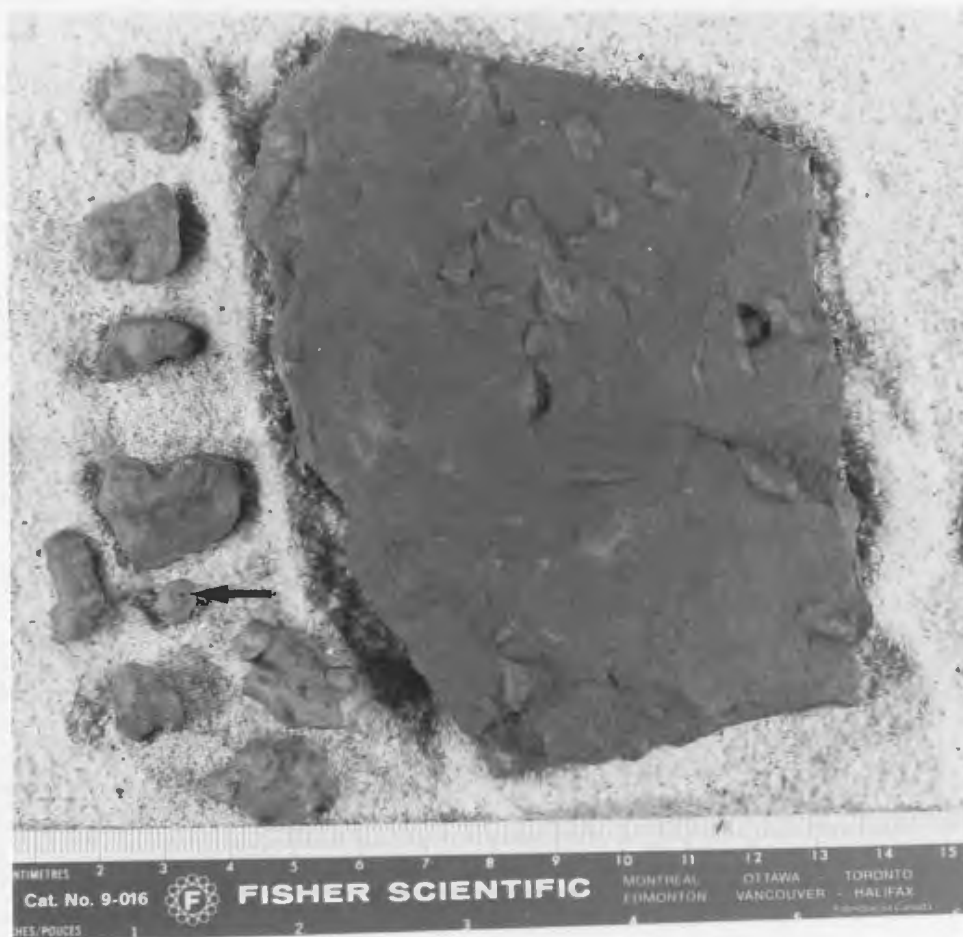


Plate 3.11: Facies H - red-brown mudstone with cylindrical and oblate-shaped calcium carbonate nodules which, in some cases, contain carbonaceous cores (arrow). The nodules are interpreted as rhizocretions (*sensu* Klappa, 1980). Outcrop #1.



Plate 3.12: Facies H - laminated grey and grey-green mudstone. BSG#1, 229.3 m.

are present, although rare in the older exposures and in the FB2-76 core. Facies H accounts for between 1% and 38% of the individual outcrops, 28% of BSG#1, and 7% of FB2-76.

PROCESS INTERPRETATION. The general lack of current-generated structures indicates that sediment comprising facies H was deposited from suspension in quiet water. Fissility may be dependent on the quantities of organic matter (Gersib and McCabe, 1981), or silt, or the intensity of bioturbation (Byers, 1974). The darker grey colour is an indication of the higher organic content of those units (Potter *et al.*, 1980). Carbonaceous laminations represent variations in the proportions of organic and clastic detritus, possibly resulting from seasonal or longer term climatic variations. Calcium carbonate nodules and segregations are generally interpreted as resulting from pedodiagenetic calcite accumulation (Wieder and Yaalon, 1982). The nodules are discussed in detail in Chapter 4.

Facies I: Sapropelic mudstone/oil shale.

DESCRIPTION. This facies consists of dark grey to black (N1 to N3) shales or mudstones with pyrite, calcium carbonate laminae, ostracodes, planispiral gastropods, and rare fish scales (the latter three occur together). Several samples were processed and examined for conodonts, but none were found. The mudstones and shales are laminated to massive, calcareous, and characterized by a brown streak,

low density (1.89-2.55 g/cc; average = 2.33 g/cc; 9 samples), and abundant disseminated organic material. Laminations consist of lighter and darker colour bands related to variations in the amount of calcium carbonate and probably to organic carbon content. The term oil shale refers specifically to rocks which produce oil upon pyrolysis (Macauley, 1984). The field identification of mudstone which contains sapropelic organic matter (defined by Hunt, 1979 as the decomposition and polymerization products of high-lipid organisms, such as spores and planktonic algae, and bacterial bodies) was primarily based upon the lack of identifiable coaly or woody debris.

The fossils were examined by C. Dewey (pers. comm., 1985), who identified the ostracode genera: Carbonita and tentatively Chamishaella. The specimens range between 0.3-1.0 mm in length and are commonly severely crushed. The disarticulated, intact valves are scattered on bedding surfaces. Both genera are notably devoid of ornamentation and have thin walls. The valves are rarely infilled with pyrite. The gastropods were not identified as to genus or species, but are 0.3-1.0 mm in diameter, loosely coiled and, in some cases have a very constricted ornamentation.

Analyses performed for this study indicate that the shales contain a maximum of 31.86% total organic carbon (Table 8.1 in Chapter 8). Extraction of one sample with

organic solvents yielded 700 micrograms of C15+ extractables per gram of organic matter (Table 8.2 in Chapter 8). The oil shales are brown when powdered and will yield up to c. 80 litres of oil/tonne of rock by pyrolysis (Table 8.4 in Chapter 8). Single beds of sapropelic mudstone reach a maximum thickness of approximately 1.5 m (224.5 to 226 m in BSG#1). This facies was only observed at one location in the field (between outcrops 15 and 15a). Oil shales or sapropelic mudstones are found at 257.5 m, 226 m, and 222 m in the BSG#1 core. Oil shales are not present in the FB2-76 core.

PROCESS INTERPRETATION. Abundant preserved organic matter and the lack of current generated structures suggests that facies I was deposited from suspension in a sediment-starved environment. Dark/light laminations probably reflect variations in the supply of organic material and calcium carbonate, caused by variations in water temperature and partial pressure of carbon dioxide. Both factors may have been the result of seasonal climatic variations such as changes in air temperature and precipitation.

The presence of a generally benthonic fauna (gastropods and ostracodes) suggest that reducing conditions were present only below the sediment water interface. However, the presence of undisturbed laminations indicates that

either fauna did not burrow into the sediment or that the the organisms were transported to their depositional site after their death.

Facies J: Coal.

DESCRIPTION. The coals in the Barachois Group are black, blocky, vitreous, in places banded, and have a rank ranging from high to low volatile bituminous (Hayes, 1949). They are composed primarily of vitrain and clarain with minor amounts of fusain and durain (R. Hyde, pers. comm.). The thickest exposed coal is located in the north bank of the Middle Barachois Brook at outcrop 17. It is about 1.0 m thick and becomes increasingly interbedded with grey shale upsection.

Bryan (1938) describes eight coal occurrences within the Barachois Group, six of which were exposed along the Middle Barachois Brook. Those along Middle Barachois Brook are named: Murray, Tom Diamond, Gale's workings, Furlong, Jukes, and Cleary. The Howley Seam is located on Robinson's River; Shear's Seam is located on the Northern Feeder. Three of the seams on the Middle Barachois Brook appear to be presently exposed: Tom Diamond Seam (outcrop 51, 4 m), Murray Seam (outcrop 21, 13 m), and Cleary Seam (outcrop 16, 7 m). Several other thin (1 to 10 cm) dirty coal (or very carbonaceous shale) occurrences were noted in the cores and exposures.

The thickest coal seams consist of up to 57 cm of coal overlain by an additional 60 cm of interbedded coal and shale (Bryan, 1938). A summary of analyses of these seams is provided in Table 3.1. The analyses indicate that the coals vary considerably in quality. Most seams are reported to be fractured and discontinuous due to subsequent tectonic deformation or stratigraphic pinch-out. Core logs provided by Hayes and Johnson (1938) tend to corroborate this conclusion.

PROCESS INTERPRETATION. Coal is the product of peat deposition in quiet shallow water and water-saturated bogs isolated from detrital input. The abundance of clarain and vitrain indicates that woody tissue formed much of the original organic matter (Bustin et al., 1983), although degraded plant remains, spore and pollen exines, and algal material are locally significant. The presence of banding (interbedded clarain and vitrain) signifies a varying depositional environment, possibly the result of water-table fluctuations. Shale beds and sandstone lenses within the coals (Bryan, 1938) and the compositional variability of the coal seams indicate that organic sedimentation was periodically disturbed by influxes of clastic material. High ash (>10%) and high sulfur (>1%) contents may be attributable, in part, to peat formation at pH values close to neutral rather than under highly acidic conditions (cf. Cecil et al., 1985).

Table 3.1

Proximate Analyses of Coals

<u>Seam</u>	<u>Fixed Carbon</u>	<u>Ash</u>	<u>Sulfur</u>	<u>Volatile Matter</u>
a Jukes	57.12%	6.67%	1.95%	36.21%
a Furlong (West of Joe MacKay's Brook)				
Upper 18cm	57.78	4.77	0.95	37.45
Lower 15cm	54.21	14.30	4.32	31.49
a Furlong (East of Joe MacKay's Brook)				
Upper 18cm	55.64	8.78	3.20	35.58
Lower 15cm	47.03	24.32	8.30	28.65
a Murray	54.20	10.26	2.80	35.54
b Cleary	55.23	6.38	3.95	30.90
b Jukes	60.14	4.52	1.96	30.34
b Howley	54.47	10.43	3.05	29.78
b Shears (58.21)		3.16	0.44	33.12
b Cleary	62.16	7.39	---	30.45
b Jukes	57.5	8.00	0.91	34.50
b Howley	61.7	6.9	---	31.70
b Cleary	60.79	6.76	---	32.45
b Howley	63.24	5.56	---	31.20
c Jukes	70.11	1.35	2.70	(29.89)
d Cleary	60.02	7.48	4.11	29.40
d Cleary	57.71	9.20	5.74	30.64
d Cleary	50.61	20.24	7.29	26.78
d Cleary	58.34	8.54	4.31	30.48
d Cleary	54.20	15.01	7.63	28.17
d Cleary	58.05	8.22	3.91	29.41
d Murray (P10)	41.11	37.14	5.39	19.42
d Outcrop 16	49.89	11.83	1.24	28.39
d Outcrop 15	48.59	20.81	7.43	27.43
d Mine Dump	57.31	9.73	2.21	28.84
d BSG220.4m	39.68	31.02	3.85	27.23
d BSG257.0m	23.16	59.09	3.11	15.29

Sources of Data: (a) Baker (1938); (b) Hayes and Johnson (1938); (c) Hayes (1949); (d) Bonnell (1984).

Howley Seam refers to coal seam on Robinson's River (Hayes and Johnson, 1938).

Shears Seam refers to coal seam on Northern Feeder (Hayes and Johnson, 1938).

---: Sulfur not analyzed.

BSG257.0: the ash content denotes a carbonaceous shale.

Facies K: Ostracodal micritic limestone.

DESCRIPTION. Facies K is a dark grey (N4) to olive grey (5Y4/1), micritic, argillaceous, faintly laminated limestone containing abundant, intact articulated and disarticulated, as well as broken thin-walled ostracodes (Plate 3.13). The ostracode valves are 0.5 mm long and disseminated evenly throughout the micrite without preferred orientation. This facies occurs only in outcrop 51 as two 10 cm beds separated by 1.0 meter of dark grey fissile shale, all within a 4.0 m-thick unit of interbedded dark grey shale and micaceous silty shale. A $\delta^{13}\text{C}$ value obtained for the micrite as part of this study is -4.4 per mil. The only carbonate mineral is calcium carbonate (as identified by X-ray diffraction).

Quartz grains with corroded edges are scattered in one thin band several mm's thick. In thin section, the texture of the micrite is uniform to somewhat clotted with traces of structured organic matter present.

PROCESS INTERPRETATION. The micrite may be an inorganic precipitate or may have formed as a result of biological activity. In either case, the presence of limestone indicates an alkaline ($\text{pH} > 7$) geochemical environment, and little detrital input at the time of deposition. Intact, but disarticulated, thin-walled ostracode valves imply lack of strong currents. The

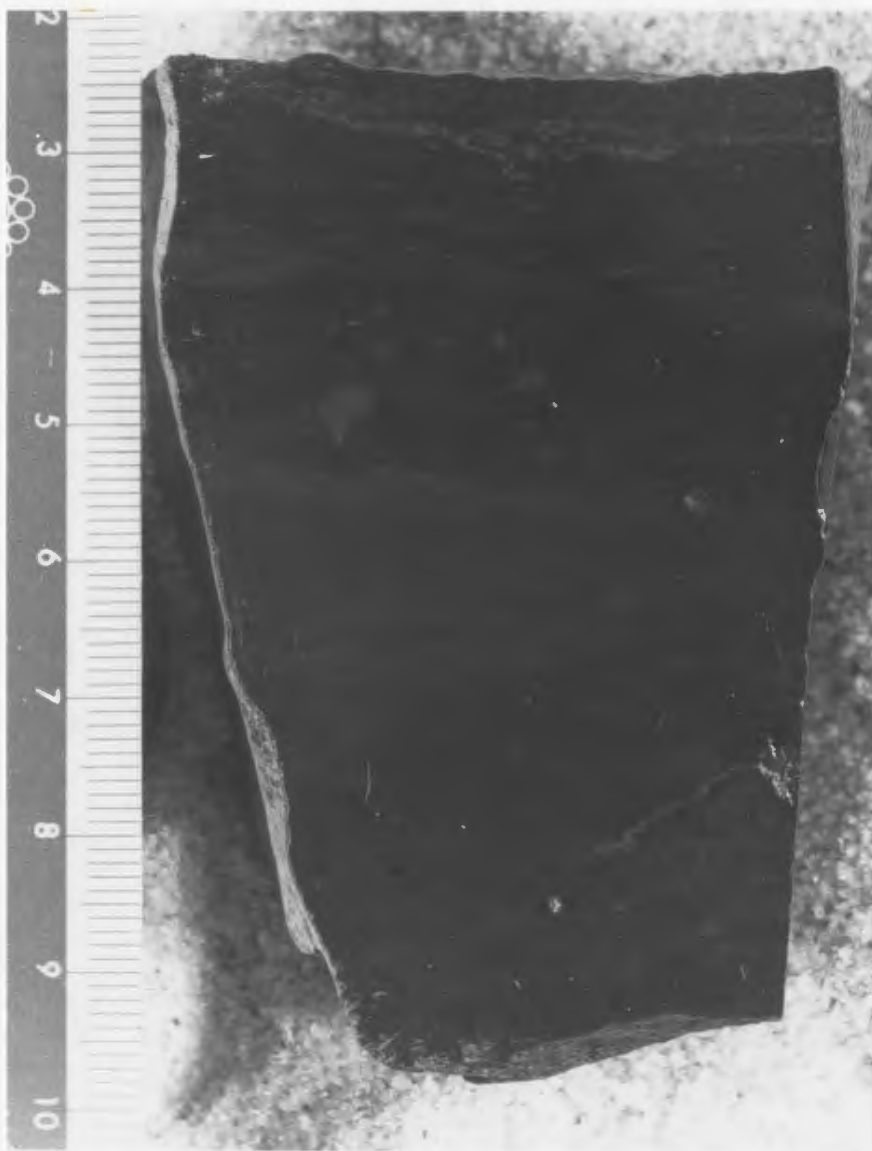


Plate 3.13: Facies K - faintly laminated ostracodal, micritic limestone. Outcrop #51.

ostracodes have not been identified, but they are similar to those identified in the sapropelic mudstones as Carbonita: a fresh water genus.

CHAPTER 4 - FACIES ASSOCIATIONS

Introduction

Facies associations are groups of facies that tend to occur together and which are genetically or environmentally related (Reading, 1978). In the Barachois Group, they fall into two broad categories : the traction-dominated deposits of facies association I; and the mixed suspension and traction deposits of facies associations II and III. Differences in grain size, proportions of facies, colour, and organic content provide the basis for further subdivision into eight subassociations (IA, IB, IIA, IIB, IIC, IIIA, IIIB, and IIIC). The description of each facies association is followed by a genetic interpretation. The legend provided in figure 4.1 contains the symbols which are common to all stratigraphic sections in this and subsequent chapters and in Appendix A.

Facies Association I: Sandstone- and Conglomerate-Dominated Deposits

Facies association I is represented by an assortment of complex multistory and relatively simple single-story sandstone and conglomerate bodies with minor thin mudstone interbeds. This facies association is subdivided into two subassociations: subassociation IA is present in the field

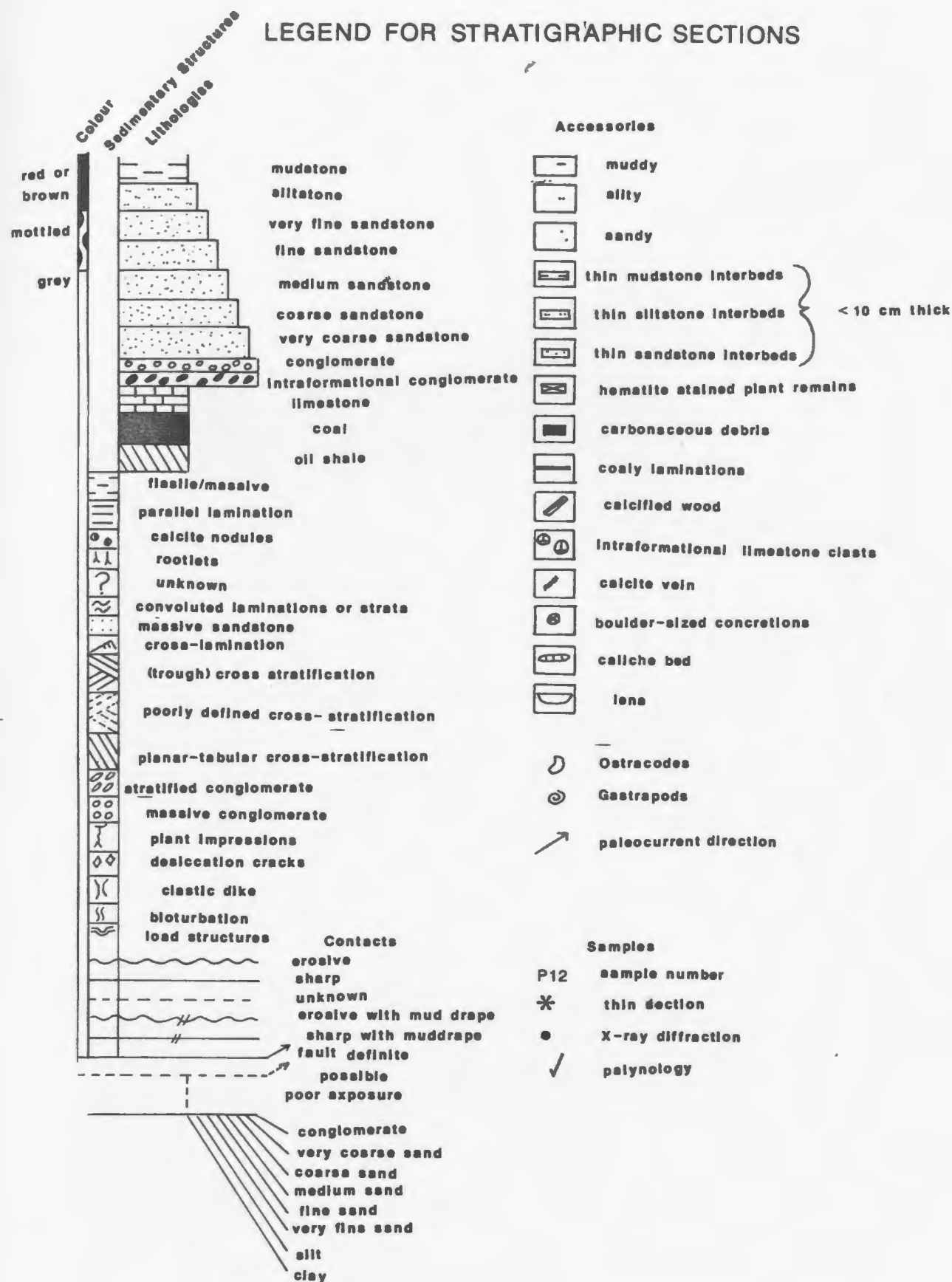


Figure 4.1: Legend for stratigraphic sections.

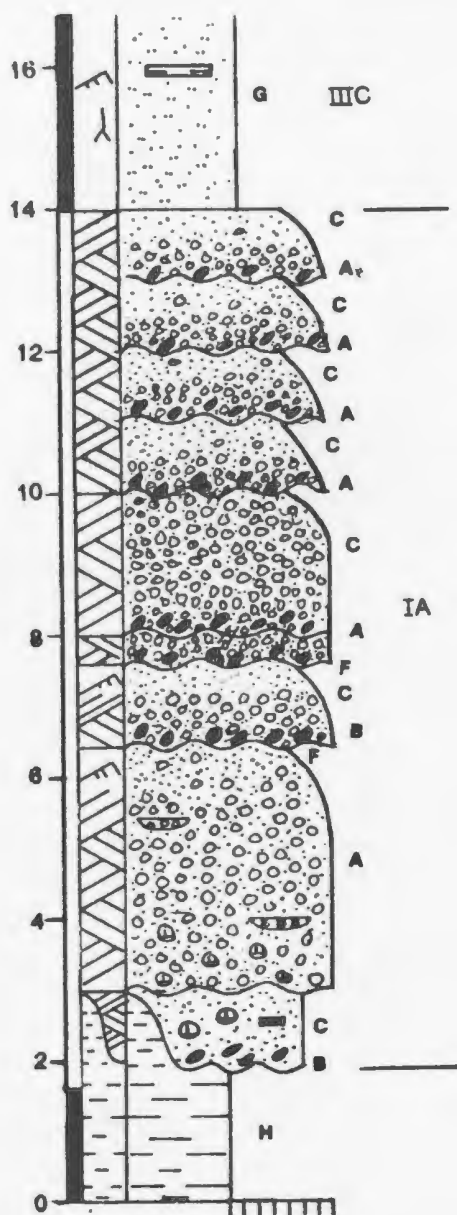
exposures and in the BSG#1 borehole, subassociation IB is present only in the FB2-76 borehole. On geophysical logs in the BSG#1 borehole (Hoffe, 1985), facies association I is recognized by high resistivity, and low spontaneous potential, gamma ray, and density.

Few outcrops were sufficiently well exposed to allow extensive paleocurrent measurements to be taken. For this reason, systematic evaluation of changes in paleocurrent direction between stories in multistory sandstone and conglomerate bodies was not attempted. Where exposures were suitable, paleocurrent measurements were made, predominantly on cross-bed foresets and along trough cross-bed axes (Figure 1.5). Paleocurrents are generally southerly directed from outcrop 38 to outcrop 23 and from outcrop 69 to 75 (along the eastern and western edges of the basinal syncline). Paleocurrents are more variable, but generally northerly and northeasterly directed, at the remainder of the outcrops.

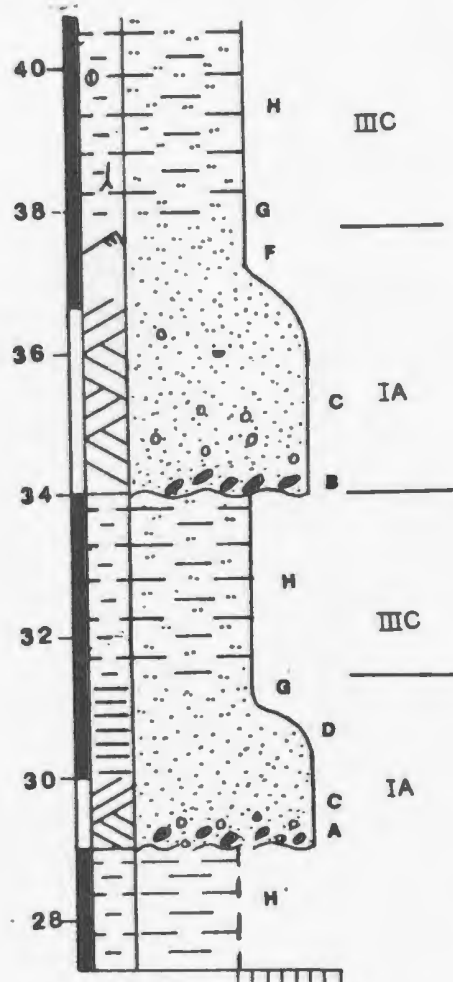
Subassociation IA: Multistory and Single Story

Sandstone Bodies in Outcrops and the BSG#1 Borehole

Subassociation IA consists of multistory (Fig. 4.2A; Plate 4.1) and single-story bodies (Fig. 4.2B; Plate 4.2) which are characterized by an erosive basal contact. Single-story sandstone bodies account for 76% of the occurrences of this subassociation. Massive, stratified, or



4.2A



4.2B

Figure 4.2A: Subassociation IA - multistory channel sandstone and conglomerate comprised of successive fining-upward sequences separated by erosion surfaces or thin mudstone beds.

Figure 4.2B: Subassociation IA - single story channel sandstone with an erosive base overlain by a fining-upward sequence.

Letters represent facies and Roman numerals followed by letters represent facies subassociations.



Plate 4.1: Subassociation IA - multistory channel sandstone, base is at left. Note the irregular, erosive base and the gradational top. See also Figure 4.2A. Outcrop 38.



Plate 4.2: Subassociation IA - single story channel sandstone sequence at outcrop #38. Top to right.

cross-stratified pebble and intraformational conglomerates (facies A and B) and cross-stratified, medium- to coarse-grained sandstone (facies C) overlie the erosive basal surface. Facies A and B may occur within local scours as well. Trough cross-stratification (as in facies C) is the dominant cross-bed type in the sandstone bodies described in the field. Ripple cross-laminated sandstone (facies F) occurs in the upper parts of individual stories, whereas parallel-bedded and structureless sandstones (facies D and E) may occur in the upper and lower parts.

Sequences of sandstone and minor conglomerate facies are separated by erosion surfaces to form stories. In the field sections, the erosion surfaces between stories have centimeter-scale relief and are usually overlain by intraformational conglomerates. The discontinuities are generally of undetermined lateral extent, although occasionally more extensive exposure allows them to be identified as local scours. In areas of restricted exposure, and in cores, stories are defined by sharp or erosive contacts overlain by intraformational and extraformational conglomerates (facies A and B). Within thick sandstone sequences, single and multistory units are commonly separated from each other by 2 to 10 cm thick mudstone layers (facies G and H) with sharp lower contacts and erosive upper contacts. As many as seven successive 2-3 m thick single-story sandstone units can be stacked, with

only several centimeters of mudstone between each unit (outcrops 28-29). Conglomerates and sandstones which overlie the erosion surfaces frequently contain rip-up clasts of the underlying material. Thin lenses of grey mudstone (1 to 5 cm thick) occur within sandstone units, but are not common (e.g. outcrop 41a, outcrop 38 at 5 m).

Individual stories of multistory units invariably fine upward. They vary from about 0.5 m to 5.0 m thick, but are usually less than 4.0 m thick. Single-story sandstone bodies range from 0.75 to 10 m thick but most are 2 to 4 m thick. They are characterized by sharp or erosive basal surfaces overlain by intra- or extraformational conglomerates (rarely more than 0.5 m thick) followed by large scale (trough?) cross-stratified, coarse grained, and pebbly sandstone (facies C). Locally, parallel-laminated sandstone (facies D) is interbedded with, or overlies, facies C. Thin, pebble-rich beds with gradational contacts may occur within facies C. Fine- to medium-grained, single-story sandstone units commonly contain thin (1 to 5 cm) mudstone beds with sharp upper and lower contacts. These mudstone interbeds are most common towards the top of the units. Convolute bedding also occurs near the top of the units. Planar tabular cross-stratification is rare, but it does occur locally. At two locations (outcrop 13/14 at 177 m and 185 m) it overlies scoured surfaces, and forms the basal coarse-grained sandstone unit of meter-scale

fining-upward sequences. At a third location (outcrop 13/14, 106 m), it occurs near the top of a fining-upward sequence in which it is sharply underlain and overlain by ripple cross-laminated sand.

Most single-story units fine upward, although upward fining is not necessarily continuous or gradational. Fining upward can take place by a simple decrease in grain size or a decrease in the amount of extraformational clasts. In outcrop 82, a single story sand body is abruptly overlain by a channel-shaped body of red-brown, massive, very fine-grained sand and silt.

Subassociation IA is almost uniformly drab, grey, or grey-green in colour, but may be more pink or green depending on the mineralogy of the dominant grains. More arkosic units tend to be pinker than quartzose units. Red-brown hematite stained units occur infrequently and are invariably less than 2 m thick (e.g. BSG#1 between 180 m and 210 m).

Subassociation IB: Multistory and Single Story

Sandstone and Conglomerate Bodies in the FB2-76

Borehole

Subassociation IB consists of an erosive base overlain by sequences of grey sandstone (facies C, D, E, and F) and conglomerate (facies A and B). Several 1 to 2 cm thick coals underlain by sandstone (facies C) or conglomerate

(facies A) are also present. Stratified and massive conglomerate facies comprise approximately 50% of the subassociation, however the proportion of sandstone facies increases upward in the core. The apparent abundance of horizontally stratified conglomerates in sections of the core may be a function of the size of sedimentary structures relative to the core diameter: the stratification may, in fact, be part of a cross bed. Similarly, some massive units may actually be stratified on a scale not visible in the core.

Multistory units are comprised of between 2 and 4 individual stories defined by sharp and erosive contacts. Sequences of single and multistory units are commonly separated by 1 to 10 cm thick beds of grey mudstone (facies G and/or facies H). Single-story units account for 65% of the occurrences of subassociation IB. Single stories and individual stories in multistory units may fine or coarsen upward (Fig. 4.3; Plate 4.3). The coarsening-upward sequences are approximately 0.75 m to 2.0 m thick, and they are characterized by an upward gradation from facies C to facies A and sharp upper and lower contacts. Fining-upward sequences typically consist of transitions from massive or horizontally stratified conglomerate to cross-stratified or parallel-laminated sandstone and pebbly sandstone (Fig. 4.4; Plate 4.4). Fining-upward may also be characterized by a gradual reduction in the abundance of pebbles.

FB2-76 519.7 m to 545.3 m: Facies Subassociation IB

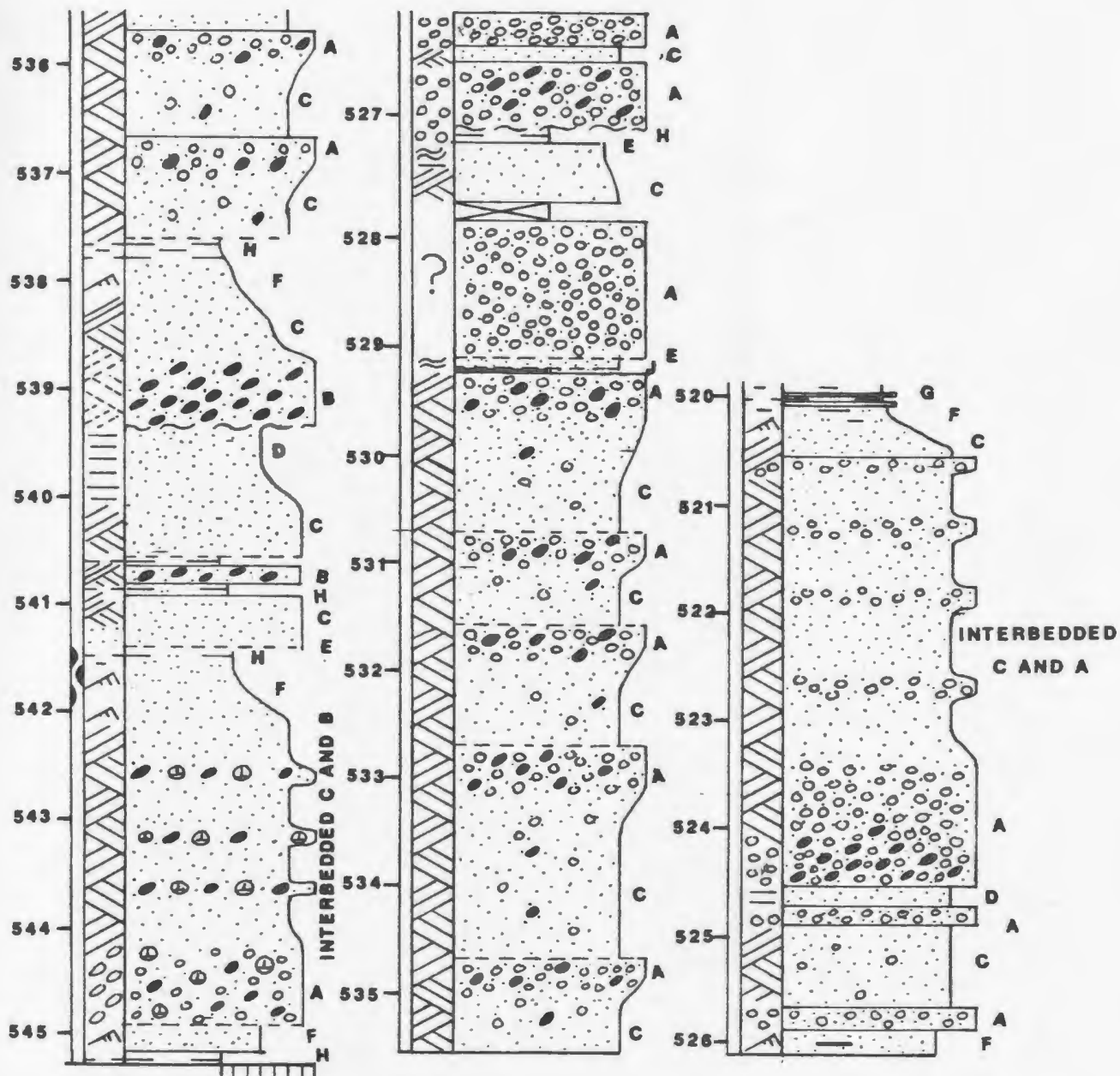


Figure 4.3: Subassociation IB - multistory conglomerate and sandstone channel deposits. FB2-76, 520-545 m. Letters represent facies.



Plate 4.3: Subassociation IB - multistory conglomerate and sandstone channel deposits. FB2-76 737.2 m to 729 m. Base is at lower left, top is at right. Core boxes are 1.5 m long.

FB2-76 601 m to 594.5 m:
Facies Subassociation IB

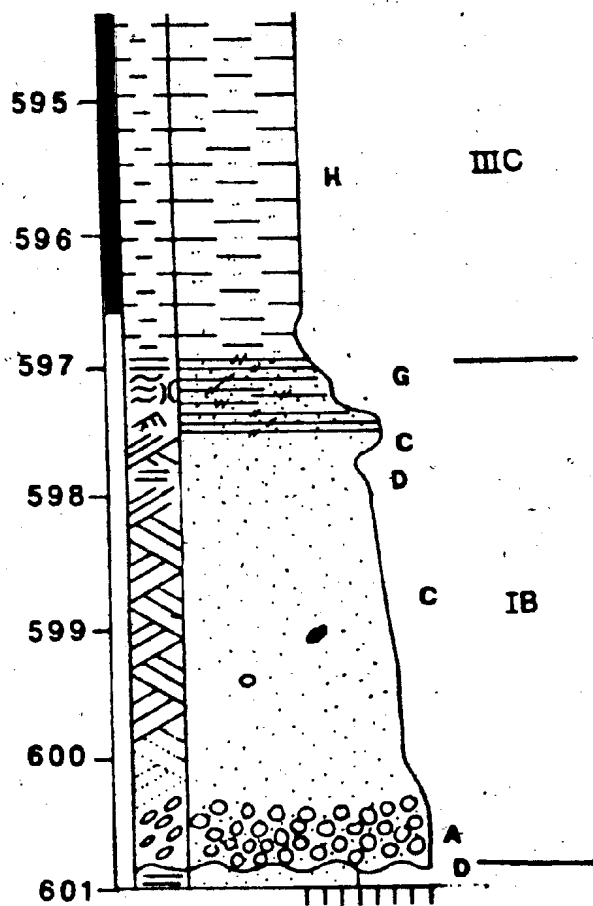


Figure 4.4: Subassociation IB - single story channel sandstone deposits. FB2-76, 601 to 594.5 m. Letters refer to facies; Roman numerals followed by letters refer to subassociations.

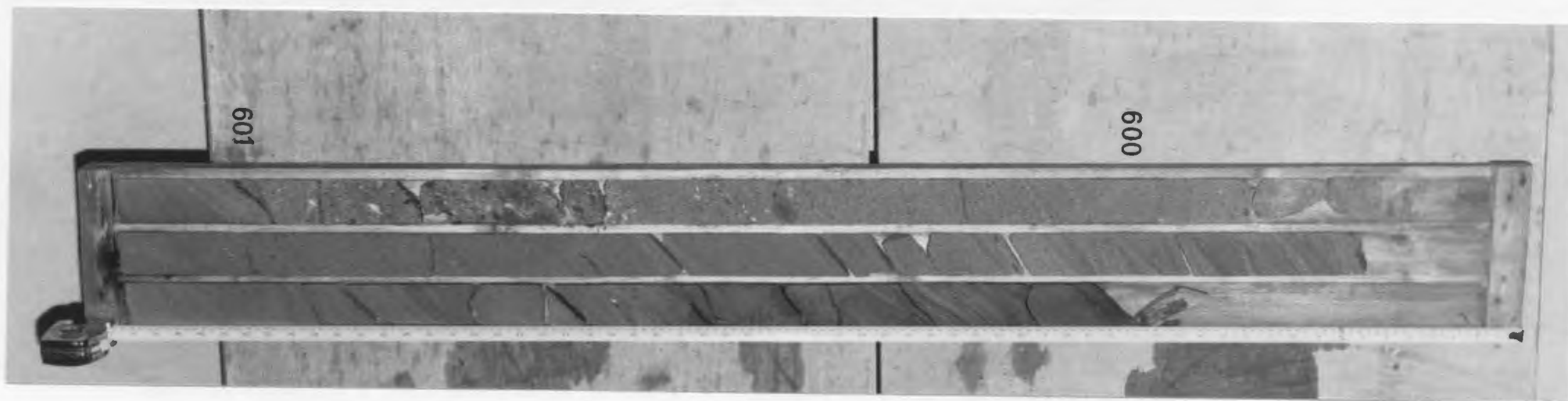


Plate 4.4: Subassociation IB - single story channel sandstone deposits. Basal erosion surface is at lower left, top is at upper right. Core boxes are 1.5 m long. FB2-76, 601 m to 597 m.

Thicknesses of rock units comprising facies in subassociation IB are highly variable. Facies A and C strata range from 0.1 m to more than 5.0 m, but are generally 1 to 3 m thick. Rocks of facies B are rarely more than 20 cm thick, but at 349 m, 4.4 m of facies B strata occurs. Individual stories in multistory units and single story units vary from 0.5 to 7.5 m thick, but most are 1 to 3 m thick. Multistory sand bodies range in thickness from 2 to 10 m. They are separated by finer units (facies associations II and III) which range from several centimeters to 18 m thick. The rocks which comprise subassociation IB are typically grey or grey-green in colour, although, within the interval 340 m to 390 m, several red-brown examples were recorded.

Subassociation IA: Interpretation

Subassociation IA is interpreted as fluvial channel deposits, a conclusion based on the following evidence:

1. channeling is indicated by basal erosion surfaces and sharp banklike contacts with adjacent sediments (the latter are rarely exposed) along with lag deposits consisting of coalified woody debris, intraformational conglomerates, and reworked concretions,
2. the presence of coal, along with paleosols, and locally abundant terrestrial plant impressions, casts, rootlets, and coalified remains in associated deposits,

3. the presence of non-marine ostracodes, gastropods and palynomorphs and the lack of any marine fossils in associated deposits.

In modern fluvial channels, basal lag deposits are overlain by the deposits of channel bars (e.g. point bars, longitudinal bars, transverse bars, diagonal bars, and sandy interbar deposits). The surfaces of active bars are molded into three- and two-dimensional bedforms (megaripples and sandwaves respectively) (e.g. Doeglas, 1962; Williams and Rust, 1969; McGowen and Garner, 1970; Bluck, 1971; Jackson, 1976b; Levey, 1978). The internal structure of the bars is often complex, reflecting a complicated accretionary history. For instance, bars may undergo several cycles of deposition and erosion, they may be actively migrating or stationary, and one bar type may evolve into another type (Reineck and Singh, 1980, p. 262).

Facies A and B (massive and stratified extraformational and intraformational conglomerate) commonly form the basal unit of subassociation IA. They are interpreted as lag or scour pool deposits.

Trough cross-stratified sandstone and conglomerate (facies C and A respectively) overlying the basal lag deposits in the field exposures were probably deposited by three-dimensional megaripples migrating over or between channel bars. Cross-stratified sands formed by the migration of three-dimensional megaripples form the major

part of some point bar sequences (Jackson, 1976a). They are commonly associated with the other types of channel bars, such as side bars (Collinson, 1970) and lateral bars (Bluck, 1974). The uncommon presence of isolated sets of relatively large, planar tabular, cross strata at the top of fining-upward sequences (e.g. outcrop 14 at 106 m) may represent deposits of chute bars (McGowen and Garner, 1970) or scroll bars (Jackson, 1976b). Erosive-based sets of planar cross-strata which form the bases of fining-upward sequences (e.g. outcrop 14 at 177 m) are either the deposits left by the migration of transverse bars, or by the lateral growth of larger bar forms (e.g. side bars, Collinson, 1970).

Parallel-laminated sandstone with parting lineation (as in facies D) interbedded with cross-stratified sandstone indicates episodes of upper and lower flow regime within a single bar deposit. This variation in flow regime is probably due to velocity fluctuations of the flow rather than depth changes. Deposits of interbedded cross-laminated and parallel-laminated fine-grained sandstone occurring in the upper parts of fining-upward sequences suggest shallow and/or waning flows. The sequence of horizontal-stratification overlain by ripple cross-lamination is found on upper bar surfaces in the Rio Grande River (Harms and Fahnestock, 1965). Ripples are found on many bar surfaces during periods of low flow (if

grain size is sufficiently small) and they may be superimposed on larger bedforms (Coleman, 1969; Karcz, 1972).

Drapes and interbeds of massive, laminated and cross-laminated mudstone with sharp contacts indicate abrupt reductions in current velocity. Channel reactivation, as evidenced by partial erosion of the finer grained interbeds and the deposition of coarser sediment, may have been gradual or abrupt. Since the upper contact between fine and coarse sediment is erosive, the total thickness and types of sediments between episodes of channel activity is not known. The presence of scoured surfaces overlain by mudclast-rich units within multistory sandstone suggests that mudstone layers were present and were completely destroyed by channel reactivation. In some cases, the mudclasts were probably derived from the collapse of cohesive river banks. Abrupt changes in current velocity may be caused by the abandonment of channels or segments of channels as a result of 1) chute or neck cut-off; 2) avulsion; 3) rapid channel switching by choking with debris; and 4) periodic floods. The same processes may produce gradual changes in current velocity as well.

The facies sequences observed in subassociation IA are not diagnostic of any one fluvial channel pattern. Upward grain size variations depend on the direction of lateral migration of channel bars with varying texture and the

position of a vertical section on a bar deposit (Bluck, 1971; Jackson, 1976; Bridge, 1985). Fining-upward sequences are common in both single and multistory sandstone units in subassociation IA. Fining-upward sequences are formed by changes in current velocity and depth. In point bar deposits, shear stress (related to mean velocity and depth) varies with position on the bar. As the bar accretes laterally, adjacent facies formed by bed response to the local shear stress will be stacked vertically forming a variety of vertical sequences of which the "fully developed" fining-upward sequence is but one (Jackson, 1975).

Occasional breaks in sedimentation caused by low flow rates, and/or minor erosion produced by floods may be preserved as lateral accretion surfaces (epsilon cross stratification, Allen, 1965). Discontinuities which separate fining-upward sequences in the multistory sandstones of subassociation IA may represent lateral accretion surfaces. However, the critical factor in the recognition of lateral accretion deposits is their lateral extent (on the order of 10's of meters) (Bridge, 1980). In restricted outcrops and cores lateral accretion surfaces cannot be unequivocally differentiated from local or large-scale scours.

Fining-upward sequences are also produced as a result of gradual abandonment of channels (e.g. Coleman, 1969) and lateral accretion of side bars (e.g. Collinson, 1970). The

multistory character of some deposits in subassociation IA may be a result of superposition of channel bars or channel belts due to a combination of aggradation and migration or avulsion (typical of all types of channel patterns), or due to aggradation and rapid channel switching (typical of braided and ephemeral streams).

The grey colour of most rocks which comprise subassociation IA is attributable to the presence of relative reducing conditions within the deposits. The rare red-coloured beds may record regional water table fluctuations (possibly due to climatic change) or instances of local river incisement, which would act to lower the local water table and to promote oxidation.

Subassociation IB: Interpretation

Deposits of subassociation IB are interpreted as non-marine alluvium for the same reasons as subassociation IA, but the abundance of conglomerate shows that there were differences in the grain size of sediment supply and/or flow characteristics of the depositional agent(s). Whereas, in outcrops, the occurrence of basal erosion surfaces with meter-scale relief and the presence of rare visible channel margins suggest deposition in channels, the inability to recognize channel margins in the core further complicates the interpretation of the deposits of subassociation IB due to the possibility that unconfined flow played an important role. Sheetfloods on alluvial fans are high magnitude, low

frequency events which originate on slopes commonly greater than 20 degrees and spread out over relatively flat surfaces (slopes of less than 10 degrees) (Hogg, 1982). Sheetfloods are on the order of 1 m or less in depth and flow velocities may range up to 10 m/s (Hogg, 1982). Clasts 5 to 10 cm in diameter (in the range of those found in subassociation IB) can be transported by flow velocities between 3-6 m/s for flow depths of 1-6 m (Gustavson, 1978). The stable bedform for medium to very coarse sand (the size of the matrix) at those velocities and depths are predominantly upper flow regime plane beds. Although the plane bed is consistent with both a sheetflood or channelized origin, only in modern sheetflood and ephemeral stream environments are they the dominant bedform (e.g. Nilsen, 1982; Tunbridge, 1981; Reading, 1978, p. 18; Ballance, 1984). Intergradation between sheetflood and stream channel deposits is expected due to the fact that depositional surfaces on which sheetfloods are deposited are composed of shallow channels and bars (Walker, 1984 p. 56), and where sheetfloods enter regions of topographic relief on fans or piedmonts they become channelized. In sections of the core where subassociation IB consists of thinly interbedded (beds 1 m thick) massive and stratified conglomerates and parallel-stratified sandstone with minor cross-stratified sandstone (e.g. 658 m to 654 m; 715 m to 710 m) deposition

could be attributable to sheetfloods.

The lack of evidence for debris flow deposits in the conglomerates (e.g. pebble imbrication, the lack of vertically-oriented pebbles, clasts are rounded rather than angular, and the lack of clasts projecting above the beds) tends to mitigate against arid/semi-arid alluvial fan environment of deposition (Nilsen, 1983; Walker, 1984 p. 60). However, in stream-dominated fans of more humid climatic regimes, debris flows tend to be important only in upper (most proximal) fan areas (Gole and Chitale, 1966; Schumm, 1977), so that sections near fan toes may not contain a record of debris-flow activity. It may not be possible to differentiate between the deposits of humid alluvial fans (which are dominated by braided stream deposition) and the deposits of braided streams on alluvial plains. Muddy drapes and thin pebble beds with abrupt contacts probably represent short term discharge fluctuations. Rapid discharge fluctuations, and the coarse bedloads imply a braided origin for the deposits of subassociation IB (Morisawa, 1985 p.106). However, rapid and extreme discharge fluctuations and a coarse bedload also characterize the Nueces River, Texas; a sinuous, single channel river (Gustavson, 1978). Differentiation between coarse-grained point bar deposits and braid bar deposits on the basis of vertical facies sequences alone does not appear to be possible (Bridge, 1985; Jackson, 1978; Miall, 1985).

Coarse-grained point bar deposits are composed primarily of cross-bedded and horizontally-bedded gravel with, in some cases, little or no sandy matrix (Gustavson, 1978).

Vertical sequences in coarse-grained point bars are typified by upward fining from gravel lags to trough cross-stratified and parallel-laminated sandy gravels to cross-laminated, finer sands (Levey, 1978; McGowen and Garner, 1970; Gustavson, 1978). Nonetheless, fining-upward is not a diagnostic criterion of coarse-grained point bars; vertical trends depend on the grain size of the sediment being transported and the location of the vertical section on the point bar (e.g. Jackson, 1976). In some cases, coarse-grained, planar, cross-stratified sands deposited by chute bars occur at the top of the sequence (McGowen and Garner, 1970). Vertical sequences in modern braided deposits have been reviewed by Miall (1977, 1978) and Rust (1978). They are characterized in general by abundant coarse sand and gravel and a variety of facies sequences, some of which are similar to sequences found in the FB2-76 borehole. These include meter-scale fining-upward and coarsening-upward cycles of gravels to cross-stratified sands.

Alternations of facies A and C (conglomerate and cross-stratified sandstone) are the most common transitions which occur in subassociation IB. Fining-upward from facies A to C may reflect waning floods or bar migration and

lateral accretion. Repetitive sequences of upward fining from facies A to C separated by erosion surfaces (i.e. multistory units) could result from rapid channel switching (as in low sinuosity, multiple channel rivers) or variations in aggradation rate and avulsion frequencies (cf. Allen, 1974; 1978; Leeder, 1978; Bridge and Leeder, 1979) overprinted on the deposits of low or high sinuosity, multiple or single channel systems. In the case of sinuous, single channel systems, confinement of channels within restricted belts by downcutting followed by a period of aggradation would tend to create multistory sands and gravels by the downstream migration of meanders (e.g. Nijman and Puigdefabregas, 1978). The upper, finer sections of point bars would be eroded away leaving only the coarse-grained sand and gravel lags and lower point-bar deposits.

Coarsening-upward sequences may represent the migration of the coarser-grained upstream portion (the "head") of a bar over the finer-grained downstream portion (the "tail") (Bluck, 1971; Smith, 1974), gradual reactivation of abandoned channels (Costello and Walker, 1972), the migration of a gravel bar into a sandy scour, or a section through the upstream end of a coarse-grained point bar (Jackson, 1976). Cross-stratified sandstones interbedded with stratified conglomerate may represent sand wedges deposited at lateral margins during falling stages of floods

(Rust, 1972).

The thin coals underlain by sandstone and conglomerate which occur in the cores are interpreted as allochthonous peat mats or pieces of coalified woody debris. This interpretation is based on the lack of a seat-earth or underclay and the presence of coal in contact with coarse clastic material.

Interpretation of Facies Association I: Summary

The deposits of facies association I are interpreted primarily as fluvial channel deposits. In a few cases, deposition from unconfined flows (i.e. sheetfloods) may have been responsible for deposits of subassociation IB. Due to limitations of data collected from restricted outcrops and cores, information by which to reconstruct paleochannel patterns is lacking. River systems were aggrading and channel abandonment occurred gradually in some instances and abruptly in others. Multistory deposits are thicker, coarser and are more common than single-story units in subassociation IB.

Facies Association II: Mixed Sandstone, Siltstone and Mudstone Deposits

Facies association II consists of interbedded mudstones, siltstones, and sandstones. The deposits form

three subassociations: IIA, IIB, and IIC. On geophysical logs run in the BSG#1 borehole (Hoffe, 1985), facies association II is characterized by a spiky appearance on all four logs (resistivity, gamma ray, spontaneous potential, and density).

Subassociation IIA: Stacked Fining-Upward Deposits

Subassociation IIA consists of stacked fining-upward sequences, each of which is 0.5 m to 2.0 m thick (e.g., Fig. 4.5). Total thickness of the stacked units ranges from 2 m to 17 m. Fining-upward sequences have sharp or erosive lower boundaries and gradational upper boundaries. Sequences of facies are variable and include the following transitions:

- 1) facies C to facies F (e.g., BSG#1, 66-68 m);
- 2) facies C to facies G (e.g., outcrop 25);
- 3) facies D to facies G (e.g., outcrop 44);
- 4) facies F to facies G or H (e.g., BSG#1, 83-86 m);
- 5) facies E to facies G (e.g., outcrop 92);
- 6) facies C to facies E (outcrop 52).

The coarsest grain size in the fining-upward units is coarse sand, but most units are comprised of fine- to very fine-grained sandstone and siltstone. Intraformational mudstone clasts may occur just above scour surfaces. Mudstones (facies H) are very thin (1-2 cm) where they are present between fining-upward units. Sedimentary structures

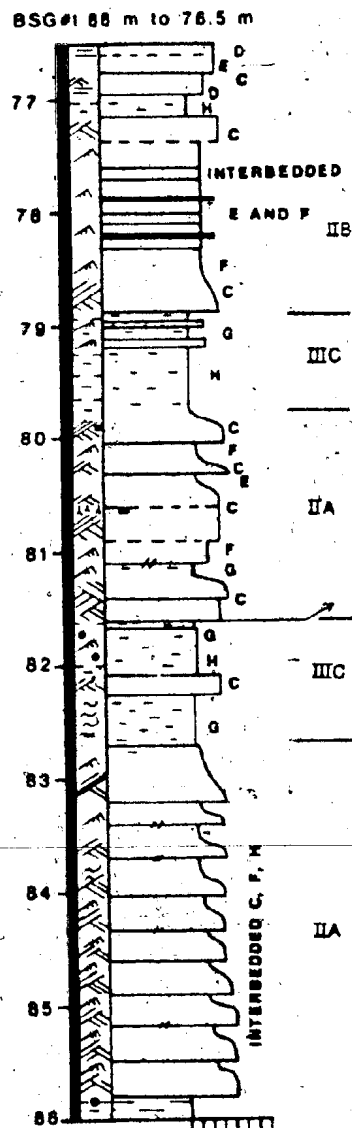


Figure 4.5: Overbank subassociations IIA, IIB, and IIIC denote proximal and distal floodplain environments. Letters refer to facies; Roman numerals followed by letters refer to subassociations.

are dominated by cross lamination, which in some cases exhibit climbing foresets, and parallel lamination. The upper parts of some of the individual fining-upward sequences contain carbonaceous filaments and greenish mottles which probably represent rootlets. Small (<2 cm) calcium-carbonate nodules and calcium-carbonate-cemented horizons are present in some sections. The colours of rocks which comprise subassociation IIA are red, grey or a mottled mixture of the two colours. In all cases, rocks assigned to this subassociation are continuous on the scale of the outcrops examined (meters to tens of meters).

Subassociation IIB: Heterogeneous Deposits

Subassociation IIB consists of a vertically heterogeneous sequence of cross-stratified, structureless, parallel- and cross-laminated sandstone and siltstone (facies C, D, E, and F), and massive to laminated siltstone and mudstone (facies G and H) (e.g. Figs. 4.6 and 4.7). These facies are interbedded on a centimeter to decimeter scale in sequences which range up to tens of meters thick. All types of contacts are present: sharp, erosive, and gradational. Sandstones range from very fine- to coarse-grained and are poorly sorted. Small (millimeter-scale) intraformational clasts and coalified woody debris are commonly present in sandstones. Siltstones and mudstones contain plant casts and

FB2-76 498.8 m to 519 m: Facies Subassociation IIB

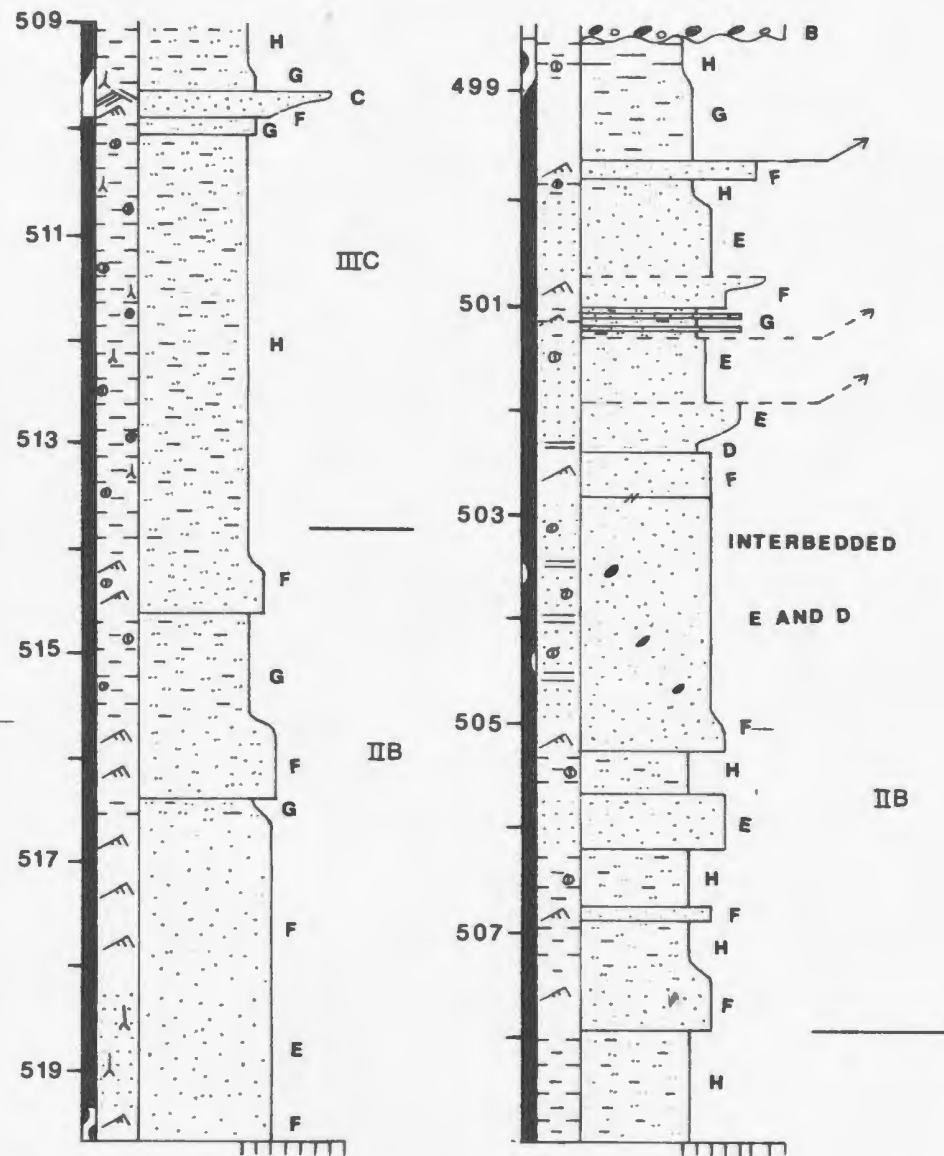


Figure 4.6: Overbank subassociations IIB and IIC denote undifferentiated floodplains and well-drained swamp environments respectively. Letters refer to facies; Roman numerals followed by letters refer to subassociations.

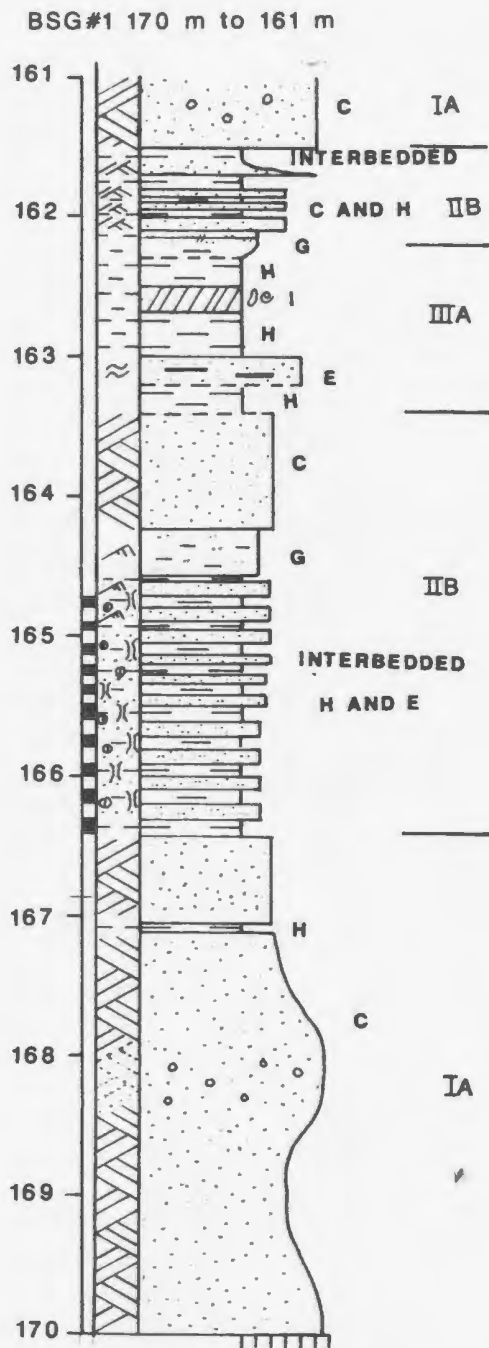


Figure 4.7: Subassociations IA, IIB, and IIIA which represent channel, crevasse splay/levee, and floodplain lake environments respectively. Letters refer to facies; Roman numerals followed by letters refer to subassociations.

impressions, coaly debris, and rootlets (preserved as coaly traces, as green mottles in red-coloured rocks, and as casts) (Plate 4.5). Desiccation cracks are found in some siltstones and mudstones. Simple, unlined burrows (?Planolites) and what may be either feeding traces or burrows (Plate 4.6) are present in some sections (e.g. outcrops 21-25; outcrop 52) within massive to cross-stratified sandstone and mudstone (facies C, E, and G). Load casts and convoluted bedding are present in several intervals (e.g. outcrop 51). Calcium carbonate nodules are locally abundant and generally restricted to the mudstones. However, calcite-cemented concretions (up to 0.5 m in diameter) are present in several sandstone beds (e.g. outcrop 11).

Locally, fining-upward sequences comprised of parallel-laminated, cross-laminated, and/or massive sandstone and siltstone (facies D, F, and G) occur. Fining-upward sequences are 10 cm to 100 cm thick and are similar to those described in subassociation IIA, but differ in that they are separated by decimeter- to meter-thick mudstone or interbedded mudstone/sandstone units. This type of sequence is common in FB2-76 (see Fig. 4.6).

The predominant colour of all lithologies which comprise subassociation IIB is red-brown (occasionally mottled with grey-green) in the FB2-76 borehole and west of outcrop 44 in the field. East of outcrop 44 and in the



Plate 4.5: Calcite root cast oriented vertically just above the pencil (arrow) in grey mudstone (facies H). Root casts (or rhizocretion) are found in facies associations II and III.

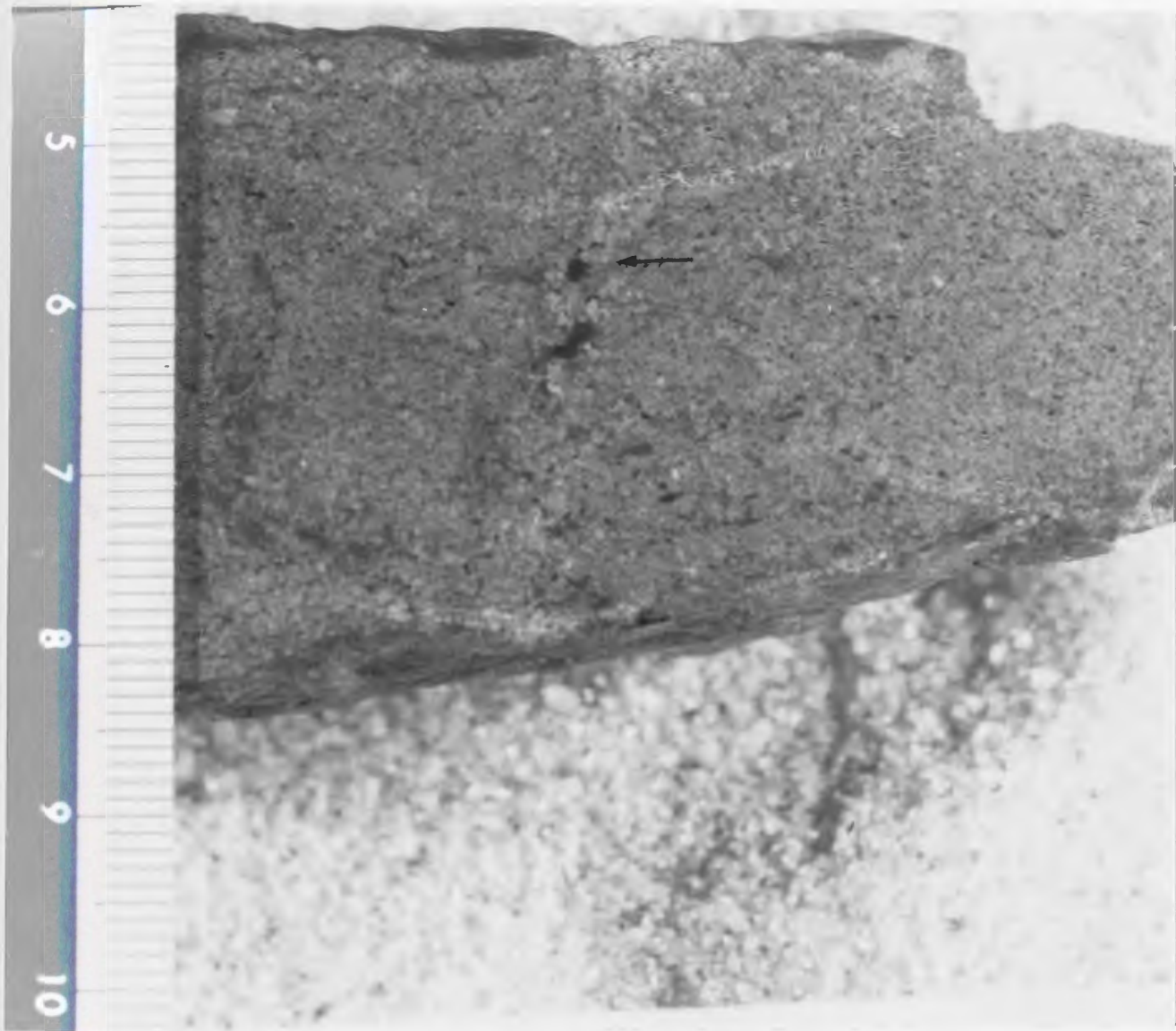


Plate 4.6: A feeding trace or burrow consisting of matrix-free sandstone (arrow) within a massive, dirty sandstone. The section from which the sample is taken consists of thinly interbedded sandstones and mudstones. Outcrop #52.

BSG#1 borehole, the colours are variable and may be grey, red-brown, or mottled.

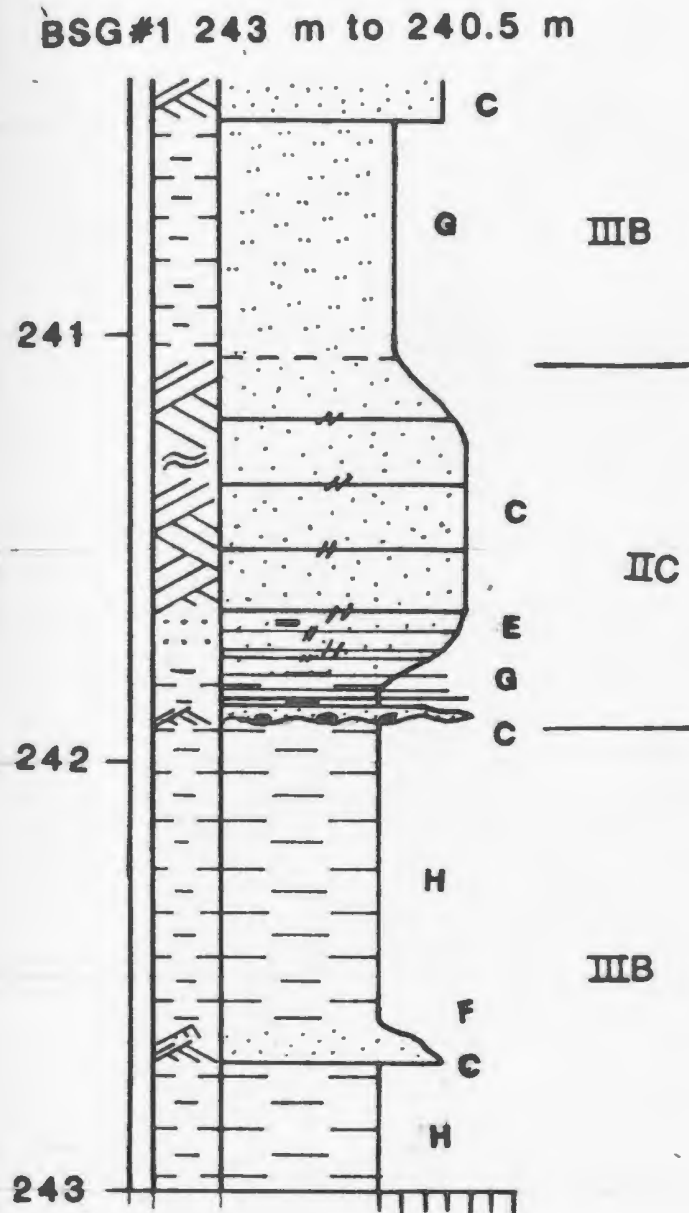
Rocks assigned to subassociation IIB are laterally continuous on the scale of the outcrops measured (meters to 10's of meters), but in some cases they pinch out within 50 m into coarser sands.

Subassociation IIC: Coarsening-Upward Deposits

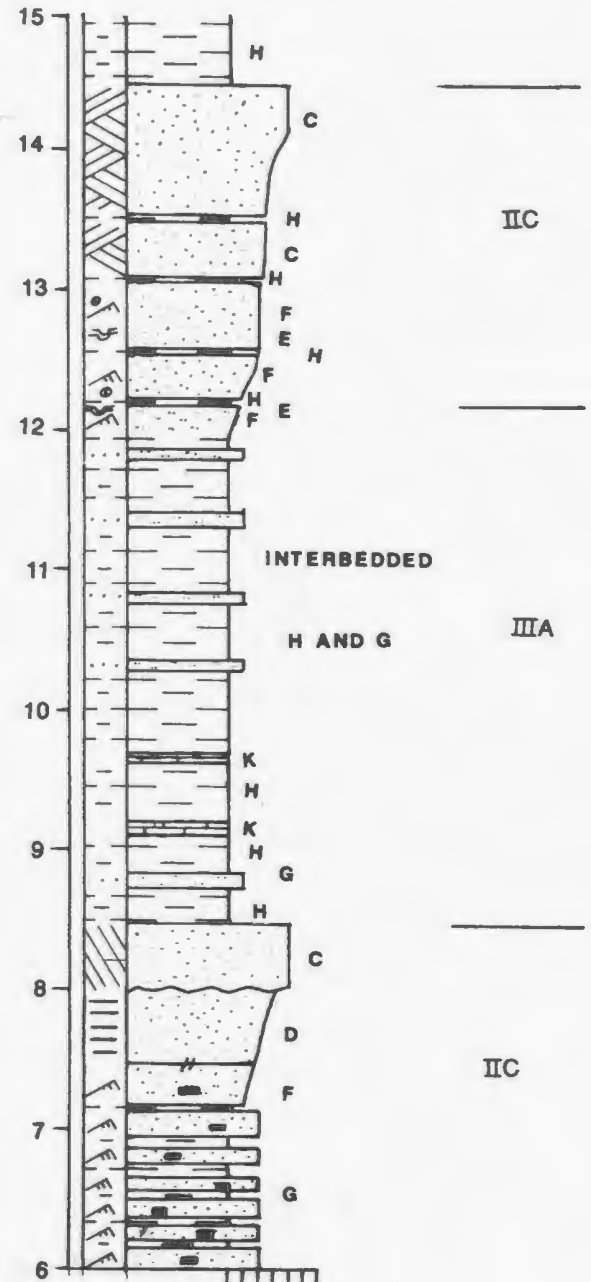
Subassociation IIC consists of a variety of facies types arranged in decimeter-to meter-scale coarsening-upward sequences (Figs. 4.8A and 4.8B). Meter-scale sequences of subassociation IIC range from 2.0 m to c. 10 m thick. Decimeter-scale coarsening-upward sequences may be stacked in units up to 4 m thick.

Stacked, decimeter-scale coarsening-upward sequences (e.g. outcrop 90, 0-3.5 m; outcrop 15, 12-14 m) have gradational bases and sharp tops. The grain size of the coarsest units is fine-grained sand. Most occurrences of decimeter-scale coarsening-upward units consist of the transition from mudstone (facies H) to cross-laminated sandstone or siltstone (facies F). At one location (BSG#1, 60-58 m) massive siltstone and very fine-grained sandstone (facies G) coarsen upward to cross-stratified fine-grained sandstone (facies C).

Meter-scale coarsening-upward sequences typically commence with grey or red (or rarely mixtures of grey and



4.8A



4.8B

Figure 4.8A: Subassociations IIIB and IIC denote poorly-drained swamp and prograding crevasse/levee or delta environments, respectively.

Figure 4.8B: Subassociations IIIA and IIC denote floodplain lake and deltaic environments, respectively.

Letters refer to facies; Roman numerals followed by letters refer to subassociations.

red), cross-laminated and/or parallel-laminated, very fine-grained sandstone or siltstone (facies F, D, and/or G) with climbing ripple cross-lamination and mudstone interbeds. These beds are gradationally overlain by grey or red, cross-stratified, cross-laminated, parallel-laminated, or structureless very fine- to medium-grained sand (facies C, F, D, or E). Small (0.75-2 m thick) channels occur at the top of several meter-scale coarsening-upward sequences (e.g., outcrop 11). Meter-scale coarsening-upward sequences are commonly capped by trough (and in one case planar) cross-stratified sandstones with erosive bases (e.g., outcrop 51b, see Fig. 4.8B).

Calcium carbonate nodules, rootlets, and desiccation cracks are present, but uncommon, in the upper beds of meter-scale sequences and within the decimeter-scale units. Calcium carbonate nodules several centimeters in diameter, load structures, convoluted beds, rare rootlets, and locally important carbonaceous debris are present in the lower beds of meter-scale sequences. Occurrences of facies sequences which comprise subassociation IIC are most common between outcrops 11 and 51 and in the BSG#1 core. Subassociation IIC is not recognized west of outcrop 43 or in the FB2-76 core.

Subassociation IIA: Interpretation

Stacked, meter-scale fining-upward sequences with sharp

or erosive bases overlain by a variety of upper and lower flow regime sedimentary structures resemble the deposits of levees and crevasse channels associated with flooding in modern rivers (e.g. Coleman, 1969; Elliot, 1974; Ray, 1976; Kumar and Singh, 1978). The presence of rootlets and pedogenic calcium carbonate nodules suggest that the environment of deposition was either shallow subaqueous, periodically, or normally subaerially exposed. In some cases, especially where rootlets separate fining-upward sequences, a single sequence is probably attributable to one flood cycle. Although vertical sedimentary sequences present in the fining-upward sequences of subassociation IIA are similar to both levee and crevasse channel sandstones, a crevasse channel origin is favored where the base of each fining-upward unit is scoured (e.g. outcrop 44). Overbank flows which form levees are not channelized and therefore contacts between units tend to be abrupt, but not erosive. Crevasse channels are formed when flood waters leave the main channel through well-defined breaches (crevasse channels) in the river banks. These channels tap deeper regions of the river flow than overbank floods and therefore generally carry coarser material.

In some types of river systems it may not be possible to differentiate between levee and crevasse splay deposits. For instance, levee deposits of the Brahmaputra River are comprised primarily of coalesced crevasse channel fills each

of which consist of decimeter- to meter-scale fining-upward sequences of fine sand and silt (Coleman, 1969). Sedimentary structures found in the Brahmaputra levees include ripple lamination, trough cross-stratification, climbing ripples, and slumping. However, in river systems where overbank flooding is more important than crevassing, crevasse channels are recognized as relatively coarser lenses within the finer levee deposits (Reineck and Singh, 1980 p.292).

In one case (outcrop 51), the stacked fining-upward sequences of subassociation IIA are overlain by an inferred channel sandstone. This sequence may represent coalesced crevasse channel deposits. The crevasse channel progressively carried larger proportions of the river flow until it enlarged (via avulsion) to become a main channel (cf. Bridge, 1985). In some respects, the stacked fining-upward sequences are similar to the deposits which comprise stacked fining-upward sequences in subassociation IA. The differences are primarily ones of scale (e.g. finer grain size and thinner sequences in the deposits of subassociation IIA). It can be difficult to differentiate between the deposits of small streams traversing the floodplains of larger rivers and the deposits of overbank floods of the larger rivers (Collinson, 1978; Bridge, 1985). In some cases, the fining-upward units of subassociation IIA may represent small, ephemeral or perennial streams.

Subassociation IIB: Interpretation

The vertically heterogeneous deposits of interbedded sandstone, siltstone and mudstone of subassociation IIB are interpreted generally as the deposits of levees, crevasse splays and overbank (unchannelized) floods. The lateral relationships between overbank deposits and their areal extent and geometry are critical in differentiating between alluvial environments. This information is often unavailable in restricted outcrops and cores making interpretation of these deposits somewhat equivocal.

Levees are deposited parallel to the river channel by floods which leave the channel by overtopping the river banks. Deposition results from a loss of competence as flows spread out and decelerate. Although deposits generally are coarsest close to the channel, coarse sand and gravel can be carried considerable distances during extreme flood events (e.g. Jahns, 1947). In modern humid climates, levees and floodplains are vegetated and may contain organic debris; in more arid climates flood deposits may contain calcium carbonate concretions (Walker and Cant, 1984).

Levee deposits of modern rivers exhibit a variety of sedimentary structures and textures. The lower Mississippi River levees consist of centimeter- to decimeter-scale fining-upward couplets of ripple laminated sand and silt (Elliott, 1974). Upper Mississippi River levee deposits are

composed of decimeter-scale, coarsening- and fining-upward sequences of cross-laminated, cross-stratified, parallel-laminated, convoluted and massive sands and silts (Ray, 1976). As mentioned previously, levee deposits of the Brahmaputra River (Coleman, 1969), consist of decimeter- to meter-scale fining-upward sequences of fine sand and silt with ripple lamination, trough cross stratification, climbing ripples, and slumping.

Overbank flood deposits consist primarily of fining-upward sequences of fine sands, silts, and muds with a variety of upper and lower flow regime bedforms deposited by episodic, waning currents (Happ et al. 1940; Jahns, 1947; Schumm and Lichty, 1963; McKee et al., 1967). In stable river systems with well-differentiated floodplains the overbank flood deposits progressively fine away from the river banks. However, in actively migrating river systems floodplain deposits are not easily differentiable into discrete environments such as levee or crevasse splay. Deposits of overbank floods from actively migrating river systems are referred to by Allen (1965) as undivided topstratum deposits. In this thesis, they are called undifferentiated overbank deposits. The variety of primary sedimentary structures in levee and overbank flood deposits can be attributed to variations in flow velocity, grain size, concentration of suspended load, and the nature of flow deceleration in a single flood cycle (Bannerjee,

1977).

In the Barachois Group, where the sandstone and mudstone sequences of subassociation IIB overlie the inferred channel deposits of facies association I (e.g., Fig. 4.6, BSG#1, 164.5-166.5 m) they are interpreted as levee deposits similar to those of modern rivers. This interpretation is based on the position within the large-scale sequence, as well as the similarity of scale and sedimentary structures in vertical facies sequences. Where these deposits do not overlie channel deposits they may represent levees which have prograded over the adjacent floodplains, distal parts of crevasse splays, and/or undifferentiated overbank deposits.

Fining-upward sequences and centimeter- to decimeter-scale beds of cross-laminated, parallel-laminated, and massive sand which characterize facies association II in FB2-76 (e.g. Fig. 4.5) and outcrops 38-43 resemble the undifferentiated floodplain deposits of modern, actively migrating rivers. Individual fining-upward unit thicknesses (30 cm to 100 cm) are comparable to thicknesses of modern flood deposits which form in a matter of hours or days (Jahns, 1947; McKee et al., 1967). The gradual change from mudstone-dominated sequences containing cross-laminated, fining-upward sandstones with calcium carbonate nodules to coarser and more abundant sandstone (with parallel lamination) is illustrated in Fig. 4.5. This change may be

due to gradually increasing flow velocities and flood frequencies in subassociation IIB. Increasing flow velocities and flood frequencies could represent progradation of a channel belt complex over the floodplain, or gradually increasing proximity to the source of the floods. In general, subassociation IIB in FB2-76 borehole does not appear to be divisible into crevasse or levee environments.

Fining-upward sequences which contain sedimentary structures typical of undifferentiated floodplain deposits also occur as channel-fill, channel-bar, and overbank deposits in sandy ephemeral stream environments (e.g. Williams, 1971; Picard and High, 1973; Karcz, 1972; Parkash et al., 1983). Bridge et al. (1980) suggest that the similarity between undifferentiated floodplain deposits and ephemeral streams is entirely consistent with the ephemeral nature of overbank flows, although ephemeral stream deposits are commonly associated with aeolian deposits, evaporites, and other deposits of desert or alluvial fan environments (Reineck and Singh, 1980 p. 310). Desiccation cracks and raindrop imprints are common in modern ephemeral stream environments. Desiccation polygons can be centimeters to meters in diameter, therefore they may not be recovered in cored intervals. In addition, thin, desiccated muddy drapes may be obliterated by wind erosion within a week (Karcz, 1972). The presence of coal, evidence of abundant

vegetation (roots, plant fragments), the lack of aeolian deposits, and the general lack of desiccation features seen in exposures of the Barachois Group suggests that ephemeral stream deposition was probably of minor importance. However, where coal and other evidence for extensive vegetation are rare (i.e., in the FB2-76 borehole), ephemeral stream deposition cannot be ruled out.

Subassociation IIC: Interpretation

Coarsening-upward sequences in the Barachois Group were probably formed as floods and splays prograded over floodplains or infilled depressions on the floodplain surface (e.g. abandoned channels and lakes) (cf. Fielding, 1984; Scott, 1978; Farquharson, 1982). As sediment was added to the toes of crevasse splays and levees during floods, or was dumped into lakes, the previously most distal (and therefore finest) sediments are overlain by progressively more proximal sediments. This process probably continued until the crevasse system became inactive, the floodplain depression (or lake) was filled in, or the local channel complex supplying the sediment was abandoned. Differences between decimeter- and meter-scale sequences are probably related more to the location on the floodplains and the depth of the depressions being filled than to differences in the filling mechanisms.

Progradation of splay/delta deposits into dominantly

subaqueous environments is indicated where evidence for subaerial exposure is lacking or where the deposits overlie demonstrably lacustrine sediments (e.g. micrites or oil shales). The drab coloured, meter-scale coarsening-upward sequence with convoluted bedding, which overlies inferred lacustrine marl deposits (Fig. 4.7, outcrop 51, 12-14.5 m), is interpreted as a small mouth bar-type delta which prograded into a lake (as in Elliot, 1974; Coleman, 1966). Where coarsening-upward deposits exhibit evidence for emergence (i.e. desiccation cracks, red colour, pedogenic nodules) they probably represent the progradation of dominantly subaerial crevasse splay and/or levee deposits over floodplains (e.g., outcrop 11, 22-32 m; outcrop 90, 0-3 m) (cf. Gersib and McCabe, 1981). In many cases, definitive evidence for deposition in permanent lakes or for deposition above the mean annual water table is lacking (e.g. Fig. 4.7, 6-8.5 m; BSG#1, 242-241 m).

The laminated and cross-laminated mudstones which form the lower parts of coarsening-upward units were deposited from suspension or by weak currents either in permanent lakes or from ponded floodwaters. Gradual introduction of coarser material with mudstone interbeds records alternations of current activity (floods or crevasse splays) with periods of quiescence. Upper beds of coarsening-upward units contain trough cross-stratification indicative of higher velocity flows (i.e., relatively more proximal to the

sediment source), erosive scours, and evidence of shallow water (rootlets) and emergence (rare desiccation cracks). Small channels and erosive-based cross-stratified sandstones at the top of meter-scale coarsening-upward sequences may represent crevasse channels within prograding levees or fluvial/distributary channels overlying deltas and crevasse splay lobes. Mirror-image coarsening/fining-upward sequences (e.g. Fig. 4.7, BSG#1, 243-240.5 m) could record gradual infill of a depression and subsequent gradual abandonment of the infilling system.

Interpretation of Facies Association II: Summary

The deposits which comprise facies association II are interpreted generally as the overbank deposits of rivers. Subassociation IIA probably represents proximal levee, crevasse channel and crevasse splay deposits. In some cases the stacked fining-upward sequences of subassociation IIA may have been deposited by small streams which traversed the floodplains of larger river systems. Subassociation IIB represents the deposits of levees, possibly crevasse splays and undifferentiated overbank floods. Undifferentiated overbank flood deposits are especially important in the FB2-76 borehole. The sequences which comprise subassociation IIC were probably deposited in prograding crevasse/levee or delta systems.

Facies Association III: Mudstone-Dominated Deposits

Facies association III is similar to and gradational with facies association II. The deposits of both facies associations consist of interbedded mudstone, siltstone, shale, and sandstone. Intervals composed primarily of mudstone, oil shale, coal, and limestone (facies H, I, J, and K) are assigned to facies association III. Facies association III is subdivided into three subassociations (subassociations IIIA, IIIB, and IIIC) based on colour and the amounts and types of organic material present in them. Although subassociations are described as end members, they are, to some extent, gradational. After the three subassociations are described, and interpreted, the implications of calcium carbonate nodules in the subassociations are discussed.

On geophysical logs run in the BSG#1 borehole (Hoffe, 1985), facies association III is characterized by low resistivity response and high gamma ray, density, and spontaneous potential responses. Oil shales which are thick enough to be recorded by the density tool (i.e. 222-226 m) exhibit slightly lower density and higher gamma ray responses than associated shales with less organic matter.

Subassociation IIIA: Grey Mudstone-Dominated Sequences
Including Sapropelic Beds

This subassociation consists of grey to black massive to fissile mudstone (as in facies G and H) interbedded with sapropelic mudstone and oil shale (facies I) (Figs. 4.7 and 4.8B). The organic-rich facies contain a restricted fauna of ostracodes and gastropods with scattered fish scales. Also included in this subassociation are argillaceous ostracodal micrites (facies K). The micrites occur in one section (outcrop 51) as two 10 cm thick beds. Thin (0.5 to 20 cm) interbeds of laminated to massive, graded, or cross-laminated siltstone and very fine- to coarse-grained sandstone (as in facies F and G), in some cases with convolute bedding are present, but uncommon.

Subassociation IIIA attains a maximum thickness of 6 m (e.g. outcrop 51, BSG#1) and ranges down to c. 1 m. The organic-rich beds range from several centimeters to 1.5 m thick. In general, field exposures are too restricted to assess the lateral continuity of the organic-rich members. However, in one location (outcrop 15), a seam of sapropelic mudstone (facies I) (poorly exposed underwater) appears to pinch out into mudstone (facies H) within 50 meters.

Organic-rich members of subassociation IIIA are restricted to locations in the vicinity of the coalfields, and are also found in the BSG#1 borehole.

Subassociation IIIB: Grey Mudstone-Dominated Sequences
With Common Coal or Carbonaceous Beds

Facies types in subassociation IIIB are massive to fissile grey (rarely green) mudstone, carbonaceous mudstone (facies H) and coal beds (facies J) up to 57 cm thick (Fig. 4.9). The mudstones contain calcium-carbonate nodules and segregations (Plate 4.7), Stigmaria and Calamites preserved as impressions (Plate 4.8), coalified plant debris, and calcified and/or coalified rootlets. Calcite- and silica-cemented cross-laminated and massive sand and silt (facies F and G) with coaly debris are present, but not common. Desiccation cracks are not abundant, but were observed at several localities (e.g., Plate 4.8). Coal seams and lenses are present between outcrops 25 and 51. Thin coal beds and laminations within shale and mudstone units are common in the BSG#1 borehole and rare in the FB2-76 borehole. At 257 m in BSG#1, 0.2 m of oil shale directly overlies 5 cm of carbonaceous shale representing a rapid transition from subassociation IIIB to IIIA.

Segregations of calcium carbonate are several mm to 2.0 cm in diameter. The segregations consist of oblate blebs with gradational boundaries in which calcium carbonate has replaced the clay matrix (cf. Wright, 1982). In contrast, nodules (Plate 4.9) have well-defined boundaries with the



Plate 4.7: Closely-packed calcium carbonate nodules in grey mudstone (facies H). The nodules are lighter grey than the surrounding mudstone. The rock hammer is 33 cm long. Outcrop #51b.



Plate 4.8: Grey mudstone (facies H) with desiccation cracks and a 1 m long, curved Stigmarella impression situated below the pencil. The pencil is 19 cm long. Outcrop #11a.

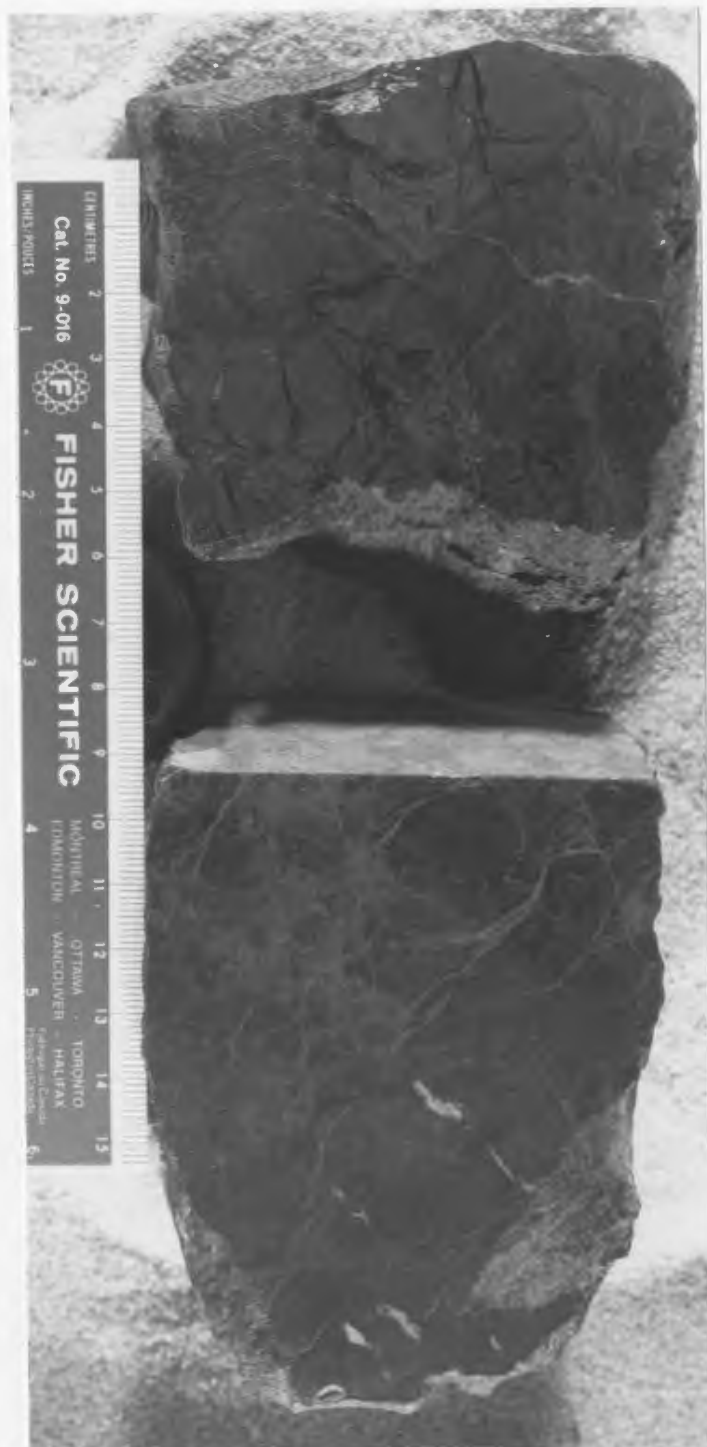


Plate 4.9: Calcium carbonate nodules containing curved spar-filled fractures which define soil peds. The nodule on the right is from outcrop 51; the nodule on the left is from outcrop 78.

Outcrop 16 6 m to 10 m

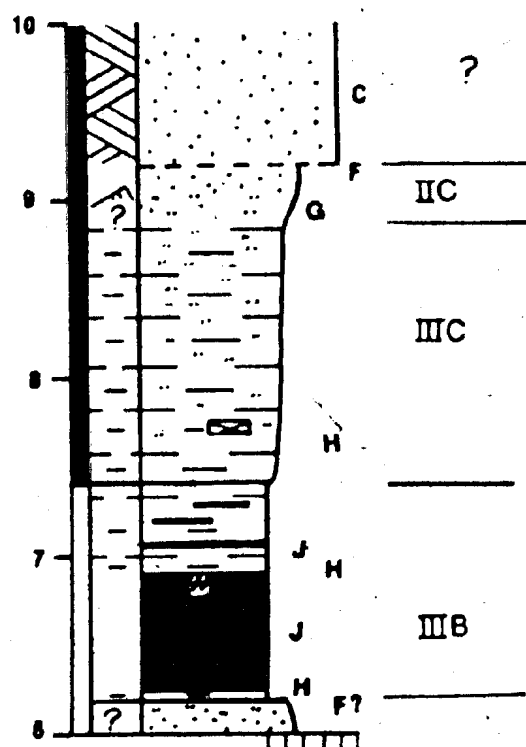


Figure 4.9: Subassociations IIIB, IIIC, and IIC illustrate the probable transition from coal swamp (IIIB) to well-drained swamp (IIIC) and gradual infilling by a prograding crevasse/levee complex (IIC). The cross-stratified sandstone at the top of the section may represent a crevasse channel. Letters denote facies; Roman numerals followed by letters denote subassociations.

surrounding sediment. They are 1 cm to 20 cm in diameter, and contain spar-filled fractures which surround and define areas of dense argillaceous micrite. The micritic zones exhibit a clotted texture and contain coalified plant material and scattered floating, corroded quartz sand grains. Nodules and segregations are commonly widely dispersed; however, in one location (outcrop 51 at 15 m) they are closely packed and protrude downward into grey mudstone (Plate 4.7).

Subassociation IIIC: Red-Brown Mudstone-Dominated Sequences

Subassociation IIIC is distinguished from the other subassociations by its red, red-brown or mottled red-brown and grey colour, and the lack of preserved organic-rich facies (e.g. Figs. 4.2, 4.4, 4.55 and 4.9). The red colour appears to be due to disseminated hematite. The mudstones which comprise the subassociation are mostly silty, micaceous, and massive, and commonly contain abundant calcareous nodules, green, calcareous reduction spots with and without coalified cores, disseminated coaly debris, and the remains of Calamites preserved as hematite coated casts (in the vicinity of coal-bearing units only). Desiccation cracks are rarely observed. Thin (3-20 cm thick) beds of cross-laminated, massive, and cross stratified silt and sand (facies F), occur sporadically. Calcium-carbonate nodules

are generally 1 to 2 cm in diameter and oblate.

Characteristics of nodules are generally the same as those described in subassociation IIIB. The small, oblate nodules appear to bifurcate downward and usually contain a thin core of coaly material (e.g., Plate 3.11).

Rocks of this subassociation ordinarily occur between successive channel sequences, and are commonly truncated by a sharp or erosive surface. Lower boundaries are gradational. Less commonly, subassociation IIIC underlies several coarsening-upward sequences and, in such cases, has a gradational top and a sharp base. It is often poorly exposed and partially covered, but is found in both cores and many of the field sections as well (e.g. outcrops 43, 14, 16, 72, 90). The thickness of subassociation IIIC ranges from about 5 cm to 7 m.

Subassociation IIIA: Interpretation

The lack of desiccation cracks in subassociation IIIA suggests deposition in a subaqueous environment with little subaerial exposure. The presence of a terrestrial aquatic fauna (fish scales, ostracodes and gastropods) strongly suggests a lacustrine depositional environment. The presence of a benthonic fauna and a general lack of pyrite indicate that strongly reducing (i.e. anoxic) conditions were not common at the lake or pond bottom. The presence of calcium carbonate in the form of fossiliferous and calcium

carbonate-rich laminae indicates that pH, as well as calcium and bicarbonate ion concentrations were high enough so that biogenically precipitated calcium carbonate was not dissolved at the site of deposition.

Carbonates similar to the ostracodal micrites of the Barachois Group are found in many pre-Modern and ancient lake deposits (e.g., Sherwood et al., 1984; Flores, 1981). The isotopic composition of the micrite (-4.40 per mil, Table 8.5, Chapter 8, pg.) is consistent with a freshwater origin (Hudson, 1977). In modern lakes endogenic precipitation of calcium carbonate is attributed to high seasonal algal productivity and/or to high concentrations of calcium and bicarbonate ions (Håkanson and Jansson, 1983 p.103). High productivity consumes carbon dioxide, thus reducing its concentration and, in some cases, raises the pH. Both factors lead to enhanced precipitation of calcium carbonate. Since the micrites are only present at one location it is difficult to interpret their origin unequivocally. Their proximity to carbonaceous beds and dark grey colour suggests that organic material was locally abundant. It is possible that concentrations of ions increased locally as lakes or ponds evaporated. However, the lack of desiccation features and evaporites in this subassociation indicate that this is unlikely. The ostracodal micrites may have been formed during occasional interludes of high algal productivity. This explanation is not inconsistent with the presence of oil shales.

Mudstones and shales, which are capable of producing liquid hydrocarbons when pyrolyzed (oil shales) contain kerogens derived predominantly from high lipid organic material such as planktonic algae, spores, and bacterial cell walls (Hunt, 1979). Oil shales are known to occur primarily in three types of deposits: 1) continental lacustrine deposits (e.g. the Green River oil shales), 2) deposits of bogs and small lakes associated with coal swamps (e.g. Permian beds of western Europe, Cenozoic intermontane basins of Thailand), and 3) the deposits of shallow seas (e.g. Miocene shales of California) (Tissot and Welte, 1978 p. 229-230). The relationship between oil shales and coals in the Barachois Group suggests that the oil shales formed in small lakes and bogs close to or within coal swamps.

The facies and facies relationships which characterize Cenozoic oil shales within small intermontane basins of Thailand (Gibling *et al.*, 1985; Gibling *et al.*, 1980) are in some ways similar to those of the oil shales in the Barachois Group. The oil shales in Thailand are dark grey to greyish brown, lean (18 to 122 litres/tonne), slightly fissile, and contain the remains of plants, and fish. As in the Barachois Group, the Thai oil shales are associated with mudstone, massive marlstone, coal, carbonaceous mudstone and calcareous mudstone (with gastropods) and are postulated to have formed in shallow lakes (Gibling *et al.*, 1985). Barachois Group oil shales are relatively lean (<90 l/tonne) and are characterized by somewhat higher densities than the

Thailand oil shales (average densities are 2.33 g/cc for the Barachois Group oil shales vs. 1.95 g/cc for the Thai oil shales).

Subassociation IIIB: Interpretation

The presence of beds of pedogenic calcium carbonate nodules (discussion to follow) and rare examples of desiccation cracks in subassociation IIIB suggest that it was deposited close to (and at times above) the mean annual water table. The relationship between coals and mudstones with Stigmaria and rooted horizons in subassociation IIIB, provides additional evidence for deposition in a higher position relative to the mean annual water table than subassociation IIIA. Banding in the thick coal seam at outcrop 16 suggests that water table fluctuations occurred during peat deposition (Stach et al., 1982 p.376). The gradual increase in clastic material suggests that peat deposition was terminated by drowning as the water table rose or the swamp subsided.

Apparently in situ rootlets and Stigmaria casts in grey, relatively organic-poor mudstones indicate that the depositional region was vegetated, but preservation of organic remains was poor. Vegetation with little organic matter preservation occurs in present-day, well-drained swamps and floodbasins (e.g. Coleman, 1966; Reineck and Singh, 1980). The relative lack of organic matter (compared to poorly drained swamps) is attributed to oxidation during

periods of emergence. Carbonaceous mudstones were formed in locations where organic debris was deposited and preserved along with abundant fine clastic material. Such locations may have been common at the edges of coal swamps where clastic material was filtered out and deposited prior to reaching the swamp. Modern poorly drained swamps (perennially saturated) are characterized by muds which contain abundant pyrite, organic matter, ostracodes and gastropods, and fewer calcium carbonate nodules than the well-drained swamp (Coleman, 1966). The carbonaceous mudstones were likely formed in an environment similar to the poorly drained swamp. Thin beds of cross-laminated silts and sands are common in some modern peat-forming environments (e.g. Styan and Bustin, 1984). Similar thin beds of sandstone and siltstone in subassociation IIIB were probably deposited by distal crevasse splays and/or overbank floods.

In general, humic coal deposits are attributed to deposition in peat swamps in which woody organic material is preserved with little or no clastic input. It has been suggested that depositional environments provided by low-lying swamps are an inappropriate model for deposition of thick, low-ash coals due to the likelihood that abundant clastic detritus would be incorporated with the peat resulting in high-ash coals and carbonaceous shales (McCabe, 1984).

Three alternative explanations for the relatively low

ash content of coals are cited (McCabe, 1984). These are:

1. the chemistry of peat waters resulted in flocculation of clastic material at swamp margins and/or dissolution of clastic material in the swamp;
2. peat formation in floating or raised swamps similar to those now forming in Borneo (Anderson, 1964);
3. clastic supply was cut-off during swamp deposition.

The thickest Barachois coals have variable, but relatively high sulfur values (0.44-8.3%) and generally high to moderate ash contents (1.35-24.3%). Peats of raised swamps are characterized by very low sulfur contents (<0.15%) and well preserved plant tissues as well as low ash content (6.5%) (Stach et al., 1982 p.30). Although high sulfur values in Barachois Group coals could be related to underlying evaporites (M. Gibling, pers. comm.), the relatively high ash contents suggest that deposition took place in low-lying peat swamps cut-off from clastic deposition and/or with highly acid waters which acted to flocculate or dissolve clastic material rather than in raised swamps.

Subassociation IIIC: Interpretation

Rare desiccation cracks, red-brown colour caused by iron oxides, pedogenic calcium carbonate nodules, and a relative lack of organic matter indicate that subassociation

IIIC was deposited under generally oxidizing conditions in an environment which was periodically submerged. The environment was vegetated as evidenced by rhizcretions and root traces. Recent floodbasins are characterized by alternating periods of emergence and submergence (Allen, 1965; Reineck and Singh, 1980 p. 296) due to overbank flooding. Deposition of suspended sediments occurs from ponded flood waters. Thin beds of cross-laminated siltstone and sandstone were probably deposited by distal crevasse splays and/or overbank floods.

Soils developed on floodbasin sediments in semi-arid conditions (i.e. under relatively oxidizing conditions) typically are reddish in colour, contain only small amounts of organic matter, and often contain pedogenic calcium carbonate nodules (caliche) (Reineck and Singh, 1980 p. 297). In some cases, where evidence of subaerial exposure is lacking (e.g. BSG#1 309-322 m), subassociation IIIC could represent deposition in small, but perennial and well-aerated lakes.

Implications of Calcium Carbonate Nodules

As discussed in the descriptions, the nodules in subassociations IIIB and IIIC are comprised of spar-filled fractures which delimit zones of argillaceous micrite with clotted texture, and which contains carbonaceous debris and floating and corroded sand grains. These characteristics

are indications of pedogenic formation (Brewer, 1964; Goudie, 1983 p. 106-107). The spar-filled fractures were probably formed by repeated wetting and drying of the sediment (Brewer, 1964). Closely packed nodules up to 5 cm in diameter resemble stage II or III caliches of Gile et al. (1966) and type A or B of Allen (1974).

Calcium carbonate segregations (gradational boundaries with the matrix) are present in subassociations IIIA and IIIB. Freytet and Plaziat (1982, p.76) draw a distinction between carbonate concentrations developed on well-drained soils (which they refer to as caliches) and hydromorphic segregations formed in the zone of water table fluctuations. It seems likely that gradations between, and mixing of the two types of carbonate segregations occur as well-drained horizons subside below the water table. This would lead to the occurrence of similar nodule types in dissimilar environments.

X-ray diffraction results on powders from six nodules (F80, F71, F77, F72, F21, F12) show that calcite is the only carbonate species present. Quartz, feldspar, and clay minerals are present in varying amounts. Stable carbon isotope determinations for the nodules range from $\delta^{13}\text{C}$ values of -7.973 to -20.552 per mil relative to PDB (refer to Table 8.5 for a summary of the values). These values are consistent with carbon isotopic compositions determined for soil calcites and diagenetic concretions (Hudson, 1977;

Salomons et al., 1978) and contrast with the more positive value of the lacustrine micrite (-4.40 per mil).

The formation of calcium carbonate nodules as caliches is a process in which calcium-carbonate is transported in solution from upper layers of a soil profile and redeposited at a lower level. The degree of calichification is dependent upon sedimentation rate, depth and range of water table fluctuation, climate, availability of calcium and bicarbonate ions and the partial pressure of carbon dioxide. Klappa (in press) emphasizes the interaction between climate, calcium carbonate supply, permeability of substrate, and biological activity in the formation of caliche. Variations in nodule size, abundance and degree of segregation from the matrix result from the interplay between these processes. Recent work suggests that decreases in partial pressure of carbon dioxide due to seasonal drought and transpiration through roots may play a significant role in the precipitation of pedogenic calcium carbonate (Schlesinger, 1985). The 1-2 cm oblate-shaped nodules with coaly cores found in subassociation IIIC strongly suggest that roots played a part in their formation. According to Klappa (1980) these nodules would be classified as rhizcretions; a term used to describe pedogenic accumulations around live or dead roots.

An analysis of the micromorphology of nodules by Wieder and Yaalon (1982) has led to a model for the formation of carbonate nodules in a variety of substrates. Their model

for nodule formation within muddy non-calcareous soil materials (as in facies association III) is divided into three stages. In stage one the nodules form within soil voids and do not include skeletal particles. As carbonate precipitation continues the nodules begin to include grains from the surrounding fabric and blocky peds are well-defined (stage two). Precipitation occurs within the larger interpedal voids. Pedoturbation (churning of the soil by soil biota and by repeated wetting and drying; Jongerius, 1970) results in repeated dissolution and reprecipitation with increased incorporation and replacement of clays. Total recrystallization of the nodule (stage three) is the end result of these processes. In this model nodule formation can occur without significant biogenic influence. Nodules occurring around live roots (rhizomorphs in the terminology of Wieder and Yaalon, 1982; rhizodcretions of Klappa, 1980) are generally micritic due to rapid precipitation of calcium carbonate as soil water evaporates, thus reducing the high partial pressure of carbon dioxide in the immediate vicinity of roots.

In light of this model as well as more generalized models of caliche formation, the nodules and segregations formed in the Barachois Group are of probable pedogenic origin. Modern climates in which nodules are common are often described as warm, with limited precipitation (400-600 mm/yr.) (e.g. Goudie, 1983, p.93). However, van de Poll (1983) argues that the presence of calcium carbonate

concretions in Carboniferous rocks may be less a climatic indicator than a reflection of the probable concentration of flora in swampy lowlands and a consequent lack of vegetative cover in the better-drained uplands (van de Poll, 1983).

The formation of calcium carbonate concretions would therefore be a result of high evaporation rates and low partial pressures in poorly vegetated soils rather than an indication of arid or semi-arid climate (van de Poll, 1983). This suggests that caution should be exercised in the use of caliche as a paleoclimatic indicator.

Interpretation Of Facies Association III: Summary

The deposits which comprise facies association III are dominated by mudstones and shales, and contain most of the organic-rich facies found in the Zaracho Group. Calcium carbonate nodules found in this facies association are generally attributed to pedogenic processes with some biogenic input. Modern environments in which similar nodules are found are often described as warm, with limited precipitation (Goudie, 1983 p. 93), however, it may not be possible to extrapolate modern climatic conditions of nodule formation back to Carboniferous time. Subassociation IIIA contains oil shales and thin limestone beds and is attributed to deposition in perennial lakes. Subassociation IIIB records deposition in poorly-drained and well-drained swamps in which carbonaceous muds and peats were deposited. Fluctuations of the water table in swamps were probably

common. Subassociation IIIC represents sediments which were deposited from ponded floodwaters on relatively well-drained parts of the floodplains. Organic material which was probably present in these localities was oxidized and destroyed. Thin beds of coarser material deposited along with the mudstones record high-magnitude overbank flood deposits and distal crevasse splay deposits.

CHAPTER 5 - MARKOV CHAIN ANALYSIS

Background

Sequences in the two boreholes were tested for the presence or absence of cyclicity ("memory") using Markov chain analysis and a chi-squared test (Miall, 1973; Harper, 1984). Outcrop sequences were too short or poorly exposed and therefore were not statistically analysed. Markov chain analysis compares the number of observed upward transitions between facies (the observed transition matrix) to a matrix of expected transitions. Calculation of the expected transition matrix is based on the assumption that facies states are mutually independent (i.e. that any facies has an equal probability of passing upward to any other facies). It is also assumed that no facies can pass upwards to itself. Since this violates the principle of independence between facies, a model of quasi-independence between successive facies states is required and the expected values matrix must therefore be calculated using iterative proportional fitting (Carr, 1982; Powers and Easterling, 1982).

The statistic used to test the hypothesis of quasi-independence has a chi-squared distribution. The test statistic is calculated by adding the quotients of the square of the difference between the observed value and the expected value divided by the expected value of each cell in

the observed transition matrix. Deviations from the hypothesis of quasi-independence are ascertained by comparison with values from tables of the chi-squared distribution. The larger the calculated chi-squared statistic (for a given degree of freedom), the stronger the evidence against the hypothesis of quasi-independence (Powers and Easterling, 1982).

Further analysis of the Markov property involves the recognition of the outliers (preferred transitions) which are responsible for the non-random behavior. Since the normalized differences between the observed and expected matrices are approximately normally distributed, outlier recognition may be performed by choosing a level of significance and extracting transitions which exceed that level of significance (Powers and Easterling, 1982). However, this method of outlier recognition may declare either too many or too few outliers, especially if one very large anomaly is present (Bradru and Hawkins, 1982; Harper, 1984). Other methods of outlier detection include a multi-step technique in which extreme normalized differences are removed from the matrix one at a time until the chi-squared statistic indicates that the matrix is random (Carr, 1982). This method is highly susceptible to "masking errors" in which fewer outliers are declared than actually exist (Harper, 1984). Outlier recognition using median tetrads and half normal plots (Bradru and Hawkins, 1982) is suggested by Harper (1984) as a supplement to the techniques

cited above.

For the borehole sequences in the Barachois Group, using the observed transition matrices were tallied, and the expected transition matrices, difference matrices, and normalized difference matrices were calculated using a BASIC program written for this study (see Appendix B). The test-statistic was calculated using a standard equation (Powers and Easterling, 1982; Billingsley, 1961, p.17; Gingerich, 1969, p. 339). The observed, expected and normalized difference matrices are illustrated in Tables 5.1 and 5.2).

Results and Interpretation: BSG#1

The BSG 1 borehole sequence is statistically non-random at the 99% level of significance. The value of the test-statistic is 146.4 with 71 degrees of freedom, which exceeds the chi-squared statistic from statistical tables (118.6 with 75 degrees of freedom) at that level of significance. Positive (i.e. upward) transitions with normalized differences which are greater than 1.645 (i.e. exceed the 90% level of significance) are from facies: J to I, A to C, B to D, B to A, C to A, I to E, H to B, H to J. Of these eight transitions, four (J to I, B to A, B to D, I to E) occur fewer than three times in the section and the one with the largest normalized difference (J to I) (and hence the largest contributor to the chi-squared statistic) occurs only once. These significant, but infrequent, facies

Table 5.1: Markov Chain Analysis - BSG#1

Observed Transitions Matrix

Facies	A	B	C	D	E	F	G	H	I	J
A	0	0	11	0	0	0	0	1	0	0
B	1	0	2	1	0	0	0	1	0	0
C	7	0	0	4	14	16	17	48	0	0
D	0	0	4	0	30	0	0	11	0	0
E	0	0	7	2	0	2	6	19	1	0
F	1	0	11	0	1	0	10	27	0	0
G	0	0	21	0	4	7	0	27	0	0
H	3	5	49	3	16	26	23	0	3	3
I	0	0	0	0	2	0	0	3	0	0
J	0	0	0	0	0	0	0	2	1	0

Expected Transitions Matrix

Facies	A	B	C	D	E	F	G	H	I	J
A	0.0	0.1	3.1	0.2	0.9	1.2	1.4	4.9	0.1	0.1
B	0.1	0.0	1.3	0.1	0.4	0.5	0.6	2.0	0.0	0.0
C	3.1	1.3	0.0	2.6	10.8	14.2	15.9	56.6	1.3	0.8
D	0.4	0.2	4.6	0.0	1.4	1.8	2.1	7.3	0.2	0.1
E	0.9	0.4	10.0	0.7	0.0	4.0	4.5	16.0	0.4	0.2
F	1.2	0.5	13.8	1.0	4.2	0.0	6.3	22.2	0.5	0.3
G	1.4	0.6	16.5	1.2	5.1	6.7	0.0	26.6	0.6	0.4
H	4.7	1.9	53.7	4.0	16.5	21.1	24.3	0.0	1.9	1.2
I	0.1	0.0	1.3	0.1	0.4	0.5	0.6	2.0	0.0	0.0
J	0.1	0.0	0.8	0.1	0.2	0.3	0.3	1.2	0.0	0.0

Normalized Difference Matrix

Facies	A	B	C	D	E	F	G	H	I	J
A	0.0	-0.3	<u>4.6</u>	-0.4	-1.0	-1.1	-1.2	-1.8	-0.3	-0.3
B	<u>2.7</u>	0.0	<u>0.7</u>	<u>3.0</u>	-0.6	-0.7	-0.8	-0.7	-0.2	-0.1
C	<u>2.2</u>	-1.1	0.0	<u>0.9</u>	1.0	0.5	0.3	-1.1	-1.1	-0.9
D	-0.6	-0.4	-0.3	0.0	1.4	-1.4	-1.4	1.4	-0.4	-0.3
E	-0.9	-0.6	-0.9	1.5	0.0	-1.0	0.7	0.7	-1.1	-0.5
F	-0.2	-0.7	-0.8	-1.0	-1.6	0.0	1.5	1.0	-0.1	-0.5
G	-1.2	-0.8	1.1	-1.1	-0.5	0.1	0.0	0.1	-0.8	-0.6
H	-0.8	<u>2.2</u>	-0.7	-0.5	-0.1	0.9	-0.3	0.0	0.8	1.7
I	-0.3	-0.2	-1.1	-0.3	<u>2.6</u>	-0.7	-0.8	0.7	0.0	-0.2
J	-0.3	-0.2	-0.9	-0.2	-0.5	-0.6	-0.6	0.7	<u>5.9</u>	0.0

Underlined normalized differences are significant at the 90% level. A=conglomerate; B=mudclast conglomerate; C=X-stratified sandstone; D=parallel-laminated sandstone; E=structureless/convoluted sandstone; F=X-laminated sandstone; G=interbedded sandstone, siltstone, and mudstone; H=mudstone; I=sapropelic mudstone/oil shale; J=coal; K=limestone.

Table 5.2: Markov Chain Analysis - FB2-76

Observed Transitions Matrix

Facies	A	B	C	D	E	F	G	H	J
A	0	7	66	13	7	9	9	27	2
B	11	0	13	1	3	0	0	2	1
C	62	11	0	6	7	11	27	16	0
D	7	1	3	0	3	3	8	6	0
E	9	2	5	0	0	2	5	6	0
F	4	2	2	1	1	0	22	3	0
G	17	5	27	5	3	7	0	24	0
H	19	3	21	7	6	8	19	0	0
J	2	0	1	0	0	0	0	0	0

Expected Transitions Matrix

Facies	A	B	C	D	E	F	G	H	J
A	0.0	8.2	47.6	8.7	7.9	8.8	26.5	24.4	0.8
B	8.1	0.0	8.8	1.6	1.4	1.6	4.9	4.5	0.1
C	47.6	8.8	0.0	9.4	8.5	9.5	28.7	26.4	0.8
D	8.1	1.5	8.8	0.0	1.5	1.6	4.9	4.5	0.1
E	7.5	1.4	8.2	1.5	0.0	1.5	4.6	4.2	0.1
F	9.2	1.7	9.9	1.8	1.6	0.0	5.5	5.1	0.2
G	25.7	4.8	27.8	5.1	4.6	5.1	0.0	14.3	0.4
H	23.9	4.4	25.9	4.7	4.3	4.8	14.4	0.0	0.4
J	0.7	0.1	0.8	0.1	0.1	0.1	0.5	0.4	0.0

Normalized Difference Matrix

Facies	A	B	C	D	E	F	G	H	J
A	0.0	-0.4	<u>2.7</u>	1.5	-0.3	-2.3	-3.4	0.5	1.4
B	1.0	0.0	<u>1.4</u>	-0.4	1.3	-1.3	-2.2	-1.2	<u>2.3</u>
C	<u>2.1</u>	0.7	0.0	-1.4	-0.5	0.5	-0.3	-2.0	-0.9
D	-0.4	-0.4	-2.0	0.0	0.3	1.1	1.4	0.7	-0.4
E	0.5	0.5	-1.1	-1.2	0.0	0.4	0.2	0.9	-0.4
F	-1.7	0.2	-2.5	-0.6	-0.5	0.0	<u>7.0</u>	-0.9	-0.4
G	-1.7	0.1	-0.2	0.0	-0.8	0.8	0.0	<u>2.6</u>	-0.7
H	-1.0	-0.7	-1.0	1.0	0.8	1.5	1.2	0.0	-0.6
J	1.4	-0.4	0.2	-0.4	-0.4	-0.4	-0.7	-0.6	0.0

Underlined normalized differences are significant at the 90% level.

Facies I does not occur in the FB2-76 borehole.

transitions probably represent rare events on the alluvial surface which are not necessarily important in evaluating normal sedimentary relationships. The remaining four transitions may provide some insight into facies relationships occurring in the BSG#1 sequences. For instance, the reciprocal transitions from C to A and A to C represent transitions between the major constituents of facies association I (the channel sequences). The transition from facies H to B records the relationship between intraformational conglomerates (facies B) and the mudstone (facies H) from which they are derived. The transitions from facies H to J indicate that coal invariably overlies mudstone.

Results and Interpretation: FB2-76

The test-statistic for the FB2-76 borehole is 155 with 55 degrees of freedom, which exceeds the chi-squared statistic from statistical tables at the 99% level of significance. Upward transitions which exceed 1.645 are from facies: A to C, C to A, B to J, F to A, F to G, and G to H. The transition facies B to J (intraformational conglomerate to coal) occurs only one time and is not considered in this analysis. The most frequent significant transitions are from facies A to C (conglomerate and cross-stratified sandstone respectively) and from facies C to A. As in the BSG#1 borehole, these transitions represent transitions between the main constituents of facies

association I; the channel association. Transitions from facies F (cross-laminated sandstone and siltstone) to G (interbedded sandstone, siltstone and mudstone) and from facies G to H (mudstone) record fining-upward sequences typical of facies associations IIA and IIB (crevasse/levee or undifferentiated floodplain deposits).

Conclusions

Markov Chain analysis as described in this section was used to evaluate the tendency of the borehole sequences to deviate from the hypothesis of totally random transitions between facies and to determine those transitions most responsible for the deviation. Both boreholes deviated from the hypothesis of randomness at the 99% level of significance. Some of the non-random behavior can be attributed to transitions which occur too few times to be of much sedimentological interest. Other, more frequent transitions between facies corroborate transitions which help to define facets of the facies associations. The most frequent, statistically significant (at the 90% level) transition in both boreholes was from facies A to C (conglomerate to cross-stratified sandstone). Almost as frequent and significant is the reciprocal transition from facies C to A. These transitions reflect interbedding of conglomerates and sandstones in facies association I. The observation that transitions between most facies states apparently occur more or less at random in the borehole

sequences suggests that most facies occur in a variety of different floodplain environments and thus appear to occur randomly through the section. For example, facies G (interbedded sandstone, siltstone and mudstone) occurs in facies associations I and II (channel and overbank deposits respectively). It is likely that the apparent random nature of the vertical transitions found in the boreholes also is also present in the outcrops, but exposures were too poor to test this hypothesis.

CHAPTER 6 - PETROGRAPHY

Introduction

Thirty three samples of sandstone from the cores and outcrops were thin sectioned and stained for calcium and potassium feldspars using the technique of Norman (1974) as modified by Quinn (1985). A minimum of 300 point counts provided data on composition. This number of counts insures that the volume of observed constituents is within plus or minus 5% of the actual volume with a 95 % level of confidence (Van der Plas and Tobin, 1965). Detrital constituents counted were categorized as follows: quartz (poly- and monocrystalline), feldspar (plagioclase and K-feldspar), rock fragments (volcanic, metamorphic and sedimentary), micas, opaques, and miscellaneous minerals (including heavy minerals). Matrix, porosity and cement were counted as well. Results of the point counts are summarized in Table 6.1. Several samples were polished, coated with carbon and examined in a scanning electron microscope (SEM) equipped with a back-scattered electron (BSE) detector and an energy dispersive xray analysis unit (EDX). The degree of back-scattering is measured in terms of the back-scatter electron coefficient which is in turn dependent upon mean atomic number of the specimen. The higher the mean atomic number, the brighter the mineral appears in photomicrographs and on the SEM screen (White

Table 6.1

Pointcount Percentages

Sample	QP	QM	P	K	LV	LM	LS	M	D	MI	MA	C	PO
F70	8	41	3	20	0	0	10	8	0	9	0	t	1
F73	16	32	13	14	t	t	8	6	1	4	4	1	1
F76	6	40	10	10	0	t	3	8	1	10	8	3	t
F54	22	21	19	12	t	2	9	2	t	3	4	0	6
F78	9	32	3	17	0	0	5	2	2	7	18	t	3
F56	11	26	8	23	0	0	t	3	t	5	t	22	t
F60	30	13	13	6	0	2	6	t	t	4	0	23	1
F36	7	30	9	20	0	0	t	14	t	2	13	0	3
F85	12	27	25	14	0	2	2	10	t	2	1	5	t
F24	13	29	12	20	0	0	4	5	t	8	3	2	3
F21	3	34	6	22	0	0	3	4	t	11	0	13	2
F13	24	29	6	4	0	0	13	3	t	t	t	13	6
F6	17	53	7	0	t	t	14	2	0	3	0	0	3
F45	4	58	5	3	0	t	9	3	1	4	3	0	6
F63	15	44	5	8	0	t	14	2	0	5	6	1	t
F39	12	41	3	5	t	t	5	4	0	5	8	11	5
F52	9	33	8	3	t	6	5	6	t	4	7	17	2
FB273.3	11	45	5	10	0	0	4	5	t	t	t	16	3
FB390.3	6	64	2	3	0	0	t	t	0	1	0	18	5
FB416.7	16	60	3	4	0	t	2	0	0	1	1	3	9
FB481.5	12	42	13	7	0	t	4	3	0	1	2	t	15
FB527.6	16	42	7	7	0	t	t	1	10	t	8	t	6
FB600	8	54	12	1	0	t	7	1	t	1	2	6	7
FB725	26	35	10	9	t	2	t	6	0	0	8	t	4
FB779	4	39	23	3	0	t	1	7	t	1	0	14	7
BSG63	5	44	29	3	0	t	t	3	t	1	0	5	8
BSG108	10	54	14	4	0	0	2	1	t	t	6	4	4
BSG146	5	42	22	6	0	0	6	3	1	1	1	10	5
BSG218	22	41	18	2	1	t	2	2	1	4	t	6	t
BSG254	t	33	38	7	t	0	1	10	0	4	t	3	1
BSG265	15	38	20	3	0	2	4	2	t	t	2	8	6
BSG285	13	45	20	4	0	t	2	2	t	3	t	8	3
SS85F3	t	24	46	2	0	0	2	5	1	4	2	7	5

QP: polycrystalline quartz; QM: monocrystalline quartz;
P: plagioclase; K: potash feldspar; LV: volcanic rock
fragment; LM: metamorphic rock fragment; LS: sedimentary
rock fragment; M: mica; D: opaque minerals;
MI: miscellaneous heavy minerals; MA: matrix; C: cement;
PO: porosity; t: trace.

et al., 1984). The BSE image and the EDX unit were used in conjunction with the conventional optical microscope to help resolve small-scale or ambiguous structures and mineralogies.

Efforts were made to distinguish between matrix and pseudomatrix (Dickinson, 1970) and to reconstruct the original composition of the sandstones by interpreting and counting altered grains as their unaltered starting components. Difficulties encountered due to alteration of samples suggests that to some degree counting errors are unavoidable.

The data generated were used to provide detrital modes (Table 6.2) for use in quartz-feldspar-lithic fragment diagrams (QFL-diagram, Fig. 6.1). Samples were classified according to Folk (1980). Using this scheme, most samples are classified as arkose and subarkose; the remainder are sublitharenite, lithic arkose, and feldspathic litharenite. Sandstones examined by Knight (1983) from both the Searston Formation and the undivided Barachois Group were compositional arkoses and subarkoses. Although all samples examined for this study are concentrated along the quartz-feldspar leg of the ternary diagram, there is considerable variability in the abundance of all of the components plotted. However, the average proportion of quartz appears to be greater and the average proportion of feldspar appears to be less in samples from the FB2-76 borehole than in samples from other locations. This is

Table 6.2

Sample	O/C#	Quartz	Detrital Modes		Grain size	Sorting
			Feldspar	LRF's		
F70	69	60%	28%	12%	c	w
F73	82	58	32	10	m/vc	m
F76	87	67	29	4	f/m	m
F54	51	51	37	12	m/c	m
F78	51	62	30	8	vf/c	p
F56	52	54	46	t	f/m	m
F60	64	60	28	12	c	m
F36	17	56	44	t	vf/m	m
F85	15	48	48	4	vf/m	m
F24	14	53	41	6	m/c	w
F21	14	54	41	5	f	w
F13	10	70	13	17	m/c	w
F6	5	76	8	16	m/c	w
F45	32	78	10	12	m/c	w
F63	28	68	15	17	f/c	m
F39	21	79	12	9	vf/m	m
F52	43	66	17	17	vf/f	m
Mean		62.4	28.2	9.5		
S.D.		9.6	13.5	5.7		
FB273.3		75	20	5	f/m	w
FB390.3		92	8	t	f/m	w
FB416.7		89	8	3	m	w
FB481.5		69	26	5	f/m	m
FB527.6		79	19	2	f/vc	p
FB600		75	16	9	f/c	m
FB725		73	23	4	f/c	m
FB779		61	36	3	vf/f	m
Mean		76.6	19.5	3.9		
S.D.		10.1	9.3	2.6		
BSG63		60	38	2	f/m	w
BSG108		76	21	3	m/vc	m
BSG146		58	35	7	vf/m	m
BSG218		74	23	3	c	w
BSG254		42	57	1	mg	w
BSG265		64	28	8	f/c	p
BSG285		69	28	3	m/c	m
Mean		63.3	32.9	3.9		
S.D.		11.6	12.2	2.6		
SS85F3		33	65	2	f/m	w

O/C#: Outcrop number; LRF: Lithic rock fragment;
w: well sorted; m: medium sorted; p: poorly sorted;
vf: very fine grained; f: fine grained; m: medium grained;
c: coarse grained; vc: very coarse grained;
S.D.: standard deviation

DETRITAL MODES (Q-F-L DIAGRAM)

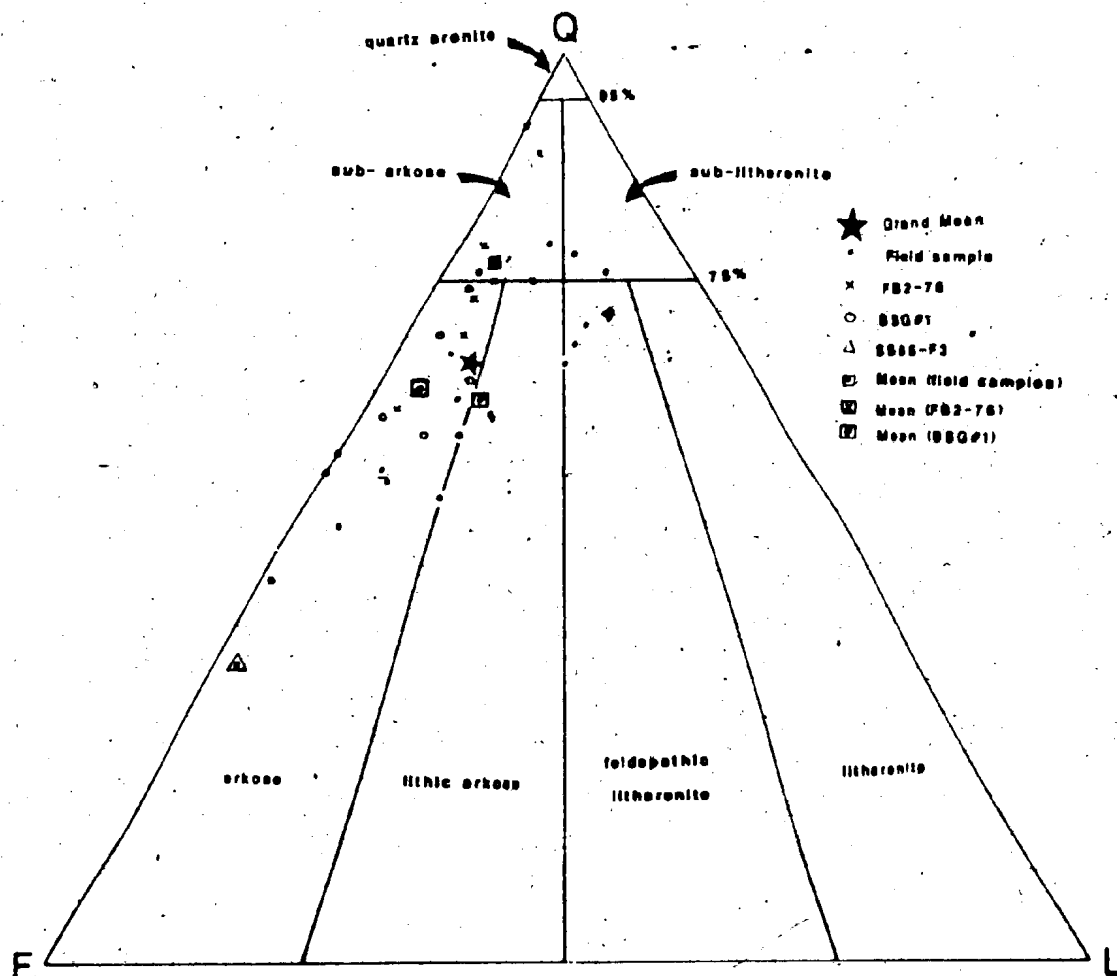


Figure 6.1: Sandstone petrology - quartz, feldspar, lithic fragment (QFL) diagram.

confirmed at the 90% level of significance by a Student's T-Test of the null hypothesis that the means are equal.

Description of Framework Grains

Monocrystalline quartz is invariably more abundant than polycrystalline quartz. Extinction is normal to undulose. Myrmekitic quartz occurs in several samples (FB527.6) and in four samples (F36, F76, F78, and F56) quartz is microfractured (Plate 6.1).

Both plagioclase and potassium feldspars are present in all but one sample. Feldspars are rarely fresh, although they appear generally less altered in samples from the FB2-76 borehole than in samples from either the outcrops or from the BSGE1 borehole. Microcline and perthitic feldspars are common. Alteration of feldspars consists of sericitization, vacuolization, albitization of plagioclase grains, and replacement by calcite and kaolinite. In the BSGE1 core, plagioclase is always more abundant than potash feldspar (Fig. 6.2). In the outcrop samples, relative abundances are variable, however, potash feldspar is usually more abundant than plagioclase. There is also a decrease in the proportion of feldspar relative to quartz and rock fragments west of outcrop 14. In the FB2-76 borehole, plagioclase is more abundant at the top and bottom of the core, but the two feldspar varieties are approximately equal.

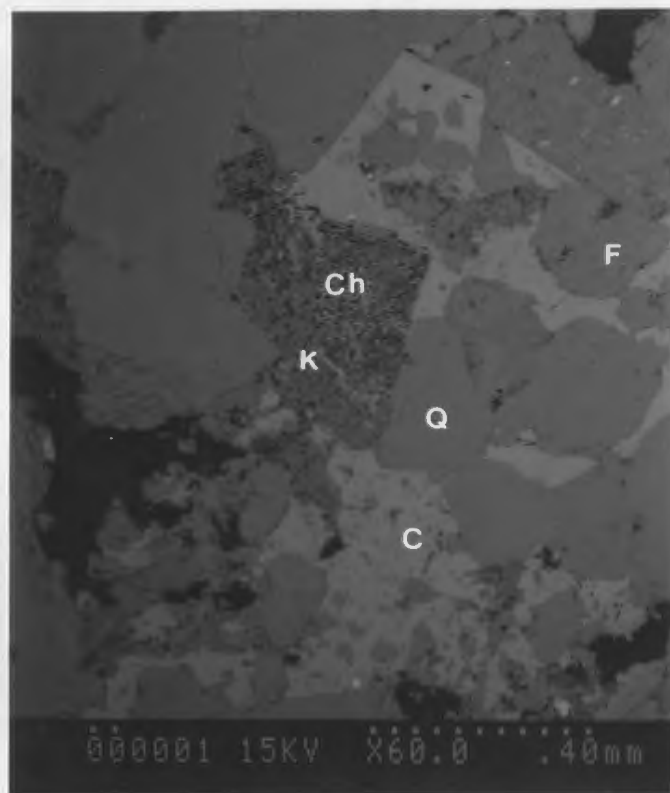


Plate 6.2: Chlorite, kaolinite and calcite grain replacements in sample F13, outcrop #10. Backscattered electron image, X60. Scale: 1 centimeter = 160 micrometers. C=calcite, Q=quartz, K=kaolinite, Ch=chlorite, F=feldspar.



Plate 6.2: Chlorite, kaolinite and calcite grain replacements in sample F13, outcrop #10. Backscattered electron image, X60. Scale: 1 centimeter = 160 micrometers. C=calcite, Q=quartz, K=kaolinite, Ch=chlorite, F=feldspar.

in the middle samples. Total feldspar content increases with depth below 417 m (Fig. 6.2).

Lithic fragments are concentrated in the medium- to coarse-grained samples. Mafic volcanic rock fragments may be underrepresented due to the degree of diagenetic alteration of the rocks. Where recognized, volcanic rock fragments consist of plagioclase laths (which may be altered to sericite) in a fine-grained chloritic groundmass. Most other lithic fragments are intraformational mudstone and siltstone fragments. Rare metamorphic rock fragments are mica schists.

Other detrital components vary unsystematically with regard to depositional environment and stratigraphic level. Heavy minerals recognized in thin section and with the use of energy dispersive X-ray analysis (EDX) include zircon, sphene, rutile, pyrite, apatite (BSG265 only), rare epidote, and possibly garnet. Biotite and muscovite may be intergrown with calcite, or pyrite. Biotite is commonly chloritized.

Description of Matrix and Cement

Matrix exceeds the 15% cut-off between arenites and wackes (Pettijohn et al., 1973, p.158) in only one sample (F78). The matrix in this sample consists of red hematite and clay. Sample F36 contains a similar matrix (13%).

Authigenic silica, calcite, and phyllosilicates

VARIATIONS IN FELDSPAR PROPORTIONS

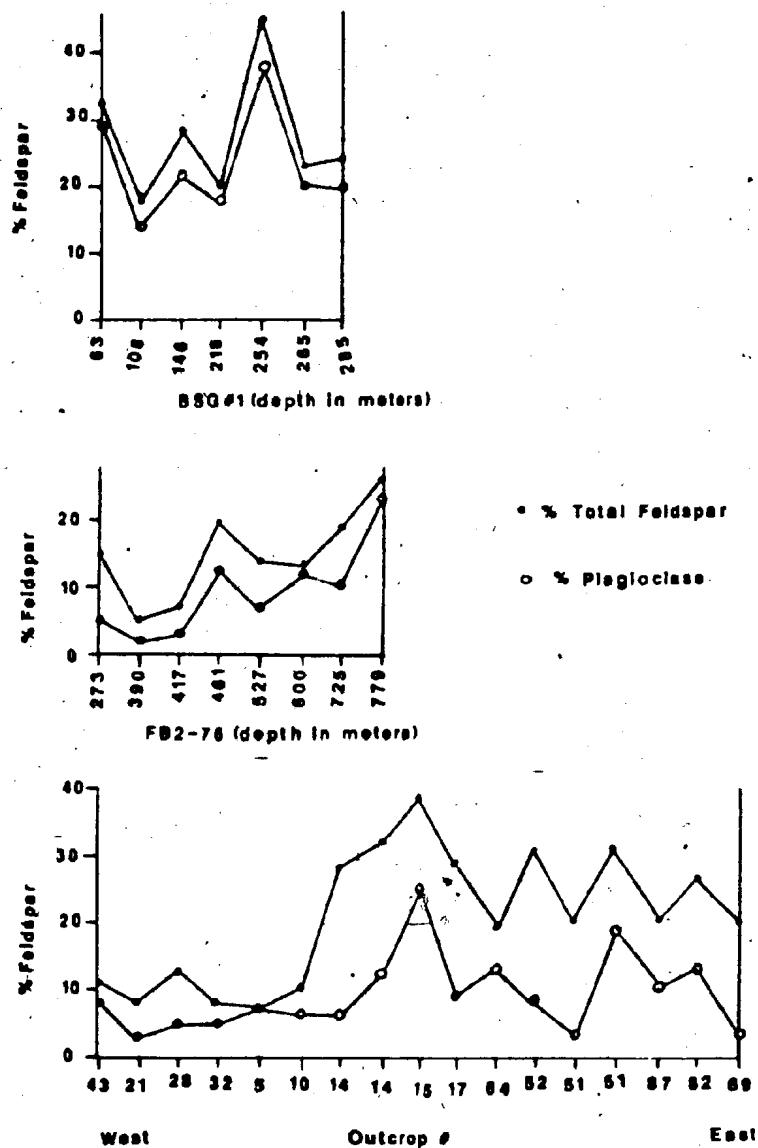


Figure 6.2: Variations in feldspar proportion in BSG#1 borehole (top), FB2-76 borehole (middle), and along Middle Barachois Brook (bottom).

(kaolinite, illite and chlorite) occur as cements and grain replacements to some degree in all samples (e.g., Plate 6.2). Pore-filling chlorite, kaolinite, chlorite-illite mixtures; and chlorite-kaolinite mixtures were identified using the BSE detector and EDX analysis. Quartz overgrowths are difficult to recognize due to a general lack of dust rims on grains; sutured and straight contacts between grains could be due to overgrowths or microquartz cementation. Silica may replace grains or line pores as well (Plate 6.3). Albite overgrowths on feldspars occur in several samples (e.g., sample F54). Calcite replacement of feldspar grains is common and may be recognized by calcite crystals in the feldspar grain (e.g., in albite in F54 - Plate 6.4). Authigenic pyrite occurs in many samples, but is only abundant in sample FB527.6 (c. 10%). EDX analysis permitted the identification of hair-like barite veins in one sample (BSG#1, 139 m), and intergrown chlorite and apatite in another (BSG#1, 264.6 m). Rare instances of iron oxide or pyrite growing displacively between mica layers were noted (e.g., sample F13).

Grain Size and Porosity

Grain size in samples ranges from very fine- to coarse-grained, but most are medium- to coarse-grained (Table 6.2). Sorting in most samples is estimated to be moderate, but ranges from poor to well-sorted (Table 6.2).

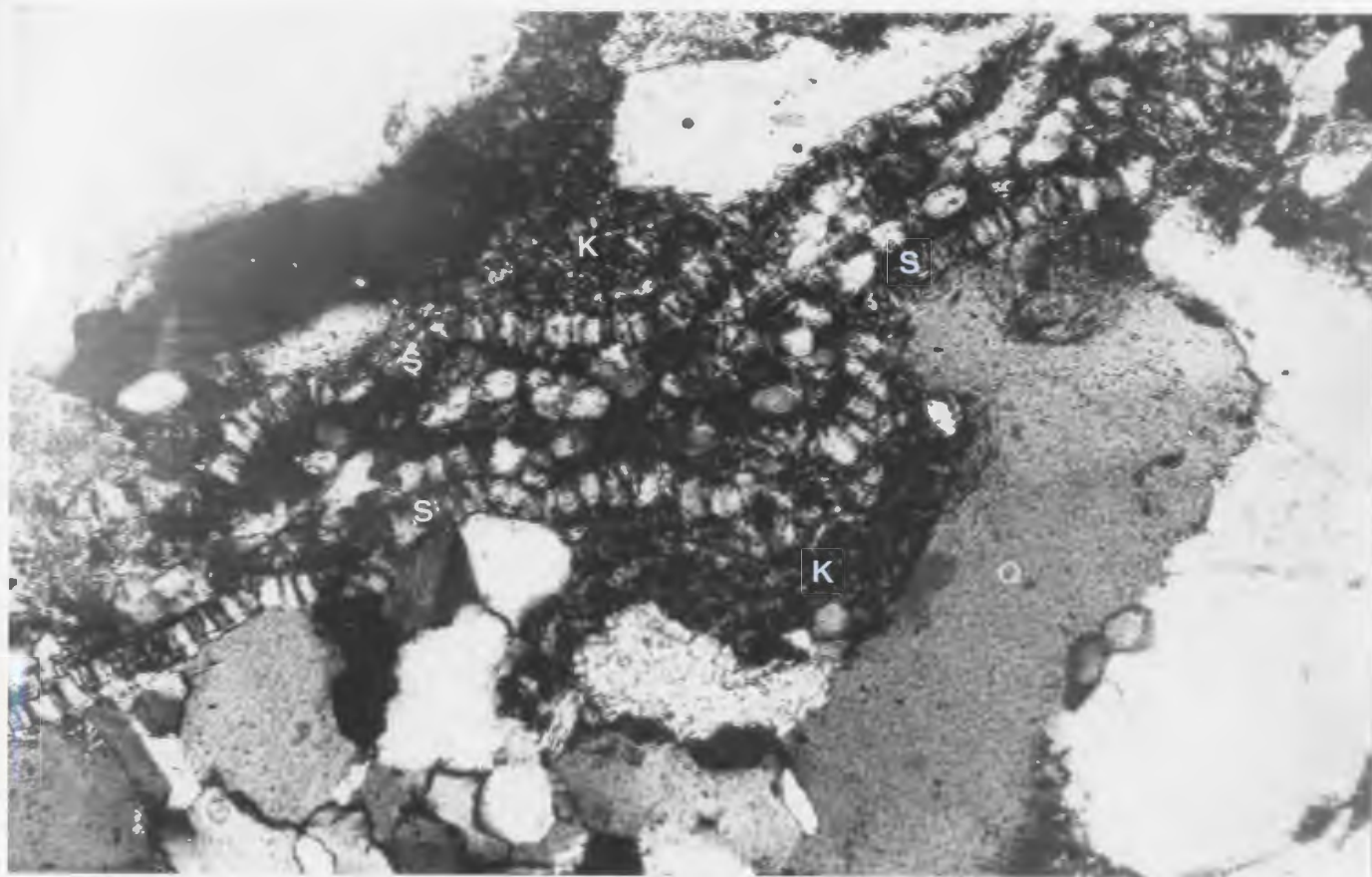


Plate 6.3: Pore-lining silica and pore-filling kaolinite in sample F13, outcrop #10. Crossed-polars. X10. Scale: 1 centimeter = 230 micrometers. S=silica, K=kaolinite, Q=quartz.

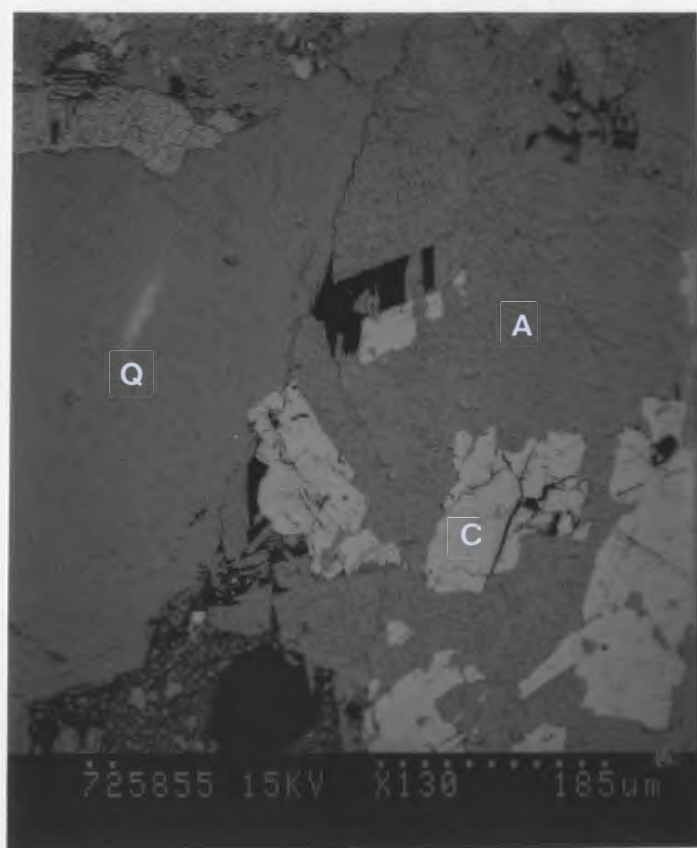


Plate 6.4: Calcite replacing sodium feldspar in sample F54, outcrop #51. Backscattered electron image, X130.
Scale: 1 centimeter = 74 micrometers.
C=calcite, A=albite, Q=quartz.

Efforts to impregnate the thin sections with coloured epoxy in order to point count porosity and recognize grain plucking were unsuccessful, probably due to a lack of permeability. Therefore, estimates of porosity (trace to 15%) are maxima. Porosity estimates from geophysical logs run in the BSG#1 borehole range from traces to a maximum of 15% (Hoffe, 1985). Visual estimates from hand specimens fall in the same range.

Interpretation

The apparent unsystematic stratigraphic and areal variability of sandstone mineralogy of the Barachois Group suggests that local source areas and drainage basins probably exercised considerable control over detrital composition. For example, the extremely high proportion of plagioclase feldspar in a sample from the Stephenville area (SS85F3) probably results from its proximity to the Indian Head Anorthosite Complex (Williams, 1985). Rapid rates of erosion, rapid subsidence and/or slow rates of weathering are implied by overall abundances of feldspars (Folk, 1980; Blatt et al., 1980). Arkoses generally signify tectonically active source areas to provide the necessary relief for rapid erosion.

The decreases in the proportion of feldspar (apparently unrelated to grain size) in exposures west of outcrop 14 and the lower average feldspar proportion in the FB2-76 borehole

are likely caused by localized source areas and/or by climatic and drainage characteristics present during the deposition of those sediments. In poorly drained areas, weathering of sediments is retarded by high water tables, thus reducing the rate of destruction of relatively unstable minerals such as feldspar (Todd, 1968). This mechanism is consistent with the abundance of feldspars in samples associated with coal-bearing units (i.e sample F85, F24, and the BSG#1 borehole). Differences in the rates of weathering of potassic and sodic feldspars and hence their relative abundance has been thought to be an indicator of palaeoclimate (Todd, 1968). However, recent work (James et al., 1981) suggests that paleoclimate is not a significant factor in the relative abundance of feldspar types. Plagioclase appears to weather more rapidly than potassium feldspar in both arid and humid climates.

Rocks which probably contributed detritus to the plagioclase-rich arkoses of the Barachois Group include diorites, gabbros, granites, and anorthosites from the Long Range Igneous and Metamorphic Complex and the Southwest Brook Intrusive Suite (Riley, 1962, Williams, 1985). These crystalline rocks presently lie to the north and east of the study area; there are other pre-Carboniferous igneous rocks which lie to the southeast (Chorlton, 1984) which could have contributed detritus as well. Knight (1983), noting the presence of granitic and silicic volcanic rock fragments in

sandstones from the St. George's coalfield, suggests that the rocks were derived from a suite of undeformed granites and felsic volcanics similar to the Siluro-Devonian Topsails Igneous Complex (Taylor et al., 1980) or the Lloyd's River Intrusive Suite (Knight, 1983). These rocks now lie to the northeast of the subbasin, but may have extended southwestward towards the subbasin margin (Knight, 1983).

Authigenic chlorite, illite, and kaolinite are typical of non-marine diagenetic assemblages which contain small amounts of volcanic debris and moderate amounts of feldspar (Carrigy and Mellon, 1964). In non-marine environments meteoric waters are usually slightly acid and undersaturated with respect to most ions (Bjorlykke, 1983). Instability of minerals such as mica and feldspar relative to the undersaturated meteoric waters may result in their being leached and degraded. Silica released during the degradation of feldspars may be reprecipitated as overgrowths on quartz grains.

Quartz overgrowths and pore-lining suggest that some of the silica cementation occurred early in the diagenetic history. In one sample (F13), a silica-coated pore (Plate 6.3) bears a resemblance to one formed in a modern petrocalcic soil (cf. Plate 10 in Flach et al., 1971). Calcite cementation and authigenic clay mineral cements record later episodes of diagenesis.

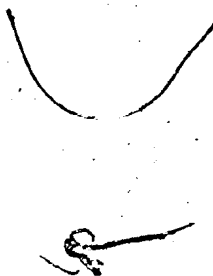
The assemblage of authigenic minerals in the Barachois Group is quite similar to that described from sandstone

cores recovered from 700-1700 m depth in a well which penetrated age-equivalent strata in the Cabot Strait, north of Cape Breton, Nova Scotia (Shell et al. North Sydney G-24; Hicks, 1984).

Summary of Petrographic Results and Conclusions

1. The primary constituents of the Barachois Group sandstones are (in order of abundance: quartz, feldspar, lithic fragments, micas, and miscellaneous opaque and heavy minerals. Most of the sandstones are classified as arkose and subarkose.
2. Common authigenetic components are silica, kaolinite, chlorite, illite and calcite. Barite and apatite are rare.
3. The general lack of apparent systematic stratigraphic and geographic variations in sandstone mineralogy suggests that local source areas exercised an overriding control on detrital compositions. Relative decreases in unstable mineral proportions could have been caused by climatic and/or drainage conditions.
4. Authigenic minerals are typical of non-marine early diagenetic assemblages. Early pore-lining silica cement may indicate active pedogenic processes.
5. From the available data, sandstone mineralogy does not identify any one distinctive provenance. Several of the

presently exposed igneous intrusive complexes in the Long Range Mountains to the southeast, east and north are potential source terranes.



CHAPTER 7 - CLAY MINERALOGY

Sample Preparation

Thirty mudstone samples collected from the two available cores (BSG#1 and FB2-76) and from the field were crushed to 2-5 mm. The crushed samples were cleaned ultrasonically, then disaggregated in a dispersing agent (1% Sodium hexametaphosphate) by applied ultrasound for three minutes. After standing for five minutes, the suspension was decanted into constricted glass tubes and allowed to settle for four hours. The remaining suspension was decanted, flocculated with magnesium chloride (which saturates the clay minerals with magnesium) and centrifuged to recover the <2 micrometer fraction. Amorphous iron was removed using the method of Mehra and Jackson (1960) in order to minimize its X-ray absorbing effects.

Two oriented mounts (0.01g per mount) were prepared by suction onto gel filters. One mount was acidified by allowing the clay suspension to stand in 6N hydrochloric acid at 90 degrees Celsius for 15 minutes in order to dissolve chlorite and allow calculation of the respective contributions of chlorite and kaolinite to the 0.7 nm peak. In some cases acid treatments of up to one hour were necessary to remove all of the chlorite. The other mount was X-rayed untreated, then exposed to ethylene glycol vapor at 70 degrees Celsius for 3 to 12 hours and re-X-rayed in

order to detect clay minerals capable of forming complexes with glycol. Four of the samples were heated to 550 degrees Celsius in order to destroy kaolinite and thus confirm the presence of chlorite.

All diffractograms were obtained using a Phillips diffractometer operating at 40 kilovolts and 20 milliamperes generating copper K-alpha radiation. A time constant of four, divergence slit of 1 degree and receiving slit of 0.2 degrees were used. The oriented mounts were scanned from 3 to 28 degrees 2-theta at 1 degree 2-theta per minute and the X-ray counts were output to a conventional paper strip chart recorder run at 1 centimeter per minute.

Several samples were rerun to evaluate the precision of the diffractometer. Other samples were reprocessed and rerun in order to evaluate the precision of the processing method. A third group of samples were rerun without the iron removal step in order to assess the effect of that technique on clay mineral quantification.

Mineral Identification

Clay minerals were identified by their characteristic XRD basal reflections. The clay mineral groups identified are illite, chlorite, kaolinite, and "mixed-layers". No discrete smectite was found, however, an interstratified chlorite-smectite was detected in one sample (F35).

Illite is identified by reflections which occur at 1.0

nm, 0.5 nm, and 0.33 nm (e.g., Fig. 7.1) and which are unaffected by acidification or ethylene glycol solvation. Although the 0.33 nm reflection coincides with that of quartz, the other reflections are generally strong and well resolved.

Kaolinite and chlorite both have strong reflections at 0.71 nm and 0.35 nm. The presence of chlorite is indicated by a 1.4 nm peak which is unaffected by ethylene glycol solvation (i.e. not smectite or swelling chlorite). In addition, the presence of both kaolinite and chlorite may be recognized by the dissolution of chlorite in warm 6N hydrochloric acid (e.g. Figs. 7.2 and 7.3), although magnesium-rich chlorites tend to be less soluble than iron chlorites (Brown and Brindley, 1980 pg. 323). Heating chlorite and kaolinite mixtures at 550 to 600 degrees Celsius may destroy the kaolinite (Carrol, 1970), but the thermal behavior of the two species may be variable and/or overlap at critical temperatures (Kodama and Oinuma, 1963).

A relative decrease in intensity of the 0.71 and the 0.35 nm peaks and the disappearance of the 1.4 nm peak (in the absence of swelling clay minerals) after acidification supports the contention that the chlorite is removed from the sample and that both chlorite and kaolinite are present.

Characterization of mixed-layer clay minerals can be difficult due to the many combinations of two or more

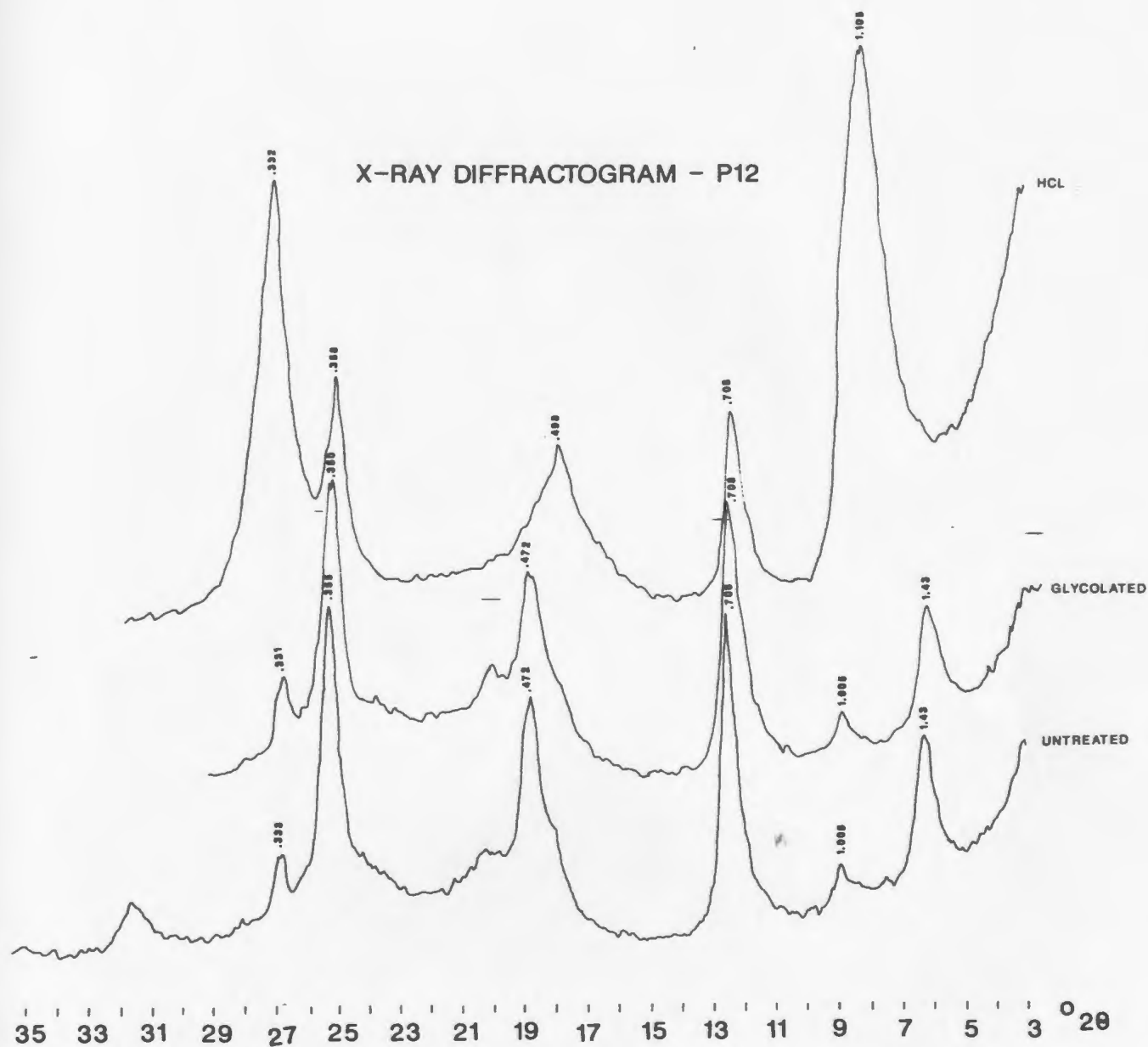


Figure 7.1: X-ray diffractogram of sample P12, outcrop #38, a grey mudstone underlying a coarse sandstone. Clay mineral proportions: 19% illite, 7% kaolinite, 74% chlorite.

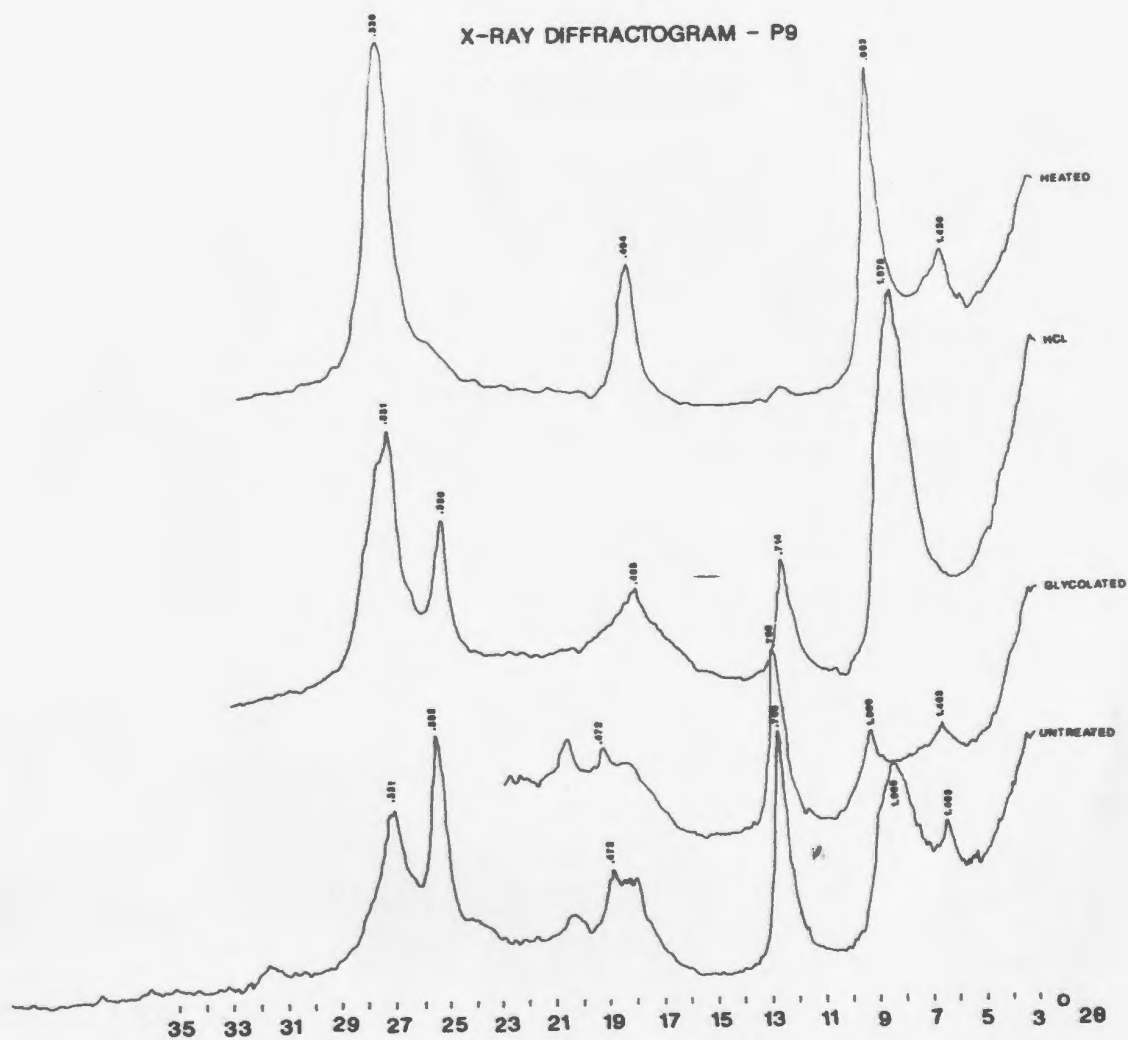


Figure 7.2: X-ray diffractogram of sample P9, outcrop #17), a light grey mudstone. Clay mineral proportions: 45% illite, 25% kaolinite, 30% chlorite.

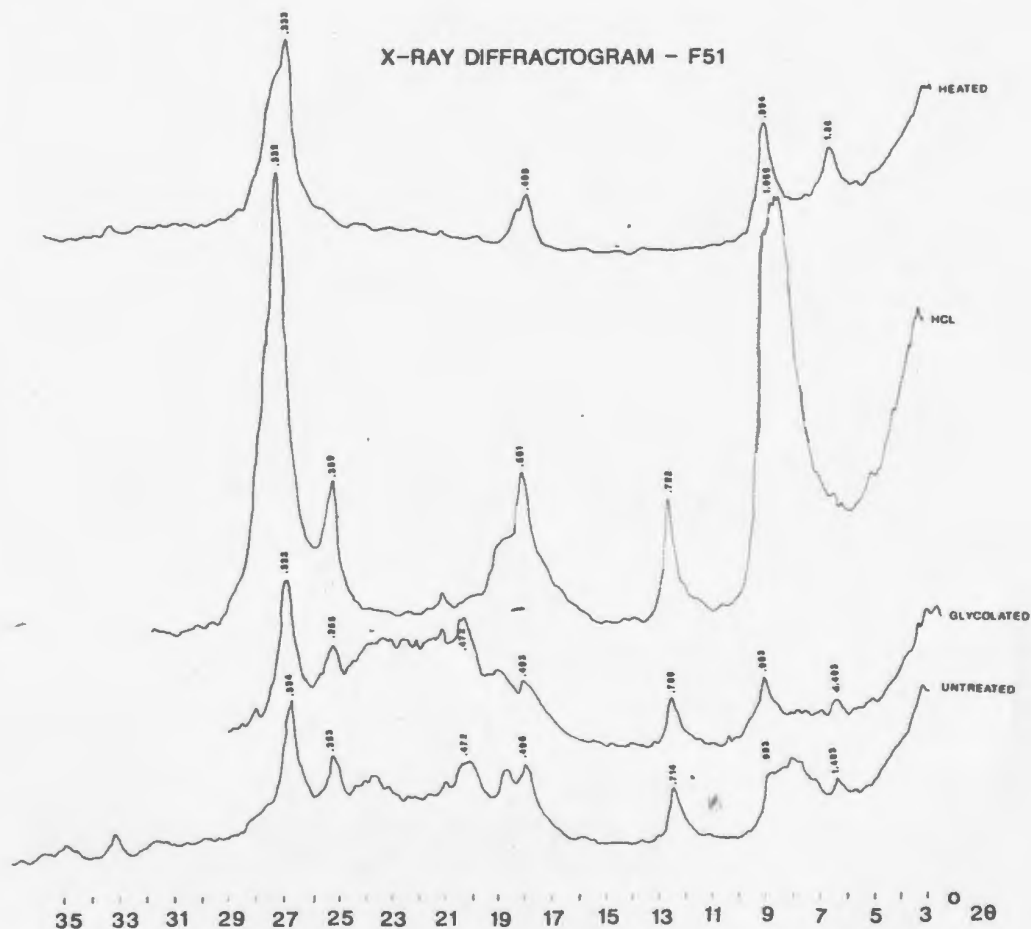


Figure 7.3: X-ray diffractogram of sample F51, outcrop £43, a red mudstone. Clay mineral proportions: 75% illite, 14% kaolinite, 11% chlorite. There is probably a significant proportion of unquantified mixed-layer illite-smectite present as suggested by the large hump between the 1.403 nm peak and the 0.983 nm peak on the untreated diffractogram.

constituents which are possible. In this study mixed-layer clays were identified by a plateau or broad hump between 1.0 and 1.4 nm or a shoulder on the low-angle side of the 1.0 nm peak or on the high-angle side of the 1.4 nm peak (Biscaye, 1965; Brindley, 1981) (e.g. Fig. 7.2). The hump was either reduced or had migrated under the 1.4 nm peak after exposure to ethylene glycol, and intensified and centered at approximately 1.1 nm after acidification. Mixed-layer clay minerals with similar behavior are thought to be interstratified illite-smectite (cf. Lee and Chadhuri, 1976). The amorphous nature of the peaks precludes quantification. The broad, intense peak at 1.1 nm after acidification is probably due to the loss of potassium from interlayer positions in mixed-layer illite-smectite clays (Ostrum, 1961).

In all heat-treated samples the 1.4 nm peaks broadened slightly and either migrated to very slightly lower d-spacings, or did not migrate. In sample BSG162.5, two peaks developed after heating, one at 1.38 nm and one at 1.33 nm. The very slight tendency of the 1.4 nm peak to migrate to larger 2-theta positions on heating, with no tendency to migrate to smaller 2-theta positions in ethylene glycol, may be caused by vermiculite interlayers in the chlorite (Brown and Brindley, 1980 p. 325).

The 1.4 nanometer peaks did not migrate after exposure to ethylene glycol except in one sample (F35 outcrop 15),

taken from beneath a thin coal seam (see Fig 8.4, Chapter 8). This sample appears to contain an interstratified chlorite-smectite mixed-layer clay mineral. This conclusion is based on the observation that the 1.4 nm peak (001) of chlorite expanded to 1.56 nm when saturated with ethylene glycol, and collapsed to 1.15 nm when heated (Fig. 7.4). In addition, the 0.7 micrometer peak becomes noticeably asymmetric after glycolation, probably as a result of a rational reflection at 0.77 micrometers. The absence of a superlattice reflection near 3.10 micrometers suggests that the mineral is randomly interstratified (April, 1981a).

Quantification

Due to the complexity of most clay-mineral assemblages, the variations in sample preparation, and variations in the crystallinity and chemical composition of clay minerals, truly quantitative evaluations of these assemblages are very difficult and time consuming and, in some cases, impossible (Biscaye, 1965; Heath and Pias, 1979; Brindley, 1980 and others). It is possible to calculate a semiquantitative "percentage" for each clay mineral in a sample by expressing the amount of each mineral as a ratio of the total mineral composition (Biscaye, 1965). This is accomplished by multiplying the basal peak areas by weighting factors, and assuming that the sum of the weighted peak areas is 100%.

Weighting factors have been calculated by Biscaye

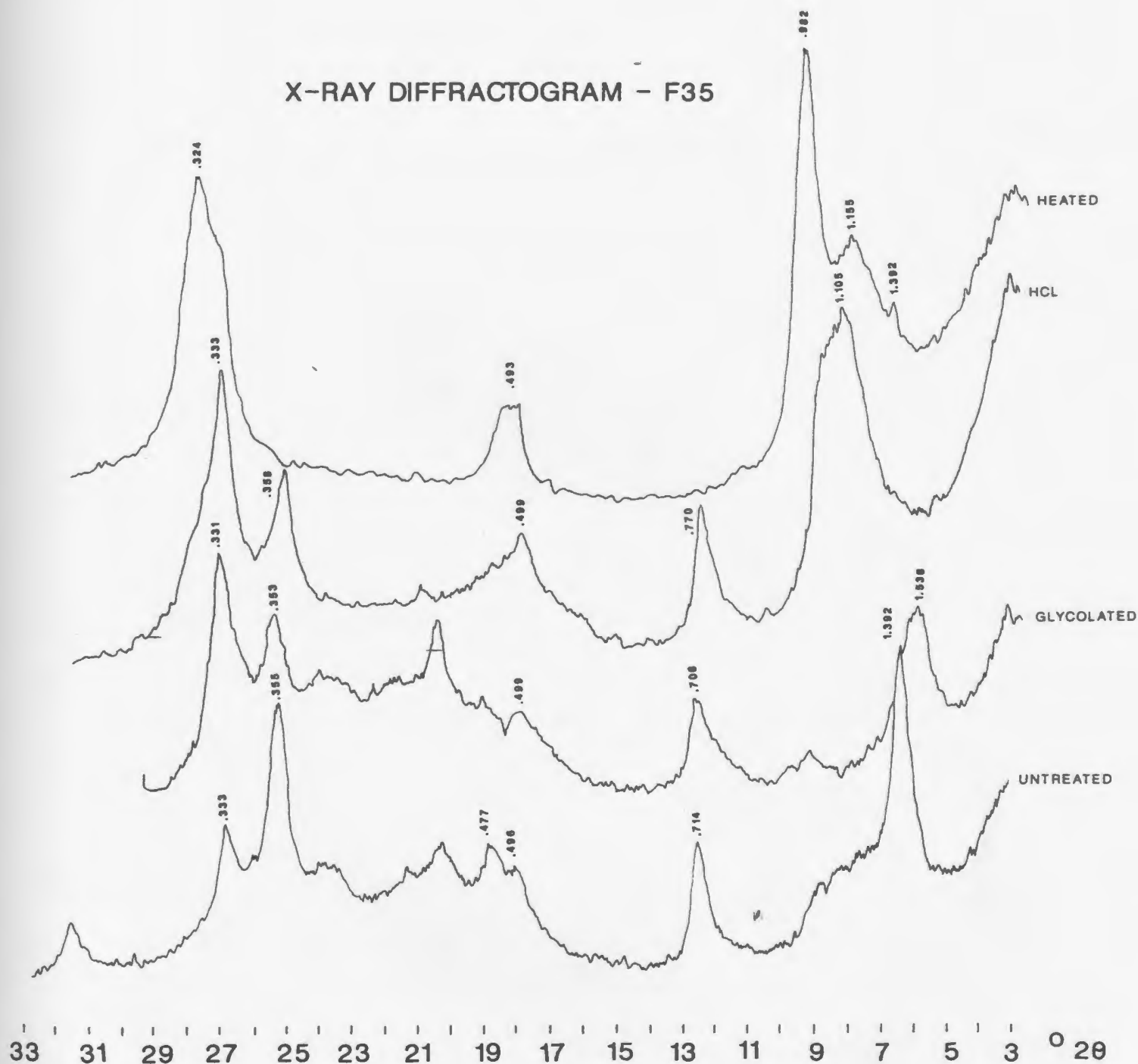


Figure 7.4: X-ray diffractogram of sample F35, outcrop #15, a yellow-grey mudstone. Clay minerals are not quantified due to the presence of mixed-layer chlorite-smectite, identified by the shift of the 1.392 nm peak on glycolation.

(1965), Cook et al. (1975) and Heath and Pisias (1979) as well as several other authors. There are significant differences in the relative amounts of clay minerals when calculated using the various weighting factors. The factors of Heath and Pisias were rejected because they were based on the unsupported assumption that the nondiffracting (i.e. amorphous) components in the clay mixtures must be minimized mathematically. The factors calculated by Cook et al. (1975) were deemed inappropriate because their method of determining weighting factors assumes that their reference minerals have the same characteristics as one's samples. Since they were concerned primarily with recent deep sea sediments this assumption is not necessarily valid for the ancient terrestrial deposits of the Barachois Group.

The factors provided by Biscaye (1965) were used in this study because they facilitate the comparison with other work in this region and with a large body of data previously generated with these factors. Any of the weighting factors will provide internally consistent "untestable approximations of real percentages" (Biscaye, 1965) within which relative changes can be recognized.

Using the weighting factors of Biscaye (1965), the percentages of illite, kaolinite, and chlorite were calculated as follows:

$$\% \text{ Illite} = \frac{4XI(1.0)}{\text{Total}}$$

$$\% \text{ Kaolinite} = \frac{2XI'(0.7)XI(.33)/I'(.33)}{\text{Total}}$$

$$\% \text{ Chlorite} = \frac{2X(I(0.7)-(I'(0.7)XI(0.33)/I'(0.33))}{\text{Total}}$$

I(0.7)= area of the ethylene glycolated 0.7 nm peak

I'(0.7)= area of the acidified 0.7 nm peak

I(1.0)= area of the ethylene glycolated 1.0 nm peak

I(.33)= area of the ethylene glycolated 0.33 nm peak

I'(.33)= area of the acidified 0.33 nm peak

Total= sum of the weighted peak areas

Peak areas were calculated by multiplying the peak height by the width at half the height.

Calculated percentages of the three clay mineral species for each sample are illustrated in Table 7.1.

Mixed-layer clays, though present, are not included in this calculation and are therefore a source of error. The apportioning of the 0.7 nm peak between chlorite and kaolinite is accomplished by subtracting the area of the acidified 0.7 nm peak (normalized using the ratio of the areas of the ethylene glycolated and acidified 0.33 nm peaks) from the area of the 0.7 nm peak.

Hiscott (1984) estimates errors in the reported abundances of clay minerals at about plus or minus 20% using Biscaye's weighting factors and computer integrated peak areas. Cook *et al.* (1975) estimates an error in the reporting of clay-mineral abundances of plus or minus 20-50%. Biscaye (1965) reported that the precision of the peak area ratio determinations (from which the percentages are calculated using the weighting factors) as expressed by the coefficient of variation (standard deviation expressed

Table 7.1

Clay Mineralogy, Organic Carbon, and Colour

Sample	TOC	%Illite	%Kaolinite	%Chlorite	Colour
F67	10.70	24	45	31	N1
BSG162.5	2.77	23	32	45	N2
P5	21.23	22	28	50	N2
P17	2.66	12	15	73	N3
FB278.7	3.64	31	13	56	N2/3
FB777.4	2.07	31	9	60	N3
FB417.7	1.76	42	16	42	N3/4
FB728	--	41	23	37	N3/4
P20	1.48	17	2	81	N3/4
P9	0.64	45	25	30	N4
P19	17.63	25	30	44	N4
FB320.5	--	60	3	37	N4
FB455.2	--	26	41	32	N4
FB538.7	0.55	17	17	66	N4
FB617.7	--	48	15	39	N4
FB557	--	34	23	43	N4/5
BSG54.9	0.19	19	5	76	N5
P12	0.59	19	7	74	N5/6
Mean	5.1	29.8	19.4	52.0	
Standard Deviation	7.0	12.9	12.5	16.2	
Coeff. of Var.	1.4	0.43	0.65	0.31	
BSG172.9	0.58	51	20	29	5R4/2
F51	--	75	14	11	5R2/2
FB364.5	--	44	50	6	10R5/4
FB357.2	--	45	41	14	10R3/4
F83	0.04	44	25	31	10R3/4
FB782.6	0.18	44	6	50	5YR3/2
BSG92	0.23	61	6	32	5YR3/2
BSG309.8	0.42	48	11	41	5YR3/2
F71	0.08	51	4	45	5YR3/2
FB617.8	--	47	15	38	5YR4/1
FB617.9	--	52	9	39	5YR4/1
BSG326.8	0.76	27	29	44	10YR2/2
Mean	0.33	49.1	19.2	31.7	
Standard Deviation	0.37	11.4	14.6	14.3	
Coeff. of Var.	1.12	0.21	0.73	0.45	

TOC=Total organic carbon (weight %); Colour: GSA rock colour chart; Coeff. of Var.: Coefficient of variation (standard deviation expressed as a proportion of the mean).

as a percentage of the mean) increases exponentially at small values. This is corroborated by the replicates run in this study. Biscaye's (1965) data on precision also indicates a wide range of peak area ratios over which the coefficient of variation is quite low (approximately 10%). Schultz (1964) found a similar relationship between the coefficient of variation and the percentage of a mineral measured. The coefficient of variation increases exponentially and the rapid rise begins at approximately 10%.

In order to assess the repeatability of the method employed in this study, five samples were prepared and run a second time (Table 7.2). Calculated clay mineral abundances differed by as much as 9% between runs. The average absolute difference between runs was 4.4% for illite, 5.6% for kaolinite, and 4.8% for chlorite. This indicates that clay mineral abundances differ by approximately 5% between runs regardless of the relative abundance of that mineral. Therefore the less abundant minerals are subject to proportionately greater errors than the more abundant minerals. The replicates suggest that plus or minus 20% is a reasonable estimate of error for abundances >20%, for abundances <20% errors of 30% to 50% are probably more realistic.

Large differences were found between successive runs of the same samples with and without the iron removal step

Table 7.2

Replicates

<u>Sample no.</u>	<u>%Illite</u>	<u>%Kaolinite</u>	<u>%Chlorite</u>	<u>Run#</u>
P9	45	21	34	1
P9	45	29	25	2
BSG533	21	30	49	1
BSG531	25	34	41	2
F51	70	10	20	1
F51	72	17	10	2
FB617.7	43	19	39	1
FB617.7	52	10	38	2
FB617.9	56	8	36	1
FB617.9	51	11	38	2

Table 7.3

Iron Removal

<u>Sample no.</u>	<u>%Illite</u>	<u>%Kaolinite</u>	<u>%Chlorite</u>	<u>Fe removed</u>
F67	13	80	7	no
F67	24	45	31	yes
FB357.2	37	36	26	no
FB357.2	45	41	14	yes
F51	72	5	22	no
F51	75	14	11	yes

(Table 7.3). Differences between the two runs vary from as little as 3% to as much as 35%. The coefficient of variation (in this case simply the difference between the two runs expressed as a percentage of the mean) varies from 4% to 126%. These observations suggest that estimates of clay mineralogical abundances are affected by removal of iron using the method of Mehra and Jackson (1960). Effects of iron removal on clay mineral x-ray diffractometry have also been noted by Brewster (1980) and Harwood et al. (1962). As mentioned previously semi-quantification of results are at best untestable approximations of real proportions.

Care should be exercised in comparing these data with other results that have not been subjected to the iron removal technique employed in this study.

Results

There is little systematic variation with stratigraphic level in either of the boreholes or among the field samples (Figs 7.5). However, there are differences in clay mineral proportions between the grey mudstones from the FB2-76 borehole and other grey mudstones, as well as variations based on colour (Figs. 7.6 and 7.7) and the abundance of total organic carbon (Fig. 7.7).

Grey mudstones from the FB2-76 borehole contain less illite than do grey mudstones from the outcrops and the BSG61 borehole. In general, however, grey-coloured

VARIATIONS IN CLAY MINERAL PROPORTIONS

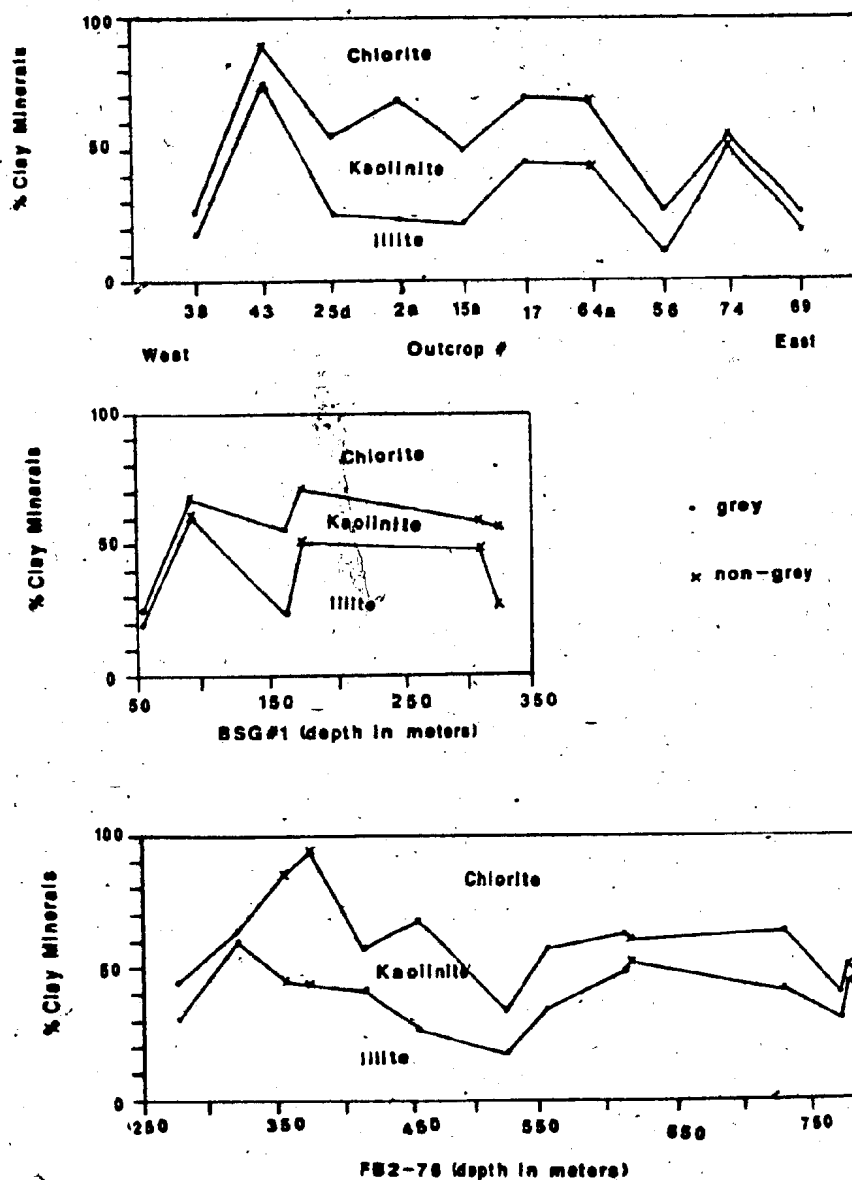


Figure 7.5: Variations in clay mineral proportions along Middle Barachois Brook (top), in the BSG#1 borehole (middle), and in the FB2-76 borehole (bottom).

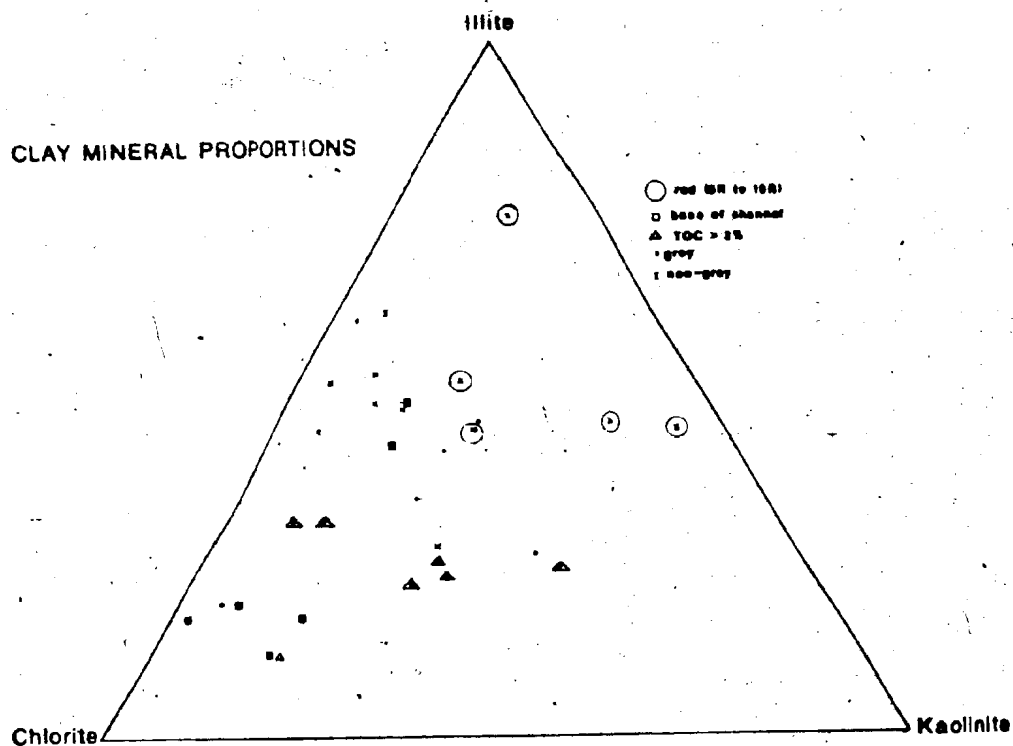


Figure 7.6: Clay mineral proportions in mudstones of the Barachois Group. Red mudstones (circled) plot closest to the illite-kaolinite line. Grey mudstones are relatively more chlorite-rich than non-grey mudstones.

DIFFERENCES IN CLAY MINERAL PROPORTIONS BASED ON COLOUR AND TOC

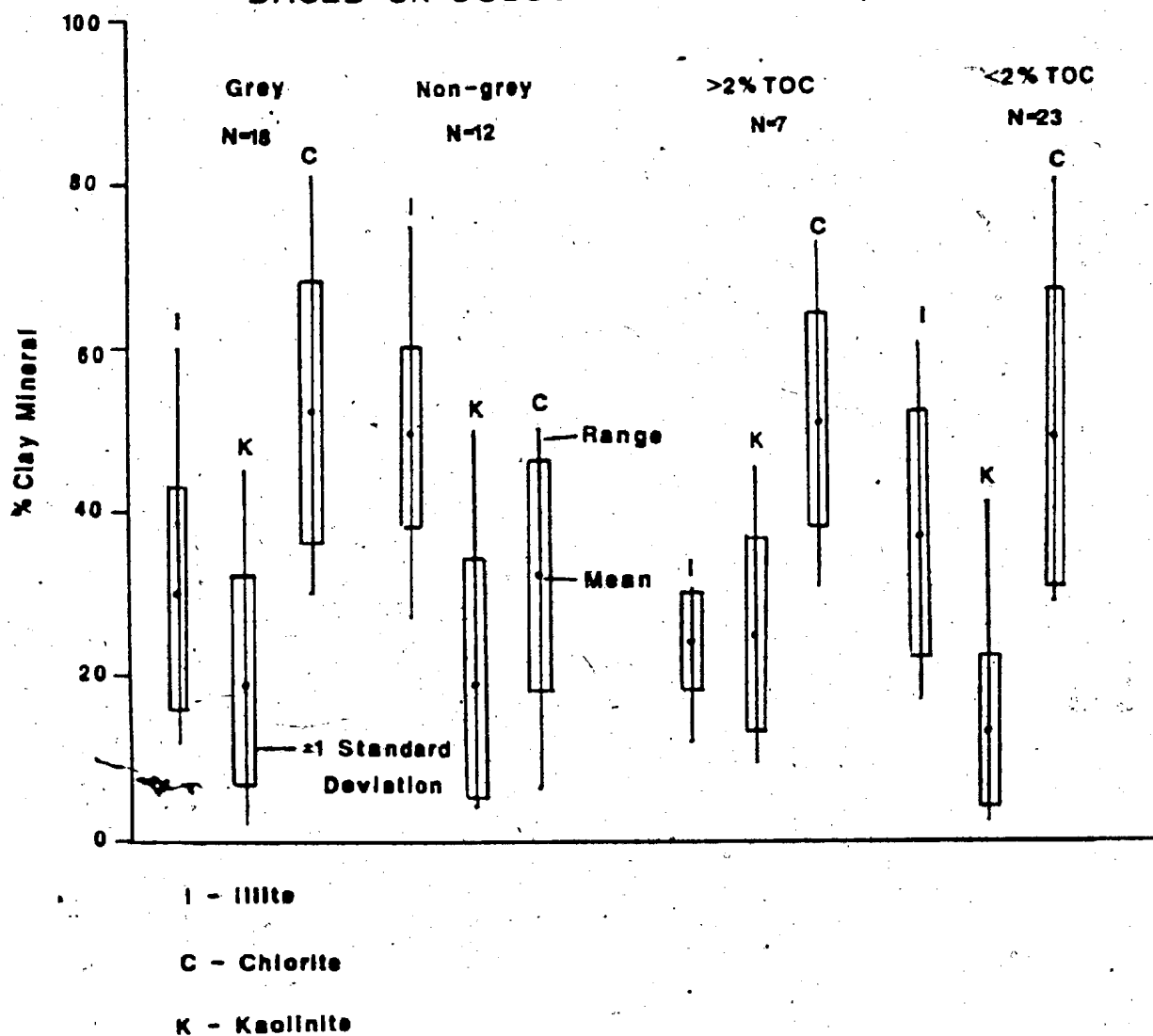


Figure 7.7: Differences in clay mineral proportions based on colour and total organic carbon (TOC). Mean chlorite and illite proportions of grey and non-grey mudstones differ significantly. TOC content has a slight impact on mean proportions of kaolinite and illite.

mudstones are relatively richer in chlorite, and non-grey (red, red-brown, brown-grey) coloured mudstones are relatively richer in illite. The samples which are richest in chlorite (i.e., P17, P12, P20, FB538.7) are mudstones which directly underlie coarse-grained sandstones and conglomerates.

A Student's t-test was performed to test the null hypothesis that the means of the grey and the non-grey mudstones are identical for each of the clay mineral species identified (Fig. 7.7). The null hypothesis was rejected at the 99% level of confidence for illite and chlorite, but not for kaolinite indicating that the mean percentage of kaolinite does not differ significantly between the non-grey and the grey mudstones. It also suggests a positive correlation between illite and non-grey mudstones and between chlorite and grey mudstones. A t-test was also performed on the average proportions of clay minerals in grey samples from the FB2-76 borehole versus grey samples from the outcrops and the BSG#1 borehole. It was found that grey mudstones from the FB2-76 borehole contain more illite (mean: 36.67%) than other grey mudstones (mean: 22.89%) at the 90% level of significance.

Similar statistical tests were performed to test the relationship between clay mineral abundances and the percentages of total organic carbon (TOC). It was found that the mean percentage of illite in mudstones with >2% TOC

is different from that of the mudstones with $< 2\%$ at the 95% level of significance. These data suggest that illite is negatively correlated with TOC. Linear regression of TOC values versus clay mineral proportions (Fig. 7.8) show that there is a slight negative correlation between illite proportion and TOC (correlation coefficient = -0.34). There is a positive correlation between kaolinite abundance and TOC (correlation coefficient = $+0.47$) and virtually no correlation between TOC and chlorite proportion (correlation coefficient = -0.014). At the 90% level of confidence, only the relationship between kaolinite and TOC is significant.

Interpretation

In general, clay minerals deposited in fluvial systems tend to reflect the mineralogy of the source area (e.g. Millot, 1970). Clay minerals are initially formed by weathering of igneous and metamorphic rocks, and may be further transformed in soils before being eroded and transported to their depositional sites. Uplifted sedimentary rocks may also be a source of clay minerals. Once deposited they may again be subjected to weathering, cation exchange, and ultimately diagenesis upon burial. The preservation of a particular suite of clay minerals is therefore a function of the stability of the clay minerals through a series of changing environments.

The clay minerals found in the Barachois Group mudstones are chlorite, kaolinite, illite and mixed-layer clays. In terrestrial environments, chlorite is stable in a poorly drained alkaline environment with an abundance of

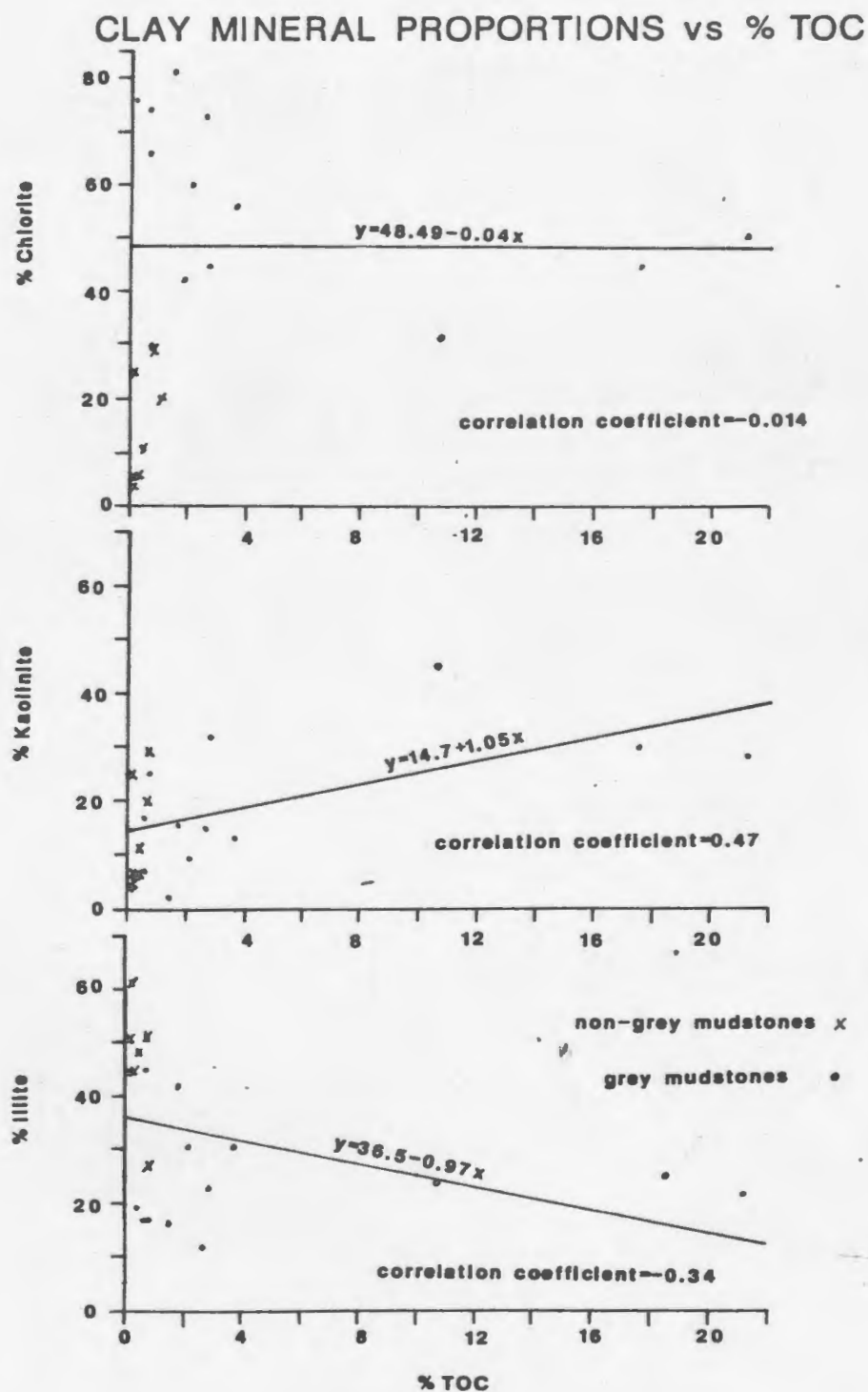


Figure 7.8: Clay mineral proportions vs. total organic carbon content (TOC). As observed in Fig. 7.7, chlorite proportion is virtually unaffected by TOC. There is a slight positive correlation between TOC and kaolinite proportion and there is a slight negative correlation between

iron and magnesium ions (Bowles, 1978, pg. 142). Illite is stable where potassium ion concentrations are high and is often found in semi-arid poorly leached environments (Bowles, 1978, pg. 136). Kaolinite is associated with highly leached, acidic soils, and is therefore often found in well drained, hot, humid environments. Kaolinite is usually quite stable once formed (Millot, 1970).

The non-grey mudstones (facies H) are the predominant facies in subassociation IIIC. They were interpreted to have formed in floodplains as a result of overbank floods and ponding of floodwaters in ephemeral and probably oxidizing lakes. The grey mudstones are typical of mudstones found in subassociations IIIA and IIIB. These subassociations were interpreted as the deposits of perennial lakes and swamps which provided a relatively more reducing geochemical milieu than the environment in which the non-grey beds were deposited. Some investigations have revealed no difference in clay mineralogy between drab and red beds (Friend, 1966; Van Houten, 1973). However, other investigators have found that illite is the most abundant clay mineral in red mudstones (e.g. April, 1981b; Gibling et al., 1985; R. Hyde, pers. comm.; McPherson, 1980).

April (1981a,b) attributes clay mineral proportions in red floodplain mudstones to a strictly detrital origin. Relative increases in chlorite in shallow lacustrine grey mudstones are attributed to neoformation of chlorite from

precursor smectite (presumably washed in from floodplains, although this is not explicitly stated) by the addition of magnesium from alkaline magnesium-rich lake and inherited pore water (April, 1981a,b). April's interpretation is based upon the relative importance of the high temperature (2M) polytype of illite (detrital illite) and the alignment of chlorite flakes in thin sections of the red mudstones. Investigation of the polytypes of illite was not undertaken for this study, so the question of a diagenetic versus detrital origin for the clay minerals in the non-grey mudstones cannot be resolved in this manner.

If illite, kaolinite, and chlorite were the dominant detrital minerals deposited in both grey and non-grey units by floods during the deposition of the Barachois Group then diagenesis was probably the agent responsible for differences in different-coloured mudstones. An alternative to the neoformation of chlorite in grey mudstones (April, 1981b) is an explanation based upon the possibility that illite is relatively less stable than chlorite under reducing conditions and that chlorite is relatively less stable than illite under oxidizing conditions. This relationship is suggested by evidence that illite increases relative to other clay minerals at the top of caliche profiles (Aristarain, 1971) and 1.4 nm chlorites decrease relative to illite under oxidizing conditions in other types

of soil profiles (Jackson et al., 1952; Velde, 1985 p.170). That illite is relatively unstable under reducing conditions is suggested by smaller amounts of potassium in some green or grey (i.e., reduced) mudstones relative to red (i.e., oxidized) mudstones (McBride, 1974; McPherson, 1980; R. Hyde, pers. comm.). The loss of potassium and sodium from green mudstones studied by McBride (1974) is ascribed to leaching by reducing fluids leaking from the sandstones which overlie them. Exceptionally high proportions of chlorites in drab shales which underlie sandstones in the Barachois Group may be caused by loss of illite and/or by formation of chlorite. Leaching by reducing diagenetic fluids probably caused degradation of illite due to the stripping of potassium (McBride, 1974; McPherson, 1980). Chlorite may be formed either from precursor smectite by the addition of magnesium (e.g., April, 1981b) or as insoluble ferric iron is reduced to the ferrous state (Velde, 1985, p.40). The overlying sandstones are presumed to be the source of the fluids responsible for cation exchanges.

Considerable variation in kaolinite proportions exists in both the grey and non-grey mudstones. Grey, organic-rich samples (i.e. oil shale and carbonaceous mudstone) have relatively high, but not the highest proportions of kaolinite. In these samples the positive correlation between kaolinite abundance and TOC probably reflects the stability of kaolinite relative to other clay minerals in a

low pH environment rather than the neoformation of kaolinite by leaching of cations (Millot, 1970 p. 164). Topography and climate (temperature and amount and temporal distribution of precipitation) are major factors in determining the degree of leaching which may occur at a particular depositional site. Variations in the kaolinite proportions in non-grey mudstones and grey mudstones with low TOC values reflect the combined effects of these factors as well as the variability of parent materials and the possibility of diagenetic kaolinite formation.

Two red (10R, GSA Colour Chart) mudstone samples (FB357 and FB364) with high kaolinite proportions are associated with rubified channel sandstones (facies association I) and the lowest recorded abundance of total feldspars (in the interval from 392 m to 338 m in the FB2-76 core). Kaolinite was probably formed by the in situ weathering of feldspars and leaching of the cations released by weathering. These red mudstones with high kaolinite proportions that are associated with feldspar-poor sandstones may have formed during relatively humid periods and/or in relatively well-drained parts of the Carboniferous floodplains (Duchaufour, 1977, p. 21).

Mixed-layer clays are commonly the products of degradation and soil formation (Millot, 1970) although they can also form by aggradation or diagenesis. They can be mixtures of any of the true clay minerals and may be either

regularly or randomly interstratified. Chlorite-smectite mixed-layer clays (as found in F35) are associated with the weathering of volcanic material in the U.S.S.R. (Sarkisyan and Kotelinkov, 1970) and are also found in Triassic lacustrine sediments in Connecticut and Massachusetts (April, 1981b) and in the Carboniferous lacustrine Rocky Brook Formation in the Deer Lake Basin, Western Newfoundland (R.Hyde, pers. comm.). In these cases, the formation of interstratified chlorite-smectite could be attributed to the diagenesis of smectite in a Mg-rich environment (c.f. April, 1981b).

The lack of smectite and the ubiquity of mixed-layer illite-smectite clay minerals could be the result of burial diagenesis. Discrete smectite is not usually found at temperatures and depths associated with coal ranks higher than medium volatile bituminous (Heroux et al., 1978; Hoffman and Hower, 1979). The coals in the Barachois Group are classified as high to low volatile bituminous. If smectite was present in the originally deposited mudstones, it could have been converted to a mixed-layer variety by the addition of potassium at temperatures in excess of about 75 degrees Celsius (Hower, 1981, p. 74-75). Potassium could have come from the diagenesis of K-feldspars (Hower, op.cit.). An alternative explanation for the lack of smectite may be its small size. Samples of <1 or <0.5 micrometer sizes could have contained discrete smectite

which was not observable in the <2 micrometer fraction. If the lack of discrete smectite is a result of source area characteristics rather than diagenesis, it is probable that the mixed-layer clays are degradation products of detrital illite and chlorite. If, on the other hand, smectite is present in a smaller size fraction, or has been diagenetically altered, then there is a difficulty in deciding whether the mixed-layer minerals are products of aggradation or degradation.

Geographic variation is exhibited by the larger proportion of illite in grey mudstones from the FB2-76 borehole than in grey mudstones from the outcrops and the BSGE1 borehole. This variation is not paralleled by significant differences in illite proportions between the non-grey mudstones from the two groups of samples. Since one would expect differences in clay mineral proportions due solely to changes in detrital mineralogy to be reflected in both grey and non-grey mudstones, the clay mineralogical differences are probably related to differences in post-depositional environments between grey mudstones in the FB2-76 borehole and other grey mudstones. As discussed above, post-depositional controls on illite abundance include a relatively more oxidizing environment or a greater depth of burial for illite-rich mudstones (e.g., grey mudstones from the FB2-76 borehole). Thermal alteration indices based on palynomorph colour do not indicate

significant differences in the degree of maturation between the FB2-76 borehole and the other sample locations (E. Burden, pers. comm.). Therefore an explanation of clay mineralogical differences based on the presence of relatively more oxidizing conditions in the post-depositional environments of grey mudstones in the FB2-76 borehole is favored.

Summary and Conclusions

A summary of the results of the XRD study of the mudstones on the Barachois Group are as follows.

1. The clay minerals recognized in the Barachois Group are illite, chlorite, kaolinite, interstratified illite-smectite, and interstratified chlorite-smectite (one sample).
2. Non-grey samples contain more illite and less chlorite than grey samples.
3. The proportion of kaolinite is very variable, but is positively correlated with TOC.
4. Grey mudstones from the FB2-76 borehole contain a higher illite proportion than grey mudstone from the combined BSG#1 borehole and outcrop samples.

The explanation of these variations are due to a combination of original detrital composition of the mudstones and the geochemical characteristics of their environment of deposition. Kaolinite variations are due in

part to the stability of kaolinite in acidic conditions (where TOC and kaolinite abundance are high) and in part to other factors such as local drainage and climate which would act to control cation and silica concentrations. The lack of discrete smectite may be attributed to original detrital compositions, size, or to burial diagenesis. Mixed-layer minerals are probably formed by degradation of original clay minerals and their partial reconstitution during burial diagenesis. Clay mineralogical differences between grey mudstones from the FB2-76 borehole versus grey mudstones from other sample locations are probably due to a prevalence of relatively more oxidizing conditions in the post-depositional environments of grey mudstones from the FB2-76 borehole.

CHAPTER 8 - ORGANIC GEOCHEMISTRY

Introduction

Organic geochemical analyses of mudstones in the Barachois Group provide information on the quantity and type of organic matter present and its level of thermal maturation. These data are necessary in order to assess the hydrocarbon resource potential of the group. Samples analyzed for organic carbon (TOC) were chosen in order to furnish information on the total range of organic content present in mudstones of the Barachois Group. Four drab coloured mudstones were further analyzed to obtain information on the quantity and quality of C15+ extractable material (i.e. bitumen). Samples for Fischer Assay and Rock-Eval pyrolysis were chosen based on their low density and lack of visible coaly material (i.e. the field attributes of sapropelic shale). Stable carbon isotope analyses on kerogens in whole rocks were performed in order to investigate their relationship to organic matter type and the source of the organic matter. Before discussing these data the methods used are described.

Methods

Total organic carbon (TOC): The technique used in this study to determine total organic carbon (TOC) is that of Bouvier and Abbey (1980). Non-dispersive infrared

absorptiometry was used to determine the percentage of carbon dioxide released upon volatilization of 20 to 200 mg of carbonate-free material. The equipment consisted of a furnace, a Beckman Model 864 non-dispersive infrared analyzer equipped with an integrator which displays absorption as millivolts, and a nitrogen carrier-gas system. The equipment is owned and operated by the geochemical laboratory of the Newfoundland Department of Mines and Energy, St. John's Newfoundland. In the case of three samples (RH83-249, RH83-252, and RH83-253) TOC content was determined by preparing the samples as for carbon isotope analysis then calculating the TOC content based upon the volume of evolved carbon dioxide gas.

Extraction: Organic content in sedimentary rocks consists of one or more types of kerogen plus bitumen. Bitumen was extracted from four samples (F35, P5, F67, and BSG162\5)... Dried samples (30-45 g) were refluxed at 35 degrees Celsius for 24 hours in an azeotrope consisting of 30% benzene:70% methane (by volume). After 24 hours the extracts were filtered, dried and weighed. Asphaltenes were precipitated by dissolving the sample in n-pentane (50:1) (Hunt, 1979 p.58). The precipitate and the extract were dried and weighed.

Liquid Chromatography (Durand et al., 1970 as modified by R. Quick, pers. comm.): Asphaltene-free samples were

separated into saturated hydrocarbons, aromatic hydrocarbons, and nitrogen-sulfur-oxygen (NSO) compounds using liquid column chromatography. The column consists of fully-activated silica gel and alumina. Solvents used for extraction of each fraction were: 50 ml hexane for saturates, 205 ml hexane:benzene (2:1) for aromatics, and 40 ml benzene:methanol (1:1) followed by 40 ml diethyl ether for NSO compounds. Flow-rate was 50 ml/hr for saturates and aromatics and was not controlled for NSO compounds.

Gas Chromatography-Mass Spectrometry (GC-MS): The saturated hydrocarbon fractions of two samples (P5 and BSG162.5) were chosen for further analysis on a coupled GC-MS (Hewlett Packard Model 5792 gas chromatograph coupled to a Hewlett Packard Model 5970A mass-selective detector). An aliquot of the saturate fraction was dissolved in redistilled hexane and injected onto a nonpolar phase, fused silical capillary column (c. 10 m length). The injection temperature was 280 degrees Celsius. Samples were separated using a temperature programmed rate of 3 degrees Celsius per minute from 70 degrees to 270 degrees. Initial time was four minutes, final time was 20 minutes. Scans for specific mass/charge (m/z) ratios were performed at $m/z=183$ (acyclic isoprenoids plus alkyl isomers), $m/z=191$ (pentacyclic triterpenoids - i.e., hopanes), and $m/z=217$ (steranes).

Saturate and aromatic fractions of three samples (P5, F67, and BSG162.5) were also analyzed on a gas chromatograph

with an 18 m column and a programmable integrator to better separate peaks and calculate relative abundances of compounds.

Fischer Assay and Rock-Eval Pyrolysis: Eight samples from the BSG#1 borehole were evaluated for their potential to produce hydrocarbons on pyrolysis by Fischer Assay. Fischer Assay involves heating a 100 g sample of crushed rock at 500 degrees Celsius for one hour (Hunt, 1979 p. 461). The analyses were done at the Hydrocarbon Processing Laboratories, Canada Centre for Mineral and Energy Technology, Ottawa, Ontario.

The five shallowest borehole samples (162.8 m to 257.3 m) plus five surface samples were submitted to the Institute for Sedimentary and Petroleum Geology (Calgary, Alberta) for Rock-Eval pyrolysis. The surface samples were collected by R. Hyde from a sapropelic bed located in the streambed of Middle Barachois Brook between outcrops 15 and 15a (Fig. 1.5), approximately 40 m upstream from outcrop 15a. The bed is only visible when the water is low. Rock-Eval pyrolysis involves the gradual heating of 100-300 mg of crushed rock in a stream of helium at a rate of 5-40 degrees Celsius/minute up to a temperature of 600-800 degrees Celsius. Due to equipment problems TOC values were not obtained for the samples submitted for pyrolysis by the pyrolytic method.

Stable Carbon Isotopes: The ratio of $\delta^{13}\text{C}$ to $\delta^{12}\text{C}$ was determined for the carbon in kerogens from shales (seven samples) and the carbon in calcium carbonate (six samples). The calcium carbonate samples contain variable amounts of quartz, feldspar, pyrite, clay minerals and possibly trace amounts of siderite and organic matter (as determined by whole rock X-ray diffractometry). The isotope ratio determinations were made on a VG Micromass 903E mass-spectrometer. Values are reported in parts per mil relative to PDB for carbon dioxide corrected for overlap of the ^{18}O peak. The equation used to calculate the ratio difference is:

$$\delta^{13}\text{C} = \frac{^{13}\text{C}/^{12}\text{C sample}}{^{13}\text{C}/^{12}\text{C std}} - 1 \times 1000$$

Samples were prepared for isotope analysis according to sample type. Shales containing kerogens were crushed and intimately mixed with purified copper oxide and high purity copper reagent in quartz tubes. The tubes were evacuated, sealed, and pyrolyzed at 850 degrees Celsius for one hour and slowly cooled. Limestone samples were crushed, placed in Y-tubes, evacuated and acidified with 100% phosphoric acid. The resultant carbon dioxide from both methods was then cryogenically purified for mass spectrometry.

Results

The results of the analyses performed on mudstones from

the Barachois Group are presented in Tables 8.1 to 8.5. Rock-Eval pyrolysis results are reported as three peaks corresponding to (a) hydrocarbons already in the rock (S1), (b) hydrocarbons produced by pyrolysis (S2), and (c) carbon dioxide liberated by pyrolysis (S3). The peaks are reported in milligrams per gram of sample. Tmax refers to the temperature at the maximum of the S2 peak. The sum of the S1 and S2 peaks have been converted to litres of hydrocarbon produced per metric ton of rock for ease in comparing the Rock-Eval results with the Fischer Assay results. Discrepancies between the results of the Fischer Assay and Rock-Eval pyrolysis may be due, in part, to the observation that the average kerogen decomposition temperature of Barachois Group samples (550 degrees Celsius) is higher than the maximum temperature attained for the Fischer Assay (500 degrees Celsius) (E. Furimsky, pers. comm.). Since samples were submitted for analysis as discrete pieces of whole rock rather than as splits of powdered samples discrepancies may also be due to real differences between samples submitted for the two types of analysis.

TABLE 8.1

TOC Analyses

Sample	Outcrop#		or Core	Colour
	%AS	%TOC		
+RH83-246	5.7	50+	15a	N1
RH83-249	13.2	18.87	sap.	N2
RH83-252	11.2	31.86	sap.	N1
RH83-253	11.3	31.76	sap.	N1
*P5	0.27	21.23	15a	N2
xP19	17.6	17.63	25	N4
*F67	27.3	10.7	2a	N1
P17	10.7	2.66	56	N3
P20	5.6	1.48	69	N3/4
*F35	8.2	0.87	15	5GY6/1
P9	5.4	0.64	17	N4
P12	0.04	0.59	38	N5/6
F51	2.8	0.27	43	5R2/2
F71	12.2	0.08	74	5YR3/2
F83	4.3	0.04	64a	10R3/4
FB278.7	6.8	3.64	FB2-76	N2/3
FB777.4	3.9	2.07	FB2-76	N3
FB417.7	3.9	1.76	FB2-76	N3/4
FB538.7	5.5	0.59	FB2-76	N4
FB782.6	11.5	0.18	FB2-76	5YR3/2
BSG256.7	21.2	3.60	BSG#1	N2/3
*BSG162.5	16.8	2.77	BSG#1	N2
BSG326.8	15.8	0.76	BSG#1	10YR2/2
BSG172.9	5.4	0.58	BSG#1	5R4/2
BSG309.8	4.9	0.42	BSG#1	5YR3/2
BSG92.1	2.4	0.23	BSG#1	5YR3/2
BSG54.9	4.4	0.19	BSG#1	N5

%AS = % acid soluble material (carbonate).

%TOC = weight % of the whole rock which is organic carbon.

+Offscale.

*Samples which were extracted and subjected to detailed geochemical analysis.
 x-shale with coal fragments
 sap.: sapropel bed c. 40 m upstream from outcrop 15a.

TABLE 8.2

Organic Geochemical Analyses

Sample #	P5	F67	BSG162.5	F35
TOC (wt. %)	21.2	10.7	2.77	0.87
Sample wt (g)	33.27825	36.17096	42.55321	44.60222
mg C in Sample	7.05	3.87	1.18	0.39
mg extract	15.6	25.32	23.5	4.58
mg extract/g Corg	2.2	6.54	19.9	11.8
mg C15+HC/g Corg	0.88	1.73	6.78	5.36
mg Sat.HC (%)	2.20(14.1)	1.10(4.3)	4.0(17)	0.6(13.1)
mg Sat.HC/g Corg	0.28	0.28	3.39	1.5
mg Arom.HC (%)	4.2(26.9)	5.6(22.1)	4.0(17)	1.5(32.8)
mg Arom/g Corg	0.60	1.45	3.39	3.86
mg NSO (%)	4.6(29.5)	7.0(27.6)	5.5(23.4)	1.9(41.5)
mg NSO/g Corg	0.65	2.23	4.66	4.88
mg Asphalt (%)	2.4(15.4)	4.9(19.4)	5.4(23)	0.94(20.5)
mg Asph/g Corg	0.34	1.81	4.58	2.4
Col. Losses mg(%)	2.2(14.1)	6.72(26.5)	4.6(19.6)	-0.36(-7.9)

(%) refers to weight percent of extract. Losses are probably due to the polymerization of NSO compounds to form asphaltenes. The very low initial extract weight of sample F35 probably resulted in large errors.

TOC: Total organic carbon (weight %)

C15+HC: hydrocarbons with more than 15 carbon atoms.

g Corg: grams of organic carbon.

Sat.HC: saturated hydrocarbons.

Arom.HC: aromatic hydrocarbons.

NSO: Organic compounds which contain nitrogen, oxygen, and sulfur.

Asph: asphaltic compounds.

Col. losses: column losses.

TABLE 8.3

Fischer Assay Results (BSG#1)			
Sample	Oil Yield		%TOC
Depth (m)	(gal/T)	(l/T)	
x162.8	1.6	7.13	5.91
x222.1	1.5	6.66	3.39
x222.6	1.2	5.33	2.79
x224.7	1.2	5.33	2.79
x225.9	2.4	10.66	2.78
257.3	0	0	1.71
325.6	0	0	0.8
326.5	0	0	0.8

TABLE 8.4

Sample#	Rock-Eval Analyses					
	Depth(m)	Tmax	S1	S2	S3	S1+S2(l/T)
x84-1A(BSG)	162.8	449	0.14	6.28	0.23	7.13
x84-2A(BGS)	222.1	456	0.10	5.44	0.03	6.15
x84-3A(BSG)	222.6	458	0.06	1.04	0.08	1.22
x84-4A(BSG)	224.7	459	0.03	1.23	0.01	1.40
x84-5A(BSG)	225.9	463	0.01	0.58	0.01	0.65
RH83-249	o/c15a	447	0.51	19.12	0.09	21.49
RH83-251	sap.	441	0.58	56.99	2.03	63.90
RH83-252	sap.	438	0.98	64.21	1.76	72.36
RH83-253	sap.	438	0.97	79.51	0.77	89.33

gal/T: gallons per metric ton; l/T: liters per metric ton.

o/c15a: outcrop 15a

sap.: sapropel bed c. 40 m upstream from outcrop 15a.

x Samples subjected to both pyrolysis and Fischer assay.

S1, S2, S3 peaks are reported in mg/g of sample.

TABLE 8.5

Stable Carbon Isotope Ratios

<u>Sample</u>	<u>Rock Type</u>	<u>Outcrop</u>	<u>$\delta^{13}C$</u>
xF35	green shale	15	-26.265
xP5	dark grey shale	15a	-25.690
xF67	black shale	2a	-26.204
RH83-246	black carbonaceous shale	15a	-24.142
BSG256.7	dark grey shale		-25.370
xBSG162.5	dark grey shale		-25.521
FB777.4	grey shale		-23.848
F7i	nodule in grey shale	6	-13.622
F80	nodule in grey shale	51	-7.977
F77	red-brown "caliche"	89	-13.353
F81	lacustrine micrite	51	-4.398
F72	grey "caliche"	78	-11.407
F2i	nodule in grey shale	1	-20.604

x extracted samples.

Interpretation

Interpretation of the results of the organic geochemical analyses will be discussed in terms of the classification, source, thermal maturity, and quantity of the organic matter, and source rock potential of the Barachois Group mudstones.

Classification and Source of Organic Matter in the Barachois Group

Disseminated organic matter in fine-grained sedimentary rocks consists of a fraction which is soluble in non-oxidizing acids, bases, and organic solvents (bitumen) and an insoluble fraction (kerogen) (Hunt, 1979). The amount of bitumen present in a rock is an indication of the amount of liquid hydrocarbons already present and is a function of thermal maturity and kerogen type. The type of kerogen and the characteristics of the bitumen are an indication of whether rocks are gas-prone or oil-prone, and can provide information on the source of the organic matter.

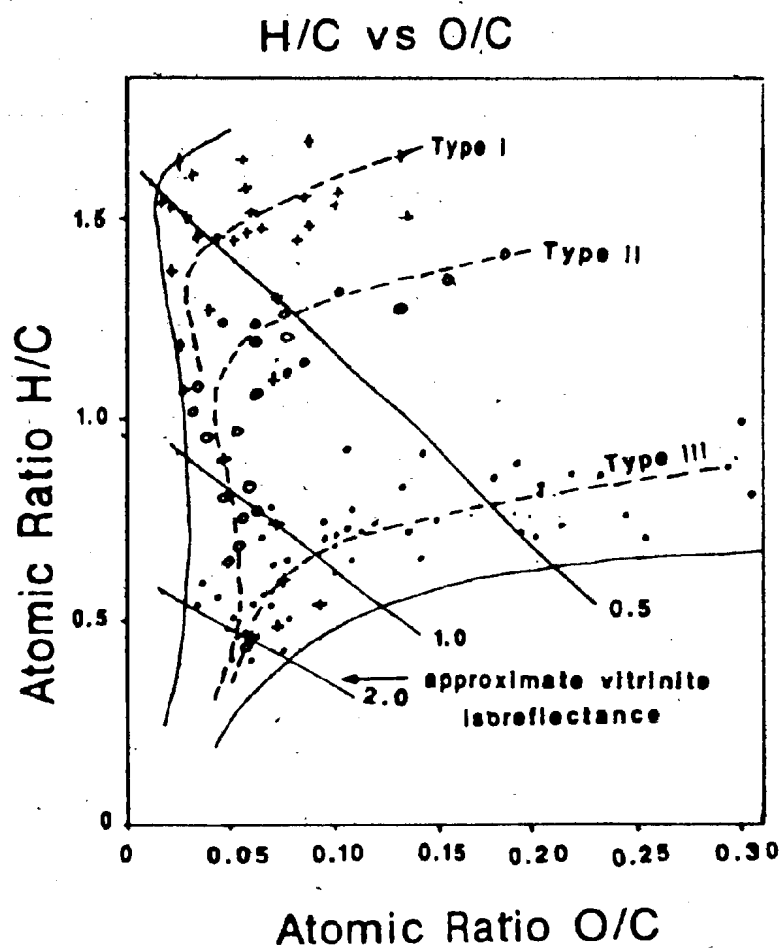
Kerogens are classified on the basis of their microscopic constituents in transmitted or reflected light or by elemental analysis. Kerogens, as classified by transmitted light microscopy, consist of algal, amorphous, herbaceous, woody and coaly types (Hunt, 1979). Algal and amorphous kerogens are usually marine or lacustrine in

origin. Amorphous kerogen is generally sapropelic (derived from the decomposition of high-lipid organic material), but may include some humic components in the form of decomposition products of terrestrially deposited plant cells, wails, plus carbonized organic matter (Tissot and Welte, 1978 p.178). Herbaceous kerogen refers to detritus from plants such as spores, cuticles, and other recognizable, discrete, nonwoody cell material. Woody kerogen is fibril material with rectangular woody structures. Coaly (inertinite) kerogen has undergone extensive carbonisation as a result of oxidation and fungal decomposition (Hunt, 1979, p. 276). Kerogens from the Barachois Group mudstones examined by transmitted light microscopy consist predominantly of the woody type (E. Burden, 1986 pers. comm.). Herbaceous and amorphous kerogens are secondary. In all samples where amorphous kerogens form more than about 8% of the kerogen types they are described as probable degraded wood based on the presence of relict structures in otherwise amorphous organic matter (E. Burden, pers. comm.).

Reflected light microscopy allows classification of kerogens based upon their maceral composition. Macerals refer to different constituents of kerogen or coal which are recognizable by their morphology and reflectance colours. Some data is available on the reflected light properties of the Barachois Group kerogens. Information provided by R.

Hyde (1986, pers. comm.) indicates that identifiable macerals in the coals and organic-rich (or sapropelic) shales of the Barachois Group contain an abundance of vitrinite (>75% of the identifiable macerals), and lesser amounts of inertinite and liptinite. The identifiable macerals are, in some cases (e.g. RH83-249), set in a matrix of clay and amorphous organic material which accounts for c. 30-40% of the sample. Vitrinite and inertinite macerals are indicative of a higher plant origin. Liptinite is derived from algae, spores, cuticle, resins, waxes, etc. (Tissot and Welte, 1979, p. 128). The origin of the amorphous material in shales like RH83-249 is unknown. It is probably algal and/or bacterially degraded humic debris.

Classification of kerogen on the basis of elemental analysis is accomplished by use of a van Krevelen diagram (Fig. 8.1) (Tissot and Welte, 1978). Oxygen to carbon (O/C) ratio is plotted on the horizontal axis; hydrogen to carbon (H/C) ratio is plotted on the vertical axis. Three starting compositions of kerogen are identified primarily on the basis of their H/C ratio. Although amorphous kerogens are usually associated with type I or II kerogens (as classified by elemental analysis), it has been found that amorphous kerogens may plot anywhere on the van Krevelen diagram (Durand and Monin, 1980, p.131; Peters, 1986). As the types of kerogen mature (with increasing time and temperature) they follow different, but convergent, evolutionary pathways



- Maturation pathway
- Boundaries of kerogen fields
- + Green River shales + algal kerogens
- o marine shale + various oil shales
- non-marine shales

Figure 8.1: The van Krevelen diagram illustrates maturation pathways for kerogen types as classified by their atomic ratios. After Tissot and Welte, 1978, p.143.

towards progressively lower H/C and O/C ratios.

Type I kerogen is characterized by the highest H/C ratio. It contains primarily aliphatic hydrocarbons and is derived from algal lipids or lipid-enriched, microbially-degraded, organic matter and contains virtually no identifiable organic remains (Durand and Monin, 1980, p. 128). It is composed of algal and amorphous kerogen (as classified by transmitted light methods). Type I kerogen is considered to be high in oil and gas generative capacity.

Type III organic matter has the lowest initial H/C ratio, relatively higher O/C ratio, and consists mostly of polyaromatic hydrocarbons and oxygenated functional groups. Hydrocarbons formed from type III kerogens are characterized in part by normal alkanes in the C₂₀-C₃₅ range (Durand and Monin, 1980, p.128). Its oil generative potential is moderate, but it may generate large amounts of gas. Type III kerogens are derived from terrestrial higher plants and is comparable to woody and coaly kerogen (Hunt, 1979 p.177).

Type II kerogen is intermediate in terms of H/C and oil- and gas-generating potential and it consists of more aromatic and naphthenic hydrocarbon compounds than type I kerogen. Type II kerogen is a mixture of amorphous, algal, herbaceous, and some woody kerogen (as classified by transmitted light microscopy) (Hunt, 1979 p. 277; Durand and Monin, 1980, p.128).

When elemental analyses are not available for kerogens it is possible to use information from pyrolysis to calculate hydrogen and oxygen indices (S_2/TOC and S_1/TOC respectively) which are in some respects analogous to the H/C and O/C ratios (Espitalie *et al.*, 1977). Van Krevelen-type diagrams based on pyrolysis results can be subject to misinterpretation due to the possibility of contamination of the S_2 peak by high molecular-weight hydrocarbons (Clementz, 1979; Snowdon, 1984). This type of contamination only appears to be a problem in samples with "large" amounts of heavy bitumen (Tissot, 1984). Hydrogen and oxygen indices have been calculated for eight of the nine samples (i.e. those for which TOC data is available) submitted for Rock-Eval pyrolysis. These values are listed in Table 8.6 and plotted on a modified van Krevelen diagram (Fig. 8.2). It can be seen that Barachois Group samples plot parallel to the mature type I and type II kerogen lines (but with a very low oxygen index). Unfortunately these samples plot on a section of the graph which is indeterminate in terms of typing kerogens.

Significant errors in the estimation of the oxygen content (i.e. S_3 peak) in Rock-Eval pyrolysis may be due to the possibility of contamination by carbonates (e.g. calcite, siderite) in the samples (Katz, 1983), and the inability of the Rock-Eval unit to measure carbon monoxide (Peters, 1984). Coals with vitrinite reflectance of 0.63

Table 8.6

Rock-Eval Assessment Parameters						
Sample		PI	S2/S3	TOC	HI	OI
BSG162.8	m	0.02	27.3	5.91	106	4.9
BSG222.1	m	0.02	181.3	3.39	160	0.88
BSG222.6	m	0.05	13	2.79	37	2.9
BSG224.7	m	0.02	123	2.79	44	0.36
BSG225.9	m	0.02	58	1.71	34	0.58
RH83-249		0.03	212	18.87	101	0.48
RH83-251		0.01	28.1	--	--	--
RH83-252		0.02	36.5	31.86	202	5.52
RH83-253		0.01	81.96	31.76	250	2.42

HYDROGEN INDEX vs OXYGEN INDEX

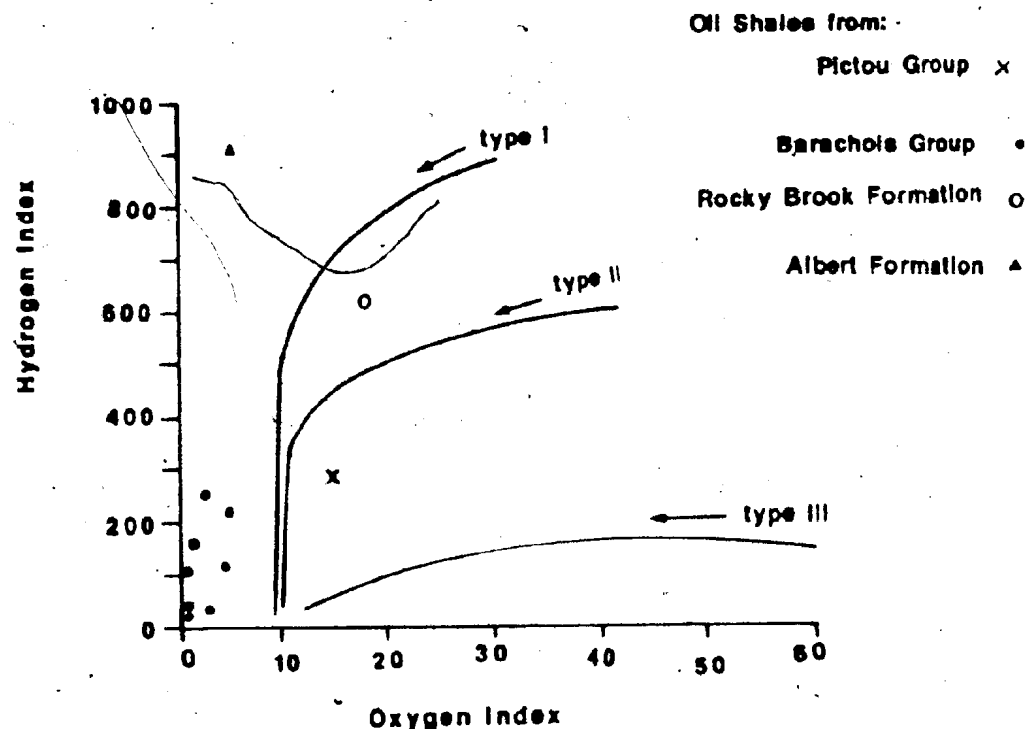


Figure 8.2: Maturation pathways, other Carboniferous oil shales and Barachois Group oil shales as defined by their hydrogen and oxygen indices (HI and OI). HI and OI are determined by pyrolysis. After Nuttal *et al.*, 1983. Data on Albert oil shales is an average of data from the Canadian Occidental Petroleum Albert Mines 2 borehole, Alberta Mines, New Brunswick, reported by (Macauley and Ball, 1982). Data on Rocky Brook Formation oil shales is an average of data from surface samples in the Deer Lake Basin, Newfoundland, reported by Hyde (1984). Data on Pictou Group oil shales is an average of data from the Coal Brook Member, Shaw Pit, near Stellarton, Nova Scotia reported by Macauley and Ball (1984).

release more pyrolytic oxygen as carbon monoxide than less mature coals so samples containing abundant coaly material may show anomalously low S3 peaks. Low S3 peaks and correspondingly low oxygen indices in Barachois Group samples may be caused by an abundance of coaly material.

An alternative method for classifying kerogens using pyrolysis data which does not make use of the S3 peak involves plotting HI vs Tmax (Espitalie et al., 1984). Pyrolysis samples from the Barachois Group are classified as type III and type II kerogens when plotted on this type of diagram (Fig. 8.3).

Additional information regarding organic matter type and source is also provided by analyses of the bitumen fraction of the organic matter. Parameters which are dependent in part on organic matter type are odd-even predominance of normal alkanes (OEP), pristane-phytane ratio (Pr/Ph), pristane-normal C17 ratio (Pr/nC17), and the relative abundances of steranes and hopanes. The data collected for the Barachois Group samples and the values for typical kerogen types are presented in Table 8.7. In general, these data lend support to the contention that the samples are dominated by terrestrial sources of organic matter. The terrestrial signature may be partially overprinted by the presence of lipids derived from prokaryotic organisms (e.g. bacteria) which participate in the degradation of any organic matter.

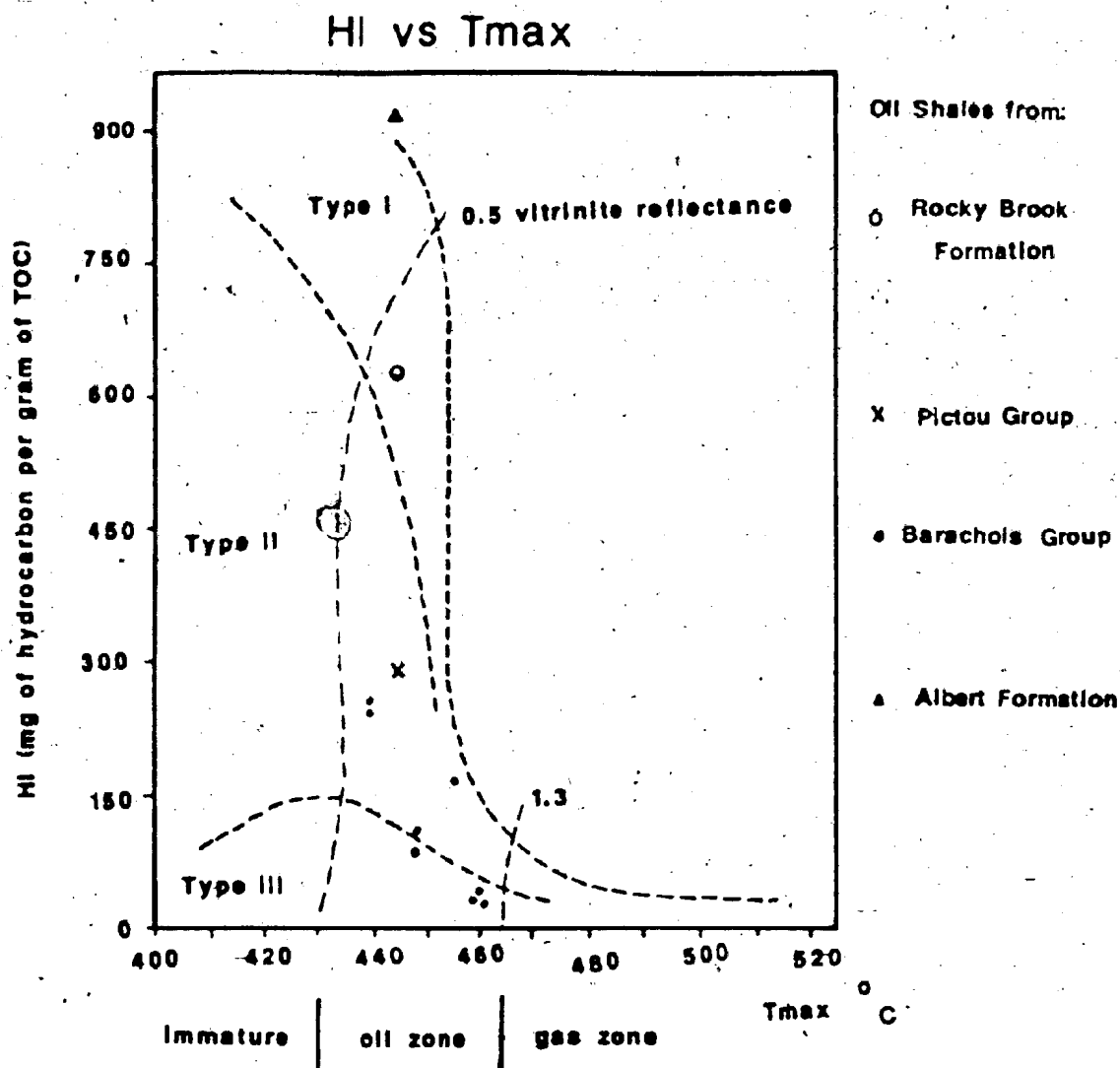


Figure 8.3: Kerogen types and Barachois Group oil shales as defined by hydrogen index (HI) and maximum temperature of the S2 peak (Tmax) determined by pyrolysis. Barachois Group oil shales plot within the oil maturation zone and within kerogen type II and III fields. Data on Albert oil shales is an average of data from the Canadian Occidental Petroleum Albert Mines 2 borehole, Alberta Mines, New Brunswick, reported by (Macauley and Ball, 1982). Data on Rocky Brook Formation oil shales is an average of data from surface samples in the Deer Lake Basin, Newfoundland, reported by Hyde (1984). Data on Pictou Group oil shales is an average of data from the Coal Brook Member, Shaw Pit, near Stellarton, Nova Scotia reported by Macauley

Table 8.7

Indicators of Kerogen Source Based on
Bitumen Extraction

Sample	BSG162.5	P5	F67	Marine or Lacustrine Terrestrial		Source Reference
				Source	Source	
Pr/Ph	3.64	4.53	1.7	<1	>1	a
Pr/nC17	0.78	1.73	0.61	<0.5	>0.5	b
OEP						
C16-C21	1.0	1.0	0.95	odd	none	a
Hopanes	present	present	--	present	present	c
Steranes	trace	trace		high	low	c

Pr/Ph: pristane/phytane ratio

Pr/nC17: pristane/normal C17 ratio

OEP: Odd-Even predominance (Scanlan and Smith, 1970)

a: Hunt, 1979, p.280

b: Lijmbach, 1975

c: Tissot and Welte, 1979, p.380

Stable carbon isotope values ascertained for kerogens of the Barachois Group also tend to corroborate a terrestrial source. Differences between the $\delta^{13}\text{C}$ values for various types of modern organic matter appear to be preserved in a somewhat reduced form in fossil kerogen (Galimov, 1980, p.280). However, there is some overlap between $\delta^{13}\text{C}$ values for ancient marine and terrestrial sedimentary rocks and coals. Therefore, although the $\delta^{13}\text{C}$ values of the Barachois Group rocks are consistent with a terrestrial origin, it is not possible to rule out a marine influence on the basis of isotopic composition only.

All the data related to kerogen classification suggest that type III kerogen is the dominant kerogen type in the Barachois Group mudstones. There appears to be some input of type II and type I kerogens in sapropelic shales (e.g. samples RH83-252, RH83-253, and BSG222). The source of these kerogens is almost certainly terrestrial.

Thermal Maturation

Thermal maturation levels for the Barachois Group rocks were established from the following types of data: vitrinite reflectance, thermal alteration index, illite crystallinity, Rock-Eval pyrolysis (production index, Tmax), organic geochemistry (odd-even predominance-OEP, pristane phytane ratio-Pr/Ph), and proximate analysis of coals (i.e. coal rank). The results are summarized in Table 8.8. The optical parameters, OEP, Pr/Ph, Tmax, and coal rank data

Table 8.8

Maturation Parameters of Ba'achois Group Rocks

<u>Parameter</u>	<u>Data</u>	<u>Correlative Ro%</u>	<u>Source of Correlative Ro</u>
OPTICAL			
Vitrinite Reflectance	0.6-1.18 (Ro%)	--	--
TAI	2-3	0.3-1.2%	Hood <u>et al.</u> , 1975
MINERAL			
Illite Crystallinity	1.12	<0.6%	Guthrie <u>et al.</u> , 1986
ROCK-EVAL			
PI	0.01-0.05	<0.6	Peters, 1986
Tmax	438-464 deg.C	0.6-1.2%	Espitalie <u>et al.</u> , 1984
ORGANIC GEOCHEMISTRY			
Pr/Ph	0.89 to 1.08	1.1-1.2	Radke <u>et al.</u> , 1980
OEP	1 to 1.08	>0.95%	Radke <u>et al.</u> , 1980
HC/Ext(%)	26-41%	>0.05	Foscolos <u>et al.</u> , 1976
COAL RANK	medium to high volatile bituminous	0.6-1.5%	Stach <u>et al.</u> , 1982

Sources of data:

Vitrinite and Illite crystallinity - R. Hyde, pers.comm.;

TAI - E. Burden, pers.comm.

Rock-Eval - I.S.P.G., pers. comm.;

Organic geochemistry - S. Macko and R. Quick, 1986, pers.comm.;

Coal Rank - Hayes, 1949; Hyde, pers. comm.

TAI: Thermal alteration index

PI: Production Index (S1/S1+S2)

Pr/Ph: Pristane/phytane ratio

OEP: Odd/Even predominance

HC/Ext(%): Extractable hydrocarbon/total extract ratio
expressed as a percentage

indicate maturation ranks which span the conventional "oil window" (Heroux et al., 1978). The illite crystallinity value and the production index both suggest immature rank (Guthrie et al., 1986; Peters, 1986). The illite crystallinity values are, in some cases, suspect due to the possibility that the illite is detrital and degraded. The production index is somewhat problematic. The extremely low values for the production indices are caused by the high values of the S2 peaks and the low values of the S1 peaks ($PI = S1 / (S1 + S2)$). This may be due to the type of organic matter in the samples. Type I organic matter may require higher temperatures in order to attain peak generation of hydrocarbons than other types of organic matter (Tissot, 1984; Rohrback et al., 1984; Harwood, 1977; Tissot et al., 1978). The presence of large amounts of type I kerogen would therefore account for low S1 and high S2 yields (and consequent low PI) at temperatures which are seemingly indicative of thermal maturity. Low yields of extractable hydrocarbons may also be accounted for by this explanation. Although the presence of abundant type I kerogen may account for the low PI in the most hydrogen-rich pyrolyzed samples (e.g. RH83-249, RH83-252, RH83-253, BSG222), the other pyrolyzed BSG#1 borehole samples are probably composed primarily of type III organic matter. This would suggest that the small S1 peak is due to the poor oil generating capacity of the type III kerogen. The large S2 peak would

therefore correspond to the generation of light gaseous hydrocarbons rather than heavier liquid hydrocarbons (the flame-ionization detector, used to detect hydrocarbons does not differentiate between light and heavy hydrocarbons, it merely counts carbon atoms). This contradicts evidence in favor of an oil-prone source provided by high values of S2/S3 (greater than L3 for all the Barachois Group pyrolysis samples) (Peters, 1986). However, potential problems with the S3 peak (as discussed above) suggest that it is not a reliable parameter in many cases, and is perhaps too low for some Barachois Group samples.

An alternative to the need for the presence of a hydrogen-rich kerogen to explain the high production indices is that the S2 peaks contain a mixture of pyrolysate and heavy solvent-extractable hydrocarbons (probably NSO compounds and asphaltenes) rather than pyrolysate only (Snowdon, 1984). This is thought to be a problem only in the case of extremely hydrogen-rich samples. The samples subjected to extraction are characterized by very small amounts of extract. Therefore it is unlikely that the relatively high S2 peaks are caused by contamination. The surface samples were not extracted, so it is not known whether or not this explanation is reasonable for those samples.

Quantity of Organic Matter

The quantity of organic matter in rocks of the Barachois Group was ascertained by determining the total organic carbon (TOC) content for a representative group of samples. TOC values range from 0.04% (weight percent) to 31.86%. The highest values are from dark grey to black shales (e.g., N1 to N2, GSA Rock Colour Chart). The lowest values are in red mudstones (e.g., 10R3/4, GSA Rock Colour Chart). In general the cut-off between potential source rocks and non-source rocks is between 0.4% and 1.0% TOC for fine-grained shales (Hunt, 1979 p. 270). It is apparent that many of the rocks sampled have TOC values well above the minimum. However, as mentioned previously, source rock potential is dependent on the type of organic matter present and its state of thermal maturation as well as the gross amount of organic carbon. Figure 8.4 illustrates the apparent stratigraphic relationship between samples with some of the highest TOC values.

Source Rock Potential of the Barachois Group Mudstones

In the previous sections the three parameters necessary to define source rock potential have been discussed (i.e. quantity of organic matter, type of organic matter, and thermal maturity). In general, there appears to be a sufficient amount of organic matter at the correct level of maturation to have produced hydrocarbons. However, the

SAMPLE LOCATIONS AND POSSIBLE CORRELATION OUTCROPS 15 AND 15A

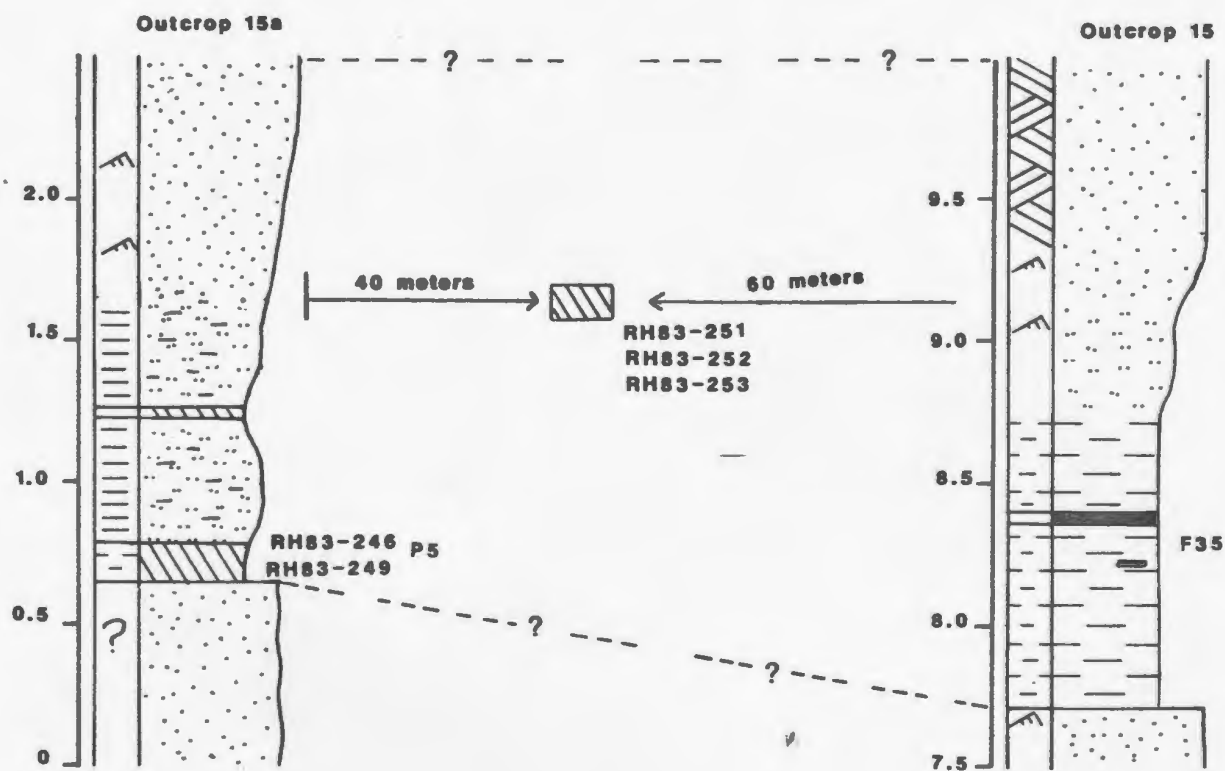


Figure 8.4: Sample locations and possible correlation between outcrops containing samples with high TOC values. The stratigraphic column at outcrop 15a is after Solomon and Hyde, 1985. Samples RH83-251 to 253 were taken from a lens of sapropelic material in the streambed of Middle Barachois Brook.

small amounts of organic extract relative to the abundance of organic matter and indications that type III (woody and coaly) kerogen is the most abundant type in Barachois Group mudstones suggest that any hydrocarbons produced were more likely to be gas rather than oil. Samples which produced relatively large amounts of hydrocarbons by pyrolysis, but which had a relatively small S1 peak (indicative of HC's already produced) may contain kerogens which require a higher thermal maturity to produce hydrocarbons (i.e. type I kerogens). These samples, which all come from the same 0.2 m bed are considered to be oil shales.

Hunt (1979) uses a plot of extractable C15+ hydrocarbons expressed as micrograms per gram of sediment versus TOC to assess source rock potential. Of the four samples for which this information is available only one (BSG162.5) plots within the empirical field for potential source rocks (Fig. 8.5). Two samples (P5 and F67) have high TOC values relative to their extractable HC content and plot towards the coal field on the diagram. The fourth sample (F35) contains too little organic matter to be of interest as a source rock. Rock-Eval parameters for assessing source potential (Table 8.9) include the abundance of TOC and the intensity of the S1 and S2 peaks (Peters, 1986). The pyrolyzed Barachois Group rocks are classified as poor to fair source rocks by these parameters.

SOURCE ROCK QUALITY

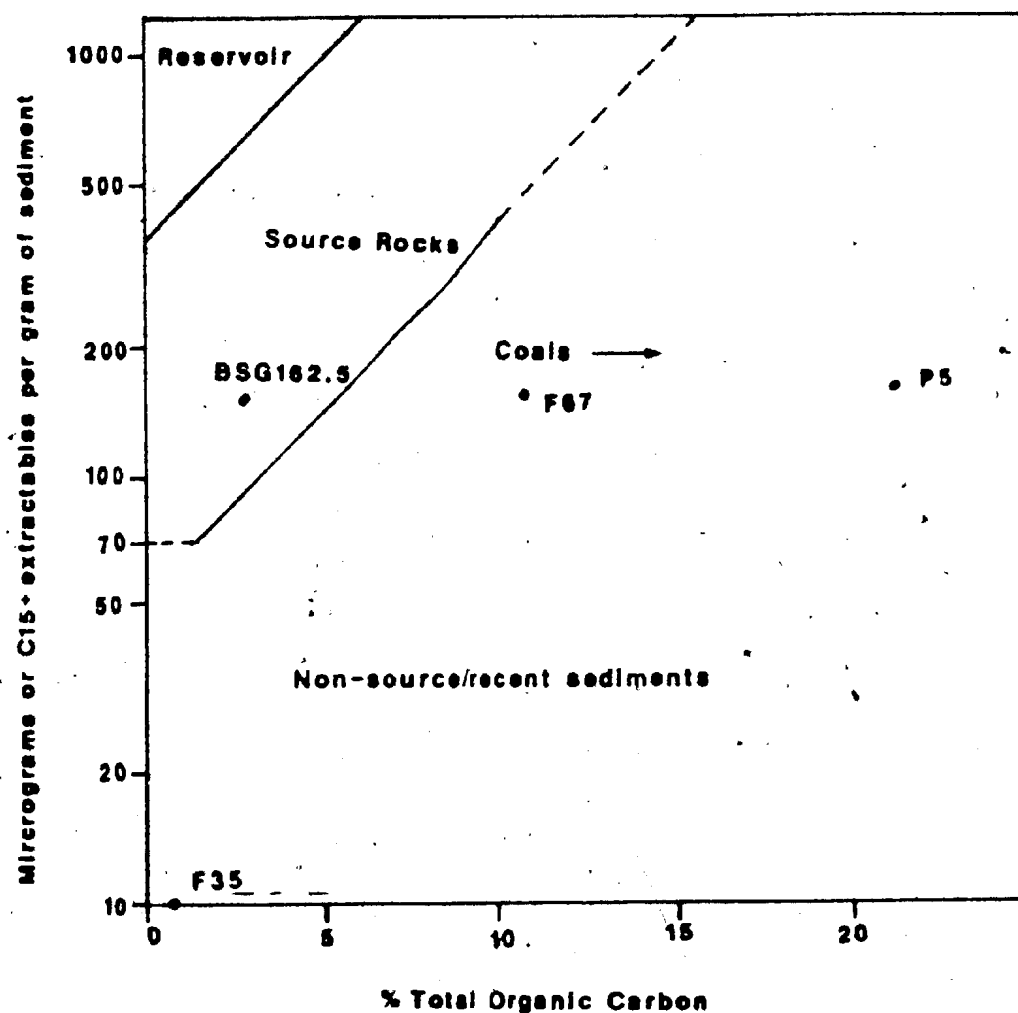


Figure 8.5: Source rock quality based on total organic carbon and the quantity of extractable hydrocarbons. Only sample BSG162.5 from the BSG#1 borehole plots in the source rock field. Samples F67 and P5 probably contain abundant gas-prone and inert material, sample F35 contains only minute amounts of organic matter. After Hunt, 1979.

Table 8.9

Rock-Eval Parameters Used to Describe Potential Source Rocks
(from Peters, 1986)

Type of Hydrocarbons Generated

$S2/S3 = 0 \text{ to } 3$	gas prone
$S2/S1 = 3 \text{ to } 5$	gas and oil
$S2/S3 = >5$	mostly oil

Source Rock Potential

Quality	TOC(%)	$S1$	$S2$
poor	0-0.5	0-0.5	0-0.5
fair	0.5-1.0	0.5-1.0	2.5-5
good	1-2	1-2	5-10
v. good	>2	>2	>10

Thermal Maturity

Maturation	$S1/S1+S2$	T_{max}
top oil window	0.1	435-445
base oil window	0.4	470

Summary

Kerogen types in the Barachois Group are dominated by woody (type III) kerogen with lesser amounts of amorphous and herbaceous kerogens (types I and II). Thermal maturation indices are indicative of temperatures which span the oil window. The presence of thermally mature organic-rich mudstones (up to 31.9% TOC) characterized by abundant woody debris suggests that the Barachois Group is probably a fair potential gas source and a poor potential oil source. Barachois Group oil shales produce from 0.65 to 89.33 liters per metric ton for samples with TOC values from 0.8% to 31.9%. Oil shales with small S1 peaks and large S2 peaks may contain organic matter which requires higher than normal temperatures to generate oil.

CHAPTER 9 - SYNTHESIS OF BARACHOIS GROUP DEPOSITION

Gross Trends in the Barachois Group

Based on the relative ages of the two cores and of the stratigraphically highest and lowest outcrops the deposits of the Barachois Group appear to define a fining-upward megasequence. Textural variations and changes in proportions of facies which provide evidence for the fining-upward megasequence sequence are:

1. an upward decrease in maximum apparent clast size in the field sections and in the FB2-76 borehole (above c. 500 m) (Fig. 9.1),
2. an upward decrease in the proportion of conglomerate facies (facies A and B) (e.g. 25% in FB2-76; 4% in BSG#1), and
3. an upward increase in the proportion of mudstone facies (facies G, H, and I) (e.g. 58% in BSG#1; 39% in FB2-76).

The fining-upward megasequence consists of a lower coarse unit and an upper fine unit which are defined by different, and possibly gradational, styles of sedimentation. The coarse unit is defined as the deposits which are characterized by alternations of thick (meters to tens of meters) grey, conglomerate-dominated channel (and minor sheetflood) deposits (facies association I) and equally thick predominantly red-brown overbank deposits

VARIATIONS IN MAXIMUM CLAST SIZE

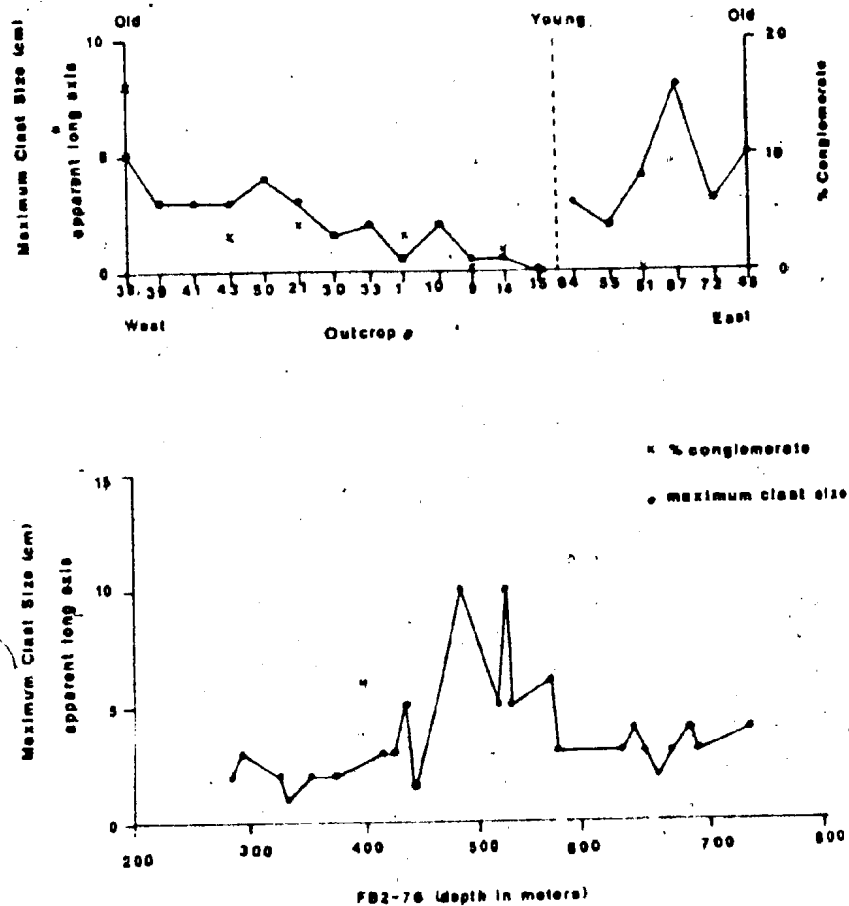


Figure 9.1: Variations in apparent maximum clast size in the FB2-76 borehole, and variations in apparent maximum clast size and percent conglomerate along Middle Barachois Brook. Clasts are smaller above about 400 m in the FB2-76 borehole than below 400 m and both clast size and percent conglomerate reach minima between outcrops 30 and 55 along Middle Barachois Brook.

(facies subassociations IIB and IIIC) (e.g. the FB2-76 core and the exposures at outcrops 38 to 39). The coarse unit comprises the oldest deposits in the study area.

The fine unit (e.g. the BSG#1 core and the exposures east of outcrop 39) consists of a predominance of overbank deposits and minor, relatively thin, channel deposits (e.g., about 80% facies associations II and III versus 20% facies association I in the BSG#1 borehole). Grey-coloured overbank deposits generally increase upward at the expense of red-coloured deposits.

The complete transition between the coarse unit and the overlying fine unit is not seen in the field (as a result of poor exposure). The upper part of the FB2-76 core (above c. 322 m) is characterised by a general thinning- and fining-upward sequence which may represent a transition between the fine and coarse units, but the lack of stratigraphic control does not allow an accurate assessment of its relationship to the other parts of the study area.

It is possible that the inferred upward-fining megasequence may be due to variations in the geographic locations of sections and cores within the paleobasin. For instance, the coarse unit is present at the westernmost outcrops and in the FB2-76 core (drilled at the edge of the present-day structural basin). The fine unit occurs in the centre of the present basin. However, the difference in general paleocurrent dispersal patterns (southerly directed

in the oldest rocks and north-northwesterly directed in the younger rocks), as well as the contrast in sedimentary styles between the oldest and youngest rocks and the presence of the fining-upward trend within the FB2-76 core (i.e. at a particular location) suggests that at least part of the variation is due to changes through time.

Depositional Contrasts Between the Coarse and Fine Units

The coarse deposits (facies association I) of the coarse unit are characterised by an abundance of conglomerate facies and were interpreted to have been laid-down predominantly in stream channels and in a few cases by sheetfloods. The fluvial systems responsible for the deposition of the rocks comprising this facies association were probably characterized by fluctuating discharges and a coarse bedload. Although these characteristics are often considered to be evidence in favor of a low sinuosity, multiple-channel pattern, recent studies of single channel, gravelly rivers suggest that unequivocal evidence for a particular channel-pattern is not provided by these criteria. The deposits of overbank facies associations (facies associations II and III) which characterise the coarse unit were interpreted as having been deposited on poorly-differentiated floodplains. Floods periodically inundated the floodplain and left interbedded

sandstone, siltstone, and mudstone which was vegetated, and usually oxidized after the ponded floodwater drained away. The contact between the channel bodies and the overlying overbank deposits is commonly abrupt, indicating rapid, rather than gradual abandonment of channels or channel-systems.

In contrast, the fine unit is characterised by better differentiation of overbank deposits and by sandstone-dominated fluvial-channel deposits (facies association I) with only minor conglomerate facies. The channel deposits within the fine unit offer little evidence of "flashy" discharge (e.g. muddy drapes) and, at two locations (outcrops 70 and 82), channels eroded into cohesive banks and with muddy channel-fills are interpreted as the deposits of a high-sinuosity fluvial regime (cf. Bridge, 1985; Jackson, 1978). In other locations, evidence for a particular channel pattern is lacking. The fine deposits (facies associations II and III) within the fine unit are red or grey in colour and contain evidence of deposition in coal swamps (subassociation IIIB), lakes (subassociation IIIA), crevasse and levee systems (subassociations IIA and IIB), and small deltas (subassociation IIC). The presence of swamp or lacustrine deposits (rocks assigned to facies subassociations IIIA and IIIB) overlying channel deposits in the fine unit indicate instances of abrupt channel abandonment. In other cases,

levee and crevasse splay deposits overlie the channel deposits gradationally suggesting gradual channel abandonment and/or channel migration. Pedogenic calcium carbonate nodules and concretionary horizons found in facies associations II and III are better developed in the fine unit.

Mineralogical Contrasts Between the Coarse and Fine Units

There are differences between rocks which comprise the fine and coarse units in terms of both clay and sandstone mineralogy. A greater proportion of illite is found in grey mudstones from the FB2-76 borehole than in grey mudstones from the combined outcrops (excluding outcrop 38) and BSC#1 borehole. This suggests that the average illite content of grey mudstones in the fine unit is less than that of the coarse unit. Both quartz and feldspar proportions in sandstones (based on average detrital modes), differ at the 90% level of significance in sandstones of the two units. The average proportion of quartz is greater in the coarse unit than in the fine unit; the average proportion of feldspar is less in the coarse unit.

Based on arguments presented in Chapter 7, the larger illite content in the coarse unit was probably due to the presence of generally more oxidizing post-depositional conditions than were present in the fine unit. The

comparative lack of grey mudstones and the nearly complete lack of organic-rich facies in the coarse unit provides additional evidence in favor of differing average geochemical conditions (e.g., Eh and pH) as determined by climate and drainage characteristics during deposition of the two members.

Differences between the fine and coarse units in terms of sandstone mineralogy could be due to differences in local or regional source area and/or increased weathering and degradation of feldspars due to climatic factors. The evidence in favor of differences in climate and/or drainage characteristics provided above suggests that the degradation of feldspars in the coarse unit may have contributed to the formation of illite (possibly by increasing the concentration of potassium in the groundwater).

Interpretation of Depositional Styles

In a general sense, the deposits of the fine unit were probably laid down in a lower energy environment (and probably on lower gradient slopes) than the coarse unit. This is suggested by the inverse relationship between the percentages of mudstone and conglomerate in the two members and the larger apparent maximum clast size in the coarse unit. Higher water tables and lower gradients (compared to the coarse unit) were probably responsible for the preservation of organic-rich swamp deposits and

grey-coloured lake and distal floodplain deposits in the upper parts of the fine unit. Although water tables were high enough to preserve organic matter and allow small perennial lakes to exist, the presence of banded coals and calcium carbonate-rich pedogenic horizons may indicate periods of relative dryness even in the wettest periods represented by the fine unit.

Factors such as the lack of marine influence, high water tables, low gradients, thick, comparatively well-differentiated floodplains, and gradual abandonment of channels (or channel systems) along with examples of high sinuosity channel deposition suggest that the fine unit was deposited on a source-distal (relative to the coarse unit) alluvial plain by rivers of generally high sinuosity. [Used in this sense, the term alluvial plain refers to laterally extensive landforms which develop down-gradient from coalesced alluvial fans (with which they are transitional) (Rust, 1978; Faniran and Jeje, 1983 p.132; Reading, 1978, p. 15).] River channel patterns at a single location on the alluvial plain may vary considerably over relatively short periods of geological time (e.g. Schumm, 1981; Leopold and Wolman, 1957; Miall, 1985). In addition, it can be difficult to differentiate between the deposits of different river channel types due to the complex interaction of variables (e.g. size of the fluvial system, subsidence rate, aggradation rate, and type and frequency of channel

migration) on which the attributes of those deposits depend (Bridge and Leeder, 1979; Leeder, 1978; Allen, 1965, 1978, Collinson, 1978; McClean and Jerzykiewicz, 1978). Therefore it is not possible to rule out deposition by rivers of a variety of channel morphologies. Multistory channel deposits in the fine unit may have formed by either lateral confinement of channels within a single channel belt or by multiple encounters of different channel belts.

Higher gradients, rare sheetfloods, flashier discharge, coarser channel deposits, and less-well differentiated floodplains suggest that the coarse unit was deposited on a more source-proximal alluvial plain or distal alluvial fan in lower sinuosity, possibly multiple channel rivers (cf. Morisawa, 1968; Schumm, 1981). The deposits of modern distal alluvial fans and proximal alluvial plains are characterized by stratified gravels and planar to cross-bedded sands along with lesser amounts of finer sands and muds (e.g. Williams and Rust, 1969; Boothroyd and Nummedal, 1978). Relatively thick units of vegetated muds with small sand-filled channels were likely deposited on inactive tracts on the alluvial plains (cf. Rust, 1981). Water tables in the coarse unit were probably lower on average than in the fine unit, but not so low that extensive oxidation of channel deposits occurred (i.e. channel deposits probably remained below the water table after their deposition). Pedogenic horizons may be poorly developed due

to frequent flooding and aggradation of the floodplain.

Differences in tectono-climatic settings and/or variations in aggradation/subsidence rates probably contributed to sedimentological differences between the two units. Schumm (1981) describes two end-member tectono-climatic regimes which are characterised by particular "transport" zones (i.e. fluvial systems) and "depositional" zones (i.e. zones of aggradation). Transport zones in sites with relatively dry climates and high relief source-areas (end-member A) are characterised by multiple channel, low-sinuosity river systems with flashy discharges and rapid deposition. Alluvial fans, internally drained alluvial plains (i.e. bajadas) with multistory sand bodies and abundant erosion surfaces comprise the depositional zone end-member A. The opposite end-member (end-member B - low relief, wet source-areas) is characterised by transport zones with bed-load-poor, high-sinuosity river systems with steady discharge and slow deposition of isolated sand bodies on alluvial plains or deltas. The coarse unit of the Barachois Group was likely deposited in a tectono-climatic setting closer to end-member A than end-member B. The fine unit was probably deposited in a setting more intermediate between Schumm's (1981) two end-members, but relatively closer to the low-relief, wet source-area regime (end-member B).

Controls on the Deposition of Organic-rich Facies

Except for coaly material associated with sandstones and two thin coaly laminations near the base of the FB2-76 borehole, coal and other organic-rich facies are restricted to the uppermost portions of the fine unit (i.e., between outcrops 51 and 21 and in the BSG#1 borehole). The compositional variability of the seams and their relatively high ash contents indicate that the peat swamps from which they were formed were subject to variable depositional conditions such as influxes of flood-borne clastic material. The one thick coal seam exposed grades upward to grey mudstone, then to a red mudstone which gradually coarsens upward to ripple-cross-laminated and parallel-stratified sandstone. This scenario represents the progradation of a crevasse splay or levee over the peat swamp thus terminating peat growth. Other coal seams in the St. George's Coalfield exhibit a similar depositional pattern (Bryan, 1938; Solomon and Hyde, 1985).

Sapropelic shales, oil shales, and carbonaceous shales (facies H and I) are rarely exposed in the field sections of the Barachois Group and comprise <1% of the BSG#1 core. These facies were deposited in lakes or ponds of probable limited extent associated with peat swamps and flood basins. The abundance of oxidized floodplain mudstones (subassociation IIIC) and the evidence of pedogenic horizons (in the form of calcium carbonate nodules) interbedded with

organic-rich deposits suggests that environments suitable for the preservation of abundant organic material were limited in time and probably in space as well. Most organic-rich mudstones were found to be generally poor in oil source rock potential and only fair in gas-generating potential. The predominance of woody kerogen in most of the samples is typical of terrestrial environments and is likely due to an abundance of arborescent flora as well as to oxidation of more easily degraded kerogens as they were being transported to their depositional sites.

CHAPTER 10 - CONCLUSIONS

Conclusions

The primary objectives of this study were the description of facies and vertical sequences in the Barachois Group, their interpretation in terms of depositional environment, and the evaluation of the fossil fuel potential of the group. Exposures of the Barachois Group along Middle Barachois Brook and in two cores have allowed the identification of 11 facies which have been grouped into 3 major facies associations and 8 subassociations. These facies associations and subassociations have been interpreted as the product of entirely non-marine, dominantly fluvial, depositional processes.

Preliminary palynological investigations coupled with the sedimentological evidence indicate that the facies associations themselves may be grouped into an older coarse unit and a younger fine unit which comprise a gross fining-upward megasequence. The coarse unit was probably deposited in a source-proximal location on a well-drained alluvial plain or distal alluvial fan. The fine unit was likely deposited in a source-distal location (relative to the coarse unit) by rivers of generally higher-sinuosity on a somewhat swampy, and comparatively well-differentiated floodplain comprised of crevasse, levee, delta, and lake deposits. Differences in clay and sandstone mineralogies

between the two units were probably due to differences in climate and drainage characteristics.

Organic-rich facies (e.g. coal and oil shale) are restricted to the youngest rocks in the fine unit. Available evidence suggests that coals were deposited in planar rather than raised bogs with variable water tables that probably prevented the development of thick extensive seams. Oil shales tend to be relatively lean (maximum c. 90 liters/tonne) and thin ($<0.5\text{m}$). The organic-rich facies in the Barachois Group appear to be mature enough to have produced hydrocarbons, but most kerogens are gas-prone. Channel sandstones are the best reservoir rocks in the Barachois Group, but extensive cementation by silica and clay minerals has reduced porosity to marginally economic levels. Coals and potential reservoir sandstones exhibit faulting and folding, thus complicated development of the hypothetical resources.

REFERENCES

- Allen, J.R.L., 1965; Review of recent alluvial sediments. *Sedimentology*, v.5:89-191.
- Allen, J.R.L., 1974; Studies in fluviatile sedimentation: implications of pedogenic carbonate units, Lower Old Red Sandstone, Anglo-Welsh outcrop. *Geological Journal*, v.9:181-208.
- Allen, J.R.L., 1978; Studies in fluviatile sedimentation: an exploratory quantitative model for the architecture of avulsion controlled alluvial suites. *Sedimentary Geology*, v.21:129-147.
- AMAX Exploration Inc., 1976; Drilling report for salt, St. George's Bay, west Newfoundland. Unpublished report, Open File 12B/7 (208), Newfoundland Department of Mines and Energy, St. John's, Newfoundland.
- Anderson, J.A.R., 1964; The structure and development of the peat swamps of Sarawak and Brunei. *Journal of Tropical Geography*, v.18:7-16.
- April, R.H., 1981a; Trioctahedral smectite and interstratified chlorite/smectite in Jurassic strata of the Connecticut Valley. *Clays and Clay Minerals*, v.29: 31-39.
- April, R.H., 1981b; Clay petrology of the Upper Triassic/Jurassic terrestrial strata of the Newark Supergroup, Connecticut Valley, U.S.A. *Sedimentary Geology*, v.29:283-307.
- Aristarain, L.F., 1971; Clay minerals in caliche deposits of eastern New Mexico. *Journal of Geology*, v.79:75-90.
- Baird, D.M. and P.R. Cote, 1964; Lower Carboniferous sedimentary rocks in southwestern Newfoundland and their relations to similar strata in western Cape Breton Island. *Bulletin of the Canadian Institute of Mining and Metallurgy*, v.57:509-520.
- Baker, H.A., 1927; The St. George's Coalfields, Newfoundland. *Transactions of the Canadian Institute of Mining and Metallurgy*, v.30:327-346.
- Ballance, P.F., 1984; Sheet-flow dominated gravel fans of the non-marine middle Cenozoic Simmler Formation,

Central California. Sedimentary Geology,
v.38:337-359.

- Bannerjee, I., 1977; Experimental study on the effect of deceleration on the vertical sequence of sedimentary structures in silty sediments. Journal of Sedimentary Petrology, v.47:771-783.
- Bell, W.A., 1948; Early Carboniferous strata of the St. Georges Bay area, Newfoundland. Geological Survey of Canada Bulletin #10:45pp.
- Belt, E.S., 1964; Revision of Nova Scotia Carboniferous units. American Journal of Science, v.262:653-673.
- Belt, E.S., 1968; Carboniferous continental sedimentation Atlantic provinces, Canada. In Late Paleozoic and Mesozoic Continental Sedimentation, ed. by G. Devries Klein. Geological Society of America Special Publication #106:127-176.
- Belt, E.S., 1969; Newfoundland Carboniferous stratigraphy and its relation to the Maritimes and Ireland. In Symposium on Stratigraphy and Structure Bearing on Continental Drift in the North American Ocean, ed. by M. Kay. American Association of Petroleum Geologists Memoir 12:734-753.
- Billingsley, P., 1961; Statistical methods in Markov Chains. Annual of Mathematics and Statistics, v.32:12-40.
- Biscaye, P.E., 1965; Mineralogy and sedimentation of recent deep-sea clay in the Atlantic Ocean and adjacent seas and oceans. Bulletin of the Geological Society of America, v.76: 803-832.
- Bjorlykke, K., 1983; Diagenetic reactions in Sandstone. In Sediment Diagenesis, ed. by A. Parker and B.W. Sellwood. D. Reidel, Dordrecht: 169-214.
- Blatt, H., G. Middleton, and R. Murray, 1980; Origin of Sedimentary Rocks. Second edition, Prentice-Hall, Englewood Cliffs, N.J.:782pp.
- Bluck, B.J., 1971; Sedimentation in the meandering River Endrick. Scottish Journal of Geology, v.7:93-138.
- Bluck, B.J., 1974; Structure and directional properties of some valley sandur deposits in southern Iceland.

Sedimentology, v.21:533-554.

Bonnel, G.W., 1984; Coal analysis results to assess the fossil fuel potential of Carboniferous basins in western Newfoundland. Cape Breton Research Laboratory, Unpublished report #84-57:4p.

Boothroyd, J.C. and D. Nummedal, 1978; Proglacial braided outwash: a model for humid alluvial fan deposits. In Fluvial Sedimentology, ed. by A.D. Miall. Canadian Society of Petroleum Geologists Memoir #5: 641-668.

Bouvier, J.L. and S. Abbey, 1980; Simultaneous determination of water, carbon dioxide and sulfur in rocks by volatilization and non-dispersive infra-red absorptiometry. Canadian Journal of Spectroscopy, v.25:126-132.

Bowles, F.A., 1978; Clay as a sediment. In The Encyclopedia of Sedimentology, ed. by R.W. Fairbridge and J. Bourgeois. Dowden, Hutchinson and Ross, Stroudsburg:136-142.

Bradu, D. and R. Hawkins, 1982; Location of multiple outliers in 2-way tables using tetrads. Technometrics, v.24: 103-108.

Braman, P.R. and L.V. Hills, 1977; Palynology and paleoecology of the Mattson Formation, Northwestern Canada. Bulletin of Canadian Petroleum Geology, v.25:582-630.

Brewer, R. 1964; Fabric and Mineral Analysis of Soils. Wiley and Sons, N.Y.:470pp.

Bridge, J.S., 1985; Paleochannel patterns from alluvial deposits: a critical evaluation. Journal of Sedimentary Petrology, v.55:579-589.

Bridge, J.S. and M.R. Leeder, 1979; A simulation model of alluvial stratigraphy. Sedimentology, v.26:627-644.

Bridge, J.S., P.M. Van Veen, L.C. Matten, 1980; Aspects of the sedimentology, palynology, and paleobotany of the Upper Devonian Southern Kerry Head Sandstone, County Kerry, Ireland. Geological Journal, v.15:143-160.

Brewster, G.R., 1980; Effect of chemical pretreatment on x-ray powder diffraction characteristics of clay

minerals derived from volcanic ash. *Clays and Clay Minerals*, v.28:303-310.

Brindley, G.W., 1980; Quantitative x-ray mineral analysis of clays. In *Crystal Structures of Clay Minerals and their X-ray Identification*, ed. by G.W. Brindley and G.Brown. Mineralogical Society of London:411-438.

Brindley, G.W., 1981; X-ray identification (with ancillary techniques) of clay minerals. In *Clay Minerals and the Resource Geologist*, ed. by F.J. Longstaffe. Mineralogical Association of Canada, short course #3:22-38.

Brown, G. and G.W. Brindley, 1980; X-ray diffraction procedures for clay mineral identification. In *Crystal Structures of Clay Minerals and their X-ray Identification*, ed. by G.W. Brindley and G.Brown. Mineralogical Society of London:305-358.

Bryan, A.M., 1938; St. George's Coalfield, Newfoundland. Geological Survey of Newfoundland Information Circular #5.

Bustin, R.M., A.R. Cameron, D.A Grieve, and W.D. Kalkreuth, 1983; Coal Petrology. Its Principles, Methods and Applications. Geological Association of Canada. Short Course Notes, v.3:273p.

Byers, C.W., 1974; Shale fissility: relation to bioturbation. *Sedimentology*, v.21:479-484.

Carr, T.R., 1982; Log-linear models, Markov chains and cyclic sedimentation. *Journal of Sedimentary Petrology*, v.52:905-912.

Carrigy, M.A. and G.B. Mellon, 1964; Authigenic clay mineral cements in Cretaceous and Tertiary sandstones of Alberta. *Journal of Sedimentary Petrology*, v.34:461-472.

Carrol, D., 1970; Clay Minerals: a guide to their x-ray identification. Geological Society of America Special Paper #126:80p.

Cecil, C.B., R.W. Stanton, S.G. Neuzil, F.T. Dulong, L.F. Ruppert, and B.S. Pierce, 1985; Paleoclimate controls on Late Paleozoic sedimentation and peat formation in the Central Appalachian Basin (U.S.A.). *International Journal of Coal Geology*, v.5:195-230.

- Chorlton, L.B., 1984; Geological development of the southern Long Range Mountains, southwest Newfoundland: A regional synthesis. Unpublished Ph.D. thesis, Memorial University of Newfoundland: 581pp.
- Clayton, G., R. Coquel, J. Doubinger, K.J. Guenin, S. Loboziak, B. Owens, and M. Streel, 1977; Carboniferous miospores of Western Europe, illustration and zonation. Mededelingen Rijks Geologische Dienst, v.29:71pp.
- Clementz, D.M., 1979; Effect of oil and bitumen saturation on source rock pyrolysis.. American Association of Petroleum Geologists Bulletin, v.63:2227-2232.
- Coleman, J.M., 1969; Brahmaputra River: Channel processes and sedimentation. Sedimentary Geology, v.3:129-239.
- Coleman, J.M., S.M. Gagliano, and J.M. Webb, 1964; Minor sedimentary structures in a prograding distributary. Marine Geology, v.1:240-258.
- Coleman, J.M. and S.M. Gagliano, 1965; Sedimentary structures: Mississippi deltaic plain. In Primary Sedimentary Structures and their Hydrodynamic Interpretation. ed. by G.V. Middleton. Society of Economic Petrologists and Mineralogists Special Publication #12:133-148.
- Coleman, L.M., 1966; Ecological changes in a massive fresh water clay sequence. Transactions of the Gulf Coast Association of Geological Societies, v.16:159-174.
- Collinson, J.D., 1970; Bedforms of the Tana River, Norway. Geografiska Annaler Series 52-A:31-56.
- Collinson, J.D., 1978; Vertical sequence and sand body shape in alluvial sequences. In Fluvial Sedimentology. ed. by A.D. Miall, Canadian Society of Petroleum Geologists Memoir #5:577-586.
- Cook, H.E., P.D. Johnson, J.C. Matti, and I. Zemmels, 1975; Methods of sample preparation and x-ray diffraction data analysis, x-ray mineralogy laboratory, Deep-sea drilling project, University of California, Riverside. D.S.D.P Report,

v.28:999-1008.

Costello, W.R., and R.G. Walker, 1972; Pleistocene sedimentology, Credit River, Southern Ontario; a new component of the braided river model. *Journal of Sedimentary Petrology*, v.42:389-400.

Dickinson, W.R., 1970; Interpreting detrital modes of greywackes and arkose. *Journal of Sedimentary Petrology*, v.40:695-707.

Doeglas, D.J., 1962; The structure of sedimentary deposits of braided rivers. *Sedimentology*, v.1:167-190.

Dowling, D.B., 1920; St. George's Coalfield, Newfoundland. Geological Survey of Newfoundland, Unpublished report, open file 12B(3).

Duchaufour, P., 1977; *Pedology*. George Allen and Unwin, London:448pp.

Durand, B. and J.C. Monin, 1980; Elemental analysis of kerogens (C, H, O, N, S, Fe). In *Kerogen*, ed. by B. Durand, Editions Technip, Paris:113-142.

Durand, B., J. Espitalie, and J.L.Oudin, 1970; Analyse geochemique de la matiere organique extraite des roches sedimentaire III. Accroissement de la rapidite du protocole operatoire par l'amelioration de l'appareillage. *Revue de L'Institut Francais du Petrole XXV*, #11:1268-1279.

Elliot, T., 1974; Interdistributary bay sequences and their genesis. *Sedimentology*, v.21:611-622.

Espitalie, J., M. Madec, B. Tissot, J.J. Mennig, and P. Leplat, 1977; Source rock characterization method for petroleum exploration. Ninth Offshore Technology Conference, OTC 2935, v.3:439-444.

Espitalie, J. F. Marquis, and J. Barsony, 1984; Geochemical logging. In *Analytical Pyrolysis*. ed. by K.J. Voorhees. Butterworths, London:276-304.

Ethridge, F.G., T.J. Jackson, and A.D. Youngberg, 1981; Floodbasin sequence of a fine grained meander belt subsystem: the coal-bearing Lower Wasatch and Upper Fort Union Formations, southern Powder River Basin, Wyoming. In *Recent and Ancient Non-marine*

Depositional Environments: Models for Exploration.
ed. by F.G. Ethridge and R.M. Flores. S.E.P.M.
Special Publication #31:191-209.

Faniran, A and L.K. Jeje, 1983; Humid Tropical
Geomorphology. Longman, London:414pp.

Farquharson, G.W., 1982; Lacustrine deltas in a Mesozoic
alluvial sequence from Camp Hill, Antarctica.
Sedimentology, v.29:717-725.

Fielding, C.R., 1984; A coal depositional model for the
Durham Coal Measures of northeast England. Journal
of the Geological Society of London, v.141:919-931.

Flach, K.W., W.D. Nettleton, and R.E. Nielson, 1971; The
micromorphology of silica-cemented soil horizons in
western North America. In Soil Microscopy. ed. by
G.K. Rutherford. Brown and Martin, Kingston,
Ontario:715-729.

Flores, R.M., 1981; Coal deposition in fluvial
paleoenvironments of the Paleocene Tongue River Member
of the Fort Union Formation, Powder River Basin,
Wyoming and Montana. In Recent and Ancient Non-marine
Depositional Environments: Models for Exploration.
ed. by F.G. Ethridge and R.M. Flores. S.E.P.M.
Special Publication #31:169-190.

Folk, R.L., 1980; Petrology of Sedimentary Rocks.
Hemphill Publishing Company, Austin, Texas:182pp.

Fong, C.C.K., 1976; Geological mapping, northern half of
the St. George's Bay Carboniferous Basin. In
Report of Activities 1975. Ed. by B.A. Greene.
Mineral Development Division, Newfoundland Department
of Mines and Energy. Report 76-1:2-9.

Foscolos, A.E., T.C. Powell, and P.R. Gunther, 1976; The
use of clay minerals and organic and inorganic
geochemical indicators for evaluating the degree of
diagenesis and oil generating potential of shales.
Geochimica et Cosmochimica Acta, v.40:953-966.

Freytet, P. and J.-C. Plaziat, 1982; Continental
carbonate sedimentation and pedogenesis - late
Cretaceous and early Tertiary of southern France.
In Contributions to Sedimentology. Ed. by B.H.
Pürser, E. Schweizerbart'sche Verlagsbuchhandlung,
Stuttgart, v.12:213pp.

- Friend, P.F., 1966; Clay fractions and colours of some Devonian red beds in the Catskill Mountains, U.S.A. Quarterly Journal of the Geological Society of London, v.122:273-292.
- Galimov, E.M., 1980; Carbon 13/carbon 12 in kerogen. In Kerogen, ed. by B. Durand, Editions Technip, Paris:271-299.
- Geldsetzer, H.H.J., 1979; Depositional development of the Late Visean Windsor Group in Atlantic Canada. Abstract. In Ninth International Congress of Carboniferous Stratigraphy and Geology, Urbana, Illinois:68-69.
- Gersib, G.A. and P.J. McCabe, 1981; Continental coal-bearing sediments of the Port Hood Formation (Carboniferous), Cape Linzee, Nova Scotia, Canada. In Recent and Ancient Non-marine Depositional Environments: Models for Exploration, ed. by F.C. Etheridge and R.M. Flores, S.E.P.M. Special Publication #31:95-108.
- Gibling, M.R. and B. Ratanasthien, 1980; Cenozoic basins of Thailand and their coal deposits; a preliminary report. Geological Society of Malaysia Bulletin, v.13:27-42.
- Gibling, M.P., B.R. Rust, A. Aksu, 1985; Mudrocks of the Pennsylvanian Morien Group, Sydney Coalfield, mud deposition and early diagenesis of an alluvial. Geological Association of Canada Programme with Abstracts, v.10:A21.
- Gibling, M.R., Y. Ukakimaphan, and S. Srisuk, 1985; Oil shale and coal in intermontane basins of Thailand. Bulletin of the American Association of Petroleum Geologists, v.69:760-766.
- Gile, L.M., F.P. Peterson, and R.B. Grossman, 1966; Morphological and genetic sequences of carbonate accumulation in desert soils. Soil Science, v.101:347-360.
- Gingerich, P.D., 1969; Markov analysis of cyclic alluvial sediments. Journal of Sedimentary Petrology, v.39:330-332.
- Gole, C.V. and S.V. Chitale, 1966; Inland delta building activity of the Kosi River. Journal of the Hydraulic

Division of the American Society of Civil Engineers,
v.92:111-126.

Goudie, A.S., 1983; Calcrete. In Chemical Sediments and
Geomorphology, ed. by A.S. Goudie and K. Pye, Academic
Press, London:93-132.

Gustavson, T.C., 1978; Bedforms and stratification types
of modern gravel meander lobes, Nueces River, Texas.
Sedimentology, v.25:401-426.

Guthrie, J.M., D.W. Houseknecht, and W.D. Johns, 1986;
Relationships among vitrinite reflectance, illite
crystallinity, and organic geochemistry in
Carboniferous strata, Ouachita Mountains, Oklahoma
and Arkansas. Bulletin of the American Association
of Petroleum Geologists, v.70:26-33.

Hacquebard, P.A., 1972; The Carboniferous of Eastern
Canada. Comptes Rendu, 7th Congres International de
Stratigraphie et de Geologie du Carbonifere,
Krefield:69-90.

Hacquebard, P.A., M. A. Barss, and J.R. Donaldson, 1961;
Distribution and stratigraphic significance of small
spore genera in the Upper Carboniferous of the
Maritime provinces of Canada. Comptes Rendu, 4th
Congres International de Stratigraphie et de
Geologie du Carbonifere, Heerlen:237-245.

Hakanson, L. and M. Jansson, 1983; Principles of Lake
Sedimentology. Springer-Verlag, Berlin:316pp.

Happ, S.C., G. Rittenhouse, and G.C. Dobson, 1940; Some
aspects of accelerated stream and valley
sedimentation. U.S. Department of Agriculture
Technical Bulletin #695:134pp.

Harper Jr., C.W., 1984; Facies models revisited:an
examination of quantitative methods. Geoscience
Canada, v.11:203-207.

Harms, J.C. and R.K. Fahnestock, 1965; Stratification,
bedforms, and flow phenomena (with an example from the
Rio Grande). In Primary Sedimentary Structures and
their Hydrodynamic Interpretation, ed. by G.V.
Middleton, S.E.P.M. special publication 12:84-115.

Harms, J.C., 1969; Hydraulic significance of some sand
ripples. Bulletin of the Geological Society of

America, v.80:363-396.

Harms, J.C., J.B. Southard, and R.G. Walker, 1982; Structures and Sequences in Clastic Rocks. S.E.P.M. Short Course #9.

Harwood, M.E., A.A. Thiesen, and D.D. Evans, 1962; Effect of iron removal and dispersion methods on clay mineral identification by x-ray diffraction. Soil Science Society of America Proceedings, v.26:535-541.

Harwood, R.J., 1977; Oil and gas generation by laboratory pyrolysis of kerogen. In Hydrocarbon Generation and Source Rock Evaluation (Origin of Petroleum III), A.A.P.G. Reprint Series #24:78-98.

Hayes, A.O., 1949; Coal possibilities of Newfoundland. Geological Survey of Newfoundland Information Circular #6:20pp.

Hayes, A.O. and H. Johnson, 1938; Geology of the Bay St. George Carboniferous Area. Geological Survey of Newfoundland Bulletin #12:62pp.

Heath, G.R. and N.G. Pias, 1979; A method for the quantitative estimation of clay minerals in North Pacific deep sea sediments. Clays and Clay Minerals, v.27:175-184.

Heroux, Y., A. Chagnon, and R. Bertrand, 1978; Compilation and correlation of major thermal maturation indicators Bulletin of the American Association of Petroleum Geologists, v.63:2128-2144.

Hicks, L.G., 1984; Sedimentology and Petrography of the Shell et al. North Sydney G-24 Well, Cabot Strait. Unpublished BSc. thesis, Memorial University of Newfoundland:157pp.

Hiscott, R.H., 1984; Clay mineral petrology and clay mineral provenance of Cretaceous and Paleogene strata, Labrador and Baffin shelves. Bulletin of Canadian Petroleum Geology, v.32:272-280.

Hobson, G.D. and A. Overton, 1973; Sedimentary refraction seismic surveys, Gulf of St. Lawrence. In Earth Science Symposium on Offshore Eastern Canada, ed. by P.J. Hood. Geological Survey of Canada Paper 71-23:325-336.

- Hoffe, B. 1985; Well-log Interpretation of BSGE1, Bay St. George Basin, Western Newfoundland. Unpublished BSc. thesis, Memorial University of Newfoundland:66pp.
- Hoffman, J. and J. Hower, 1979; Clay mineral assemblages as low-grade metamorphic geothermometers: applications to the thrust-faulted Disturbed Belt of Montana, U.S.A. In Aspects of Diagenesis, ed. by P.A. Scholle and P.R. Schluger. S.E.P.M. Special Publication #26:55-80.
- Hogg, S.E., 1982; Sheetfloods, sheetwash, sheetflow, or....? Earth Science Reviews, v.18:59-76.
- Hood, A, C.C.M. Gutjahr, and R.L. Heacock, 1975; Organic metamorphism and the generation of petroleum. Bulletin of the American Association of Petroleum Geologists, v.59:986-996.
- Hower, J., 1981; Shale diagenesis. In Short Course in Clays and the Resource Geologist, ed. by F.J. Longstaffe. Mineralogical association of Canada, Short Course Handbook, v.7:60-80.
- Howie, R.D. and M.S. Barss, 1975; Upper Paleozoic rocks of the Atlantic Provinces, Gulf of St. Lawrence and adjacent continental shelf. In Offshore Geology of Eastern Canada v.2, ed. by W.J.M. van der Linden and J.A. Wade. Geological Survey of Canada paper 74-30:35-50.
- Howley, J.P., 1896; Newfoundland, Mineral resources of the Colony. Government of Britain Colonial Reports, Miscellaneous #7:13-18.
- Howley, J.P., 1913; Our Coal Areas. Lecture delivered before the Board of Trade, April 1, 1913. Open File Newfoundland 17, Newfoundland Department of Mines and Energy, St. John's.
- Howse, A. and J. Fleischman, 1982; Coal assessment in the Bay St. George Carboniferous Basin. In Current Research 1982, ed. by C.F. O'Driscoll and R.V. Gibbons. Mineral Development Division, Newfoundland Department of Mines and Energy Report #83-1:214-218.
- Hudson, J.P., 1977; Stable isotopes and limestone lithification. Journal of the Geological Society of London, v.133:637-660.
- Hunt, C.B., 1972; Geology of Soils. Freeman and Company,

San Francisco:344pp.

Hunt, J.M., 1979; Petroleum Geochemistry and Geology. Freeman and Company, San Francisco:617pp.

Hyde, R.S., 1984; Oil shales near Deer Lake, Newfoundland. Geological Survey of Canada, Open File Report OF1114:10pp.

Jackson, M.L., S.A. Tyler, A.L. Willis, G.A. Bourbeau, and R.D. Pennington, 1952; Weathering sequence of clay-sized minerals in soils and sediments. International Journal of Physical Colloidal Chemistry, v.52:1237-1260.

Jackson, R.G. II, 1975; Velocity-bedform-texture patterns of meander bends in the Lower Wabash River of Illinois and Indiana. Bulletin of the Geological Society of America, v.86:1511-1522.

Jackson, R.G. II, 1976a; Depositional models of point bars in the Lower Wabash River. Journal of Sedimentary Petrology, v.46:579-594.

Jackson, R.G. II, 1976b; Large scale ripples of the Lower Wabash River. Sedimentology, v.23:593-623.

Jackson, R.G. II, 1978; Preliminary evaluation of lithofacies models for meandering streams. In Fluvial Sedimentology, ed. by A.D. Miall, Canadian Society of Petroleum Geologists Memoir #5:543-576.

Jahns, R.H., 1947; Geological features of the Connecticut Valley as related to recent floods. U.S.G.S. Water Supply Paper #996:158pp.

James, W.C., G.H. Mack, and L.J. Suttner, 1981; Relative alteration of microcline and sodic plagioclase in semi-arid and humid climates. Journal of Sedimentary Petrology, v.51:151-164.

Johnson, S.Y., 1984; Cyclic fluvial sedimentation in a rapidly subsiding basin, northwestern Washington. Sedimentary Geology, v.38:361-391.

Jongerius, A., 1970; Some morphological aspects of regrouping phenomena in Dutch Soils. Geoderma, v.4:311-331.

Jopling, A.V., 1965; Laboratory study of the distribution

of grain sizes in cross-bedded deposits. In Primary Sedimentary Structures and their Hydrodynamic Interpretation, ed. by G.V. Middleton, S.E.P.M. Special Publication #12:53-65.

Jukes, J.B., 1843; General Report of the Geological Survey of Newfoundland, John Murray, London.

Karcz, I., 1972; Sedimentary structures formed by flash floods in southern Israel. Sedimentary Geology, v.7:161-182.

Katz, B.J., 1983; Limitations of "Rock-Eval" pyrolysis for typing organic matter. Organic Geochemistry, v.4:195-199.

Klappa, C.F., 1980; Rhizoliths in terrestrial carbonates; classification, recognition, genesis, and significance. Sedimentology, v.27:613-629.

Klappa, C.F., in press; A process response model for the formation of pedogenic calcretes. Journal of the Geological Society of London.

Knight, I., 1979; Coal in the Bay St. George Basin: a geofiles review. Mineral Development Division, Newfoundland Department of Mines and Energy, unpublished report.

Knight, I., 1983; Geology of the Carboniferous Bay St. George Subbasin, western Newfoundland. Mineral Development Division, Department of Mines and Energy Memoir #1:358pp.

Kodama, H. and K. Oinuma, 1963; Identification of kaolin minerals in the presence of chlorite by x-ray diffraction and infra-red absorption spectra. Clays and Clay Minerals, v.11:236-249.

Kumar, S. and I.B. Singh, 1978; Sedimentological study of Gomti River sediments, Uttar Pradesh, India. Examples of a river in an alluvial plain. Senckerbergiana Marit., v.10:145-211.

Lee, M.J. and S. Chadhuri, 1976; Clay mineral studies of the Lower Permian Havenville Shale in Kansas and Oklahoma. Clays and Clay Minerals, v.24:239-245.

Leeder, M.R., 1978; A quantitative stratigraphic model for alluvium with special reference to channel deposit

density and interconnectedness. In Fluvial Sedimentology, ed. by A.D. Miall, Canadian Society of Petroleum Geologists Memoir #5:587-596.

Leopold, L.B. and M.G. Wolman, 1957; River channel patterns; braided, meandering, and straight. U.S.G.S. professional Paper #282B:39-85..

Levey, R.A., 1978; Bedform distribution and internal stratification of coarse grained point bars, Upper Congaree River, South Carolina. In Fluvial Sedimentology, ed. by A.D. Miall, Canadian Society of Petroleum Geologists Memoir #5:105-127.

Lijmbach, G.M.G., 1975; On the origin of petroleum. In 9th World Petroleum Congress Proceedings, London, v.2:357-369.

Lowe, D.R., 1982; Sediment gravity flows: II. Depositional models with special reference to the deposits of high-density turbidity currents. Journal of Sedimentary Petrology, v.52:279-297.

Lowe, D.R. 1975; Water-escape structures in coarse-grained sediments. Sedimentology, v.22:157-204.

Macauley, G., 1984; Geology of the oil shale deposits of Canada. Geological Survey of Canada Paper #81-25:65pp.

Macauley, G. and F.D. Ball, 1982; Oil shales of the Albert Formation, New Brunswick. Mineral Resources Division of the Department of Natural Resources, New Brunswick, Open File Report #82-12:173pp.

Macauley, G. and F.D. Ball, 1984; Oil shales of the Pig Marsh and Pictou areas, Nova Scotia. Geological Survey of Canada, Open File Report OF1037:57pp.

McBride, E.F., 1974; Significance of colour in red, green, purple, olive, brown, and grey beds of the Difunta Group, northeast Mexico. Journal of Sedimentary Petrology, v.44:760-773.

McCabe, P.J., 1984; Depositional environment of coal and coal-bearing strata. In Sedimentology of Coal and Coal-bearing Sequences, ed. by R.A. Rahmani and R.M. Flores, International Association Of Sedimentologists Special Publication 7:13-42.

- McClellan, J.R. and T. Jerzykiewicz, 1978; Cyclicity, tectonic, and coal: some aspects of fluvial sedimentology in the Brazeau-Paskapoo Formations, Coal Valley Area Alberta, Canada. In *Fluvial Sedimentology*, ed. by A.D. Miall, Canadian Society of Petroleum Geologists Memoir #5:441-468.
- McGowen, J.H. and L.E. Garner, 1970; Physiographic features and stratification types of coarse-grained point bars: modern and ancient examples. *Sedimentology*, v.14:77-111.
- McKee, E.D., E.J. Crosby, and H.L. Berryhill Jr., 1967; Flood deposits, Bijou Creek, Colorado, June, 1965. *Journal of Sedimentary Petrology*, v.37:829-851.
- McPherson, J.G., 1980; Genesis of variegated redbeds in the fluvial Aztec Siltstones (Late Devonian), southern Victoria Land, Antarctica. *Sedimentary Geology*, v.27:119-142.
- Mehra, O.P. and M.L. Jackson, 1960; Iron oxide removal from soils by a dithionite-citrate system buffered with sodium bicarbonate. In *Clays and Clay Minerals*, ed. by E. Ingerson, Monograph #5 Earth Science Series, Pergamon Press:317-327.
- Miall, A.D., 1973; Markov chain analysis applied to ancient alluvial plain successions. *Sedimentology*, v.20:347-364.
- Miall, A.D., 1977; A review of the braided river depositional environment. *Earth Science Reviews*, v.13:1-62.
- Miall, A.D., 1978; Lithofacies types and vertical profiles in braided river deposits: a summary. In *Fluvial Sedimentology*, ed. by A.D. Miall, Canadian Society of Petroleum Geologists Memoir #5:597-604.
- Miall, A.D., 1985; Architectural element analysis: a new method of facies analysis applied to fluvial deposits. In *Recognition of Fluvial Depositional Systems and their Resource Potential*, ed. by R.M. Flores, S.E.P.M. Short Course Notes #19:33-82.
- Millot, G. 1970; *Geology of Clays*. Springer-Verlag, New York:429pp.
- Morisawa, M., 1968; *Streams: their dynamics and morphology*.

McGraw-Hill, New York:175pp.

Morisawa, M. 1985; Rivers: Form and Process. Longman, London:222pp.

Murray, A., 1873; Report of the Geological Survey for the year 1872. Geological Survey of Newfoundland:298-350.

Nijman, W. and C. Puigdefabregas, 1978; Coarse grained point bar structure in a molasse type fluvial system, Eocene Castisent Sandstone Formation, southern Pyrenean Basin. In Fluvial Sedimentology, ed. by A.D. Miall, Canadian Society of Petroleum Geologists Memoir #5:487-510.

Nilsen, T.H., 1982; Alluvial fan deposits. In Sandstone Depositional Environments, ed. by P.A. Scholle and D. Spearing, American Association of Petroleum Geologists Memoir #31:49-86.

Norman, M.B., 1974; Improved techniques for selective staining of feldspar and other minerals using amaranth. U.S.G.S. Journal of Research, v.2:73-79.

Nuttall, H.E., Tian-Mingus, S. Schrader, and D.S. Thakur, 1983; Pyrolysis kinetics of several key world oil shales. In Geochemistry and Chemistry of Oil Shales, ed. by F.P. Miknis, and J.F. McKay, American Chemical Society, Washington, D.C.:269-300.

Ostrum, M.E., 1961; Separation of clay minerals from carbonate by using acid. Journal of Sedimentary Petrology, v.31: 123-129.

Parkash, B., A.K. Anashti, and K. Gohain, 1983; Lithofacies of the Markanda Formation, Kurukshetra District, Haryana, India. In Modern and Ancient Fluvial Environments, ed. by J.D. Collinson and J. Lewin, Special Publication of the International Association of Sedimentologists, v.6:337-344.

Peters, K.E., 1986; Guidelines for evaluating petroleum source rock using programmed pyrolysis. Bulletin of the American Association of Petroleum Geologists, v.70:318-329.

Pettijohn, F.S., P.E. Potter, and R. Siever, 1973; Sand and Sandstone. Springer-Verlag, Berlin:618pp.

Picard, M.D. and L.R. High, 1973; Sedimentary Structures of

- Ephemeral Streams. Developments in Sedimentology, v.17, Elsevier, Amsterdam:223pp.
- Poole, W.H., 1967; Tectonic evolution of the Appalachian region of Canada. In Hugh Lilly Memorial Volume, Geological Association of Canada Special Paper #4:9-51.
- Potter, P.E., J.B. Maynard, and W.A. Pryor, 1980; Sedimentology of Shale. Springer-Verlag, Berlin:306pp.
- Powers, D.W. and R.G. Easterling, 1982; Improved methodology for using embedded Markov chains to describe cyclical sediments. Journal of Sedimentary Petrology, v.52:913-923.
- Quinn, L. 1985; The Humber Arm Allochthon at South Arm, Bonne Bay, with extensions in the Lomond Area western Newfoundland. Unpublished MSc. Thesis, Memorial University of Newfoundland:188pp.
- Radke, M., R.G. Schaefer, and D. Leythausen, 1980; Composition of soluble organic matter in coals: relation to rank and liptinite fluorescence. Geochimica et Cosmochimica Acta, v.44:1787-1800.
- Ray, P.K., 1976; Structure and sedimentological history of the overbank deposits of a Mississippi River point bar. Journal of Sedimentary Petrology, v. 46:788-801.
- Reading, H.G. 1978; Sedimentary Environments and Facies. Blackwell, Oxford:557pp.
- Reineck, H.E. and I.B. Singh, 1980; Depositional Sedimentary Environments. Springer-Verlag, Berlin:549pp.
- Riley, G.C., 1962; Stephenville map area, Newfoundland. Geological Survey of Canada Memoir 323:72pp.
- Rohrback, B.G., K.E. Peters, and I.R. Kaplan, 1984; Geochemistry of artificially heated humic and sapropelic sediments II: Oil and gas generation. Bulletin of the American Association of Petroleum Geologists, v.68:961-970.
- Rust, B.R., 1972; Structure and process in a braided river. Sedimentology, v.18:221-245.

- Rust, B.R., 1975; Fabric and structure in glaciofluvial gravels. In Glaciofluvial and Glaciolacustrine Sedimentation, ed. by A.V. Jopling and B.C. McDonald. S.E.P.M. Special Publication #23:238-248.
- Rust, B.R., 1978; Depositional models for braided alluvium. In Fluvial Sedimentology, ed. by A.D. Miall, Canadian Society of Petroleum Geologists Memoir #5:605-625.
- Rust, B.R., 1981; Alluvial deposits and tectonic style: Devonian and Carboniferous successions in Eastern Gaspe. In Sedimentation and Tectonics in Alluvial Basins, ed. by A.D. Miall, Geological Survey of Canada Special Paper #23:49-76.
- Rust, B.R. and E.H. Koster, 1984; Coarse alluvial deposits In Facies Models, ed. by R.G. Walker. Geoscience Reprint Series 1:53-69.
- Salomons, W., A. Goudie, and W.G. Mook, 1978; Isotopic composition of calcrete deposits from Europe, Africa, and India. Earth Surface Processes, v.3:43-57.
- Sarkisyan, S.G. and D.D. Kotelnikov, 1972; Genesis and thermodynamic stability of dioctohedral and trioctohedral mixed-layer minerals in sedimentary rocks. Proceedings of the International Clay Conference, Madrid:281-289.
- Scalan, R.S. and J.E. Smith, 1970; An improved measure of the odd-even predominance in the normal alkanes of sediment extracts and petroleum. Geochimica et Cosmochimica Acta, v.34:611-620.
- Schlesinger, W.H., 1985; The formation of caliche in soils of the Mojave Desert, California. Geochimica et Cosmochimica Acta, v.49:57-66.
- Schultz, L.G., 1964; Quantitative interpretation of mineralogical composition from x-ray and chemical data for the Pierre Shale. U.S.G.S. Professional Paper #391C:31pp.
- Schumm, S.A. and R.W. Lichty, 1963; Channel widening and floodplain construction along Cimarron River in southwest Kansas. U.S.G.S. Professional Paper #352D: 71-88
- Schumm, S.A. 1977; The Fluvial System. J. Wiley,

N.Y.:338pp.

Schumm, S.A., 1981; Evolution and response of the fluvial system, sedimentological implications. In Recent and Ancient Non-marine Depositional Environments: Models for Exploration, ed. by F.G. Etheridge and R.M. Flores. S.E.P.M. Special Publication #31:19-29.

Scott, A.C., 1978; Sedimentological and ecological control of Westphalian B plant assemblages from West Yorkshire. Proceedings of the Yorkshire Geological Society, v.41:461-508.

Sherwood, N.R., A.C. Cook, M.R. Gibling, and C. Tantisukrit, 1984; Petrology of a suite of sedimentary rocks associated with some coal-bearing basins in northwest Thailand. International Journal of Coal Geology, v.4:45-71.

Smith, A.H.V. and M.A. Butterworth, 1967; Miospores in the Coal Seams of the Carboniferous of Great Britain. Special Papers on Paleontology & Paleontological Society of London:324pp.

Smith, N.D., 1972a; Flume experiments on the durability of mudclasts. Journal of Sedimentary Petrology, v.42:378-383.

Smith, N.D., 1972b; Some sedimentological aspects of planar cross-strata in a sandy braided river. Journal of Sedimentary Petrology, v.42:624-634.

Smith, N.D., 1974; Sedimentology and bar formation in the upper Kicking Horse River, a braided outwash system. Journal of Geology, v.82:205-224.

Snowdon, L.R., 1984; A comparison of "Rock-Eval" pyrolysis and solvent extract results from the Collingwood and Kettle Point shales, Ontario. Bulletin of Canadian Petroleum Geology, v.32:327-334.

Solomon, S.M., and Hyde, R.S., 1985; Stratigraphy and sedimentology of some coal seams in the Carboniferous Bay St. George basin, southwest Newfoundland. In Current Research for 1984, ed. by K. Brewer, D. Walsh, and R.V. Gibbons. Mineral Development Division, Newfoundland Department of Mines and Energy, Report 85-1:168-176.

Stach, E., M.-Th. MacKowsky, M. Teichmüller, G.H. Taylor, D.

- Chandra, and R. Teichmuller, 1982; Stach's Textbook of Coal Petrology. Gebrouler Borntraeger, Berlin:535pp.
- Styan, W.B., and R.M. Bustin, 1984; Sedimentology of Fraser River delta peat deposits: a modern analogue for some deltaic coals. In Sedimentology of Coal and Coal-Bearing Sequences, ed. by R.A. Rahmani and R.M. Flores. International Association of Sedimentologists Special Publication #7:241-274.
- Summers, W.F., 1948; Report on the geology and diamond drilling operations in the St. George's coalfield area, Newfoundland in the summer of 1947. Geological Survey of Newfoundland, Unpublished report, Open File 12b/2(41).
- Taylor, R.P., D.F. Strong, and B.F. Kean, 1980; The Topsails Igneous Complex: Siluro-Devonian peralkaline magmatism in Western Newfoundland. Canadian Journal of Earth Sciences, v.17:425-439.
- Tissot, B.P., 1984; Recent advances in petroleum geochemistry applied to hydrocarbon exploration. Bulletin of the American Association of Petroleum Geologists, v.68:545-563.
- Tissot, B.P. and D.H. Welte, 1978; Petroleum Formation and Occurrence. Springer-Verlag, Berlin:538pp.
- Tissot, B.P., G. Deroo, and A. Hood, 1978; Geochemical study of the Uinta Basin: formation of petroleum from the Green River Formation. Geochimica et Cosmochimica Acta, v.42:1469-1485.
- Todd, T.W., 1968; Paleoclimatology and the relative stability of feldspar minerals under atmospheric conditions. Journal of Sedimentary Petrology, v.38:832-844.
- Tunbridge, I.P., 1981; Sandy high energy flood sedimentation - some criteria for recognition with an example from the Devonian of southwest England. Sedimentary Geology, v. 28:79-95.
- Utting, J., 1966; Geology of the Codroy Valley, southwest Newfoundland including results of a preliminary palynological investigation. Unpublished MSc. Thesis, Memorial University of Newfoundland:89pp.
- Van de Poll, H.W., 1983; The Upper Carboniferous Clifton.

- Formation of northern New Brunswick: coal bearing deposits of a semi-arid alluvial plain: Discussion. Canadian Journal of Earth Sciences, v.20:1212-1215.
- Van Houten, F.B., 1973; Origin of red beds: a review, 1961-1972. Annual Review of Earth and Planetary Science, v.1:39-61.
- Velde, B., 1985; Clay minerals: A Physico-chemical Explanation of their Occurrence. Developments in Sedimentology #40, Elsevier, Amsterdam:427pp.
- Van der Plas, L. and A.C. Tobi, 1965; A chart for judging the reliability of point counting results. American Journal of Science, v.263:87-90.
- Walker, R.G. and D.J. Cant, 1984; Sandy fluvial systems. In Facies Models, ed. by R.G. Walker, Geoscience Canada Reprint Series #1:71-90.
- White, S.H., H.F. Shaw, and J.M. Hugget, 1984; The use of back-scattered electron imaging for the petrographic study of sandstone and shale. Journal of Sedimentary Petrology, v.54:487-494.
- Wieder, M. and D.H. Yaalon, 1982; Micromorphological fabrics and developmental stages of carbonate nodular forms related to soil characteristics. Geoderma, v.28:203-220.
- Williams, E.P., 1974; Geology and petroleum possibilities in and around the Gulf of St. Lawrence. Bulletin of the American Association of Petroleum Geologists, v.58:1137-1155.
- Williams, G.E., 1971; Flood deposits of the sand-bed ephemeral streams of central Australia. Sedimentology, v.17:1-40.
- Williams, H., 1978; Tectonic lithofacies map of the Appalachian Orogen. Memorial University of Newfoundland, Map #1.
- Williams, H., 1985; Geology, Stephenville map area, Newfoundland. Geological Survey of Canada Map 1579A.
- Williams, H., M.J. Kennedy, and E.R.W. Neale, 1972; The Appalachian structural province. In Tectonic Styles in Canada, ed. by R.A. Price and R.J.W. Douglas. Geological Association of Canada Special Paper

11:181-261.

Williams, H., M.J. Kennedy, and E.R.W. Neale, 1974, The northwestward termination of the Appalachian Orogen. In The Ocean Basins and Margins v.2 - North Atlantic, ed. by A.E.M. Nairn and F.G. Stehli, Plenum, New York:79-123.

Williams, P.F. and B.R. Rust, 1969; The sedimentology of a braided river. Journal of Sedimentary Petrology, v.39:649-679.

Wright, V.P., 1982; Calcrete paleosols from the Lower Carboniferous Llanelly Formation, South Wales. Sedimentary Geology, v.33:1-33.

APPENDIX B

BASIC PROGRAMME FOR MARKOV CHAIN ANALYSIS

```
999 REM MATRIX INPUT ROUTINE
1000 Input "# of Columns";K
1100 Input "# of Rows";N
1150 DIM A1(N)
1155 DIM B1(K)
1160 DIM A2(N)
1165 DIM B2(K)
1170 DIM ND(N,K)
1200 DIM F(N,K)
1201 DIM R(N)
1202 DIM C(K)
1203 DIM D(N,K)
1204 DIM P(N,K)
1205 DIM I(N,K)
1206 DIM US(N,K)
1210 INPUT "Input from Keyboard?" Y/N";B$
1220 If B$ = "Y" and B$ <> "N" then Goto 1210
1230 If B$="N" then Gosub 13600:Goto 1999
1300 For I=1 to N
1400 For J=1 to K
1500 Print "Enter F(";I;",";J;")="
1600 Input F(I,J)
```

```

1700 Next J
1800 Next I
1999 REM Calculate Row and Column Totals
2000 G1=0
2010 For I=1 to N
2030 R(I)=0
2040 For J=1 to K
2050 R(I)=R(I)+F(I,J)
2060 Next J
2070 G1=G1+R(I)
2080 Next I
2090 For J=1 to K
2110 C(J)=0
2120 For I=1 to N
2130 C(J)=C(J)+F(I,J)
2140 Next I
2150 Next J
3000 REM Calculate Probability Matrix
3020 For I=1 to N
3030 For J=1 to K
3040 P(I,J)=F(I,J)/R(I)
3050 Next J
3060 Next I
4000 REM Calculate Ind. Trials Matrix
4010 NI=0
4020 AS=0

```

```

4030 For I=1 to N
4040 A1(I)=R(I)/(N-1)
4050 AS=A1(I)+AS
4060 Next I
4070 BS=0
4080 For J=1 to N
4090 B1(J)=C(J)/(AS-A1(J))
4100 BS=B1(J)+BS
4110 Next J
4120 AS=0
4130 For I=1 to N
4140 A2(I)=R(I)/(BS-B1(I))
4150 AS=A2(I)+AS
4160 Next I
4170 BS=0
4180 For J=1 to N
4190 B2(J)=C(J)/(AS-A2(J))
4200 BS=B2(J)+BS
4210 Next J
4220 NI=NI+1
4230 For J=1 to N
4240 TA=(ABS(A2(J)-A1(J)))*ABS(A2(J))
4250 TB=(ABS(B2(J)-B1(J)))*ABS(B2(J))
4260 If TA<.001 and TB<.001 then NK=0
4261 If TA>.001 or TB>.001 then NK=1
4263 Next J

```

```

4264 If NK=1 then GOSUB 13310
4265 If NK=1 then GOTO 4120
4270 Print"# of Iterations=";NI
4280 For I=1 to N
4290 For J=1 to K
4300 I(I,J)=A2(I)*B2(J)
4305 If I=J then I(I,J)=0
4310 Next J
4320 Next I
5000 REM Calculate Difference Matrix
5010 For I=1 to N
5020 For J=1 to K
5030 D(I,J)=F(I,J)-I(I,J)
5033 If I(I,J)=0 then ND(I,J)=0
5034 If I(I,J)=0 then goto 5040
5035 ND(I,J)=D(I,J)/SQR(I(I,J))
5040 Next J
5050 Next I
5100 REM Calculate CHI SQ. Method I
5110 X1=0
5120 For I=1 to N
5130 For J=1 to K
5135 If I=J then GOTO 5145
5140 C1=((F(I,J)-I(I,J))2/I(I,J))
5145 If I=J then C1=0
5170 X1=X1+C1

```

```

5180 Next J
5190 Next I
5200 REM Calculate degrees of freedom
5210 D1= ((N-1)2 )-N
5220 Print "CHI SQ I=" ;X1
5230 Print "degrees of freedom=";D1
10000 REM Print routines
10020 Dim A$(4)
10040 For I=1 to N
10060 For J=1 to K
10080 U$(I,J)=STR$(F(I,J))
10100 Next J
10120 Next I
10140 A$="Transition Count Matrix"
10160 Gosub 13000
10180 For I=1 to N
10200 For J=1 to K
10220 U$(I,J)=STR$(P(I,J))
10222 If Val(U$(I,J))<.01 then U$(I,J)=Left$(U$(I,J),4)
      +Right$(U$(I,J),4)
10224 If Val(U$(I,J))>=.01 then U$(I,J)=Left$(U$(I,J),5)
10226 If Val(U$(I,J))=0 then U$(I,J)=" 0"
10240 Next J
10260 Next I
10280 A$="Probability Matrix"
10300 Gosub 13000

```

```

10320 For I=1 to N
10340 For J=1 to K
10360 U$(I,J)=Str$(I(I,J))
10362 If Val(U$(I,J))<.01 then U$(I,J)=Left$(U(I,J),4)
      +Right$(U$(I,J),4)
10364 If Val(U$(I,J))>=.01 then U$(I,J)=Left$(U$(I,J),5)
10366 If Val(U$(I,J))=0 then U$(I,J)=" 0"
10380 Next J
10400 Next I
10420 A$="Independent Trials Matrix"
10440 GOSUB 13000
10460 For I=1 to N
10480 For J=1 to K
10500 U$(I,J)=Str$(ND(I,J))
10502 If Abs(Val(U$(I,J)))<.01 then U$(I,J)=Left$(U$(I,J),4)
10504 If Abs(Val(U$(I,J)))>=.01 then U$(I,J)=Left$(U$(I,J),5)
10506 If Val(U$(I,J))=0 then U$(I,J)=" 0"
10520 Next J
10540 Next I
10550 A$="Normalized Difference Matrix"
10560 GOSUB 13000
10561 For I=1 to N
10562 For J=1 to N
10563 U$(I,J)=Str$(D(I,J))
10564 If Abs(Val(U$(I,J)))<.01 then U$(I,J)=Left$(U$(I,J),4)
10565 If Abs(Val(U$(I,J)))>=.01 then U$(I,J)=Left$(U$(I,J),5)

```

```

10566 If Val(US(I,J))=0 then US(I,J)=" 0"
10568 Next J
10570 Next I
10572 AS="Difference Matrix"
10612 End
13000 REM Screen Print
13020 Print AS
13040 For I=1 to N
13060 For J=1 to K
13080 Print US(I,J);
13085 Next J
13090 Print
13100 Next I
13110 Print"Hit any key to continue"
13120 Get DS:If DS=""then 13120
13200 Return
13310 For I=1 to N
13320 A1(I)=0:B1(I)=0
13330 A1(I)=A2(I):B1(I)=B2(I)
13340 A2(I)=0:B2(I)=0
13350 Next I
13360 Return
13599 REM Data statement input; start data statements
      at 14000
13600 For I=1 to N
13610 For J=1 to K

```

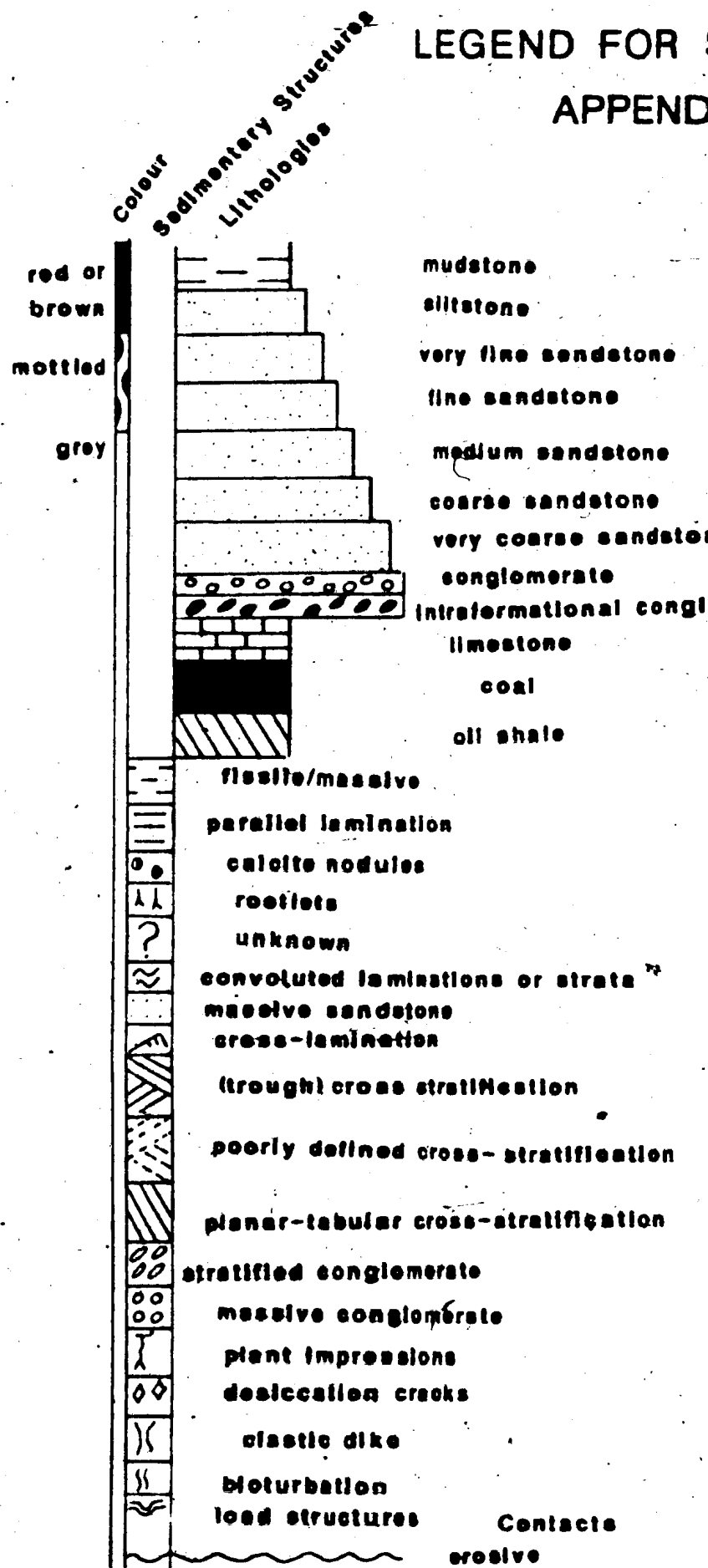
13620 Read F(I,J)

13630 Next J

13640 Next I

13650 Return


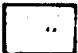
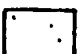



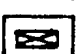

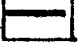

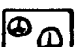
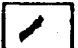
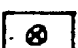
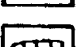
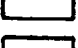
LEGEND FOR APPEND



STRATIGRAPHIC SECTIONS

INDEX A FIGURE 1

Accessories

-  muddy
-  silty
-  sandy
-  thin mudstone interbeds
-  thin siltstone interbeds
-  thin sandstone interbeds
-  hematite stained plant remains
-  carbonaceous debris
-  coaly laminations
-  calcified wood
-  intraformational limestone clasts
-  calcite vein
-  boulder-sized concretions
-  caliche bed
-  lens

< 10 cm thick

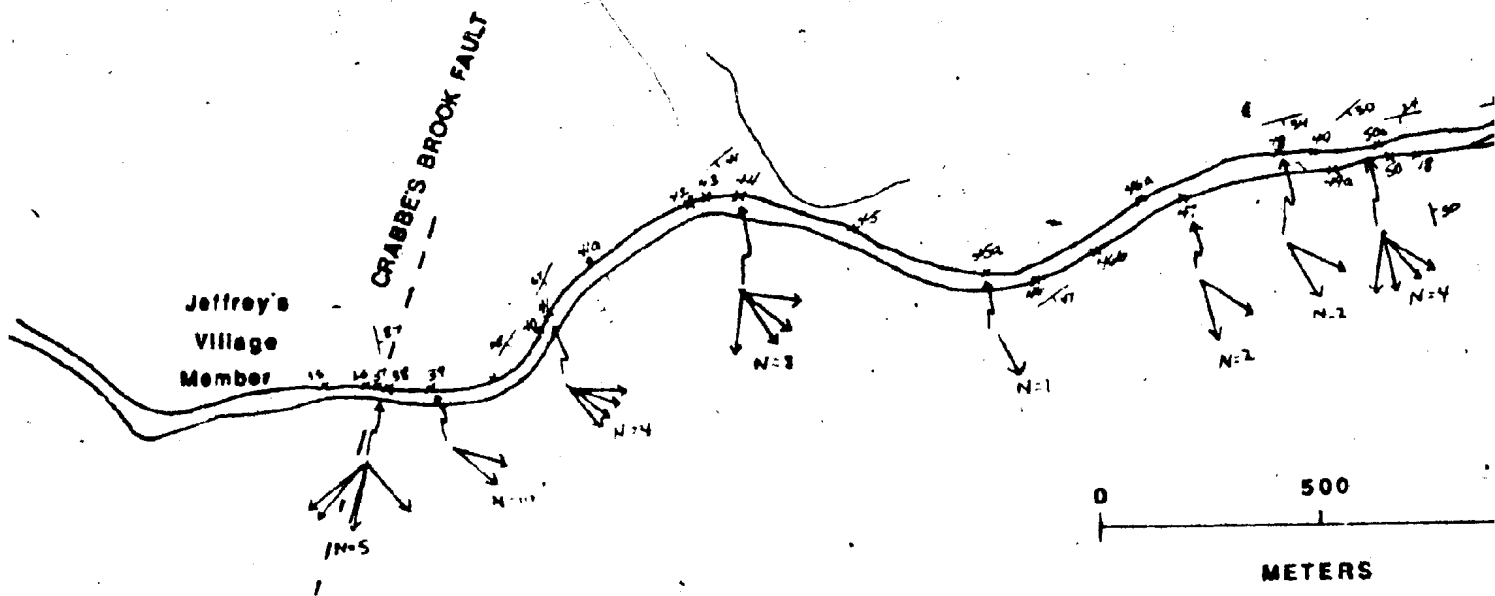
 Ostracodes

 Gastropods

 paleocurrent direction

Samples

sample number



METERS

← paleocurrent

N=4 number of

outcrop at v

x38 outcrop

possible fa

approximate

LOCATION MAP

N

Joe Mackey's Brook



1000

irrent direction

of paleocurrent measurements

t which paleocurrent directions were measured

fault

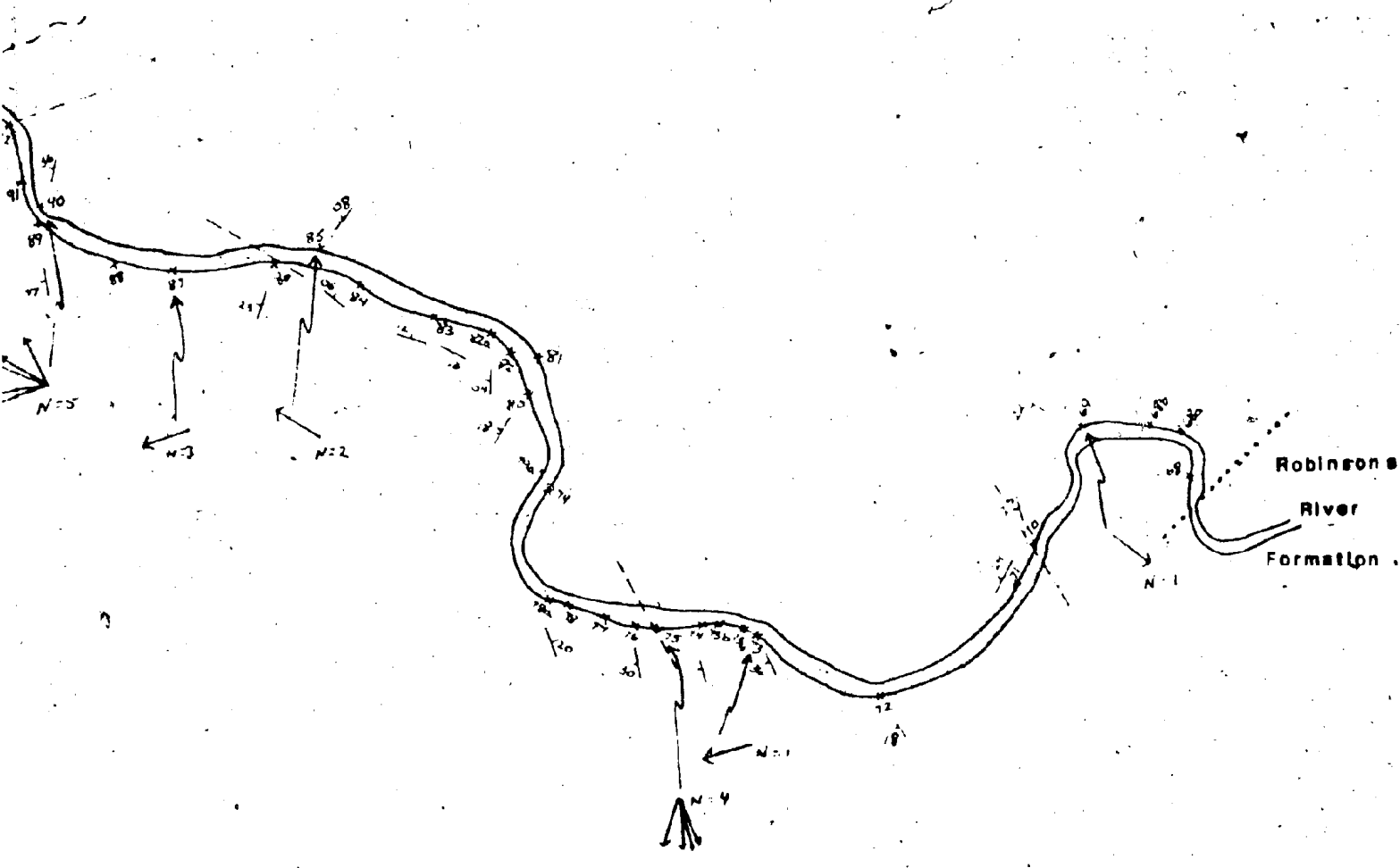
ate geological boundary

LOCATION MAP - BARACHOIS GROUP OUTCROPS ALO

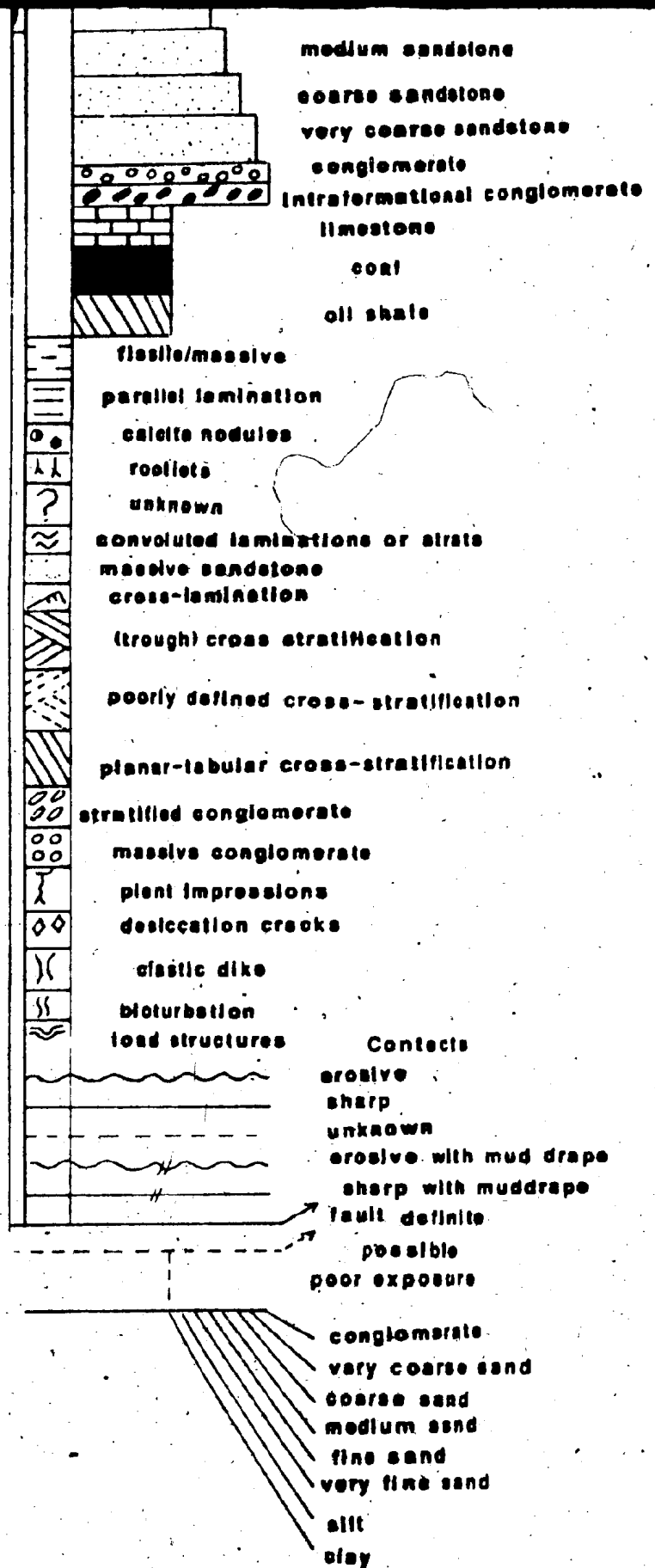
FIGURE 1.5

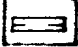

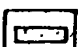


ONG MIDDLE BARACHOIS BROOK



grey




 thin mudstone interbeds
 thin siltstone interbeds
 thin sandstone interbeds

< 10 cm thick

 hematite stained plant remains

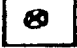
 carbonaceous debris

 coaly laminations

 calcified wood

 intraformational limestone clasts

 calcite vein

 boulder-sized concretions

 caliche bed

 lens

 Ostracodes

 Gastropods

 paleocurrent direction

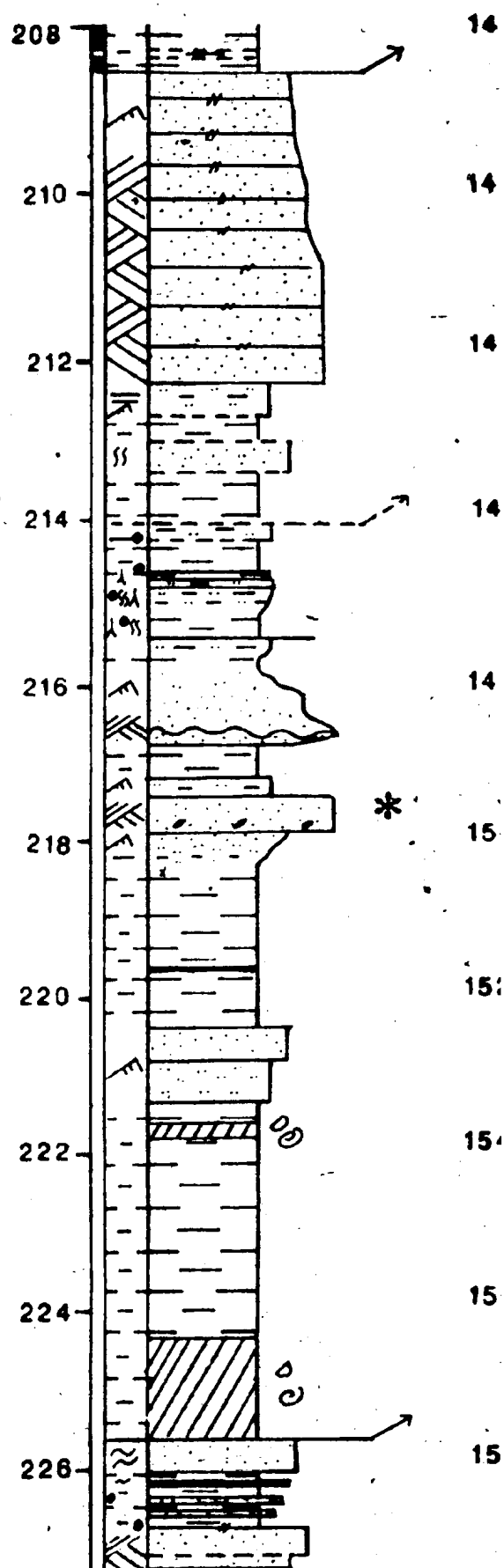
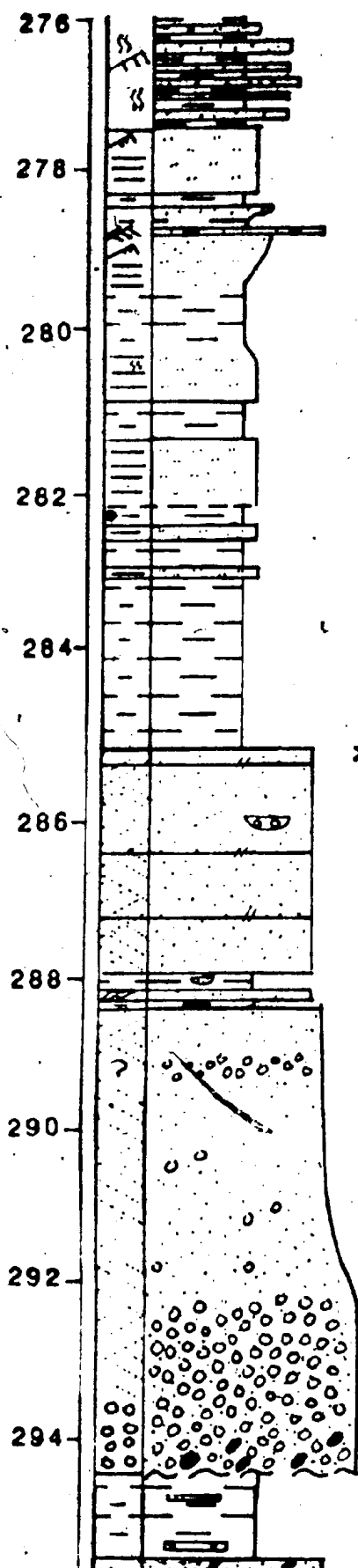
Samples

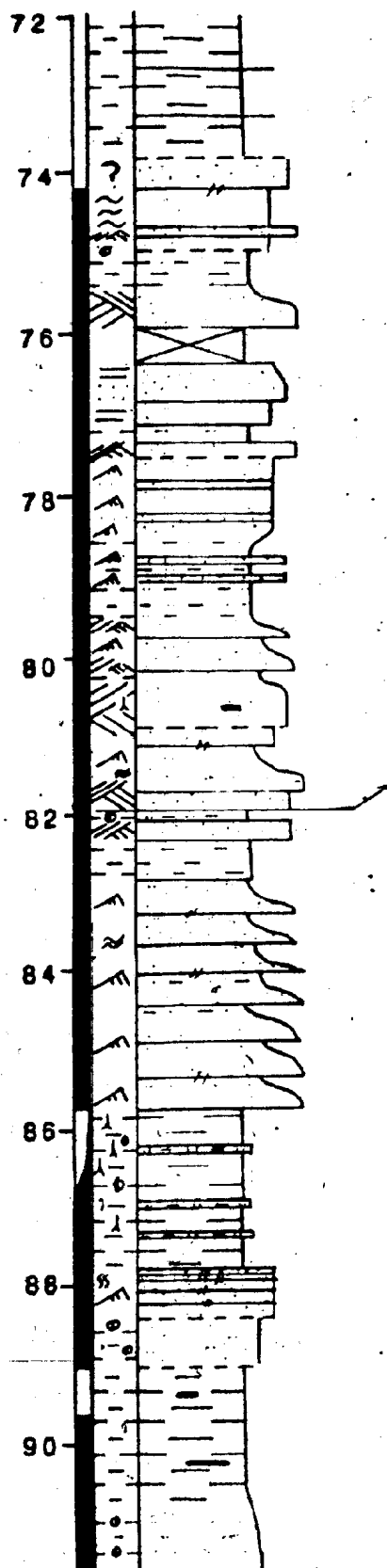
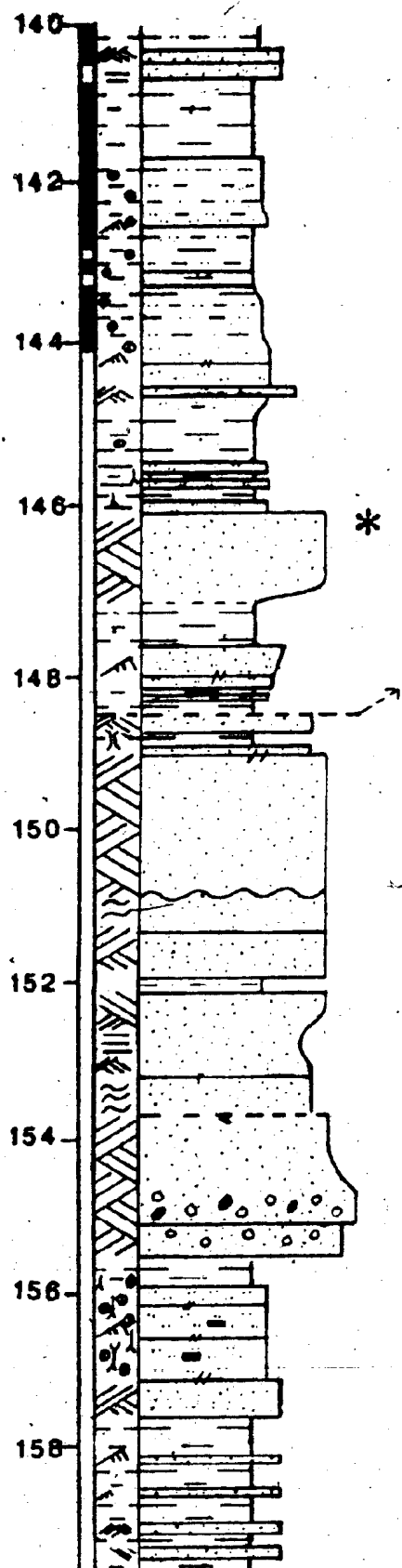
P12 sample number

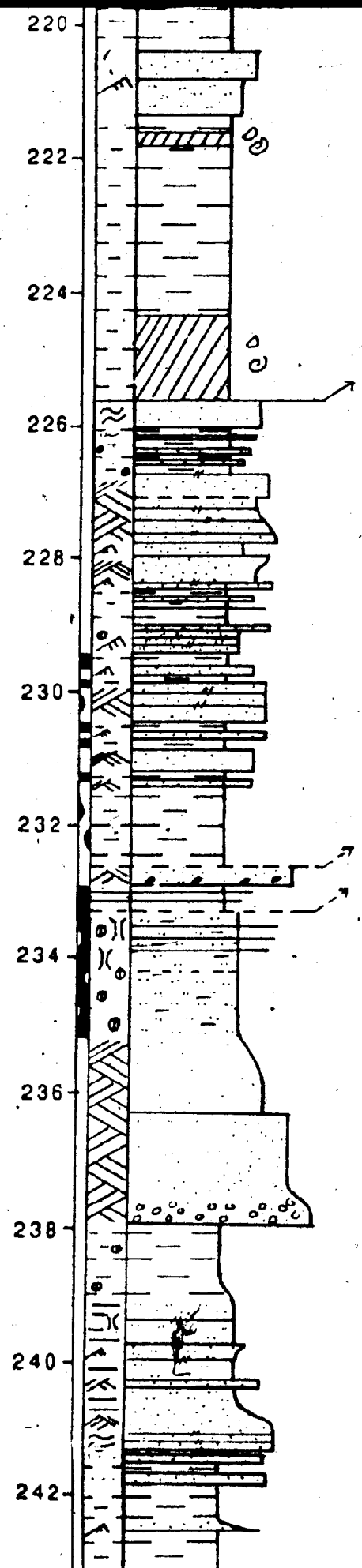
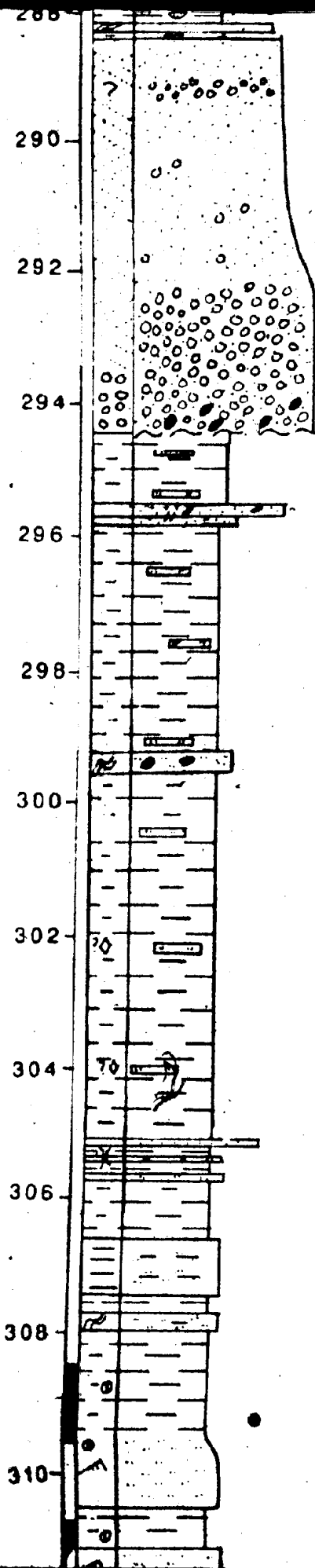
* thin section

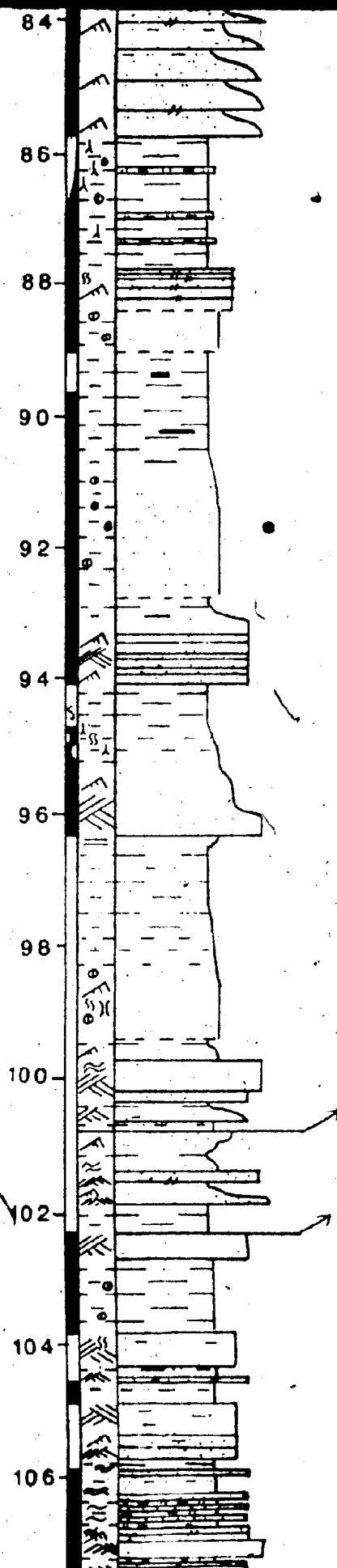
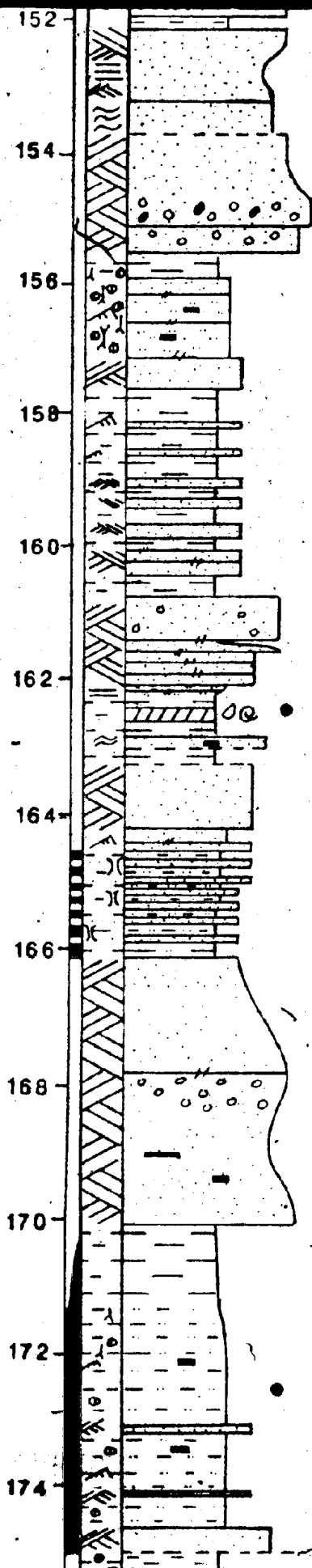
• X-ray diffraction

✓ palynology





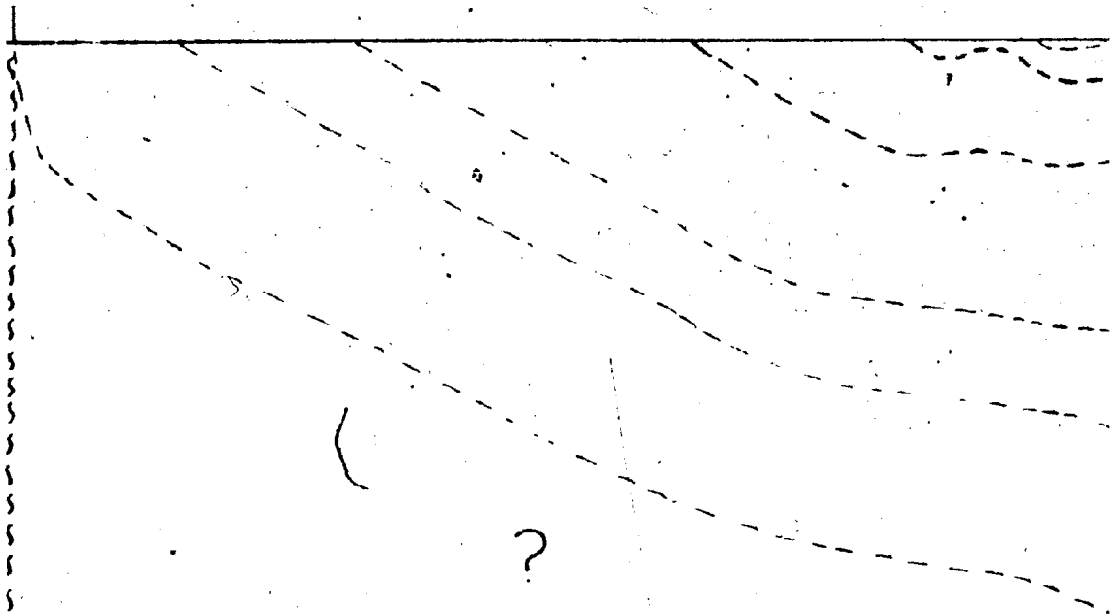




outcrop 38

Jeffrey's Village Member

CRABBS BROOK FAULT



outcrop 25

outcrop 11

outcrop 14

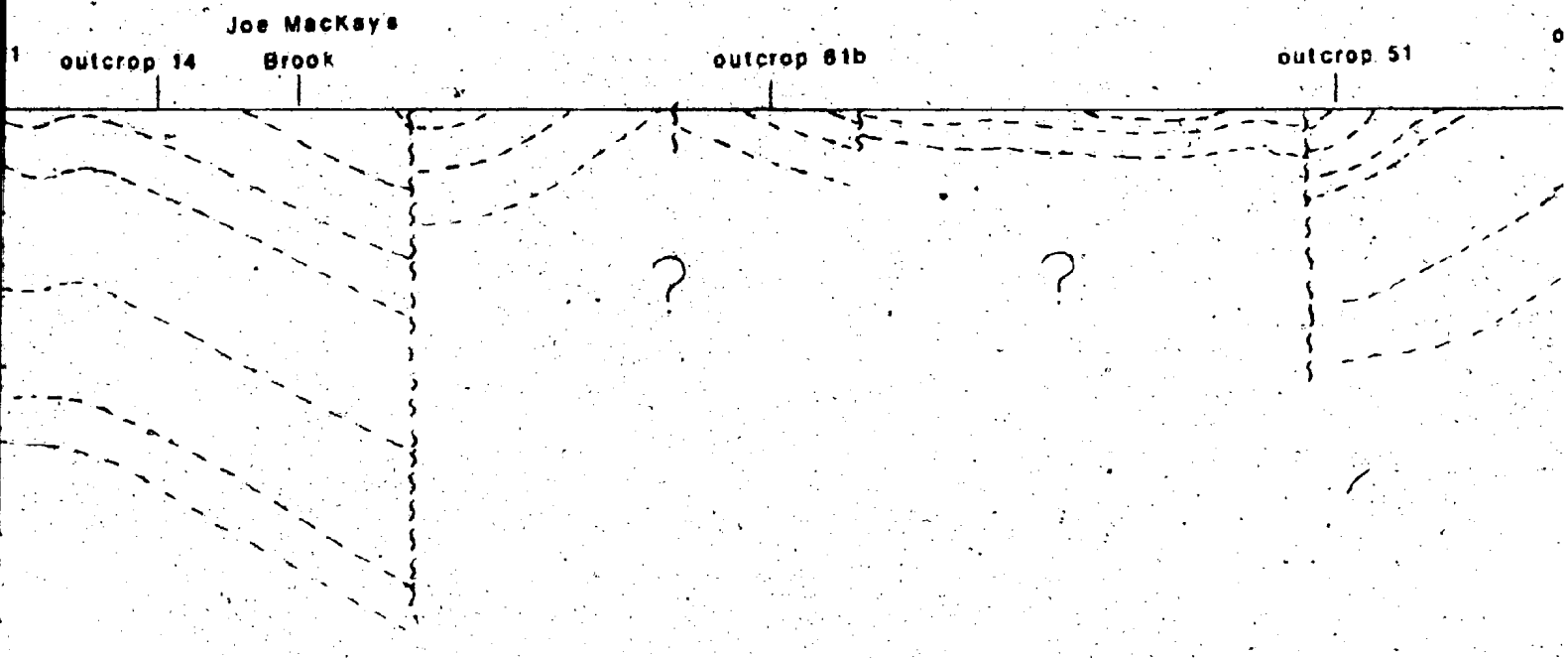
Joe Mack
Brook

0 500 1000
METERS

bedding extrapolated from

possible fault

approximate geological



DIAGRAMMATIC CROSS-SECTION

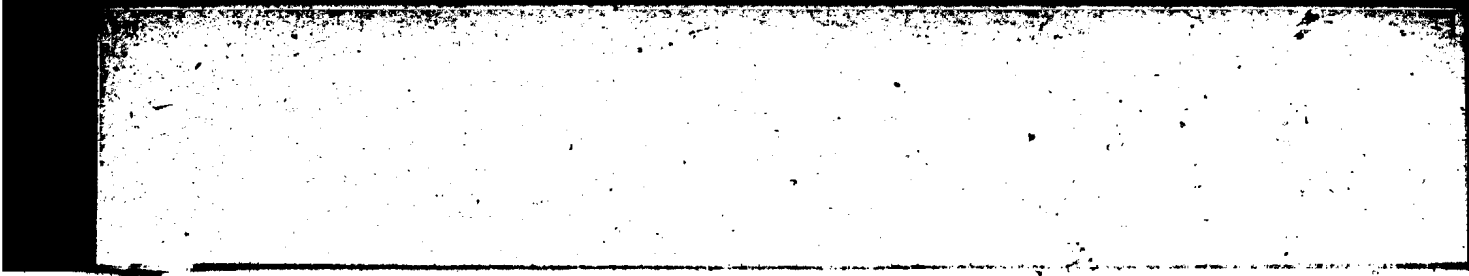
— bedding extrapolated from surface dip angles

— possible fault

- - - approximate geological boundary

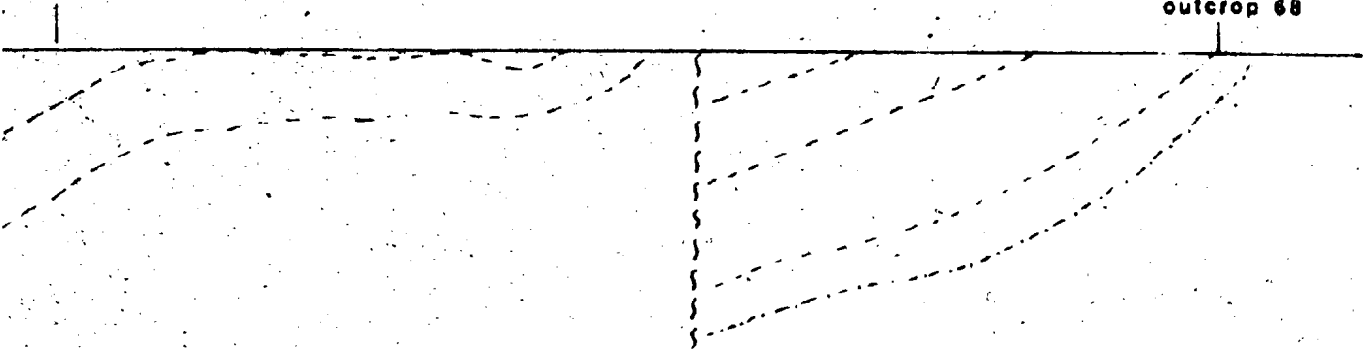
line of section S28E along

FIGURE



outcrop 87

outcrop 68



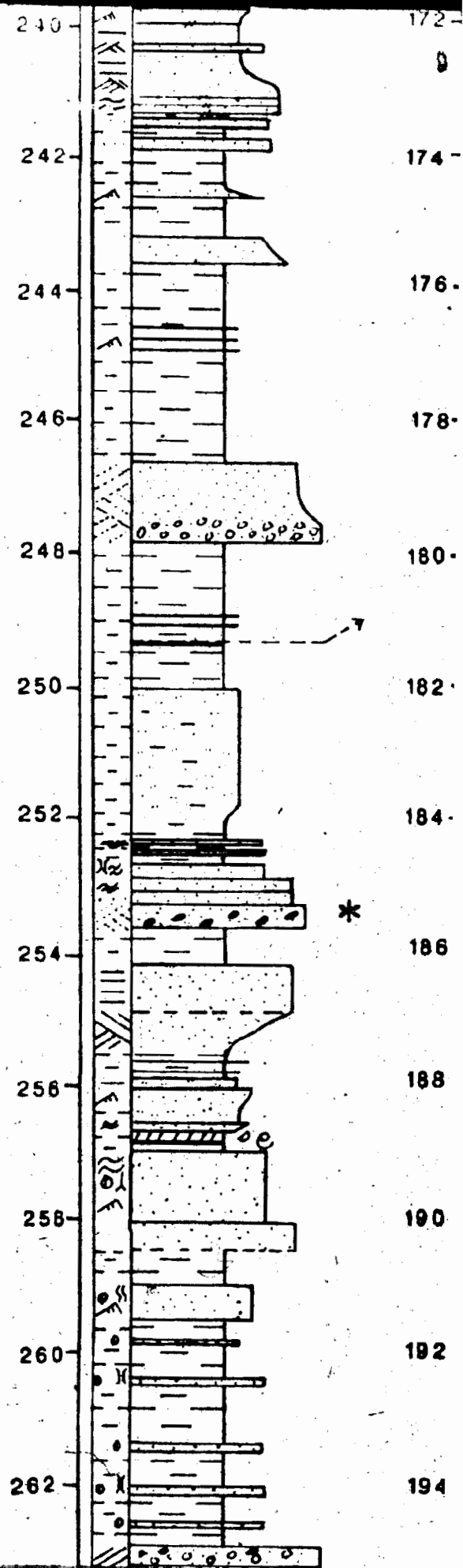
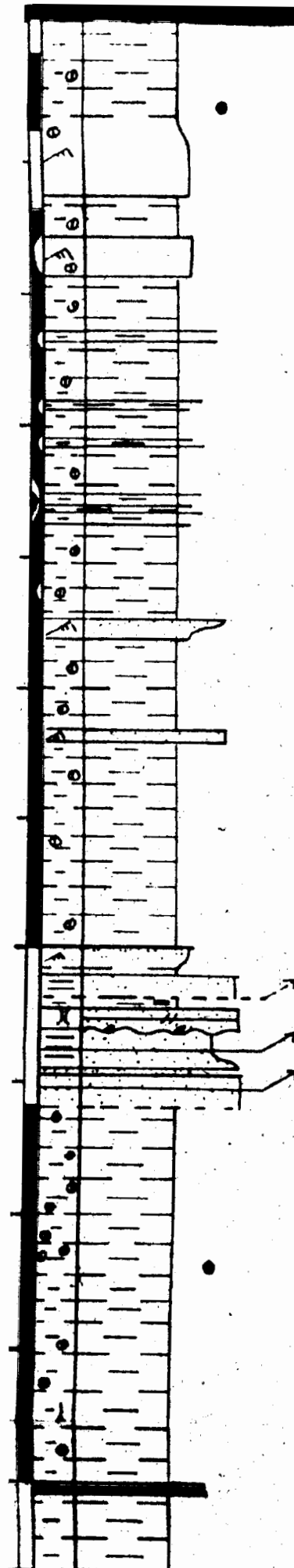
Robinson's River Formation

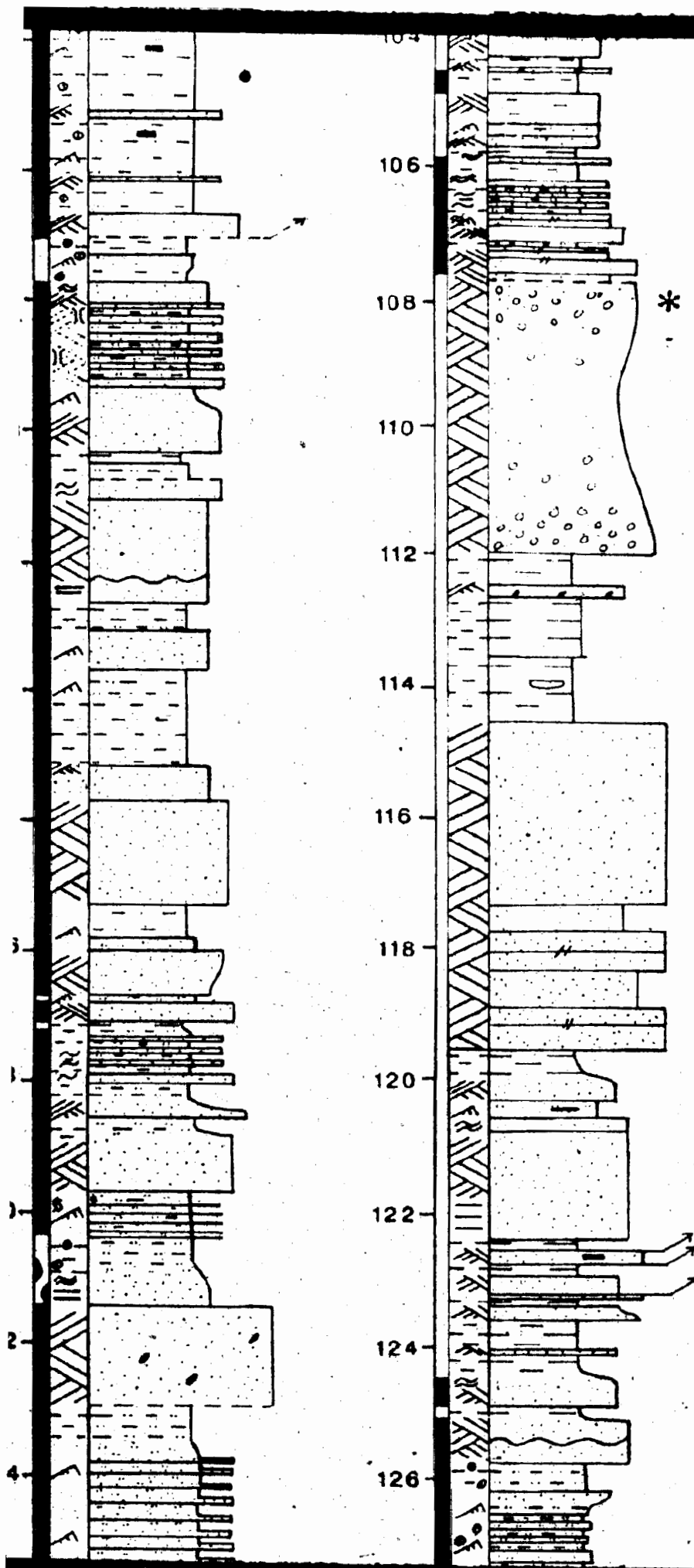
?

I ALONG MIDDLE BARACHOIS BROOK

ng Middle Barachois Brook

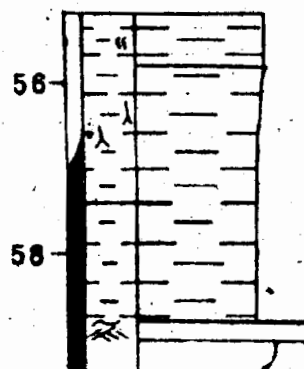
E 2.1

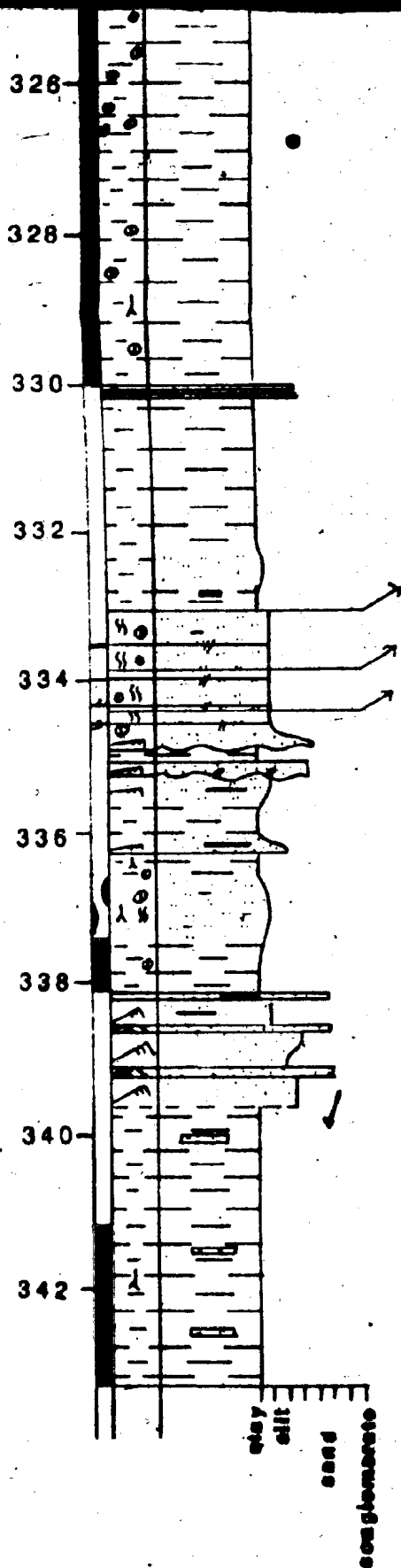




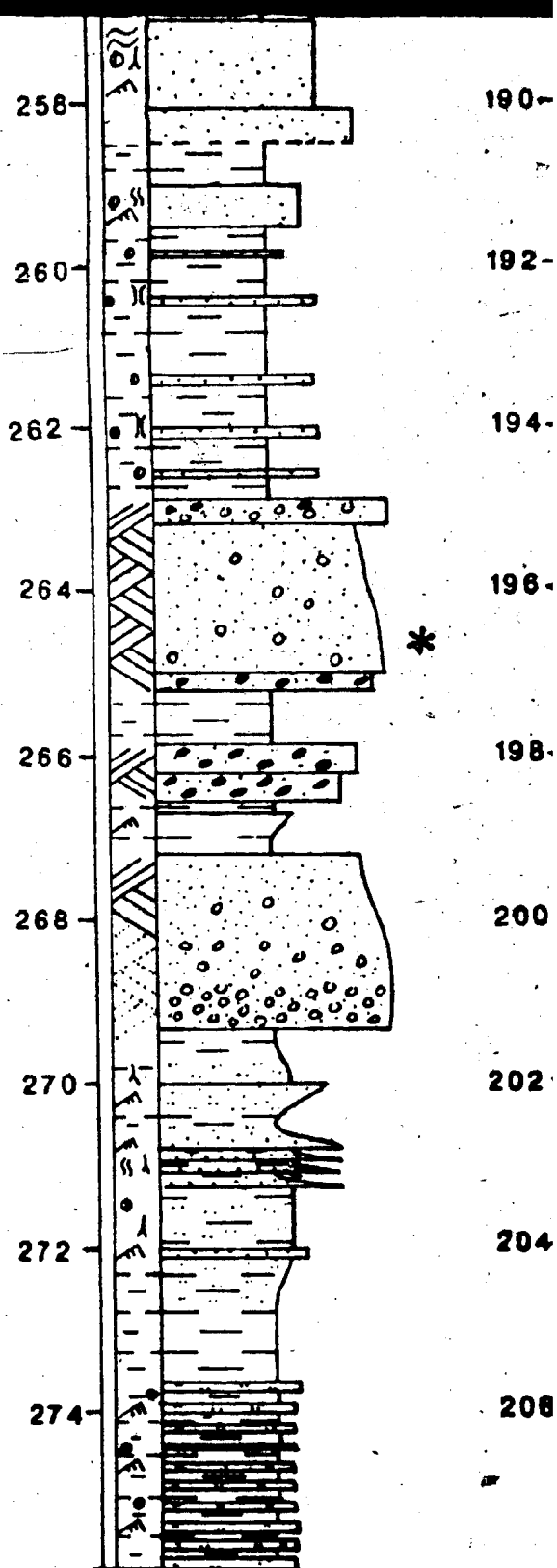
APPENDIX A FIGURE 2

BSG#1

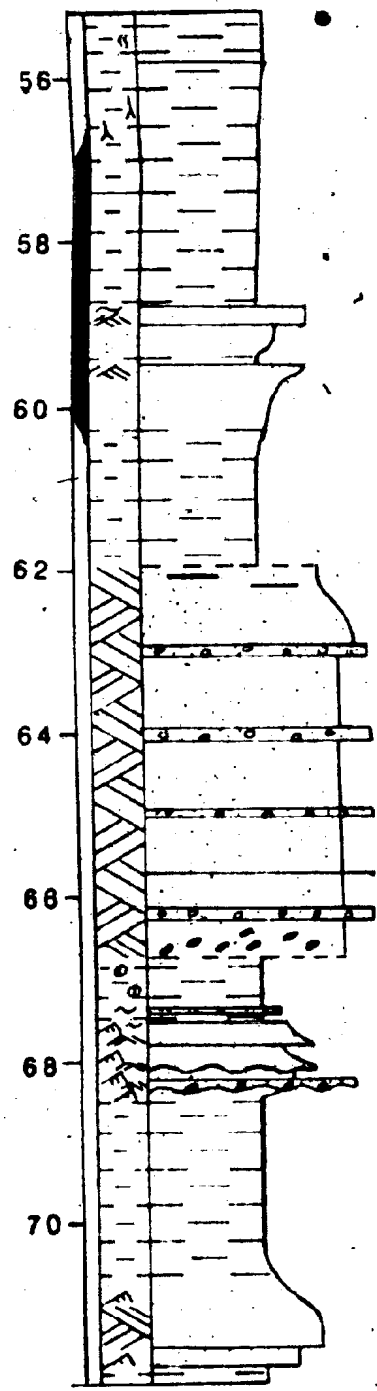
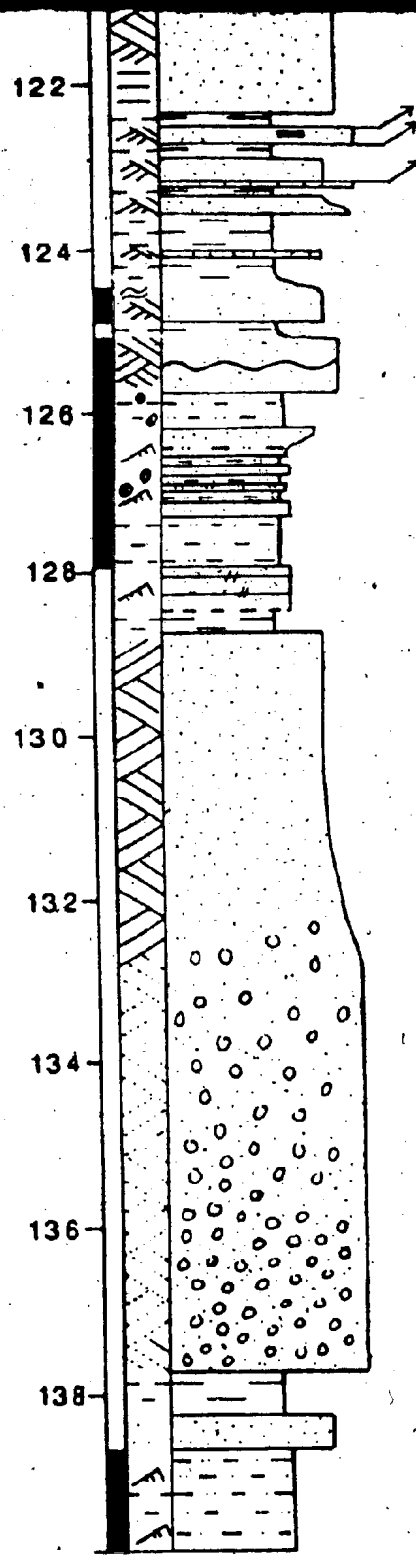
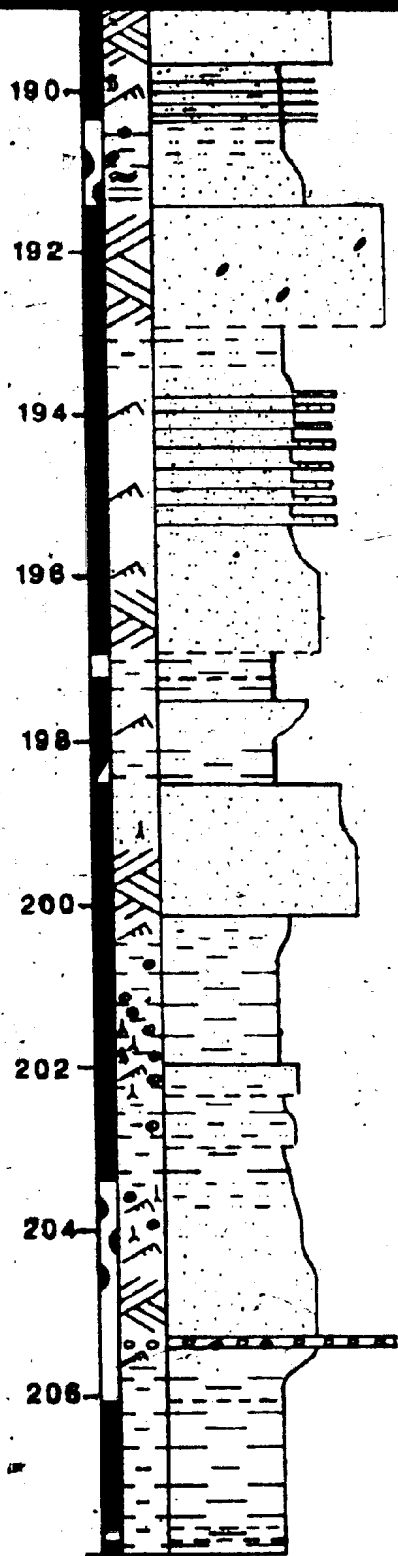


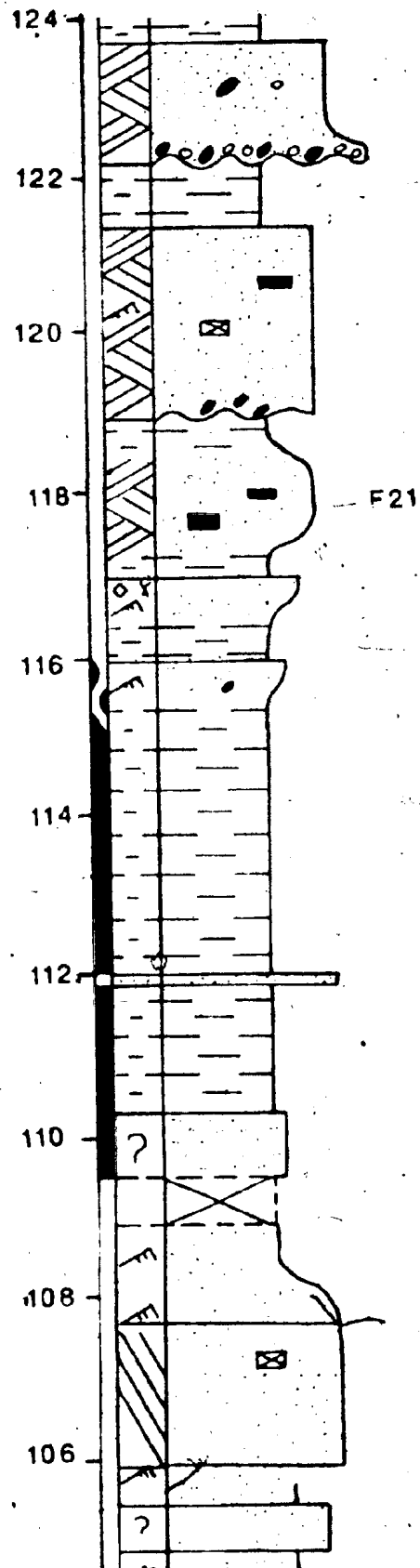
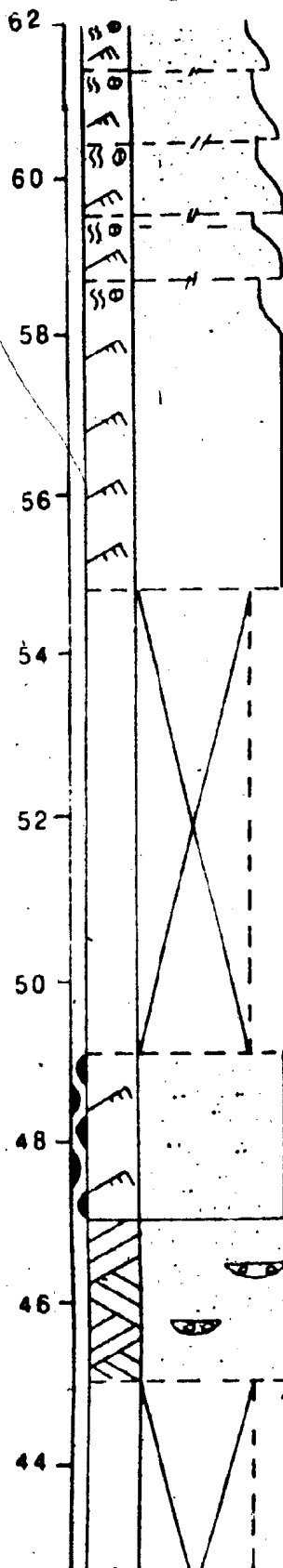


Total Depth - 343 m

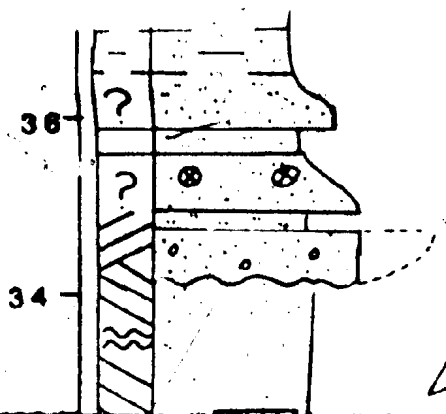


BSG#1





OUTCROP 11

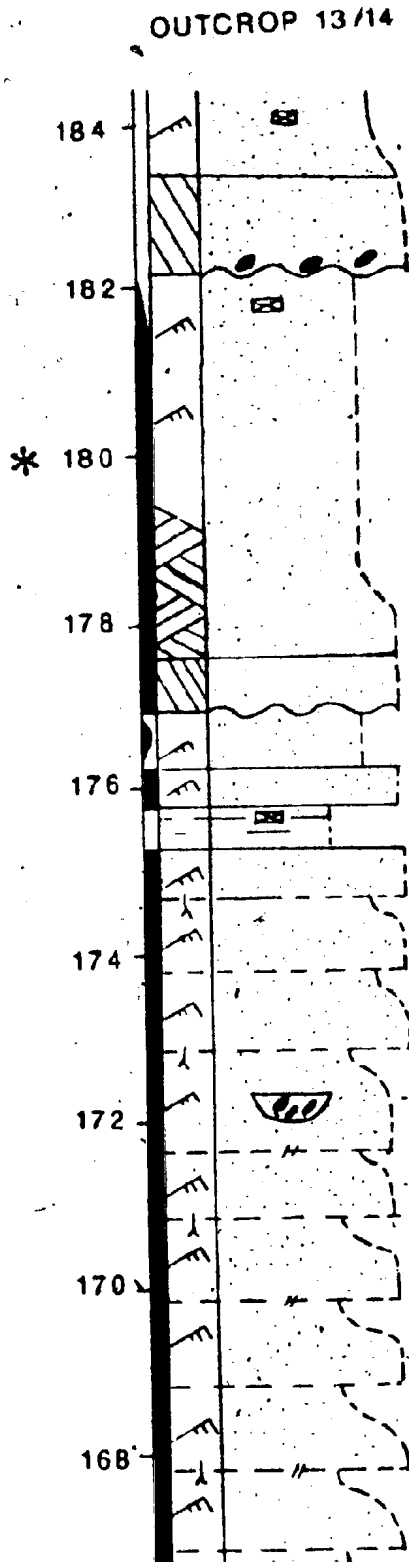


cross-strata

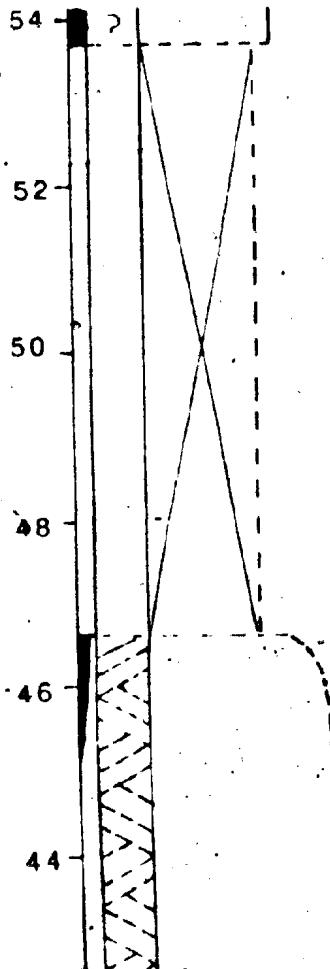
cross-strata

APPENDIX A FIGURE 4

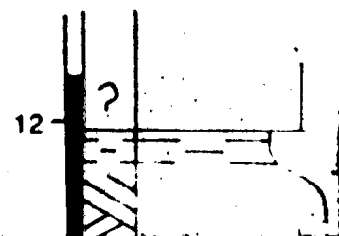
OUTCROPS 10, 11, 10, 13-14, 16, JOE MACKAY'S BROOK



JOE MACKAY'S BROOK



OUTCROP 16

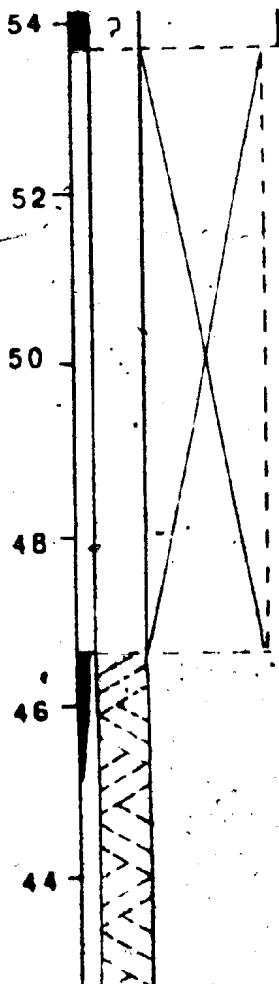


APPENDIX A FIGURE 4

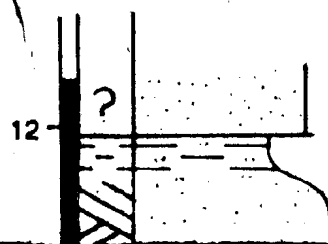
OUTCROPS 10, 11, 10, 13-14, 16, JOE MACKAY'S BROOK

JOE MACKAY'S BROOK

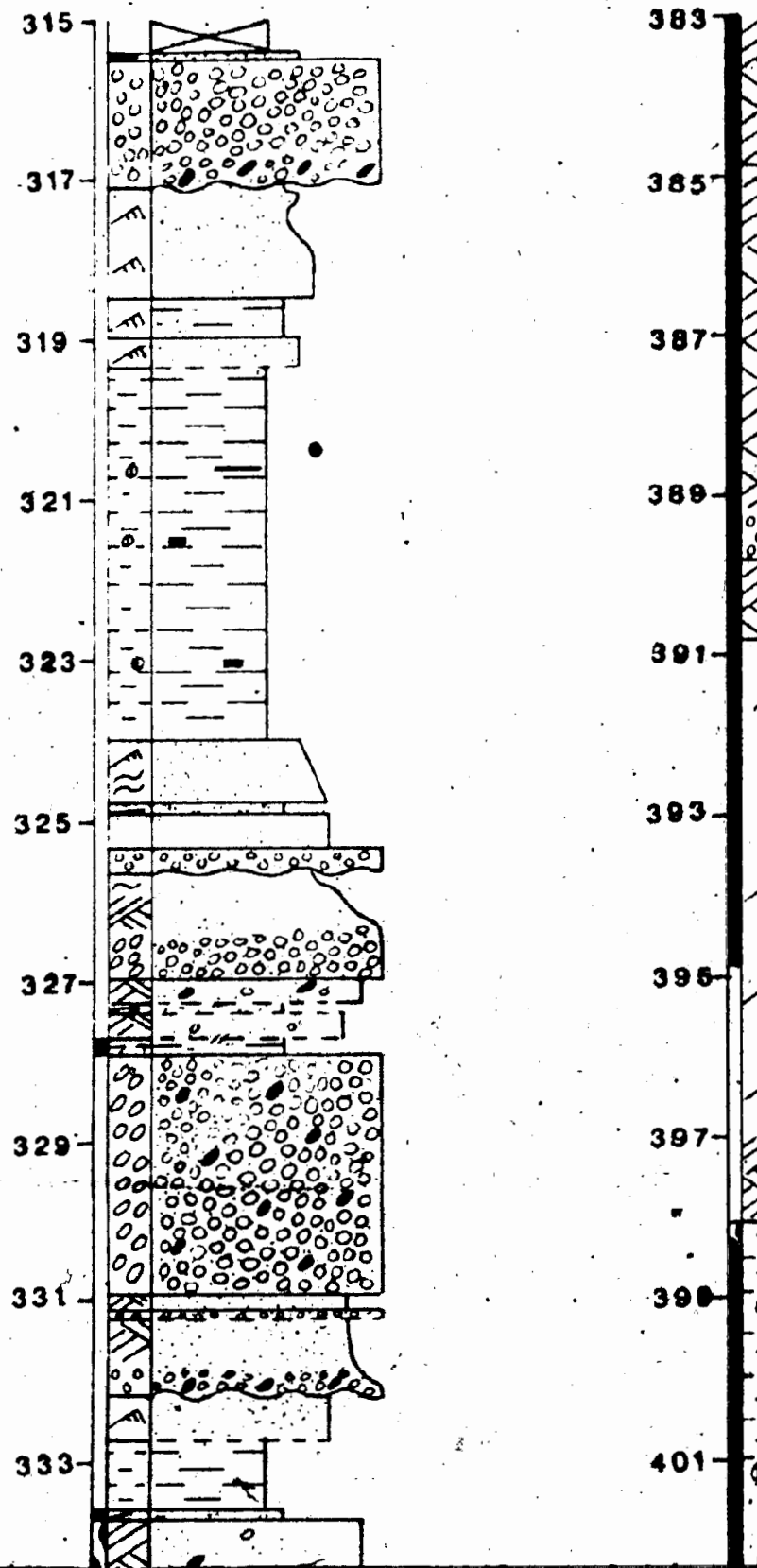
F24 *

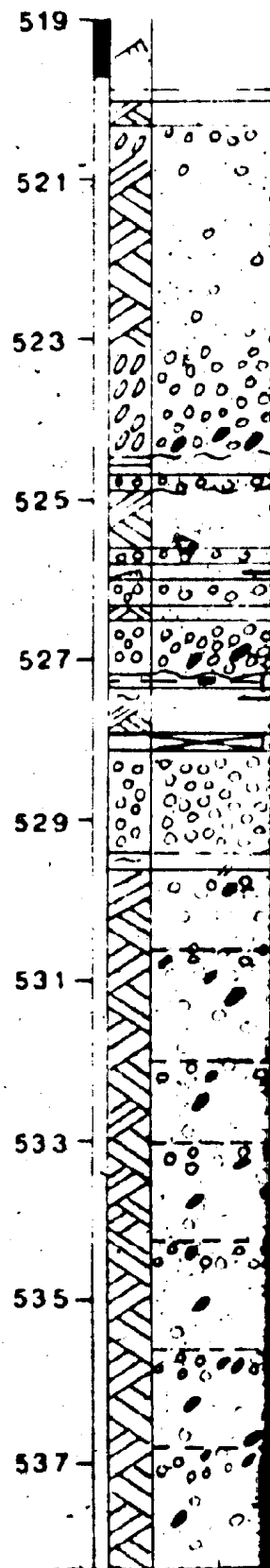
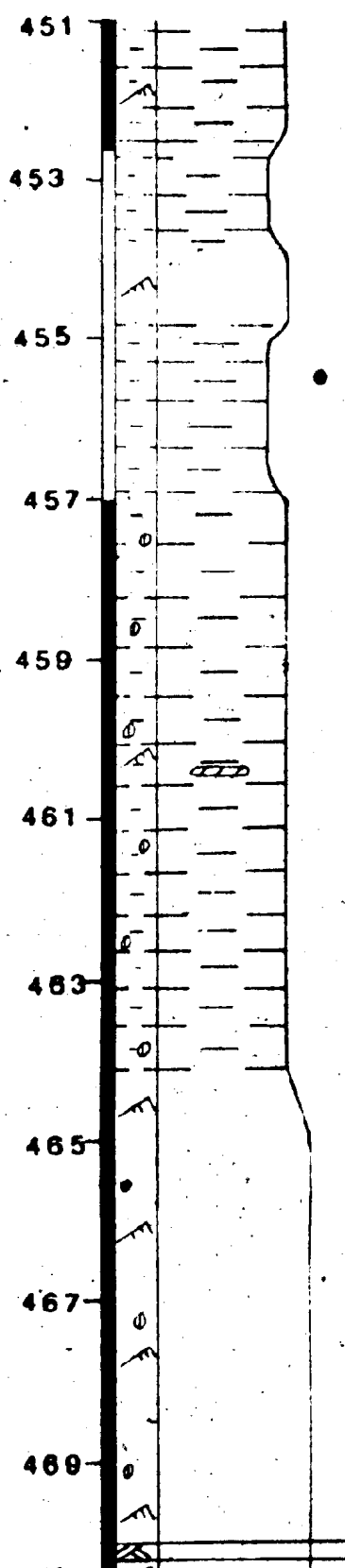
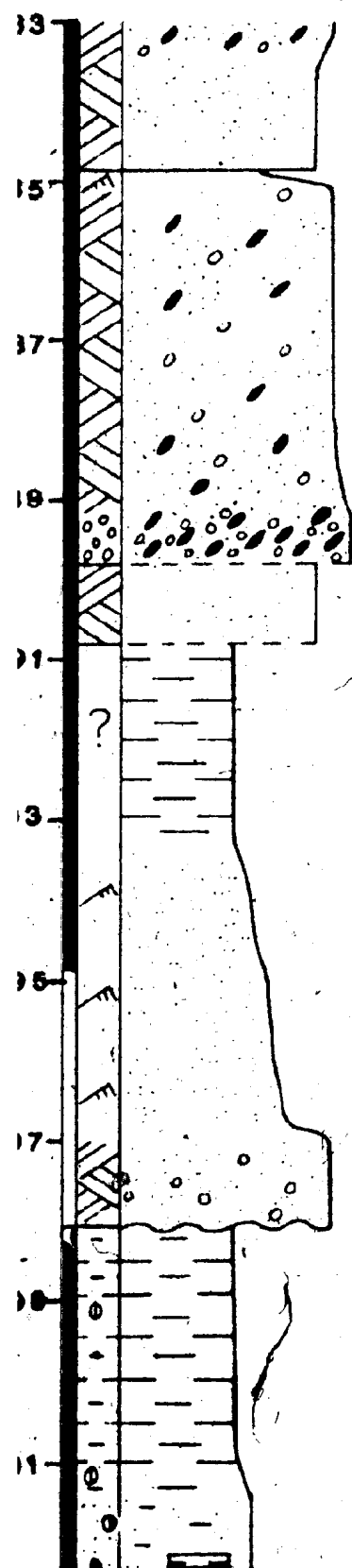


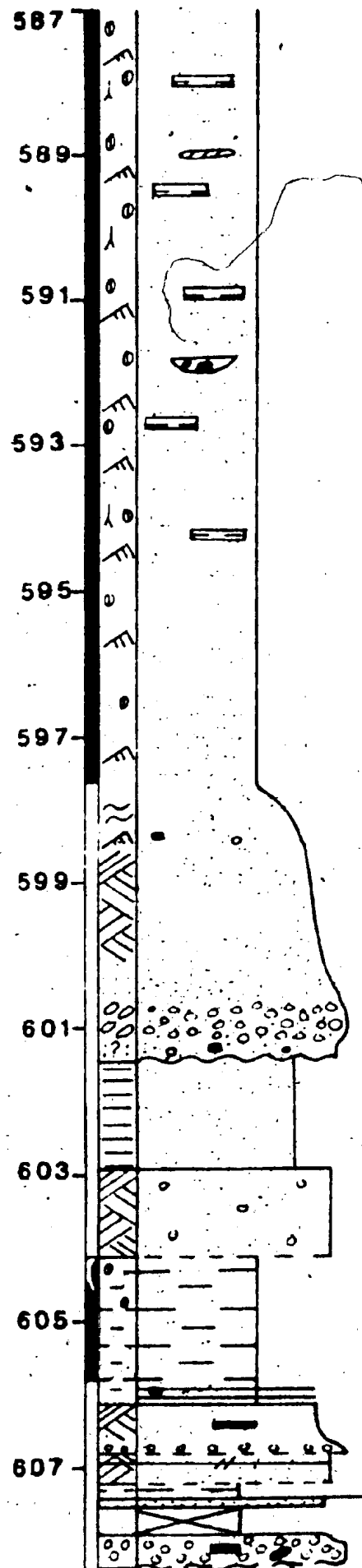
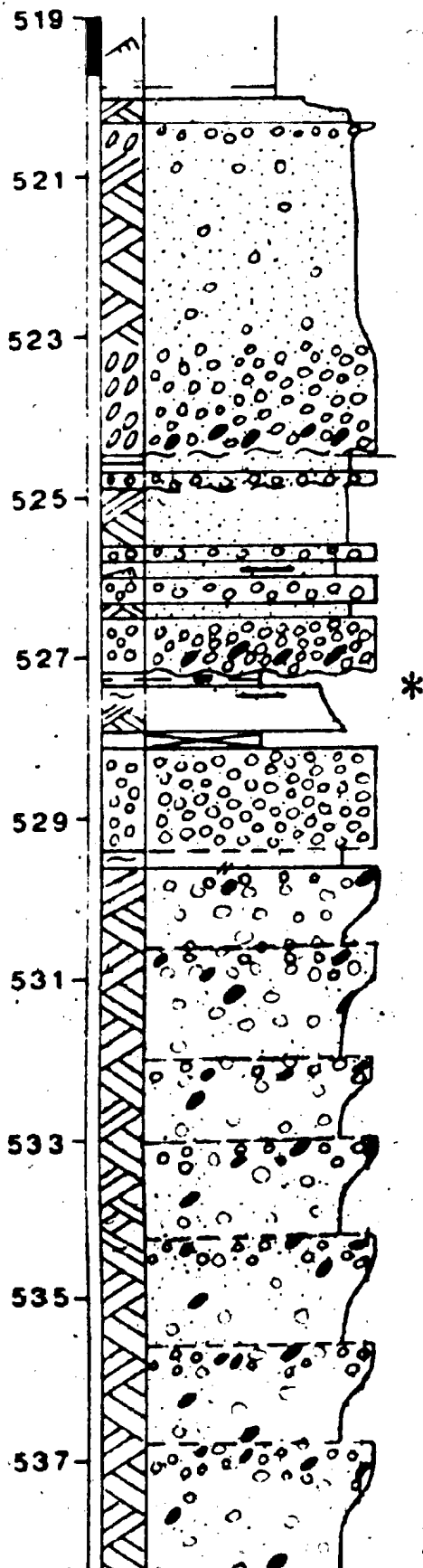
OUTCROP 16

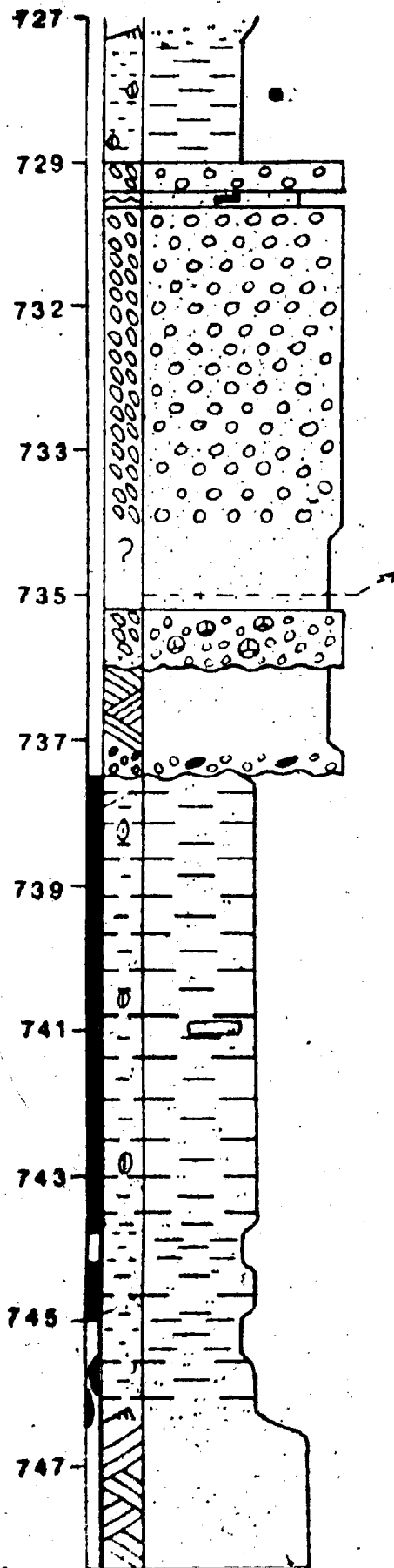
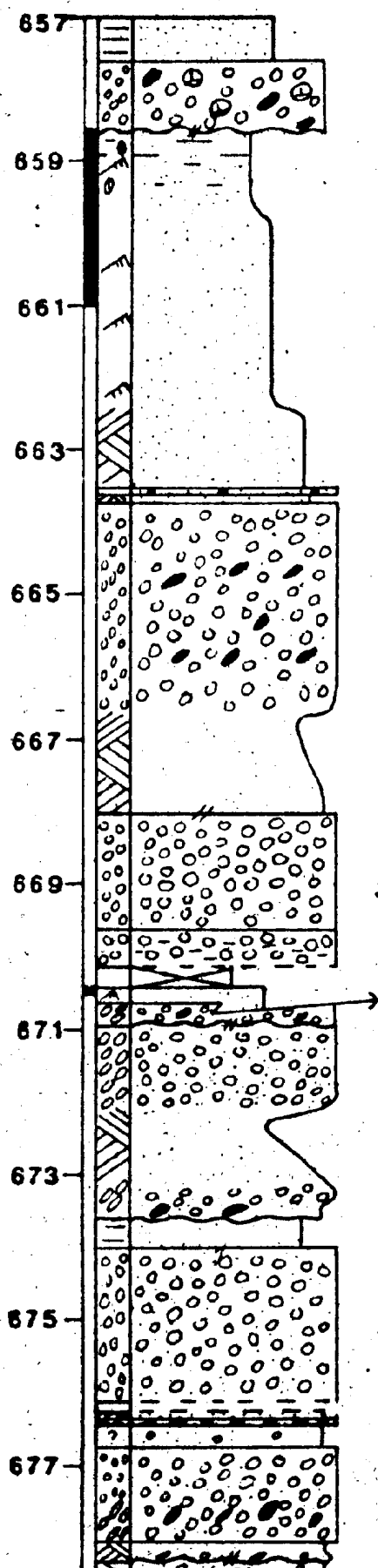


cross-strata

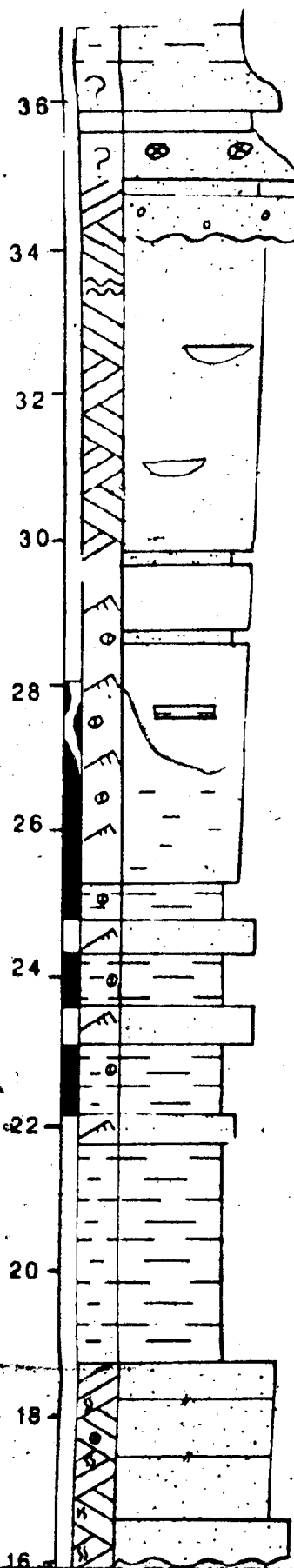






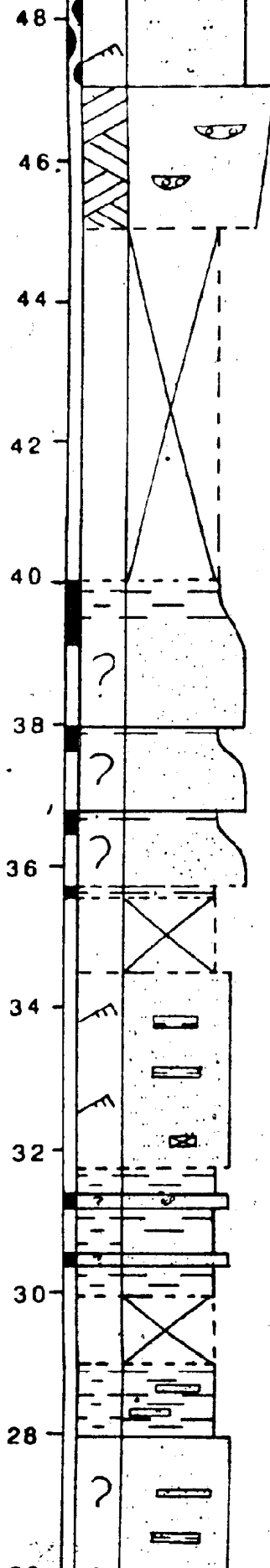


OUTCROP 11

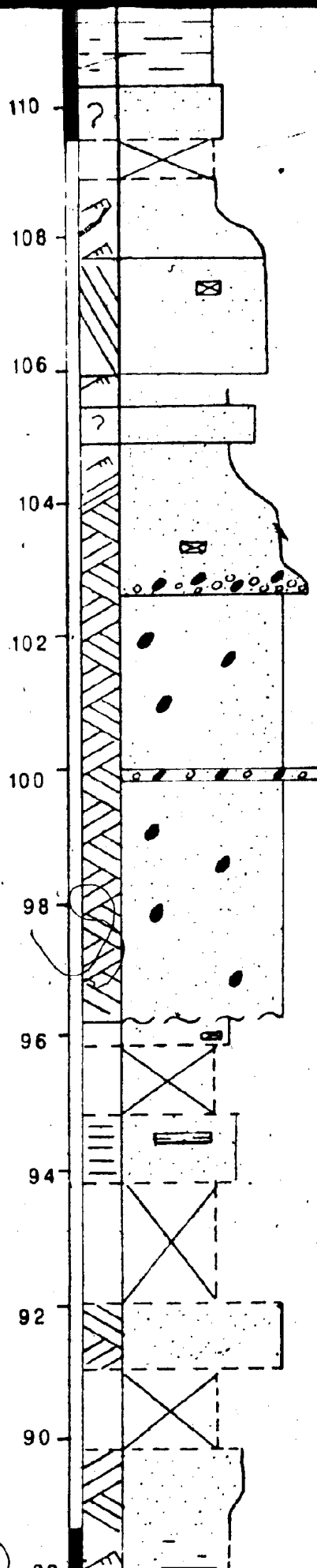


cross-strata

cross-strata



cross-strata



172

F24 *

48

170

46

168

44

166

42

164

40

162

38

160

36

158

34

156

32

154

30

152

28

OUTCROP 16

12

10

8

6

4

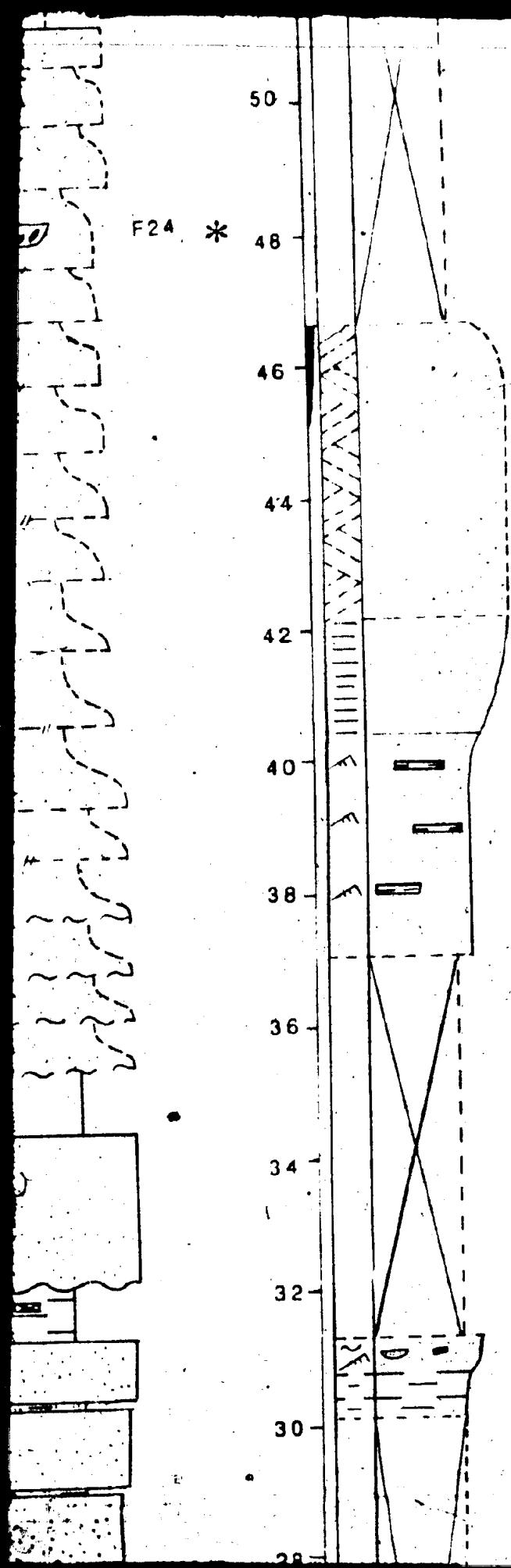
2

0

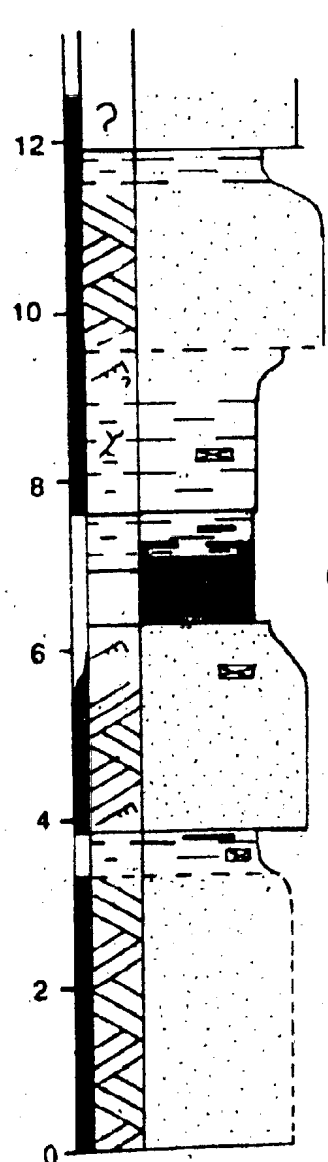
OUTCROP 15

28

26



OUTCROP 16



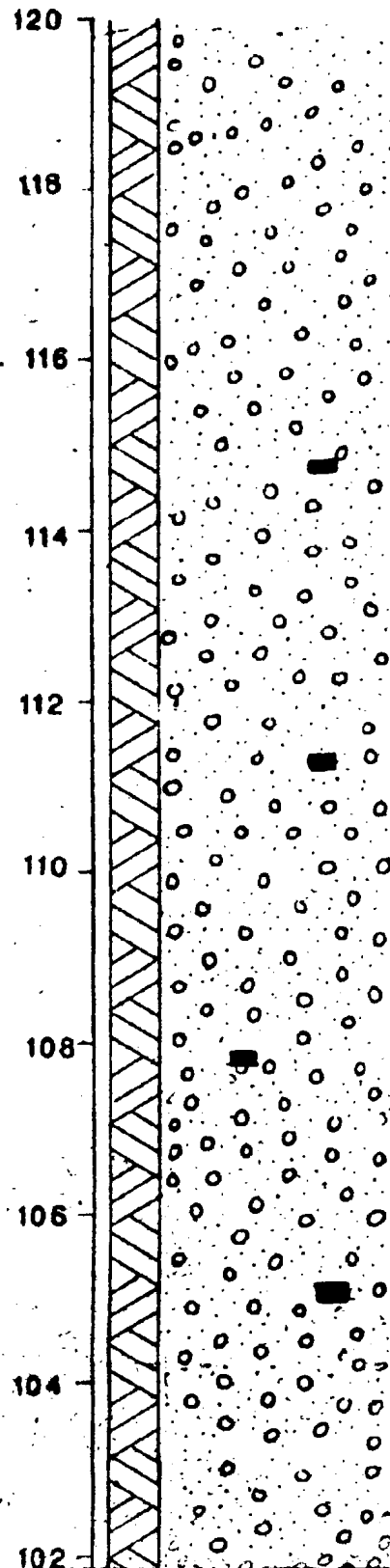
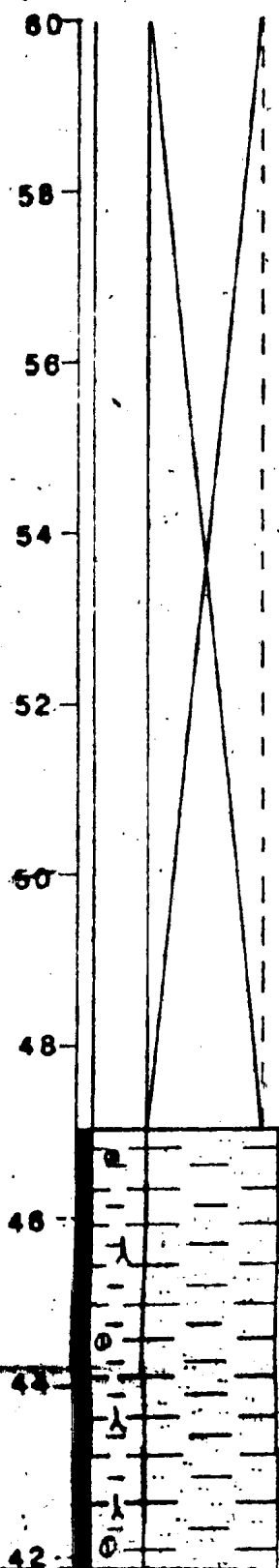
Cleary Seam (?)

OUTCROP 15



↗ cross-strata

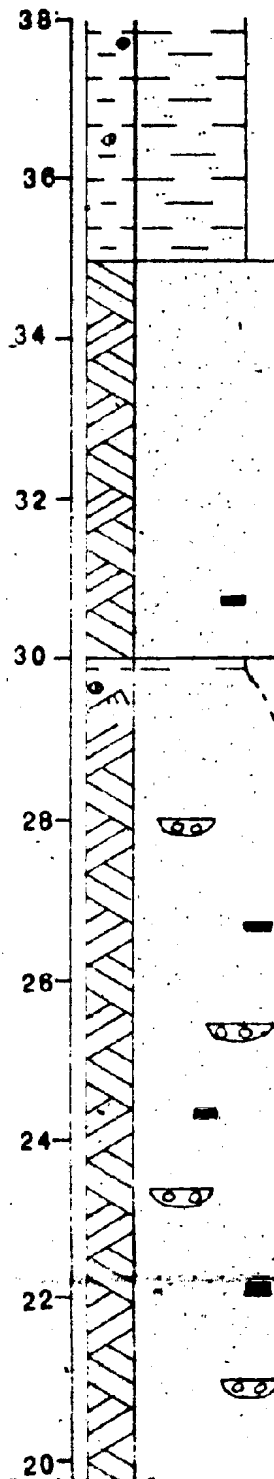
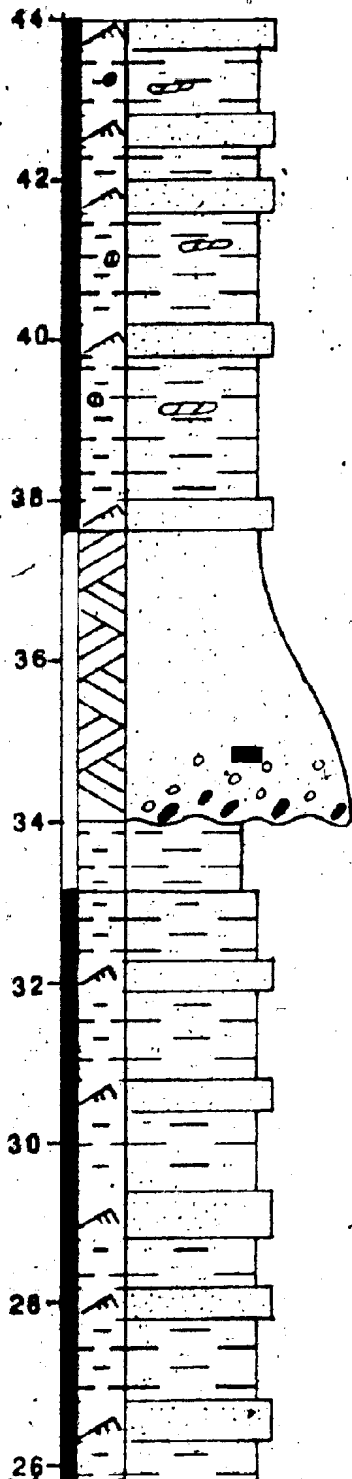
OUTCROPS 38-39



cross-strata

APPENDIX A FIGURE 5

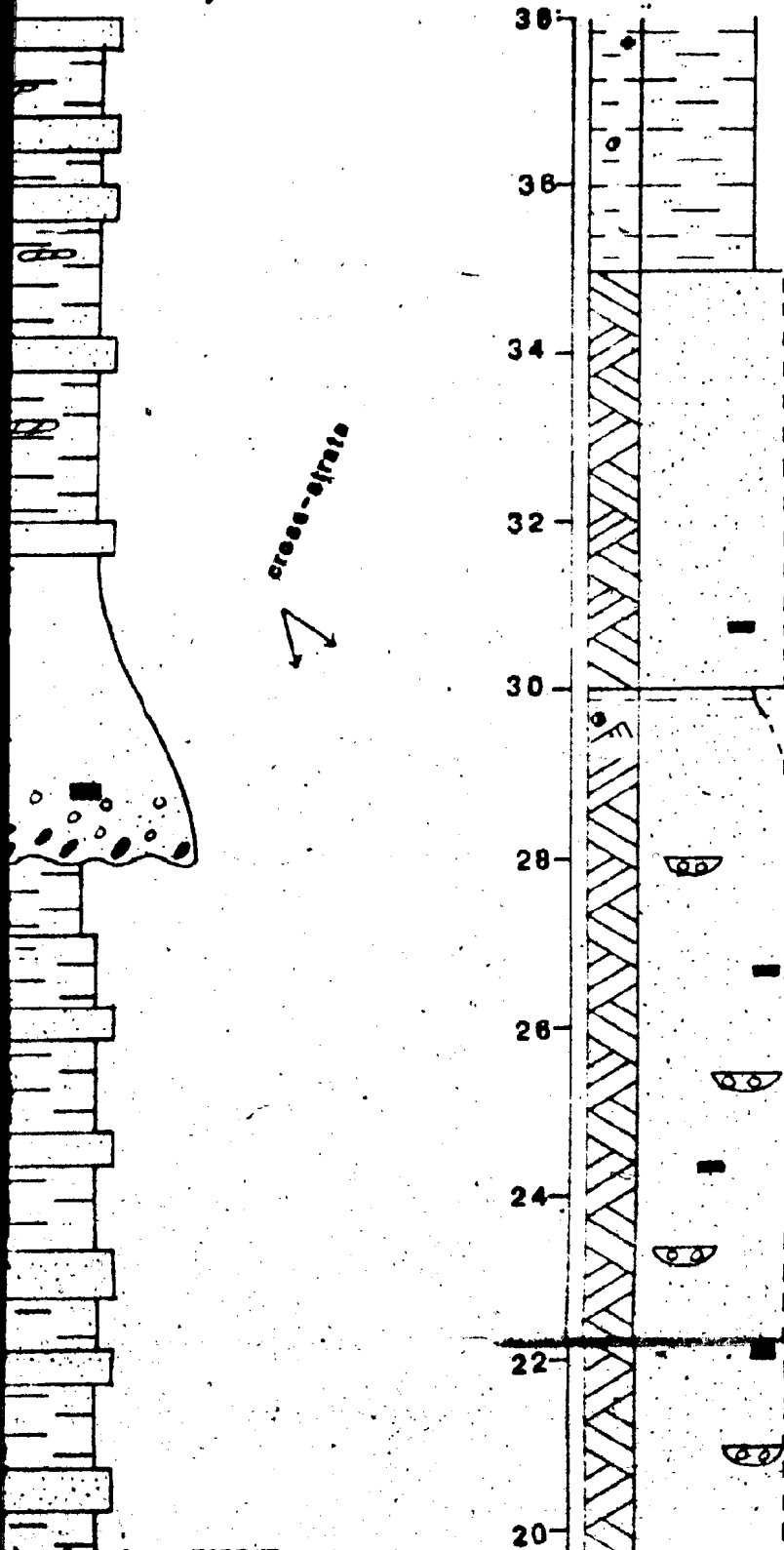
OUTCROPS 38-39, 43, 44, 48, 49, 49a,



OUTCROP

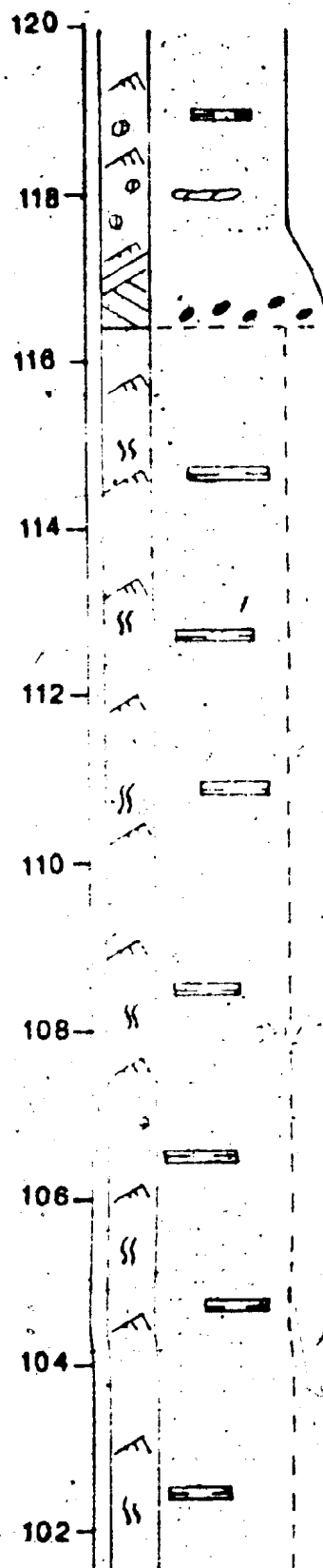
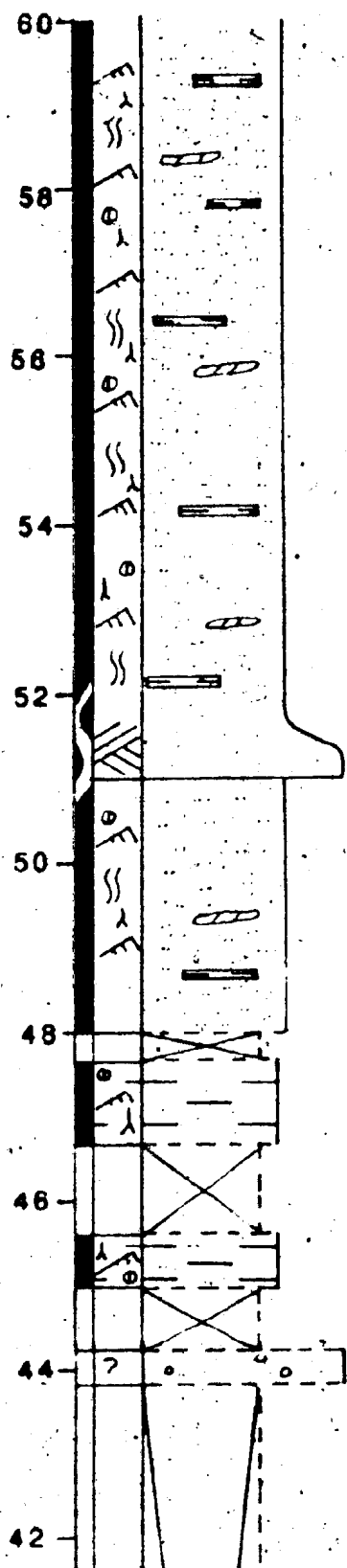
APPENDIX A FIGURE 5

OUTCROPS 38-39, 43, 44, 48, 49, 49a, 50, 21



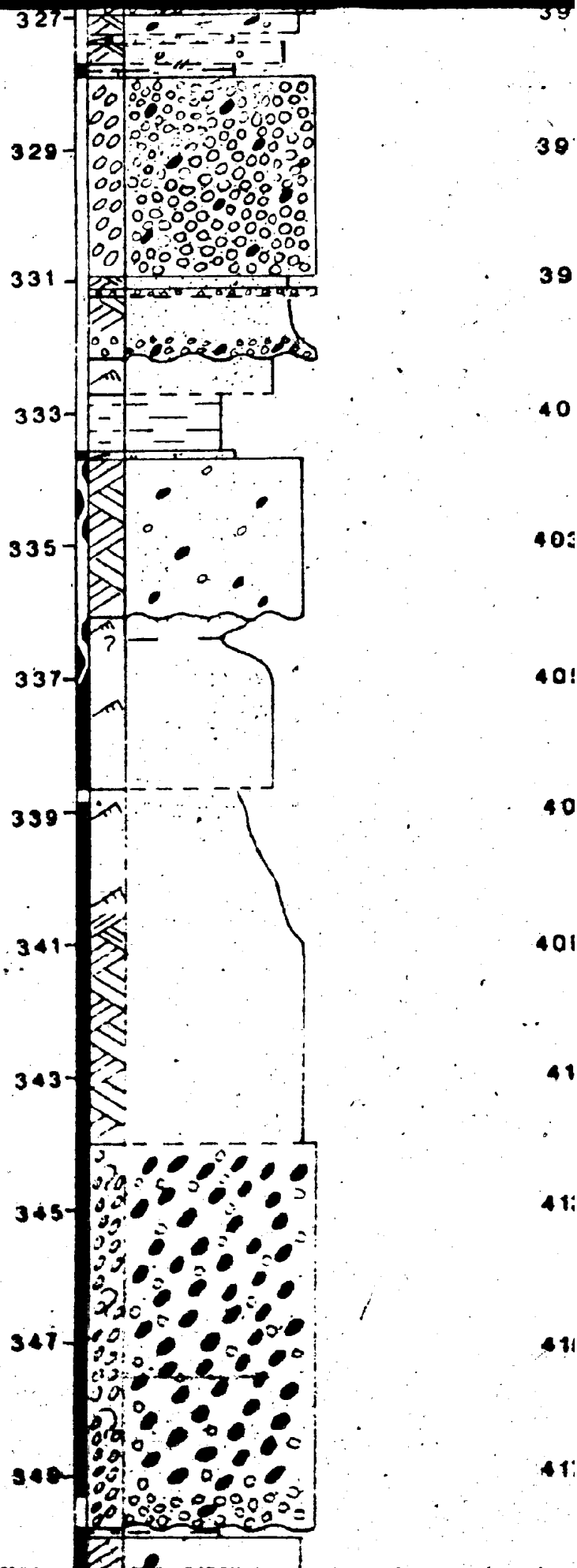
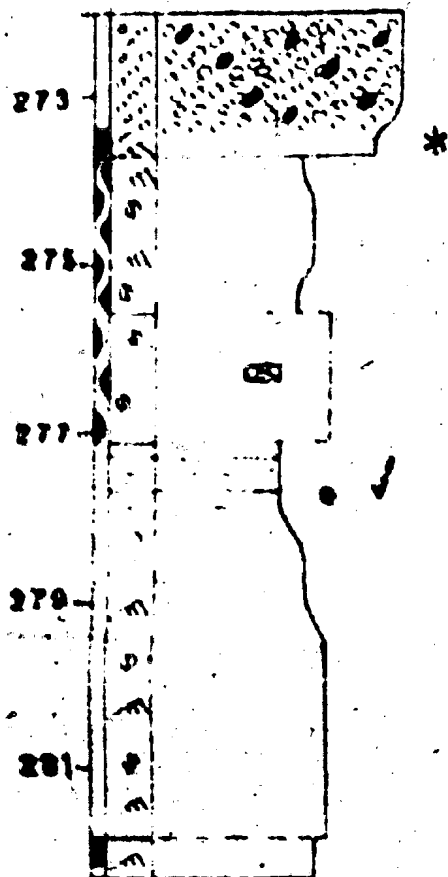
OUTCROP 50

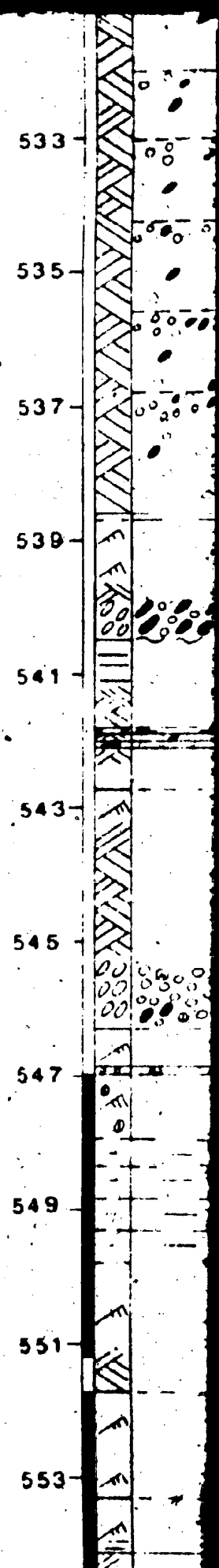
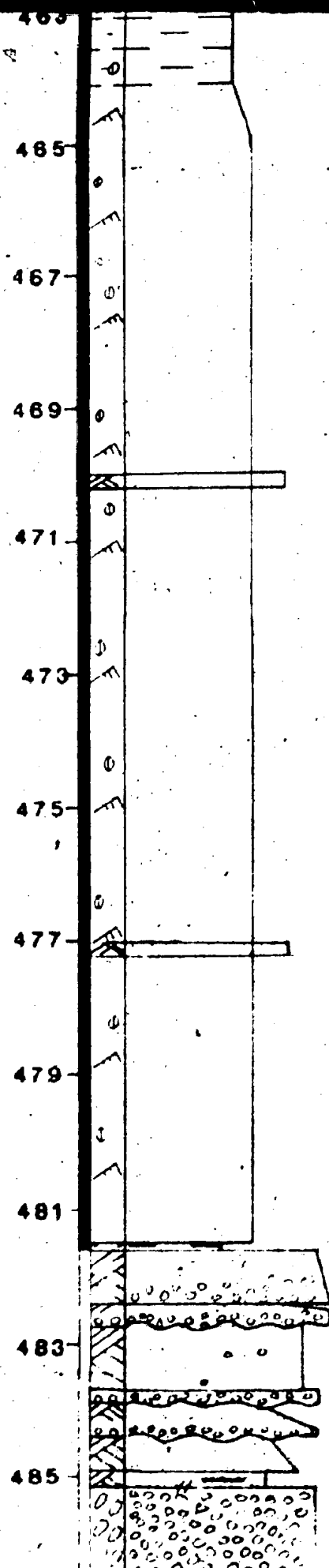
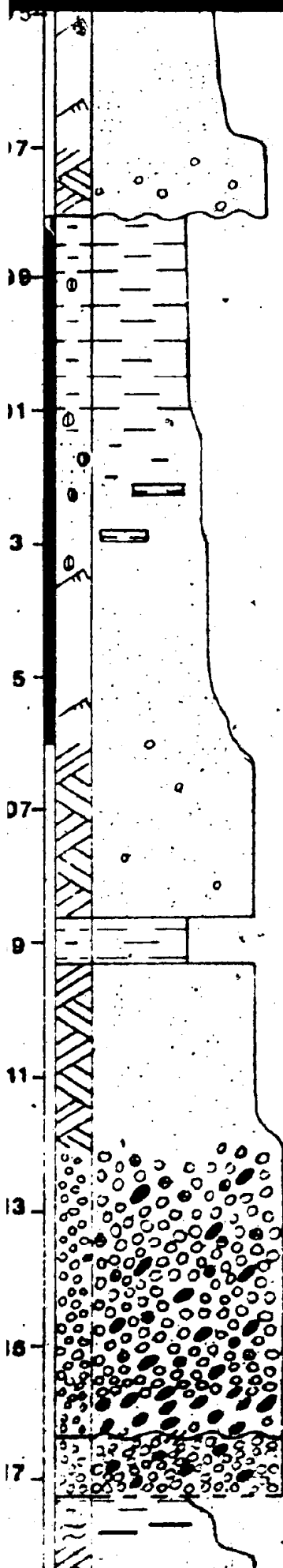
OUTCROPS 21-25

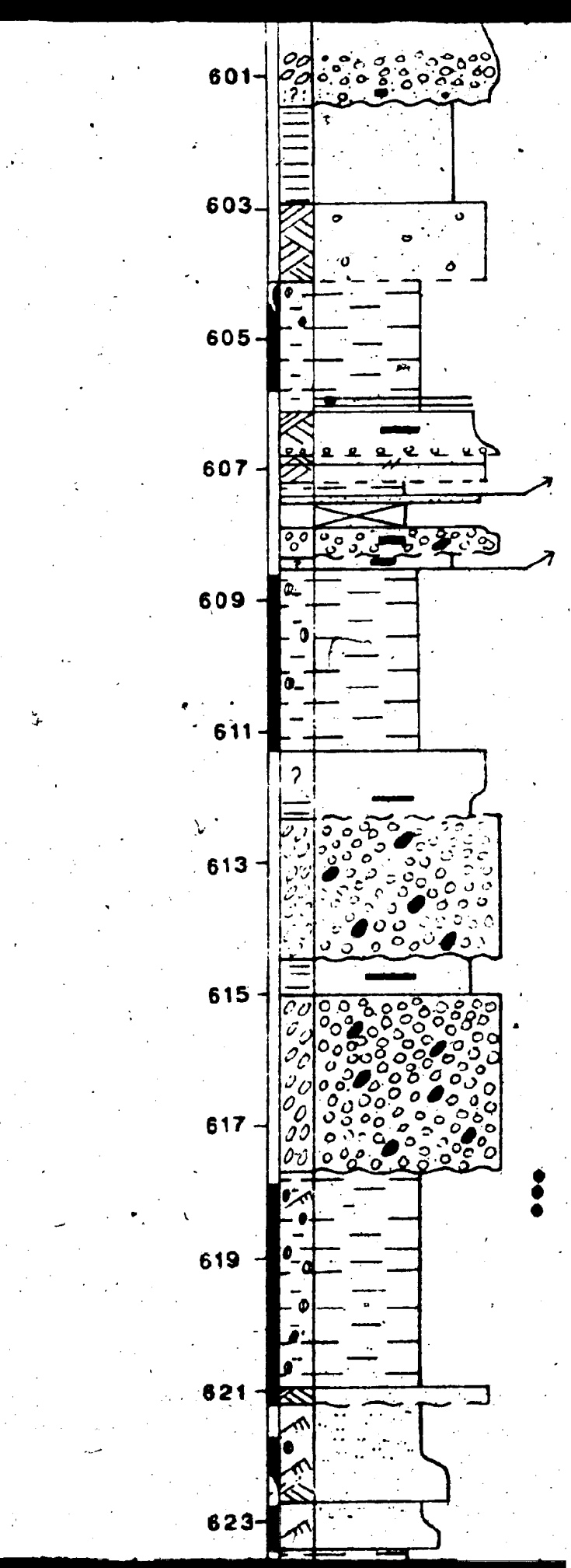
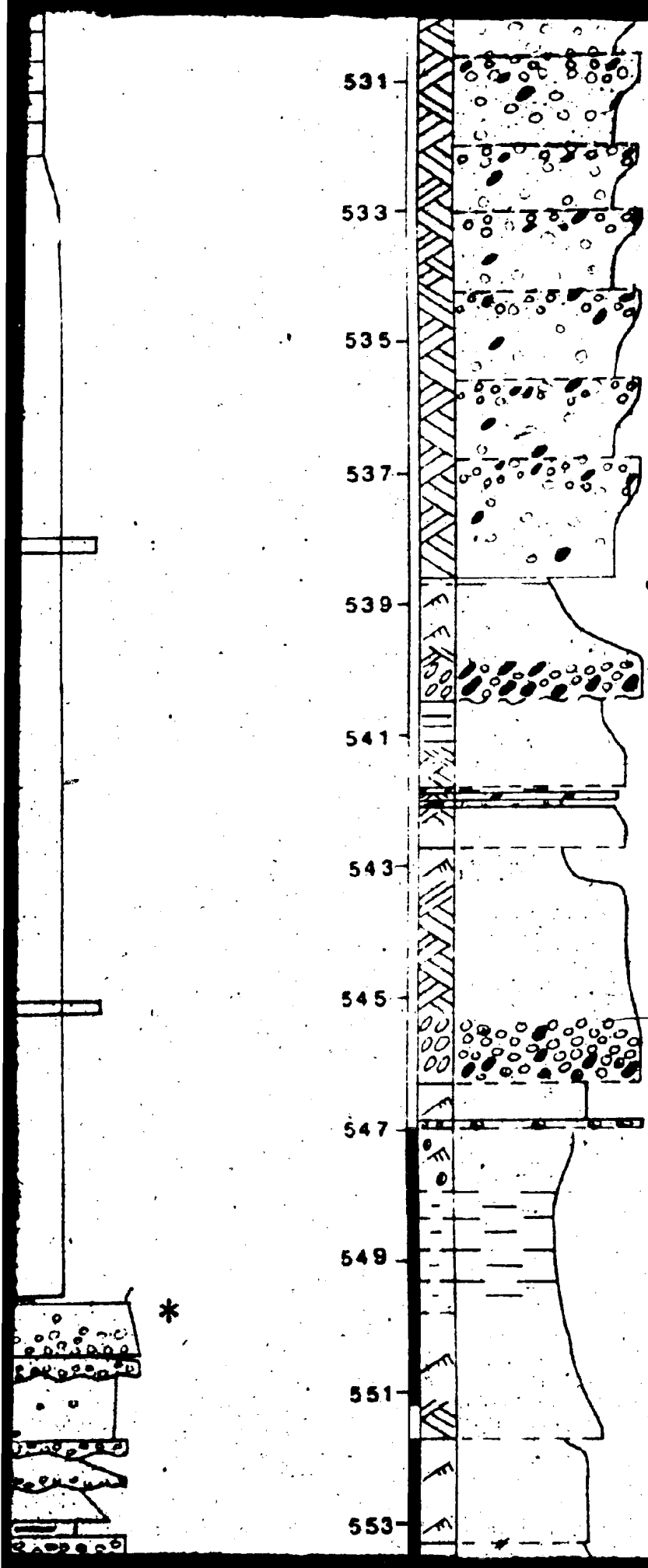


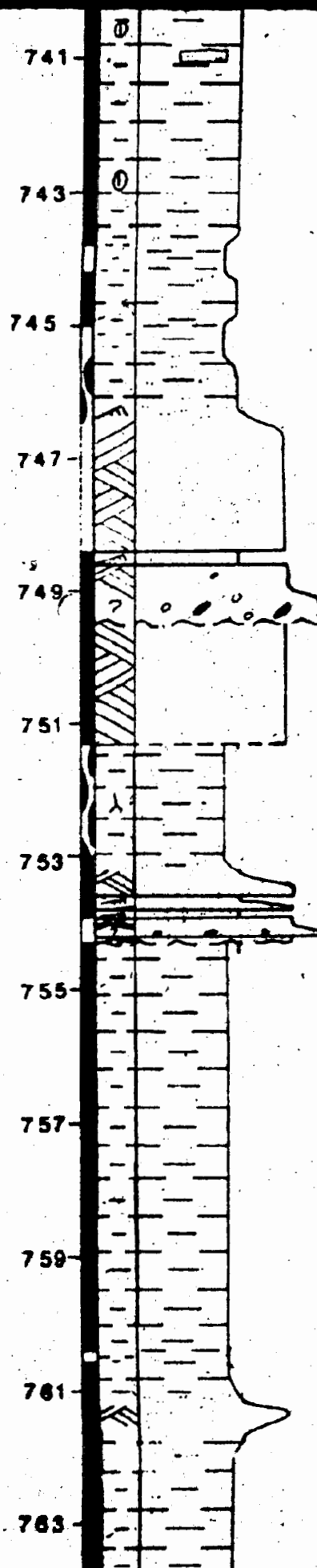
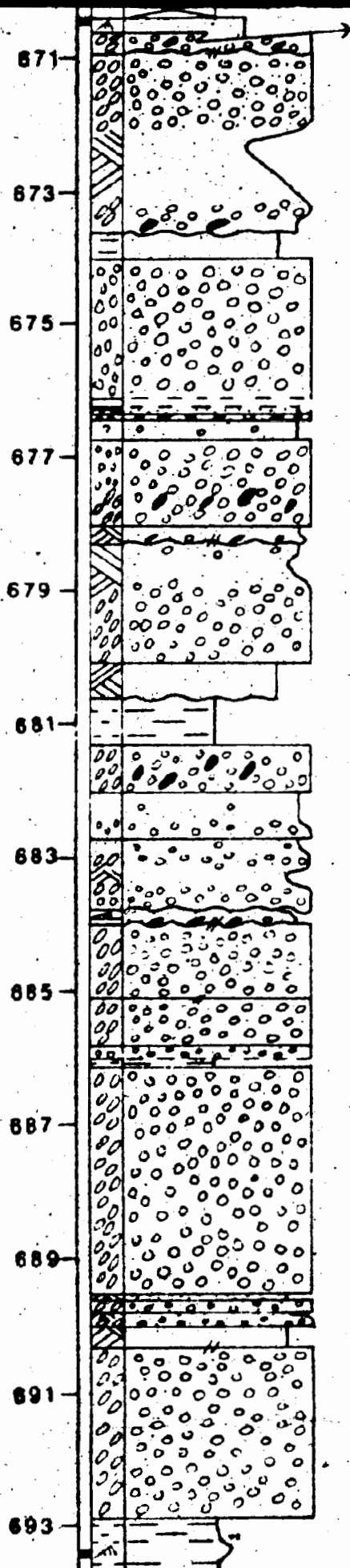
APPENDIX A FIGURE 3

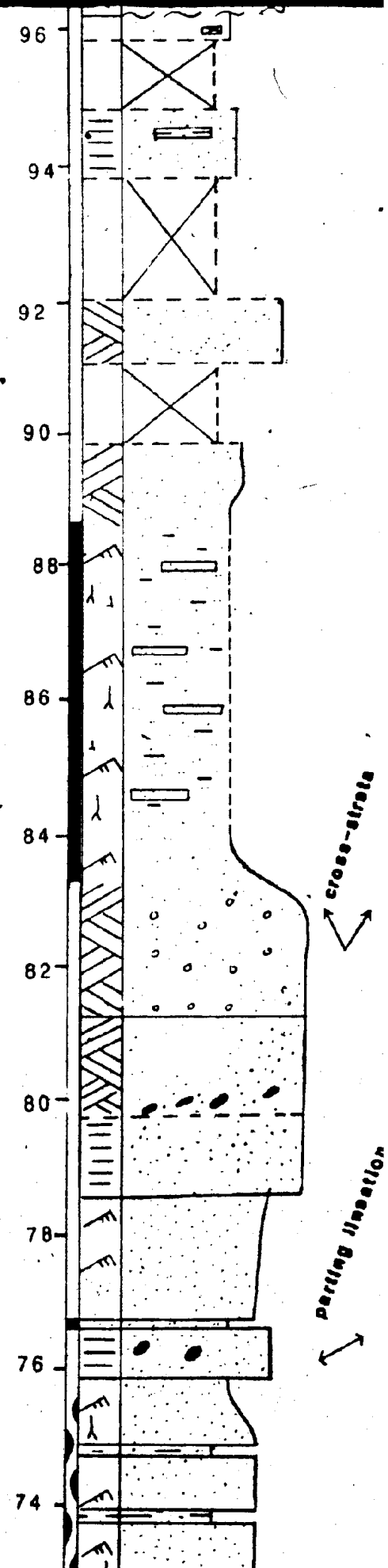
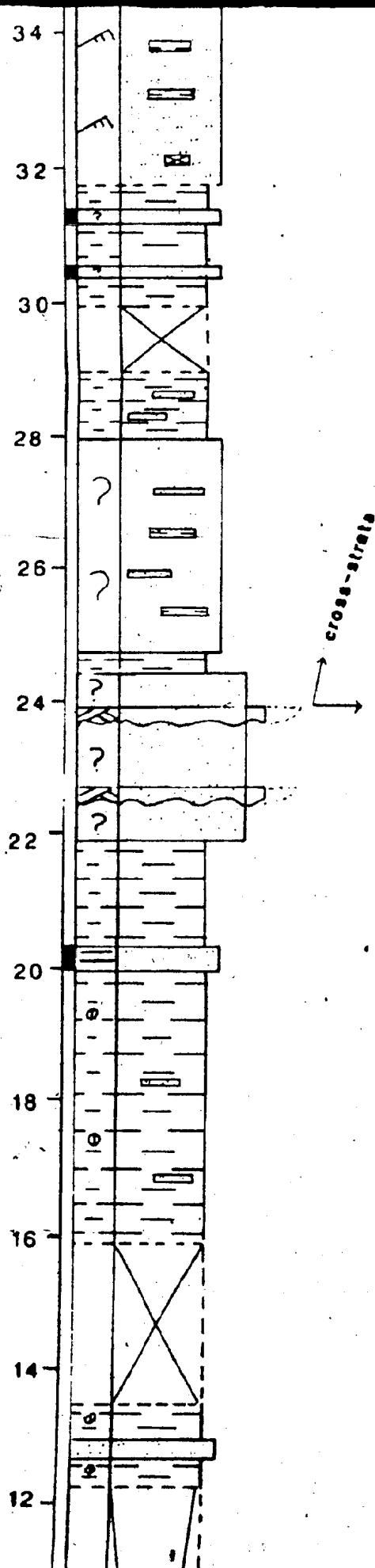
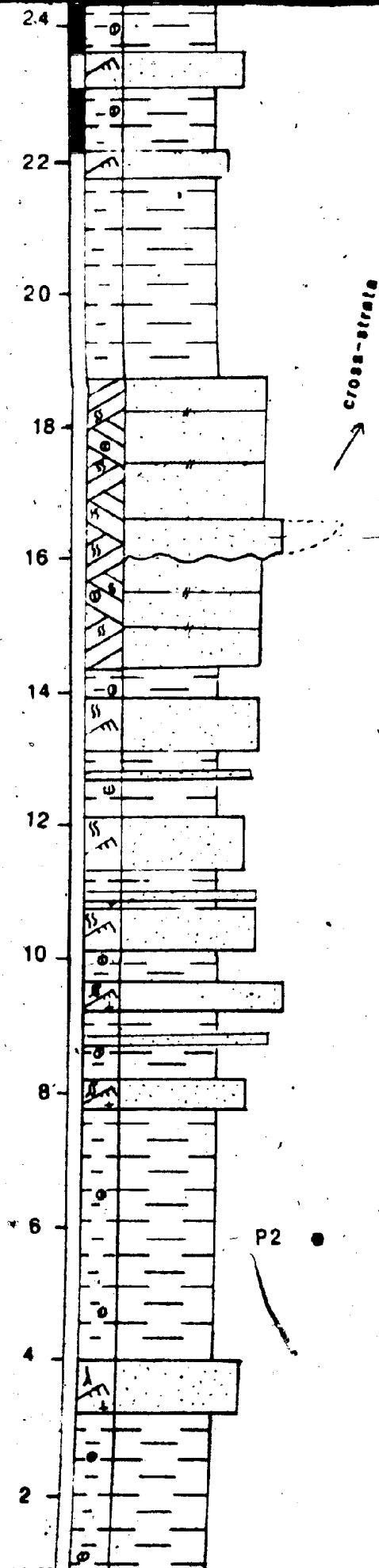
FB2-76

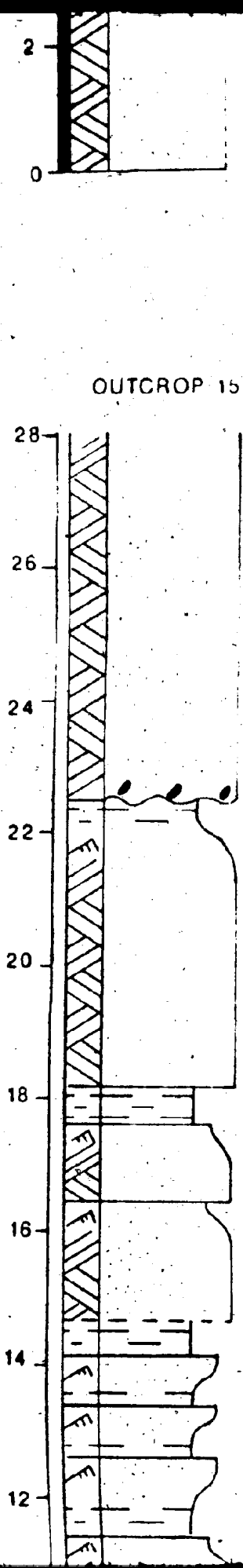
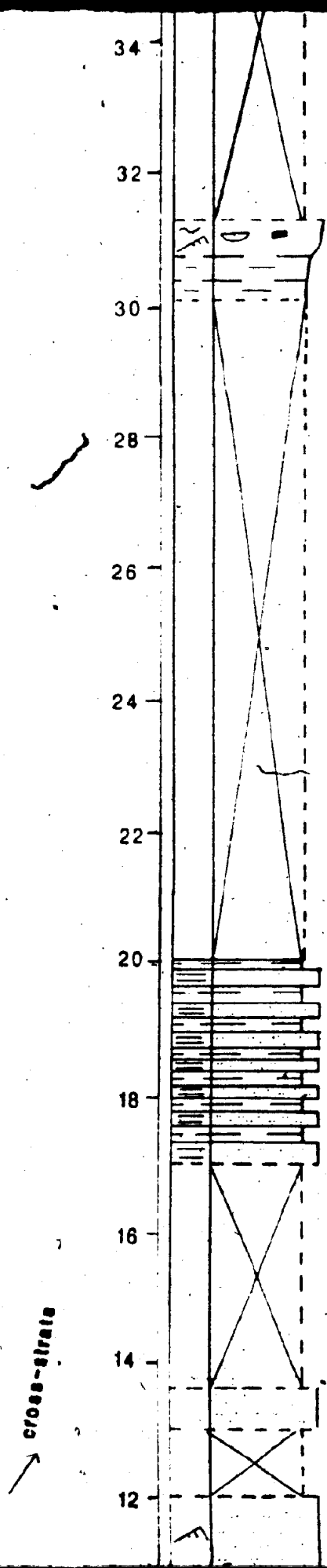
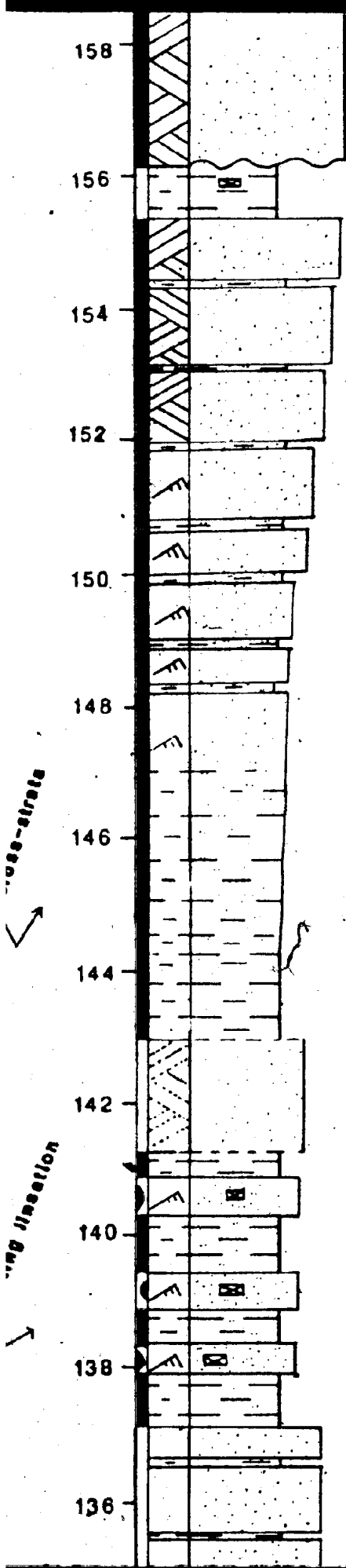


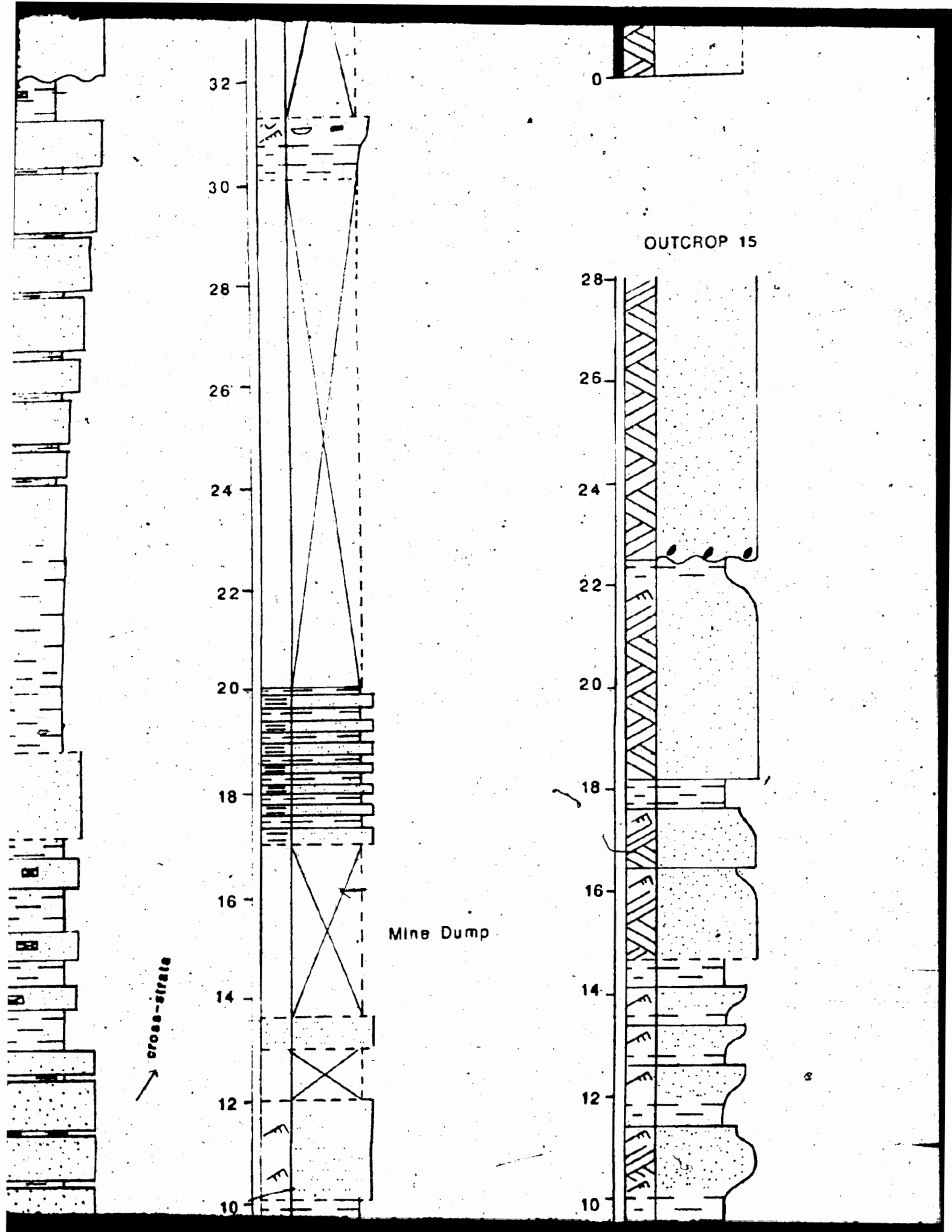


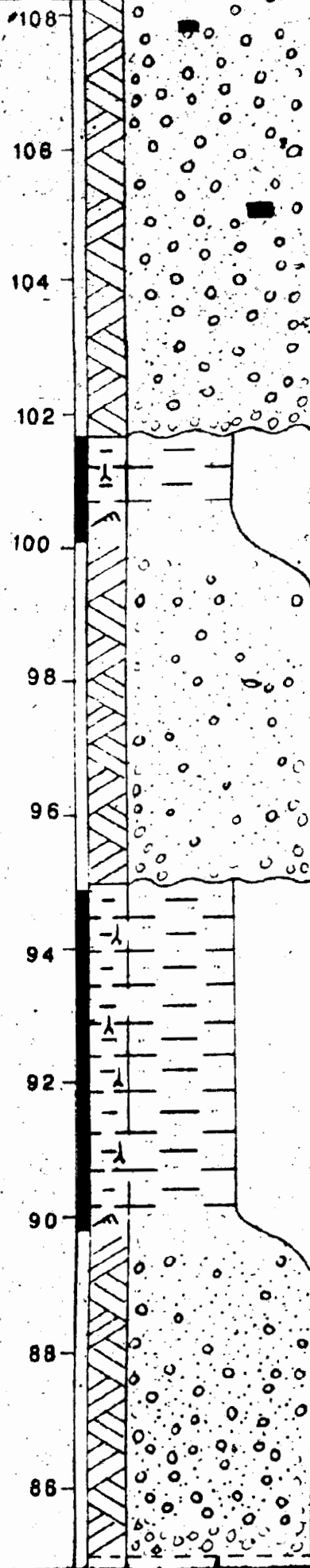
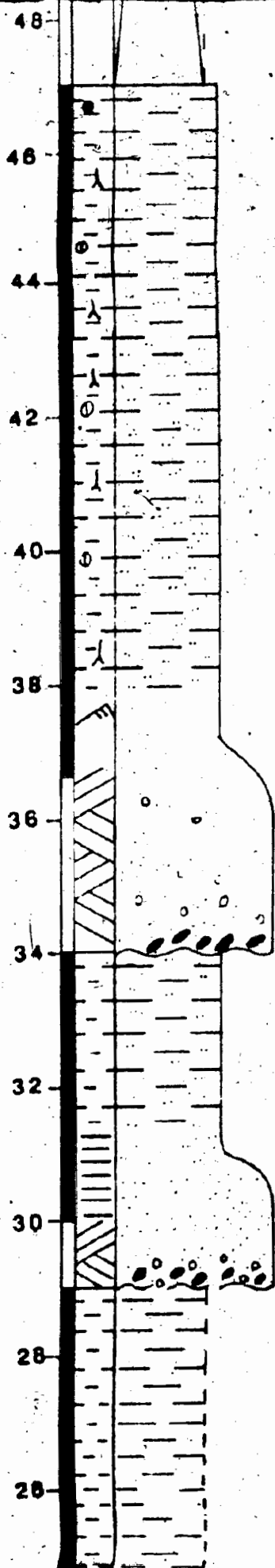




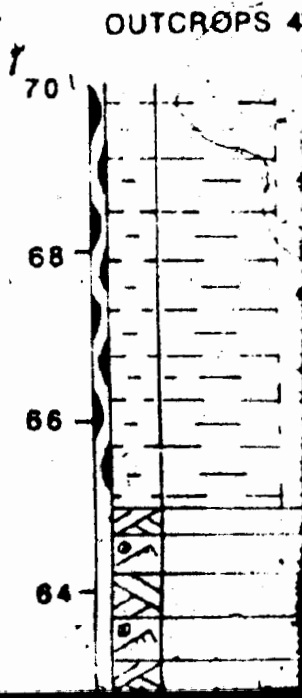
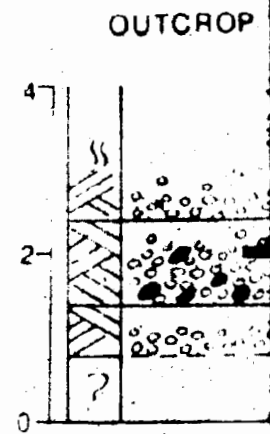
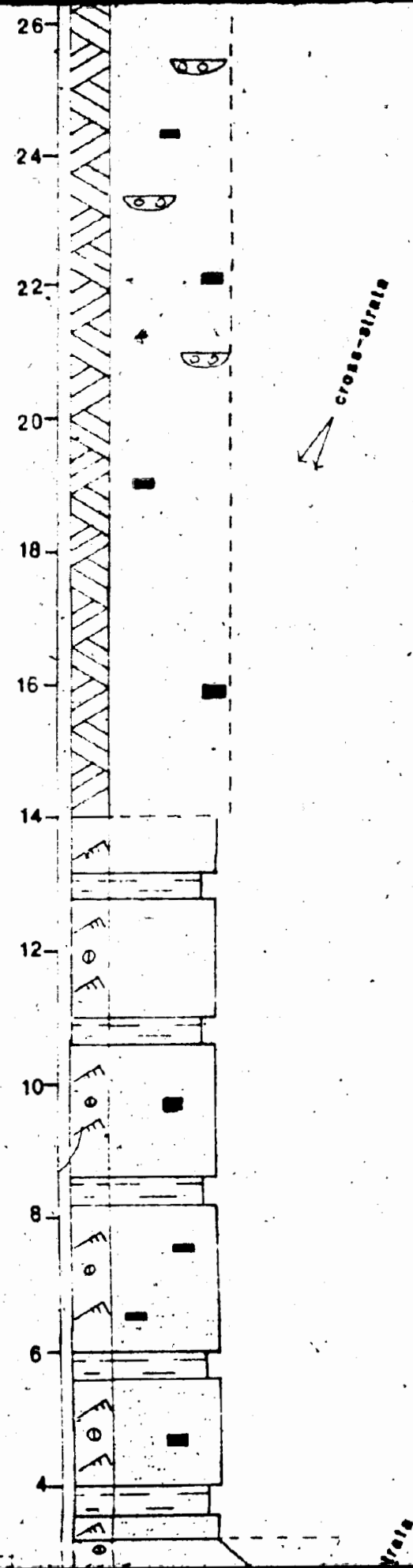
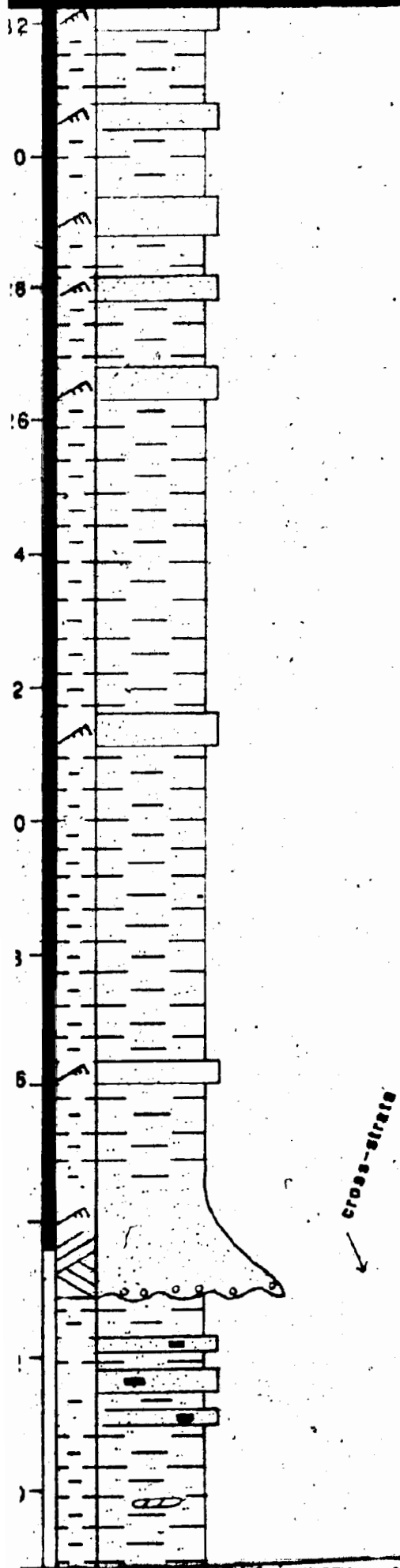


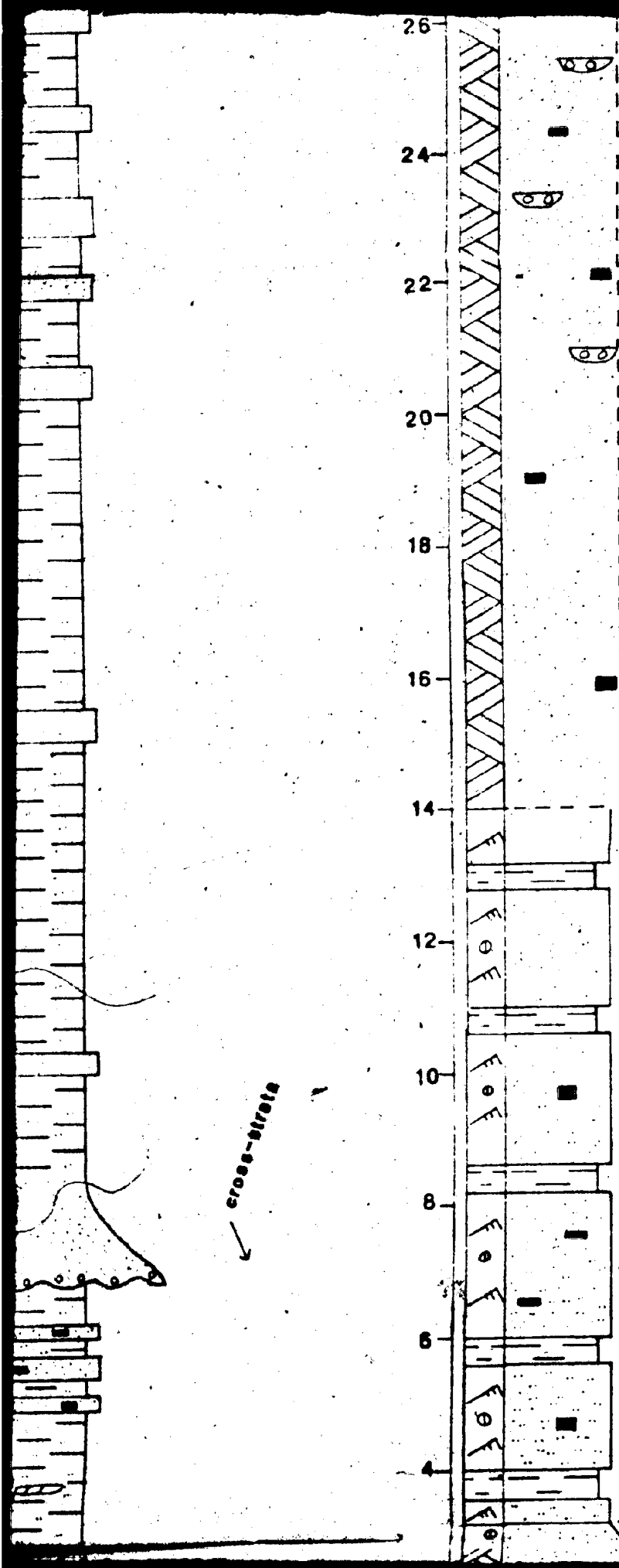






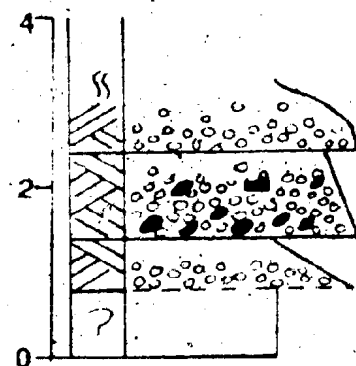
cross-section



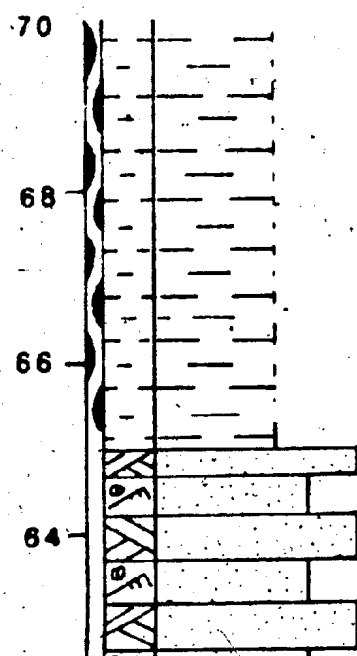


cross-strata

OUTCROP 50

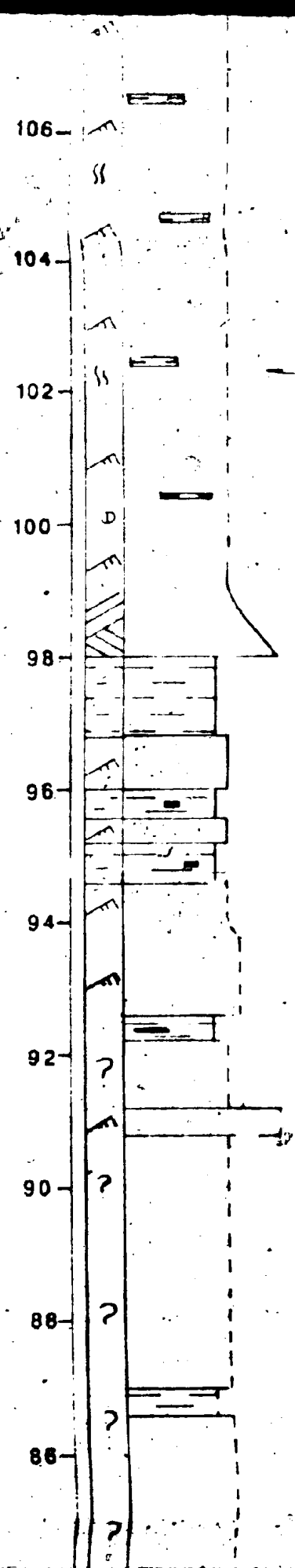
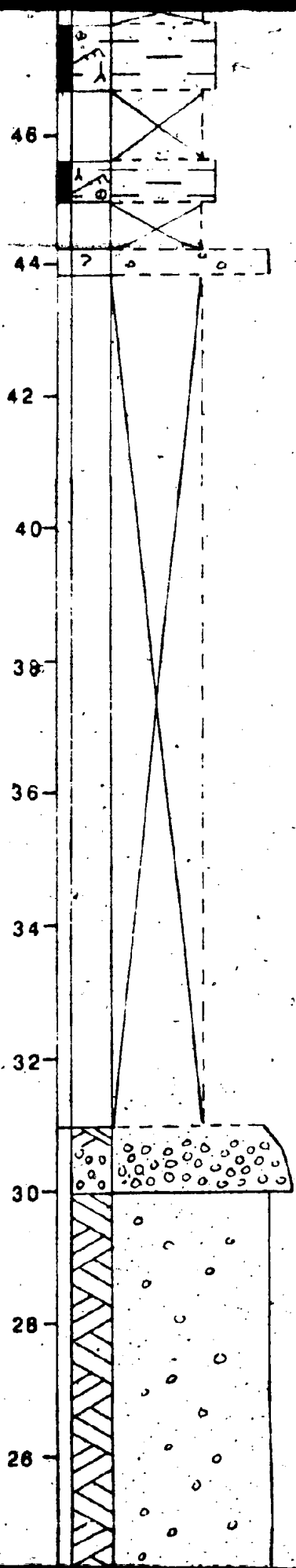


OUTCROPS 48, 49, 49



7 1000

9,49a



275

277

279

281

283

285

287

289

291

293

295

297

343

345

347

349

351

353

355

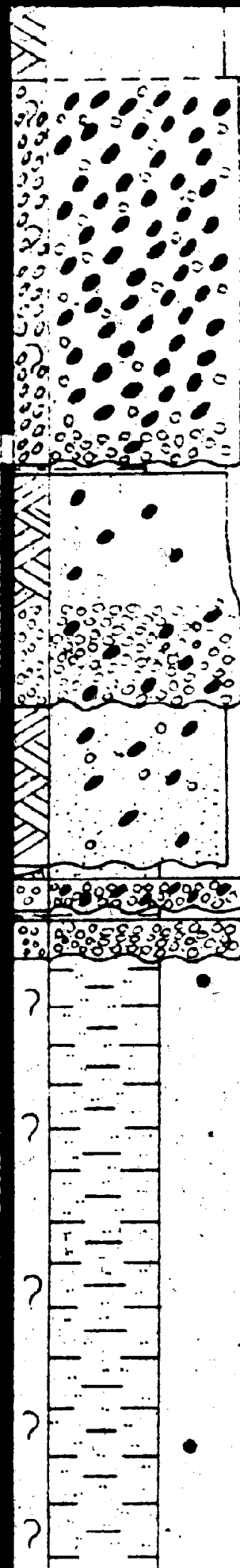
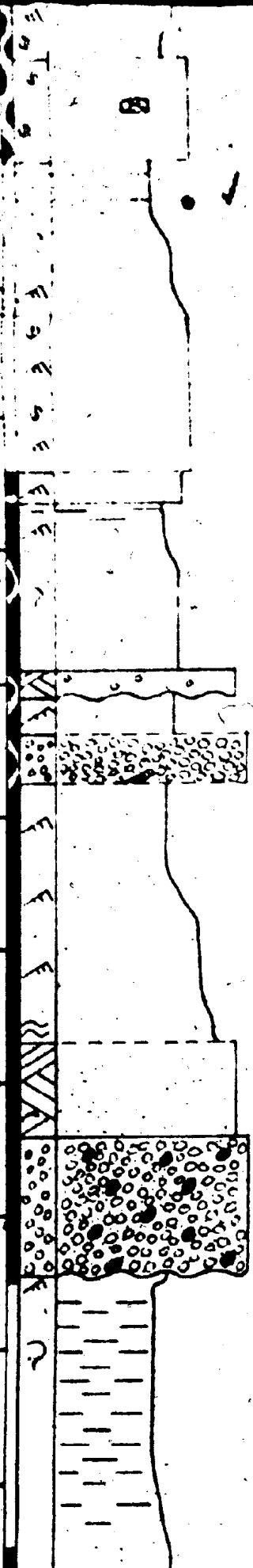
357

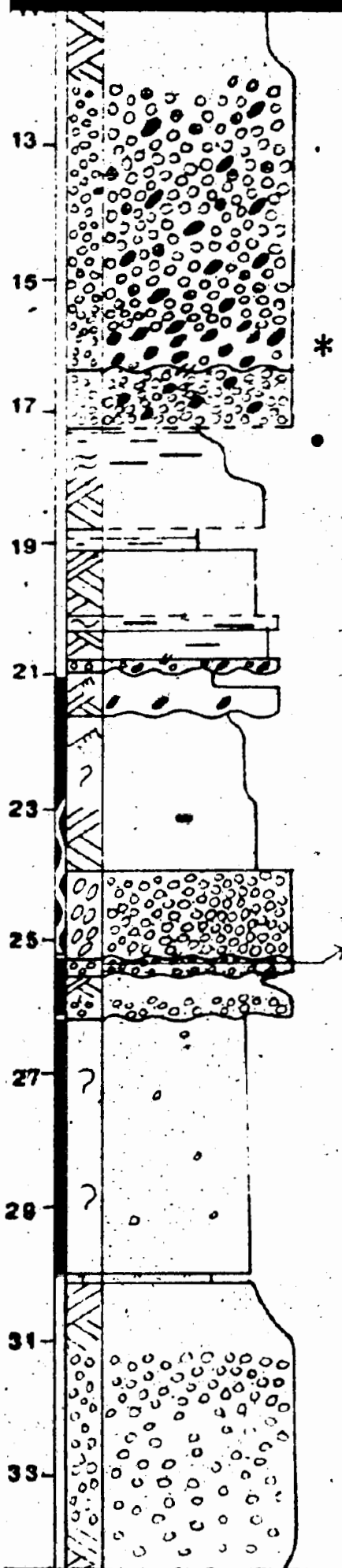
359

361

363

365





481

483

485

487

489

491

493

495

497

499

501

549

551

553

555

557

559

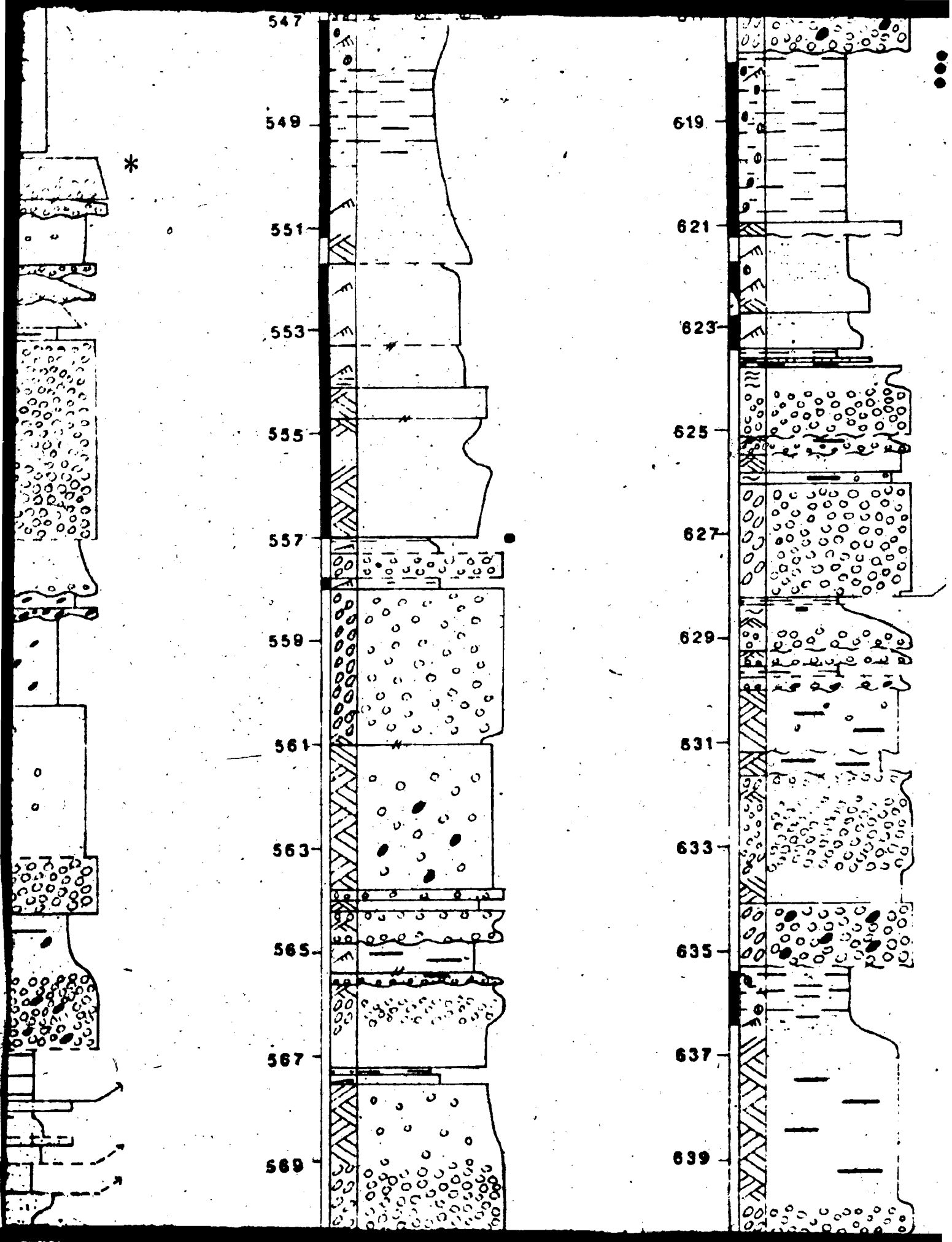
561

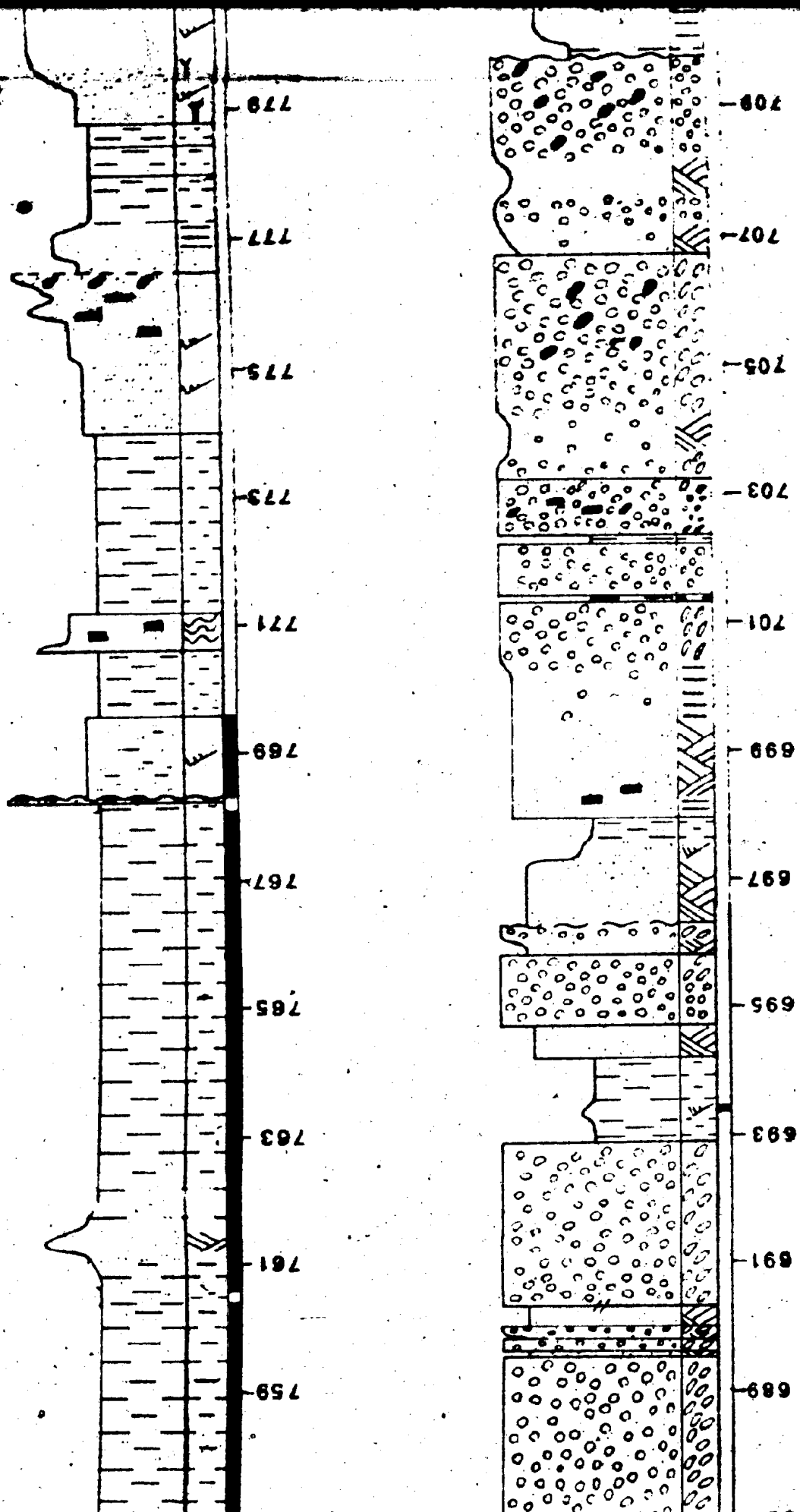
563

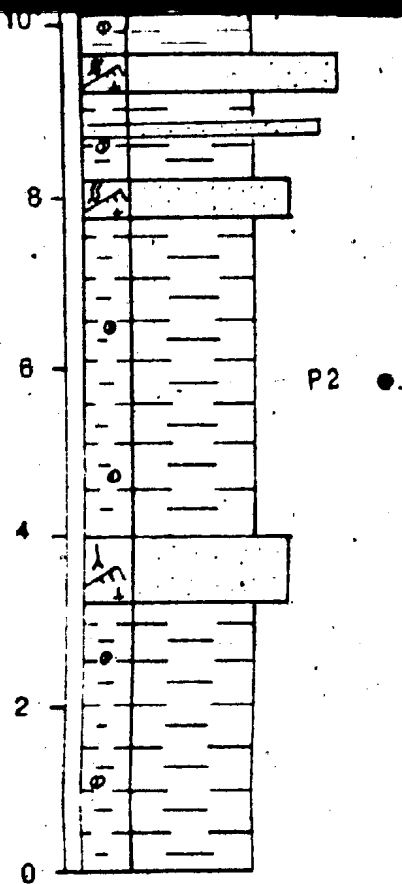
565

567

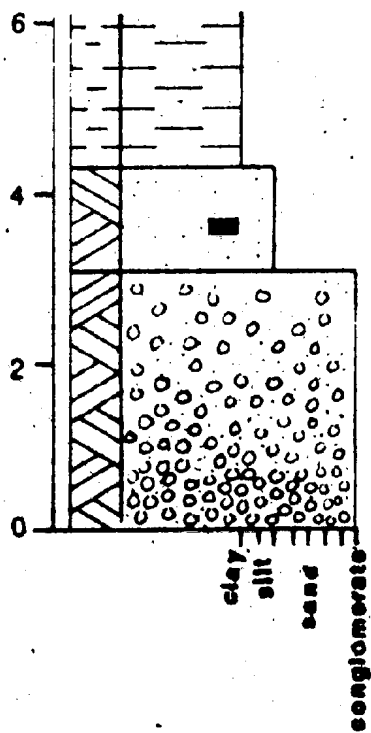
569



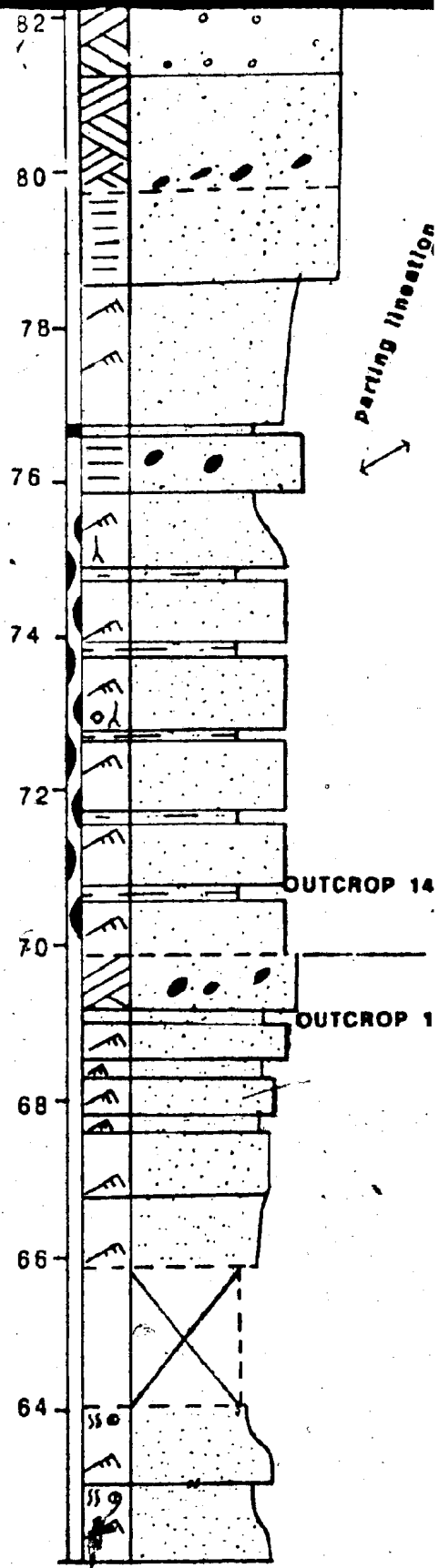
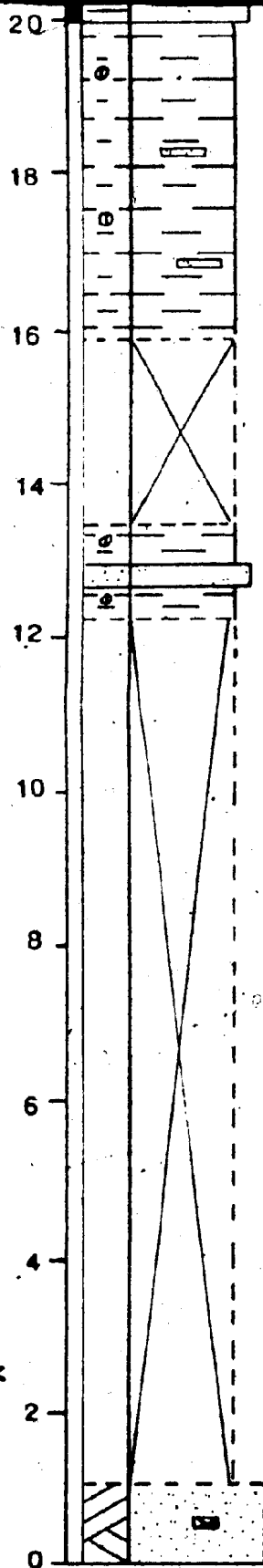


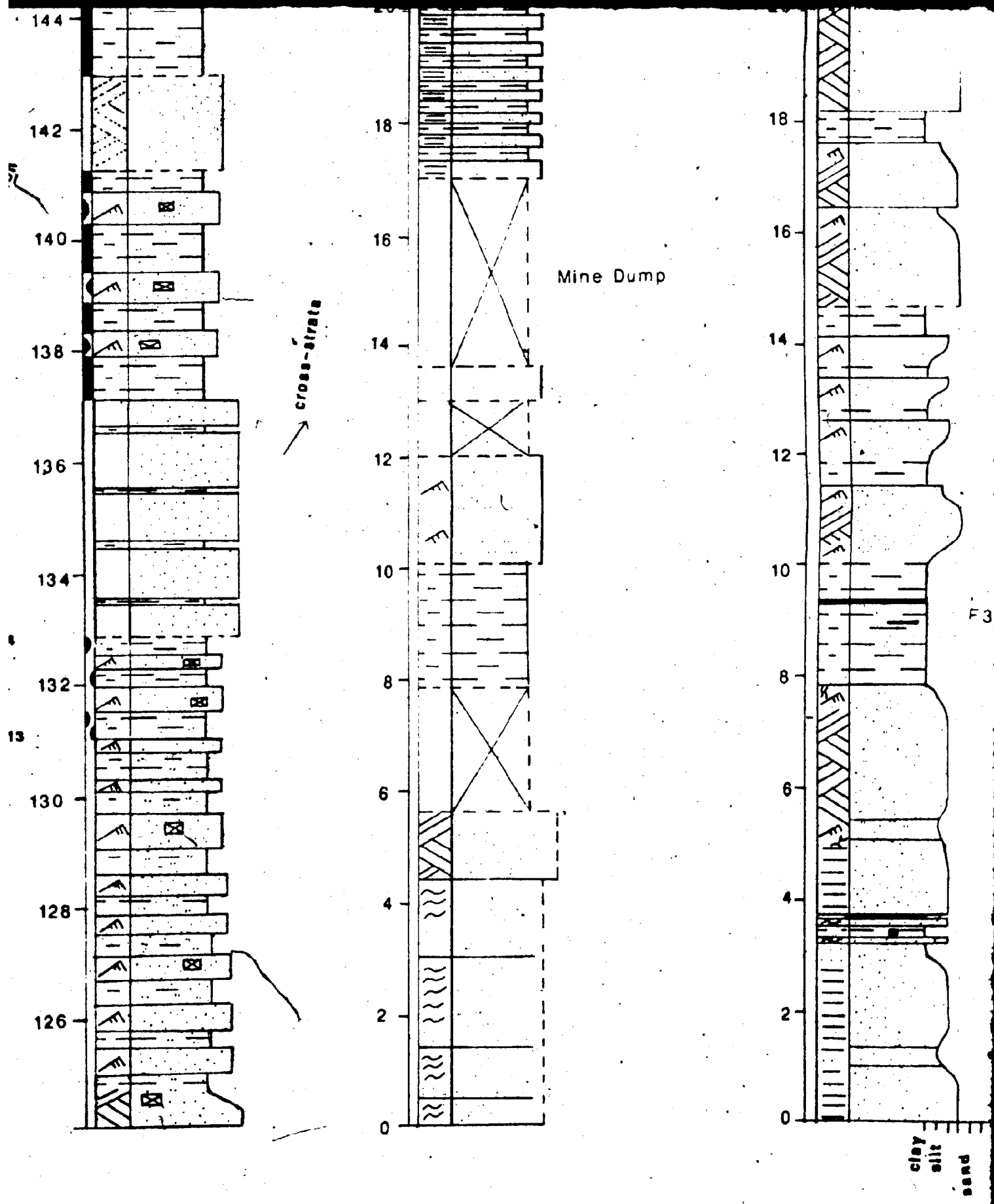


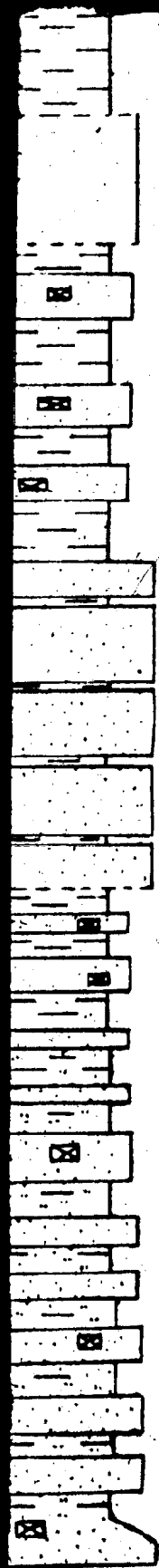
OUTCROP 10



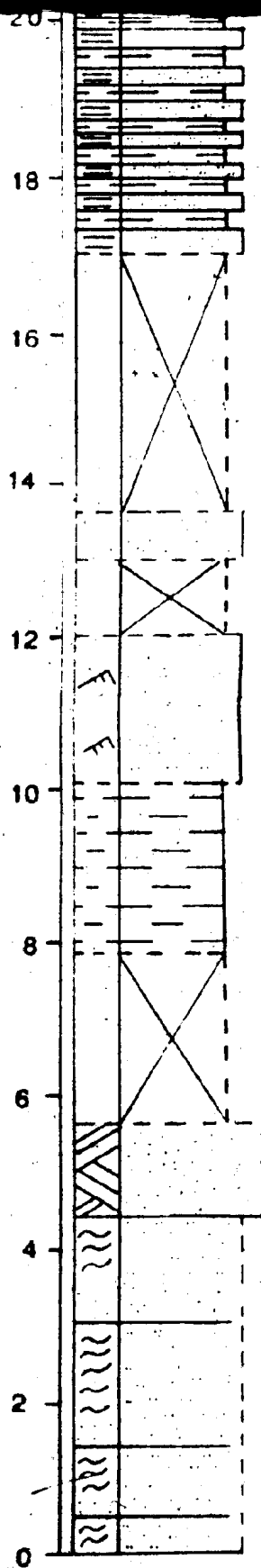
F13 *



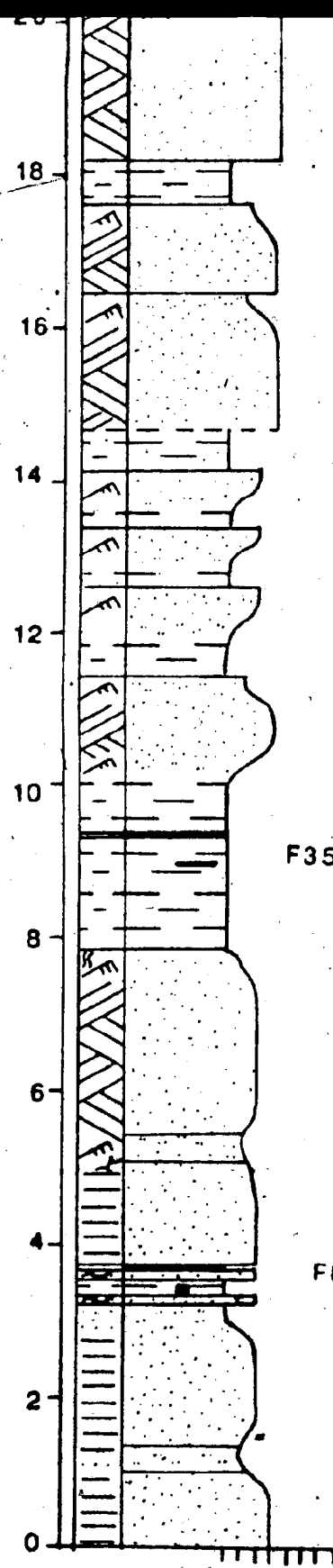




↗ cross-strata



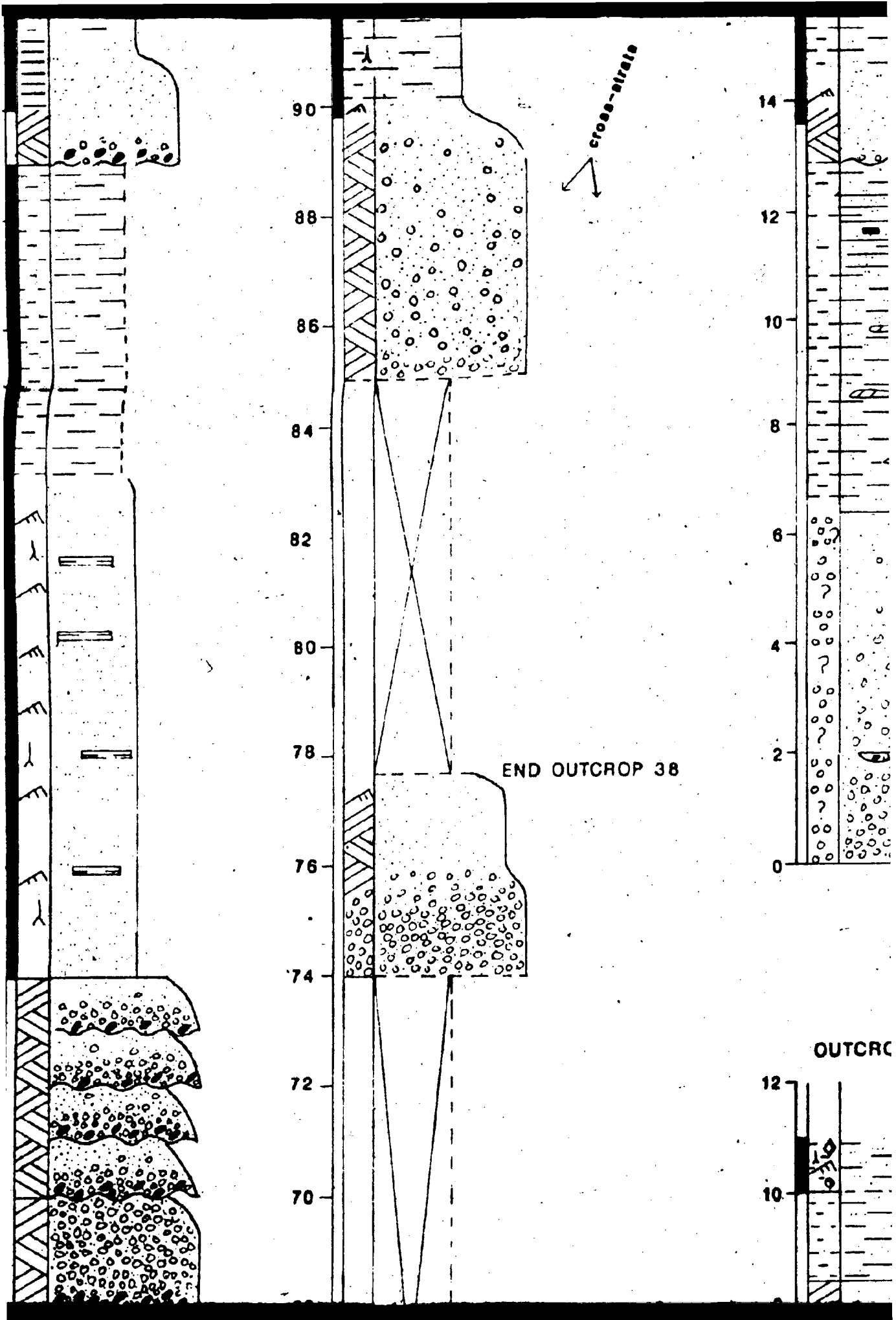
Mine Dump

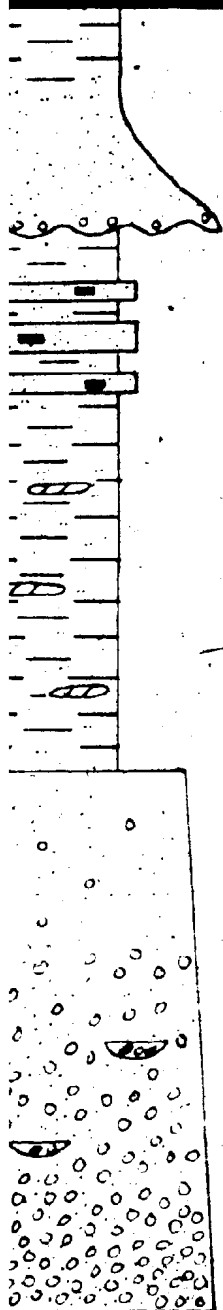


F35 •

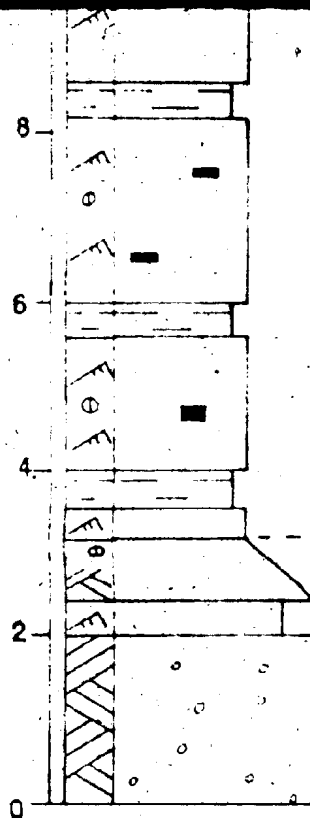
F85 *

clay
alt.
sand
conglomerate

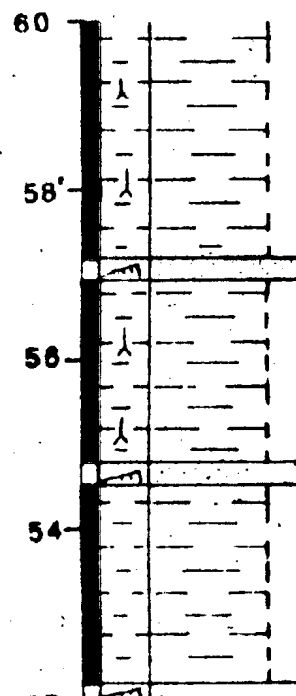




F51 ●

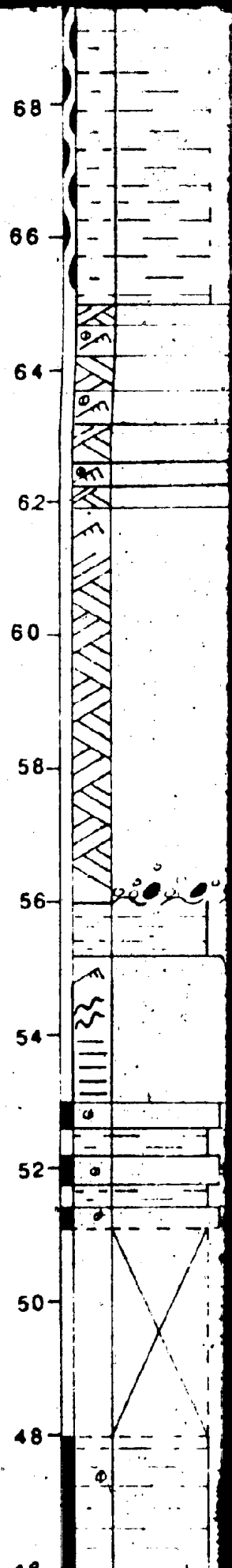


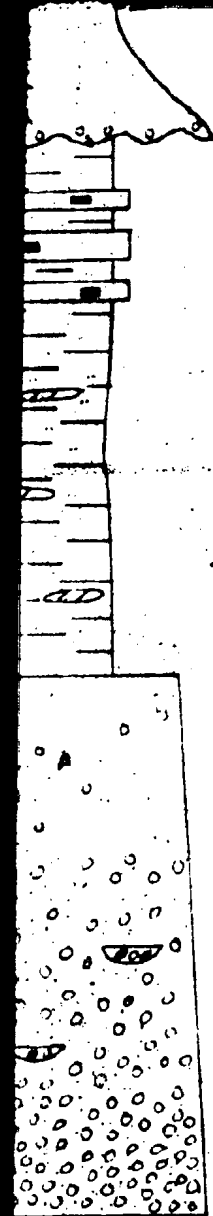
OUTCROP 44



cross-laminated
cross-strata

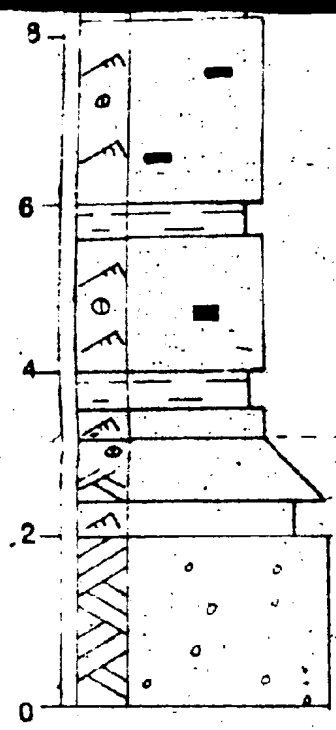
cross-laminated





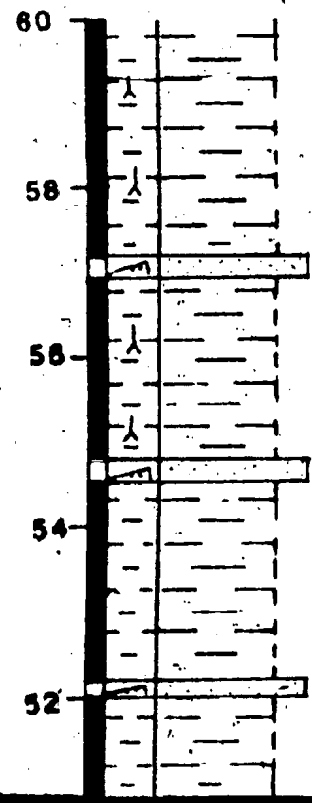
ROP 43

F5T ●



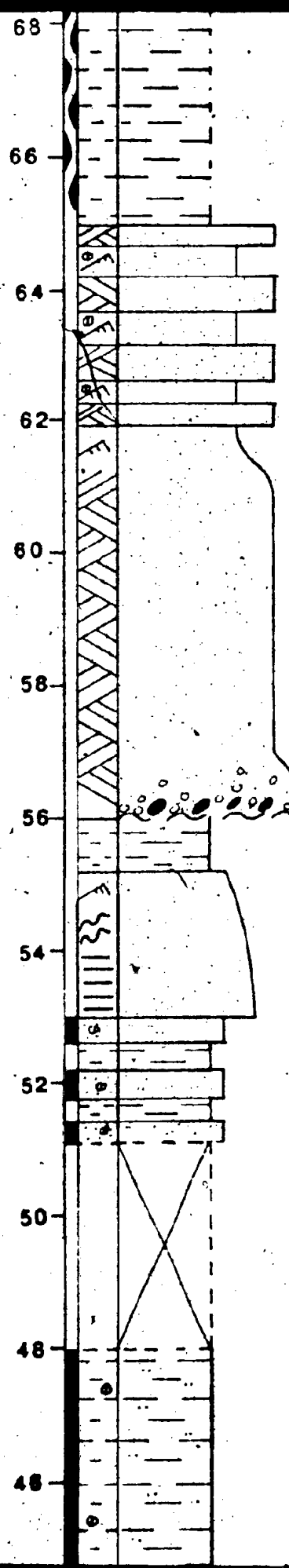
cross-strata

OUTCROP 44

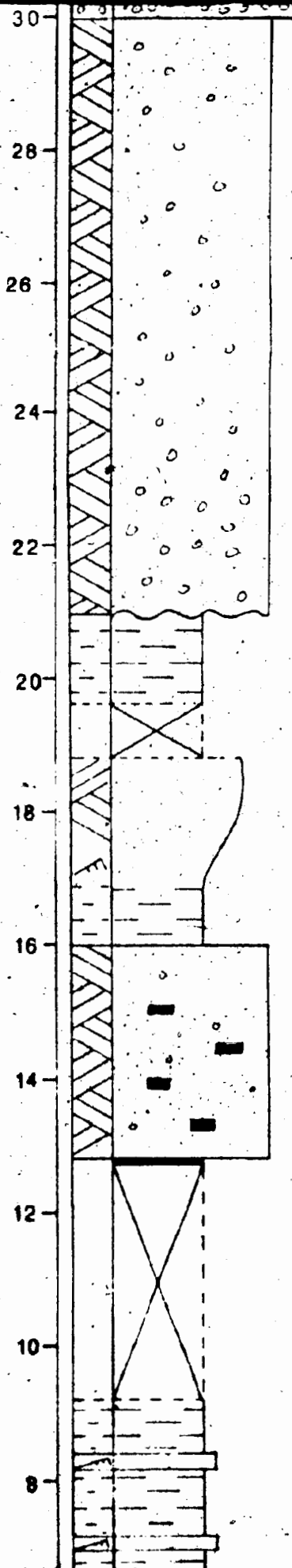


cross-laminated
cross-strata

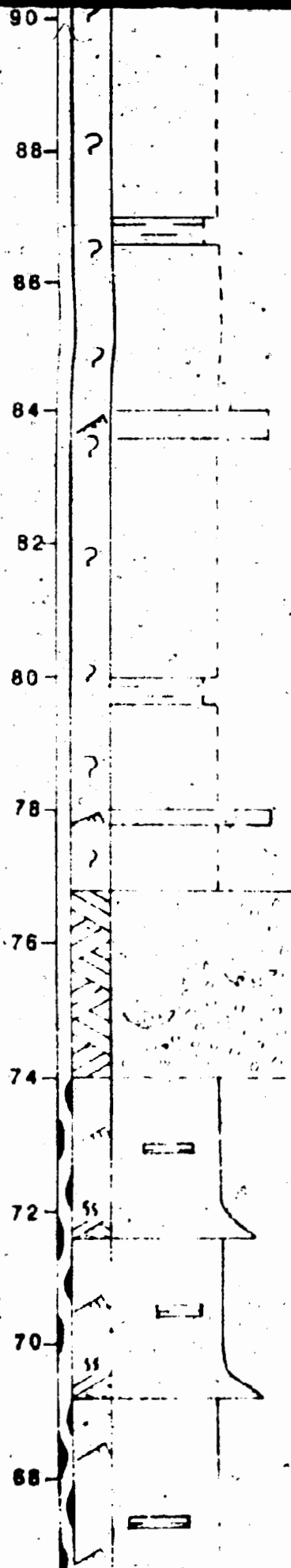
cross-laminated



cross-l.



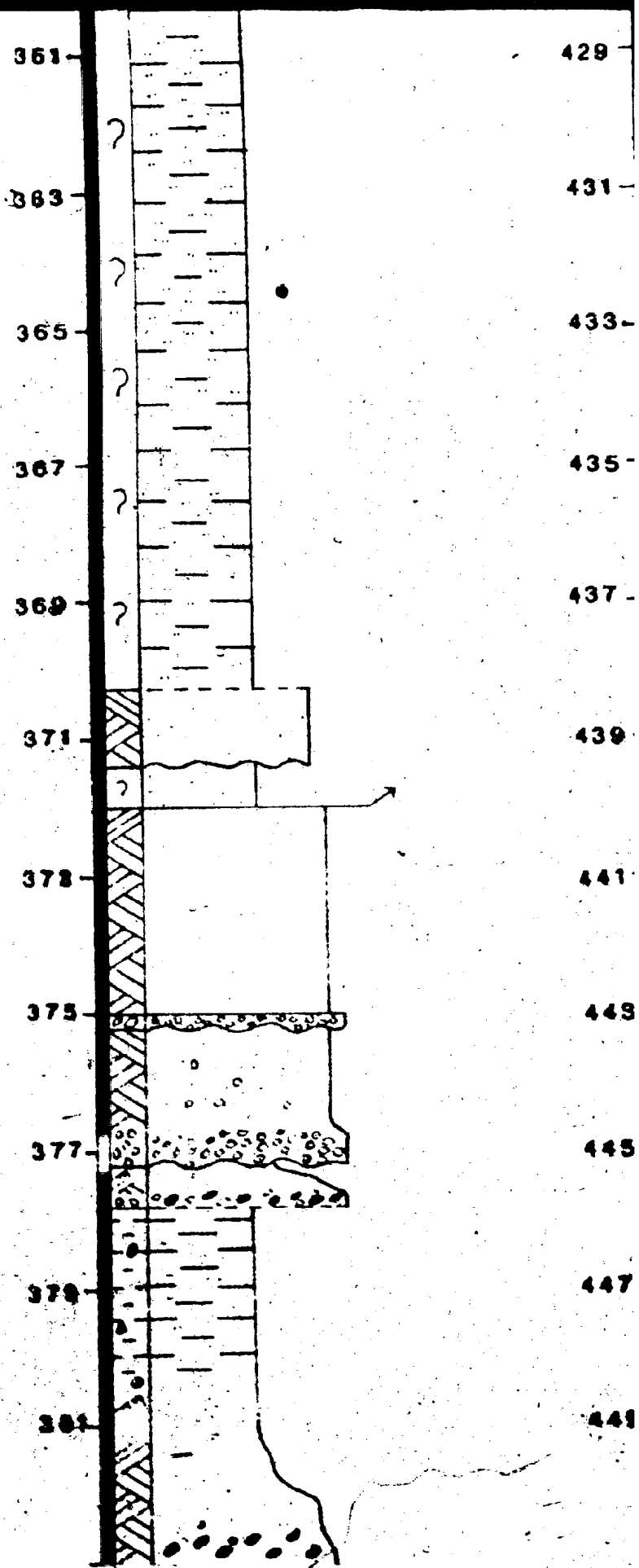
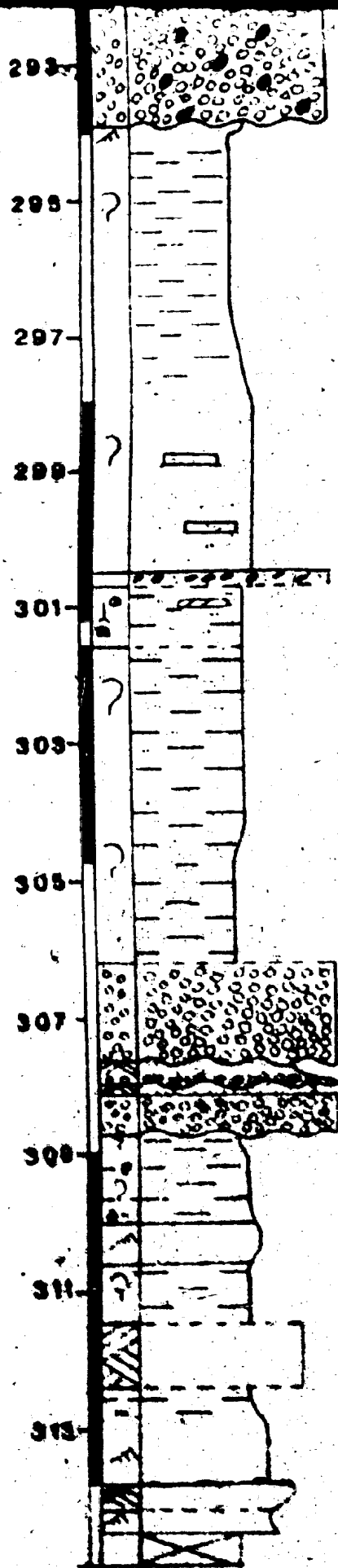
F39 *

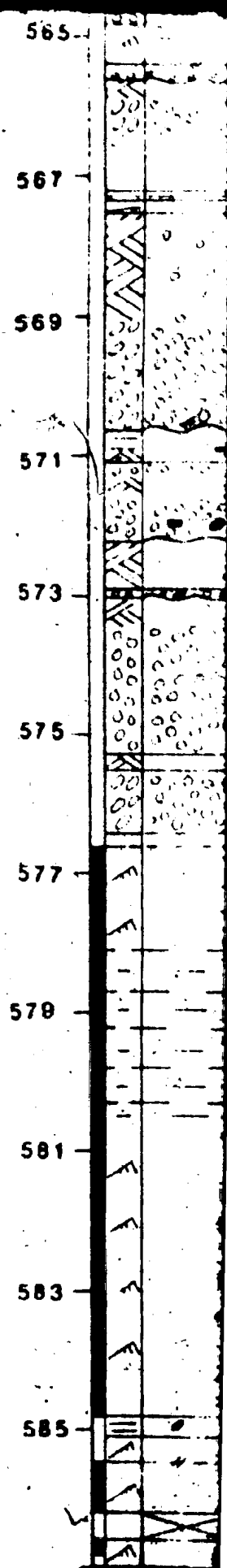
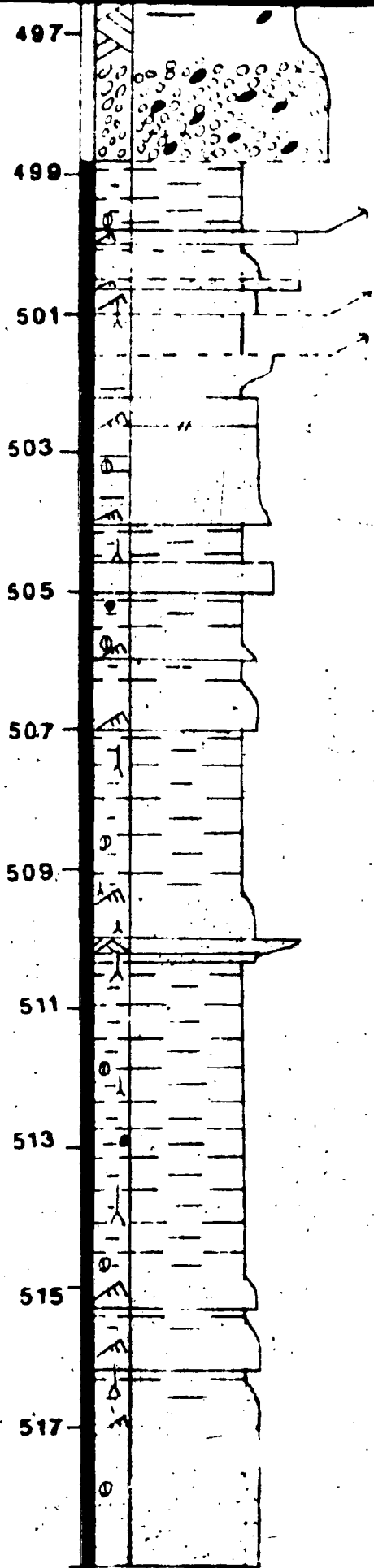
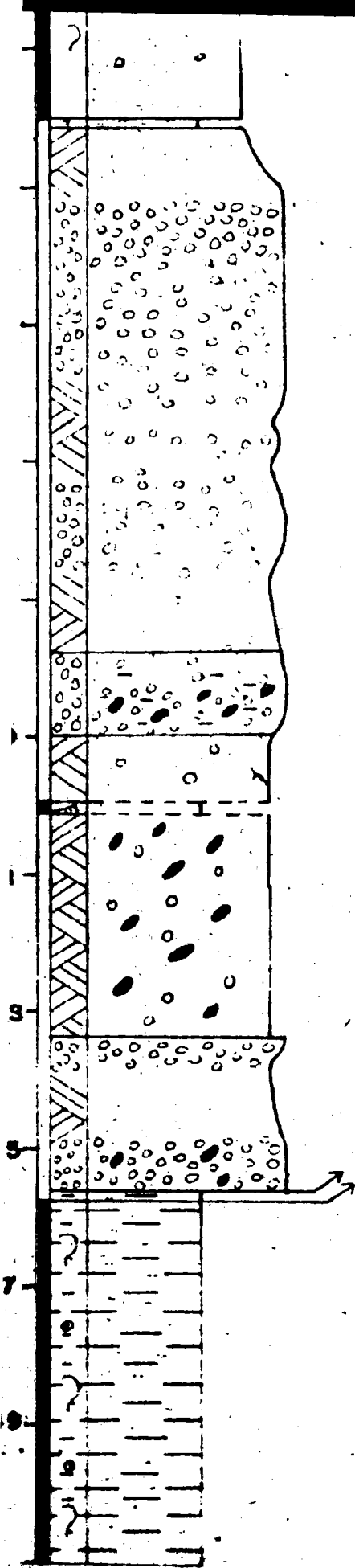


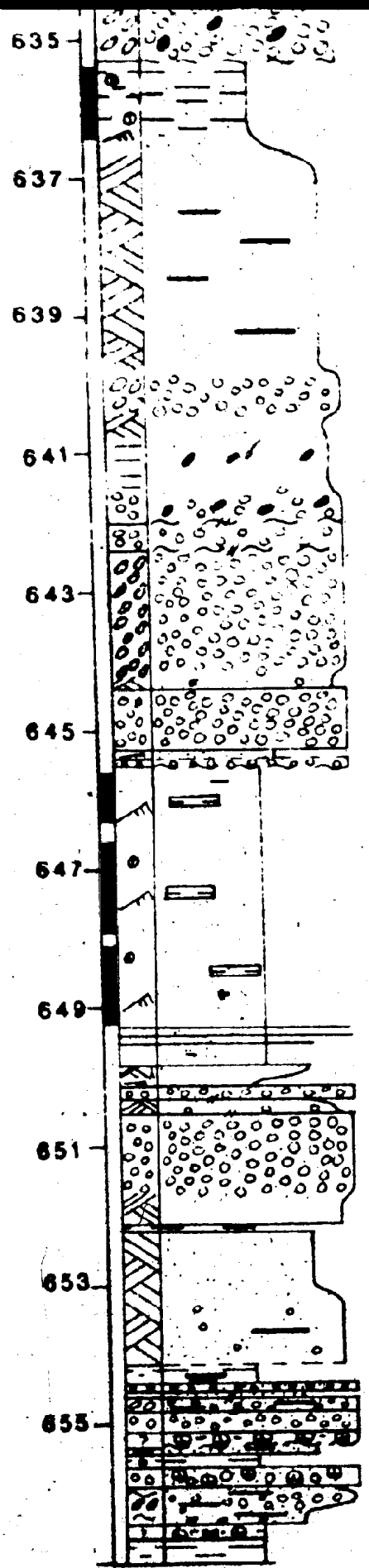
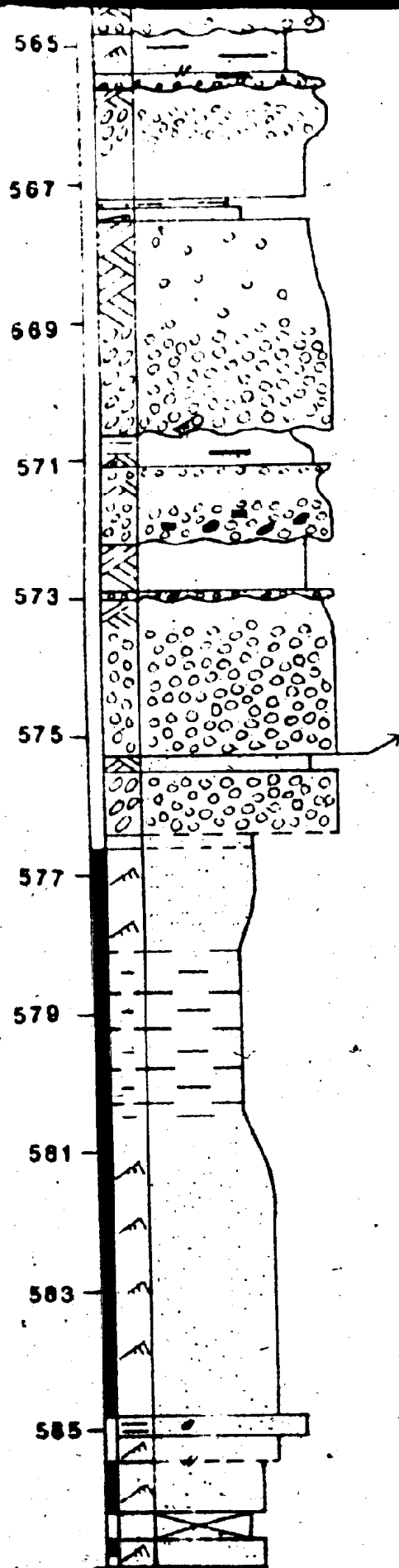
cross-strata
parting lineation

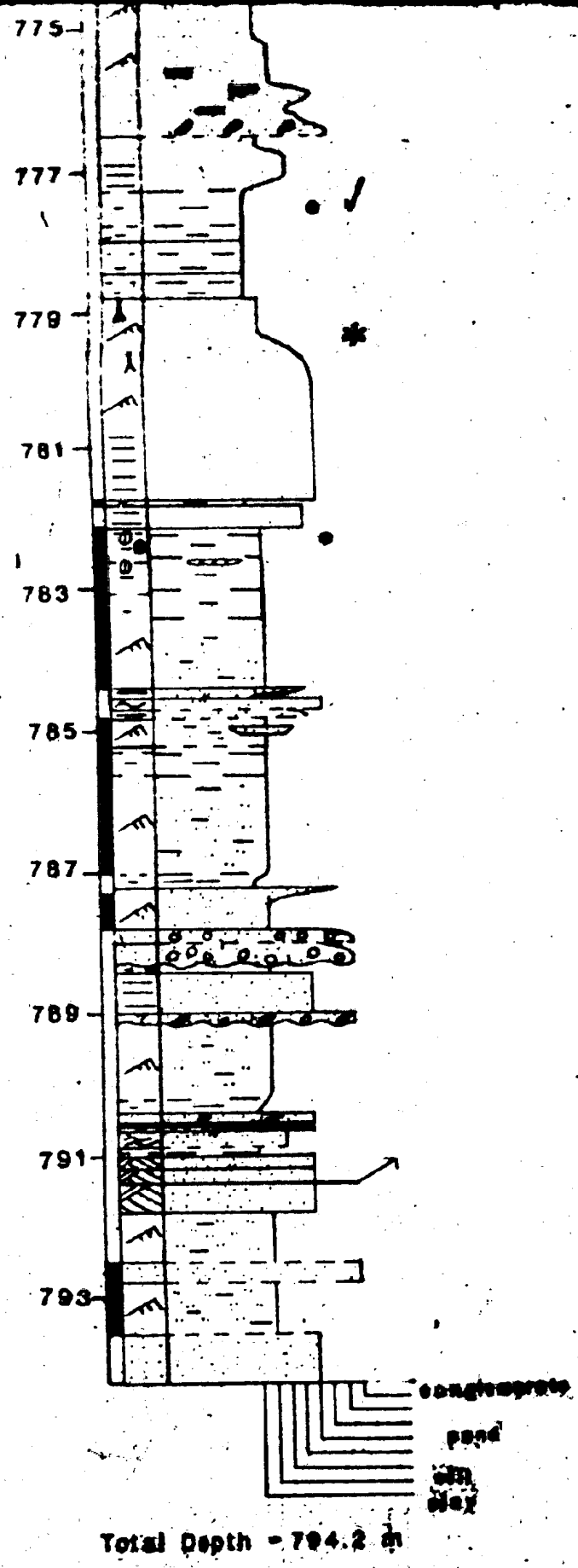
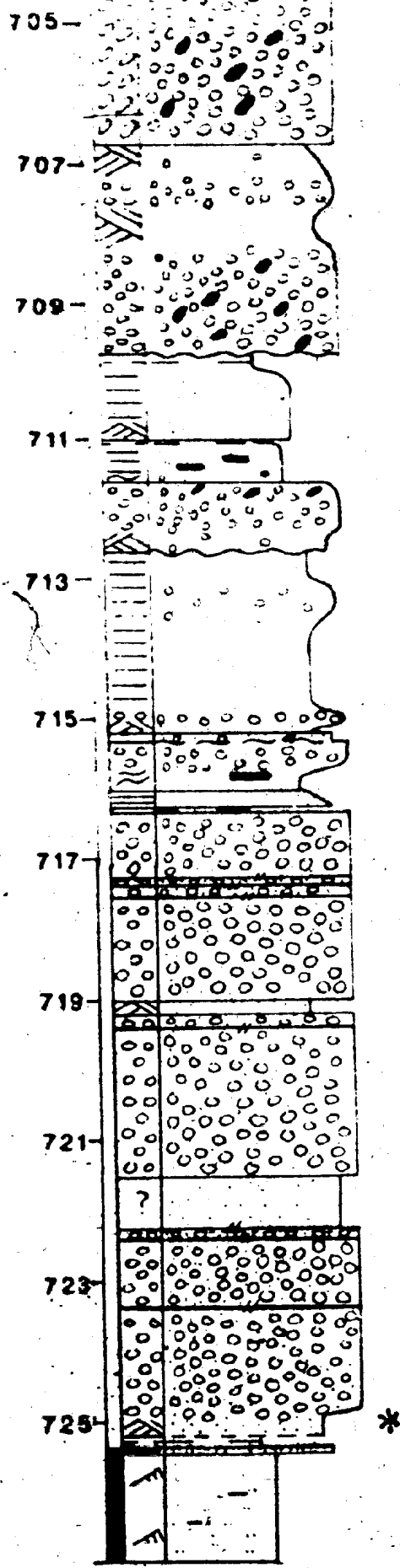
cross-strata

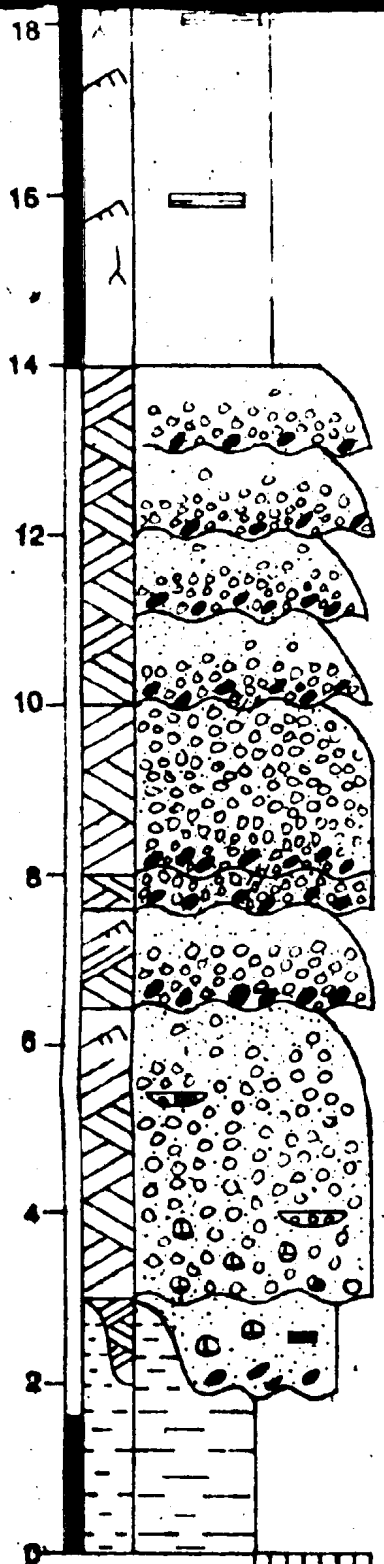
strata





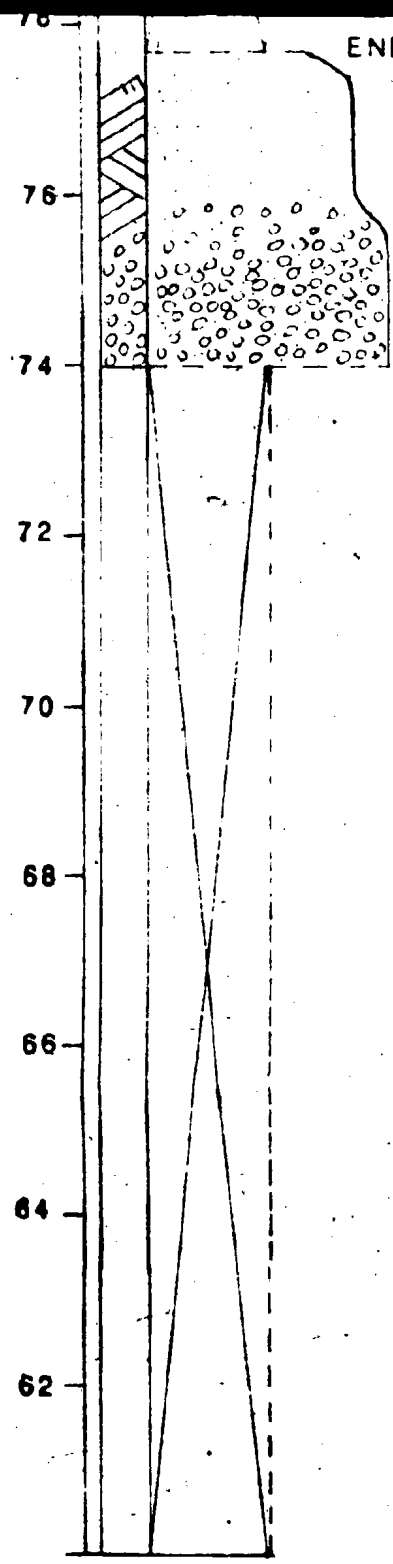




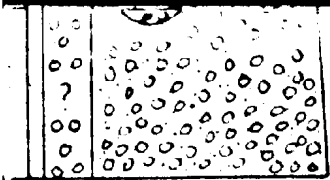


clay
silt
sand
conglomerate

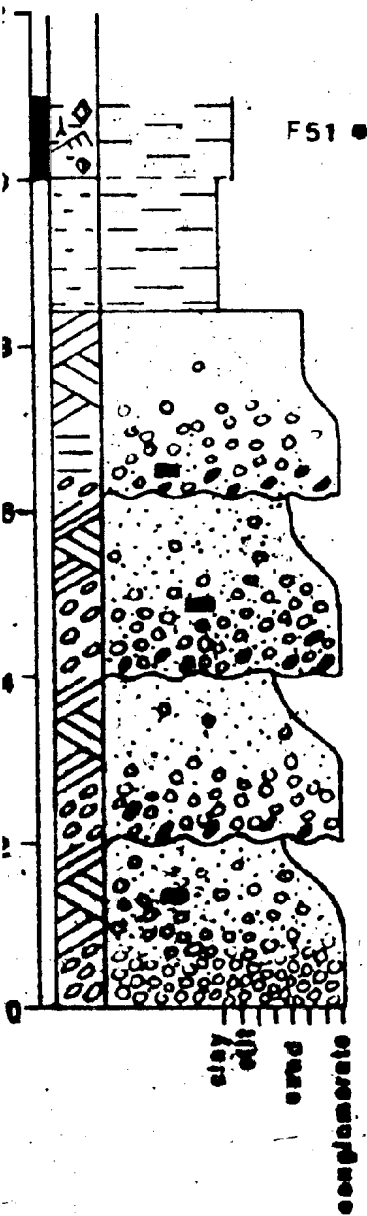
P12 •



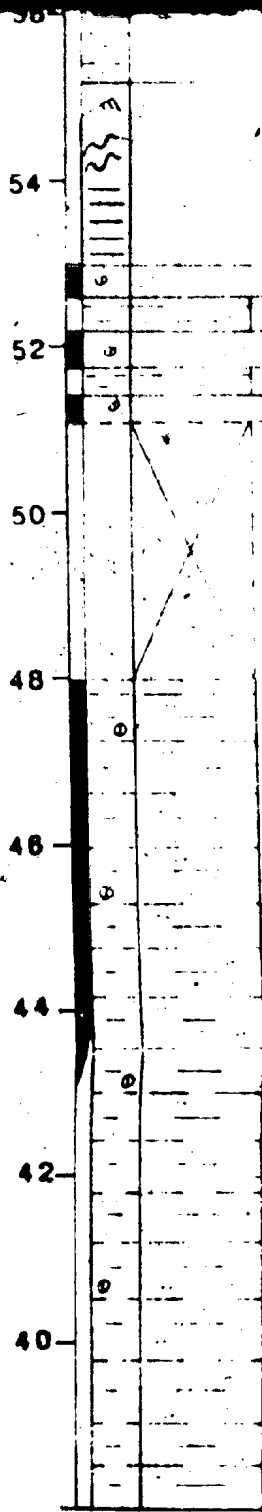
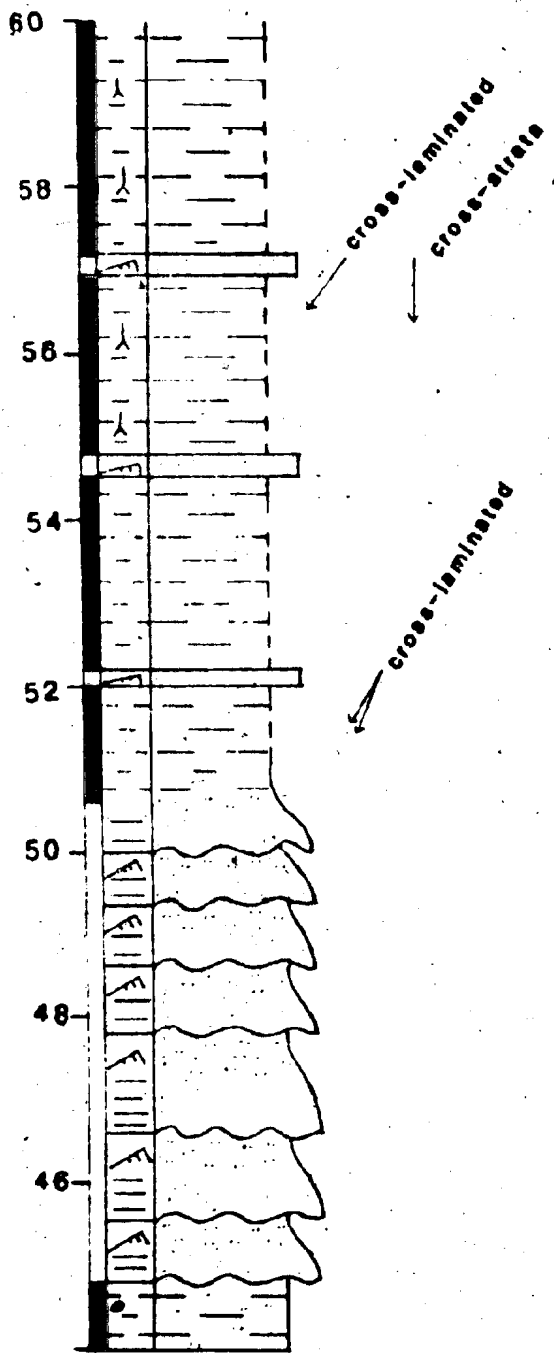
END OUTCROP 38



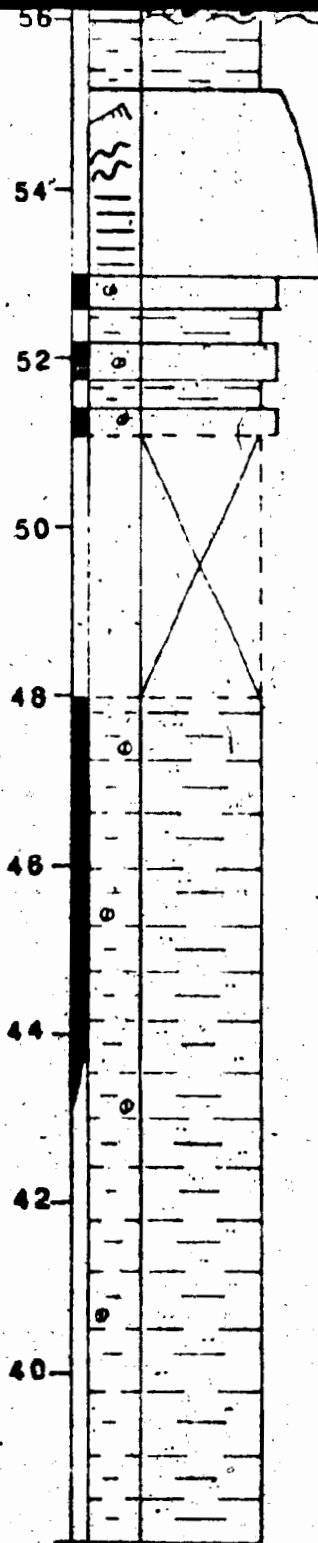
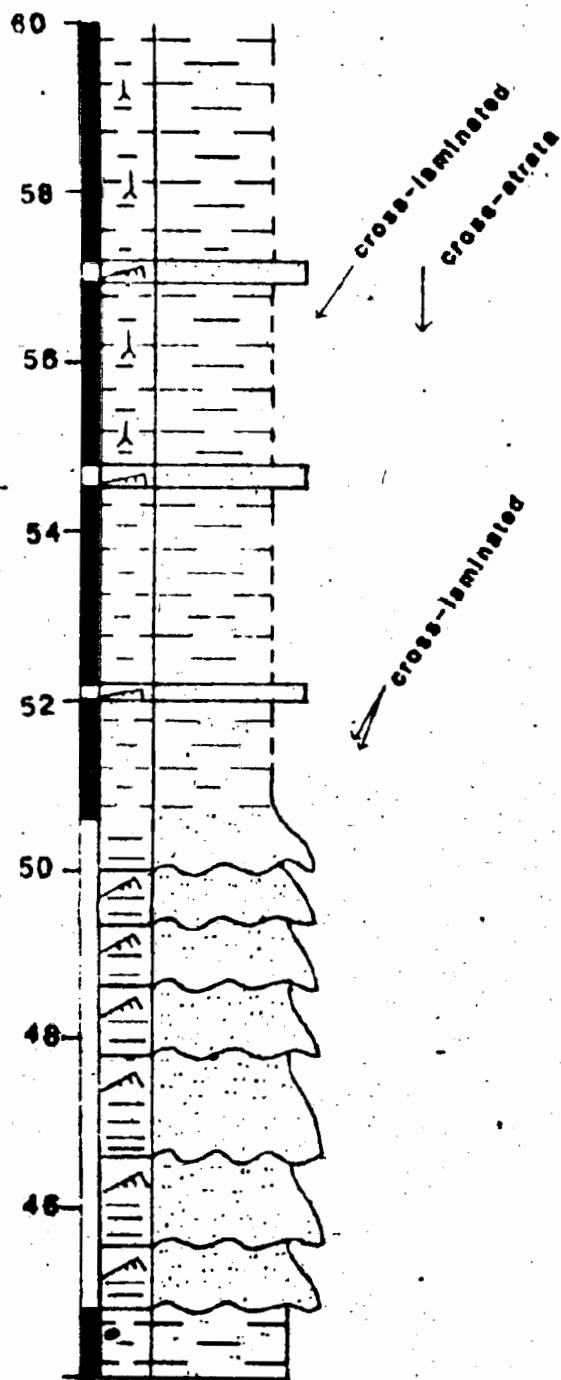
OUTCROP 43



OUTCROP 44



OUTCROP 44

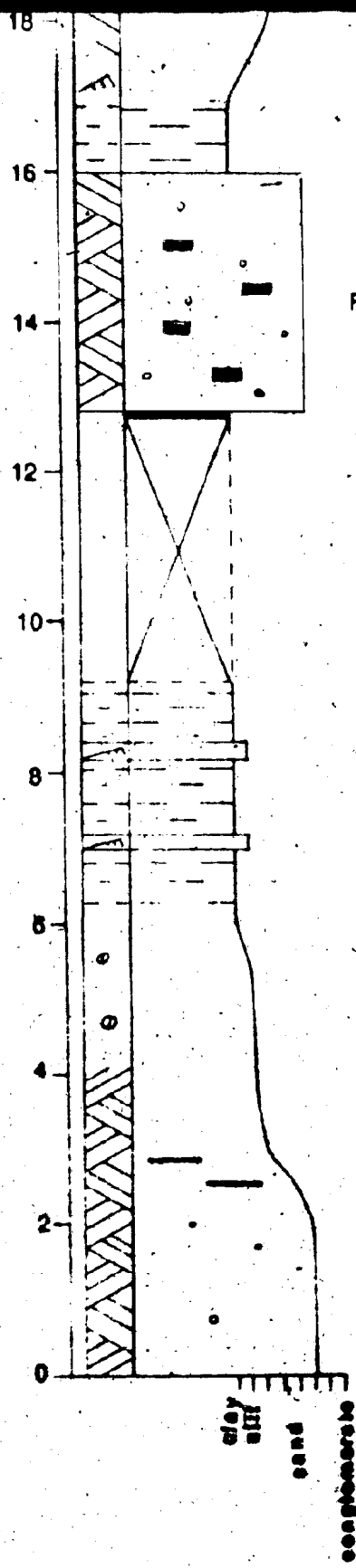


ROP 43

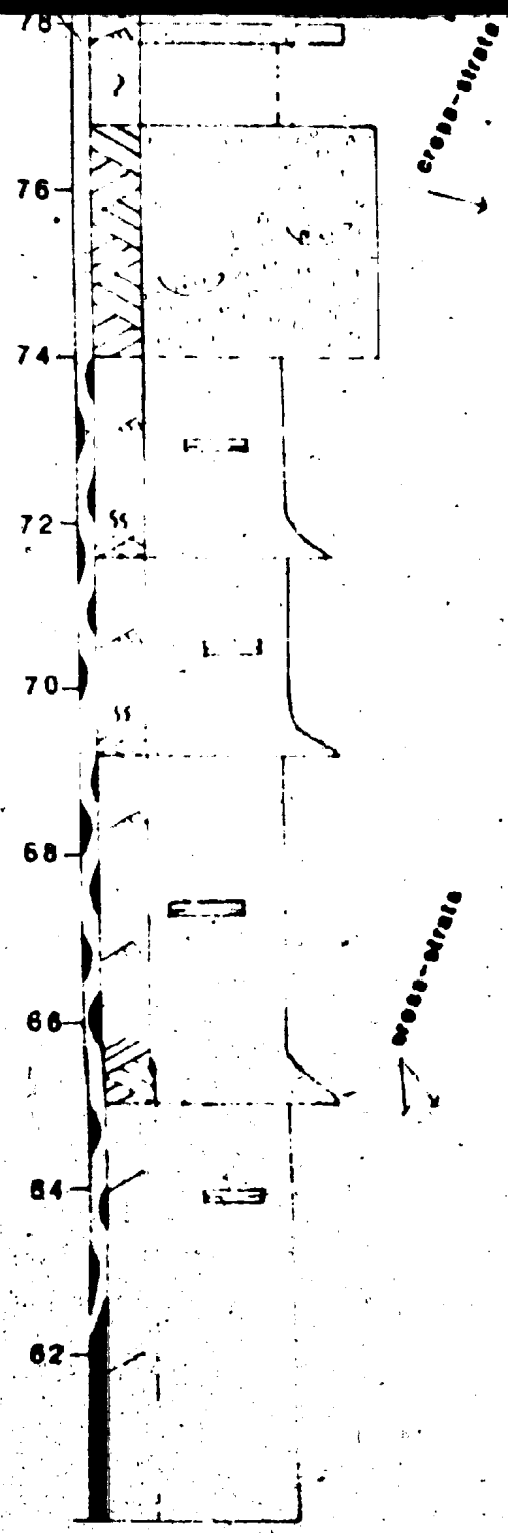
F51 •



clay
silt
sand
conglomerate



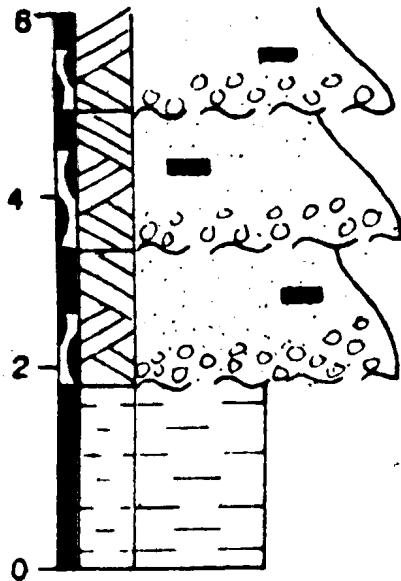
F39 *



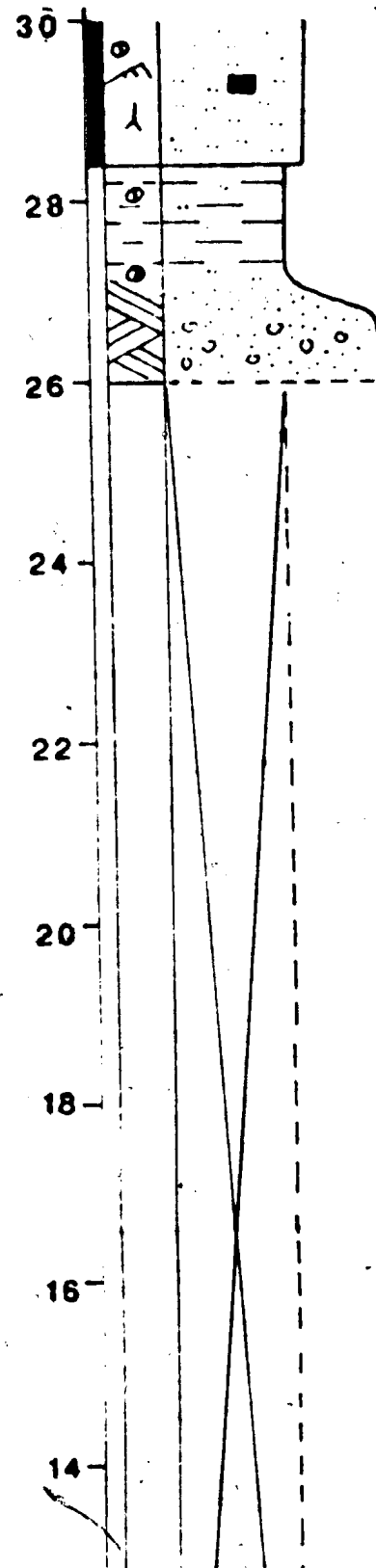
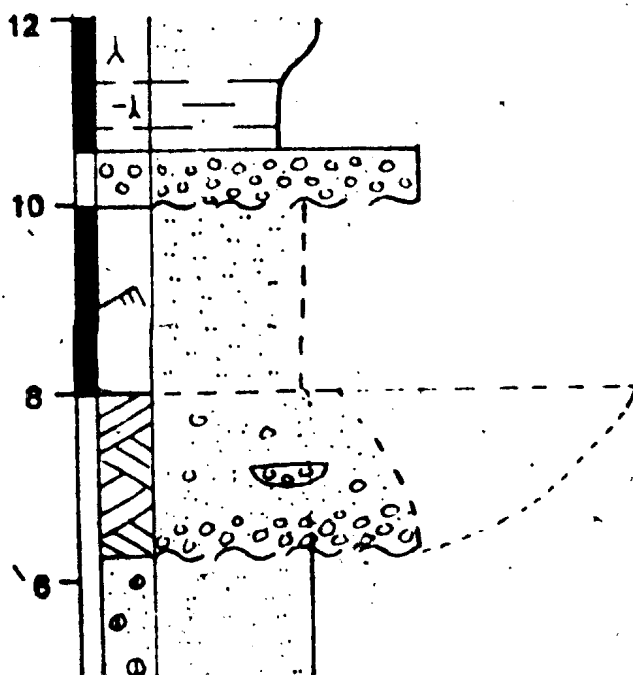
APPENDIX A FIGURE

OUTCROPS 28, 29, 30, 31,

OUTCROP 31

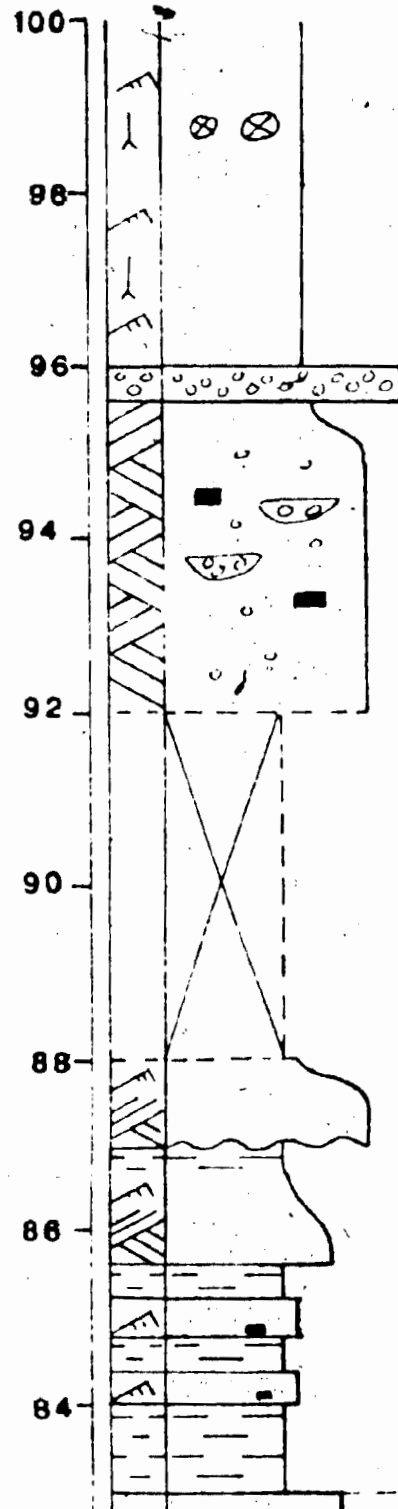
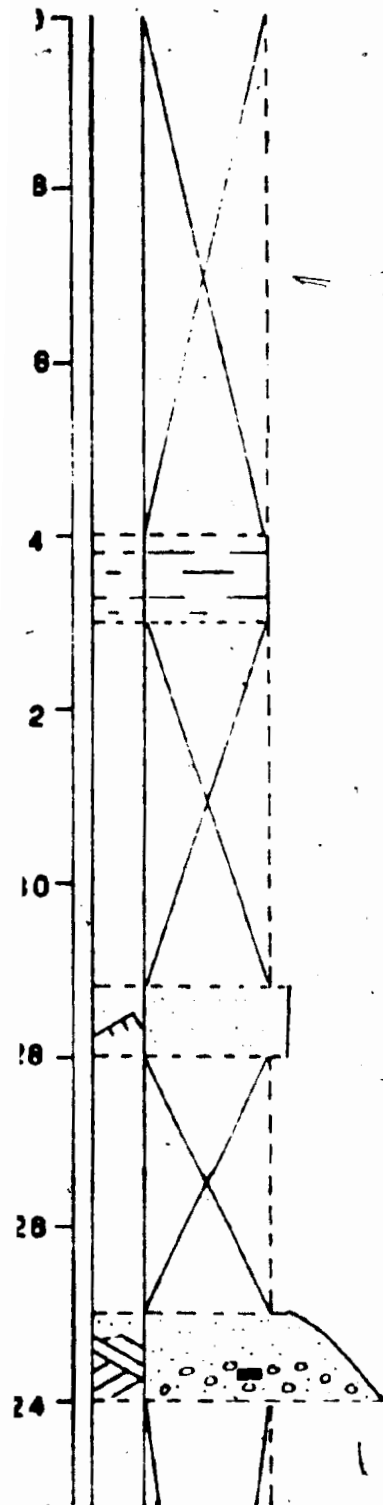


OUTCROP 30

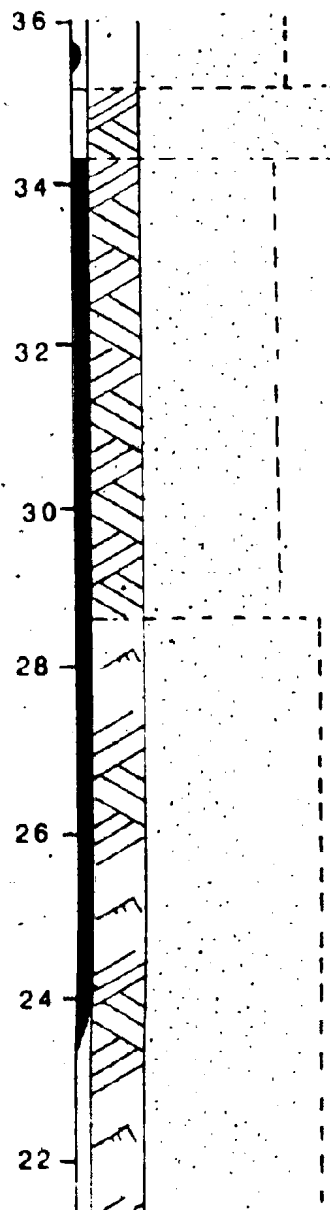


RE 6

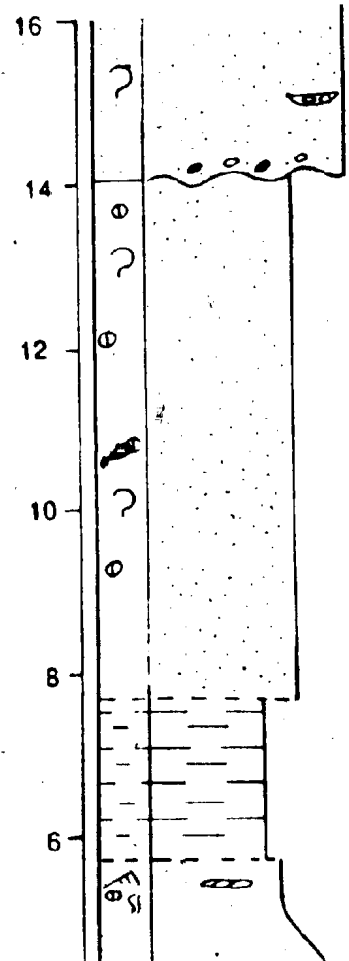
1, 33, 1, 2-7



OUTCROPS 68, 68a, 68b, 70, 7

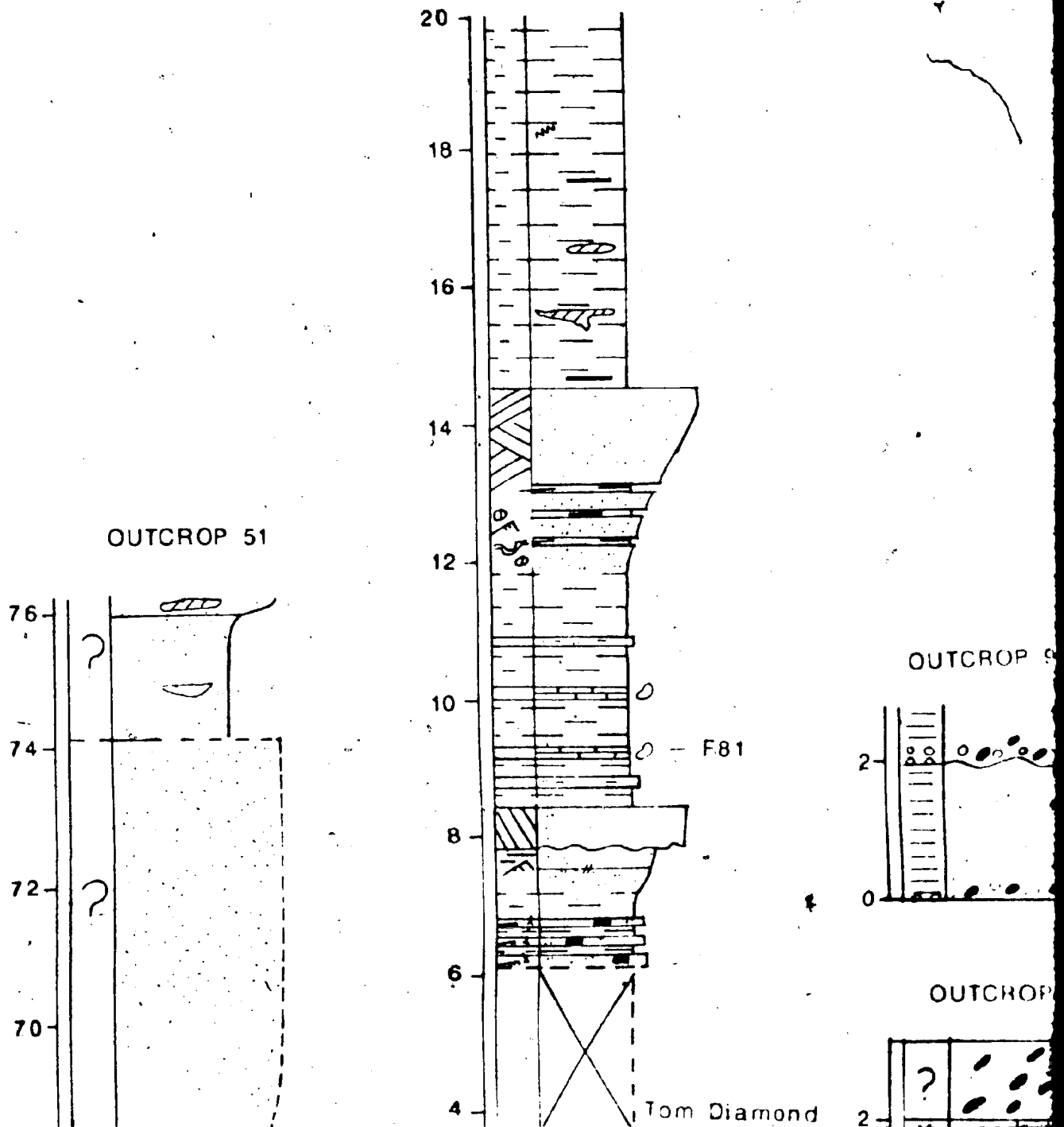


OUTCROP 62c

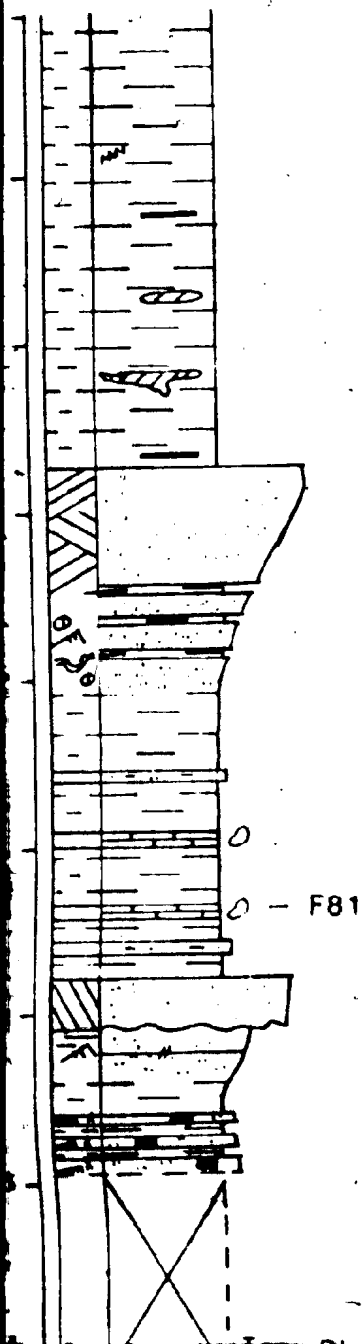


APPENDIX A FIGURE 7

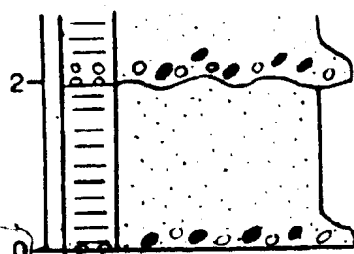
72, 73, 73b, 82, 85, 92, 93, 89, 90, 51, 51a, 51b, 54, 61, 62c, 52, 63, 62a, 64, 65a



a, 51b, 54, 61, 62c, 52, 63, 62a, 64, 65a



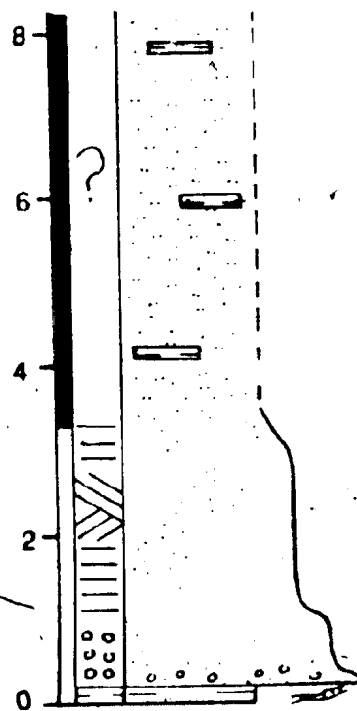
OUTCROP 93



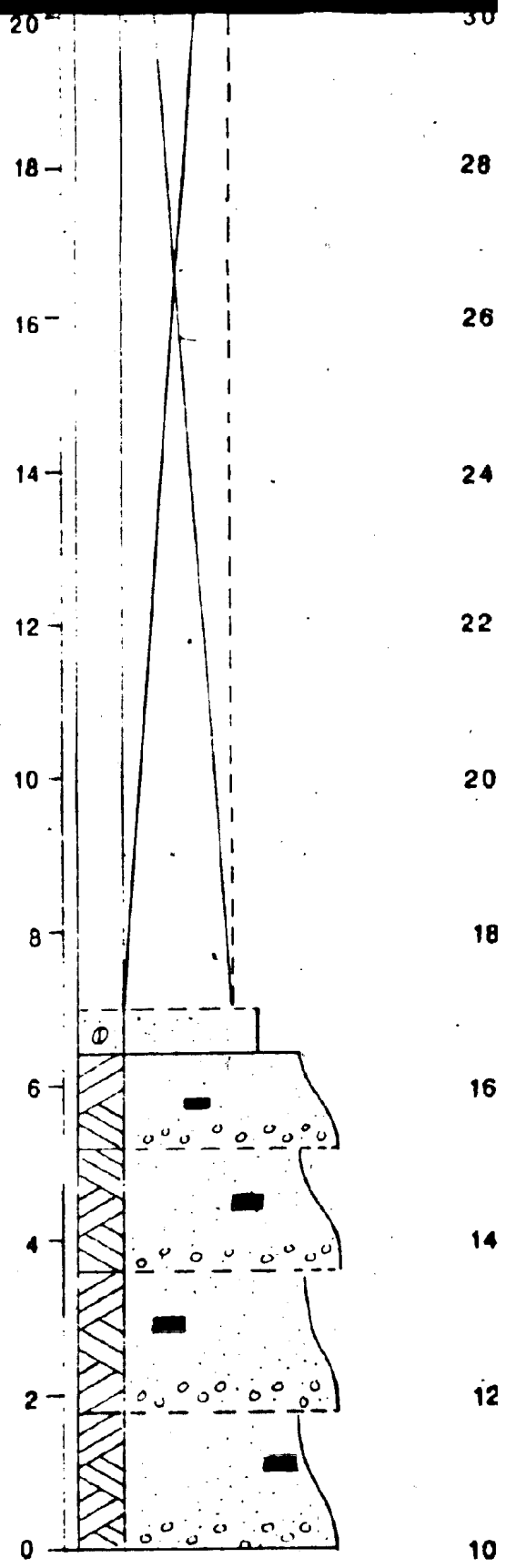
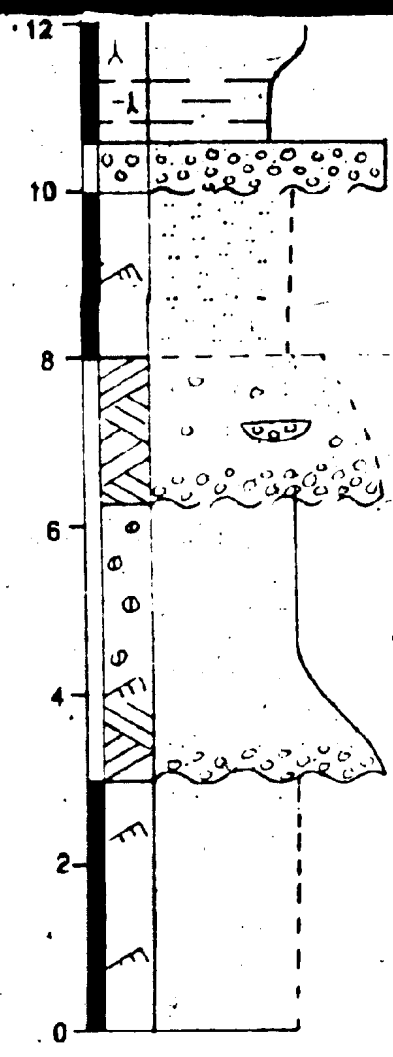
OUTCROP 92



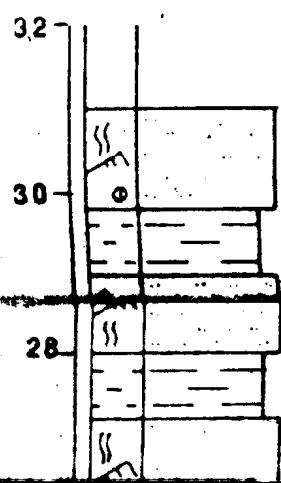
OUTCROP 85



cross-strata



OUTCROP 28/29



30

28

26

24

22

20

18

16

14

12

10

8

F6 *

88

86

84

82

80

78

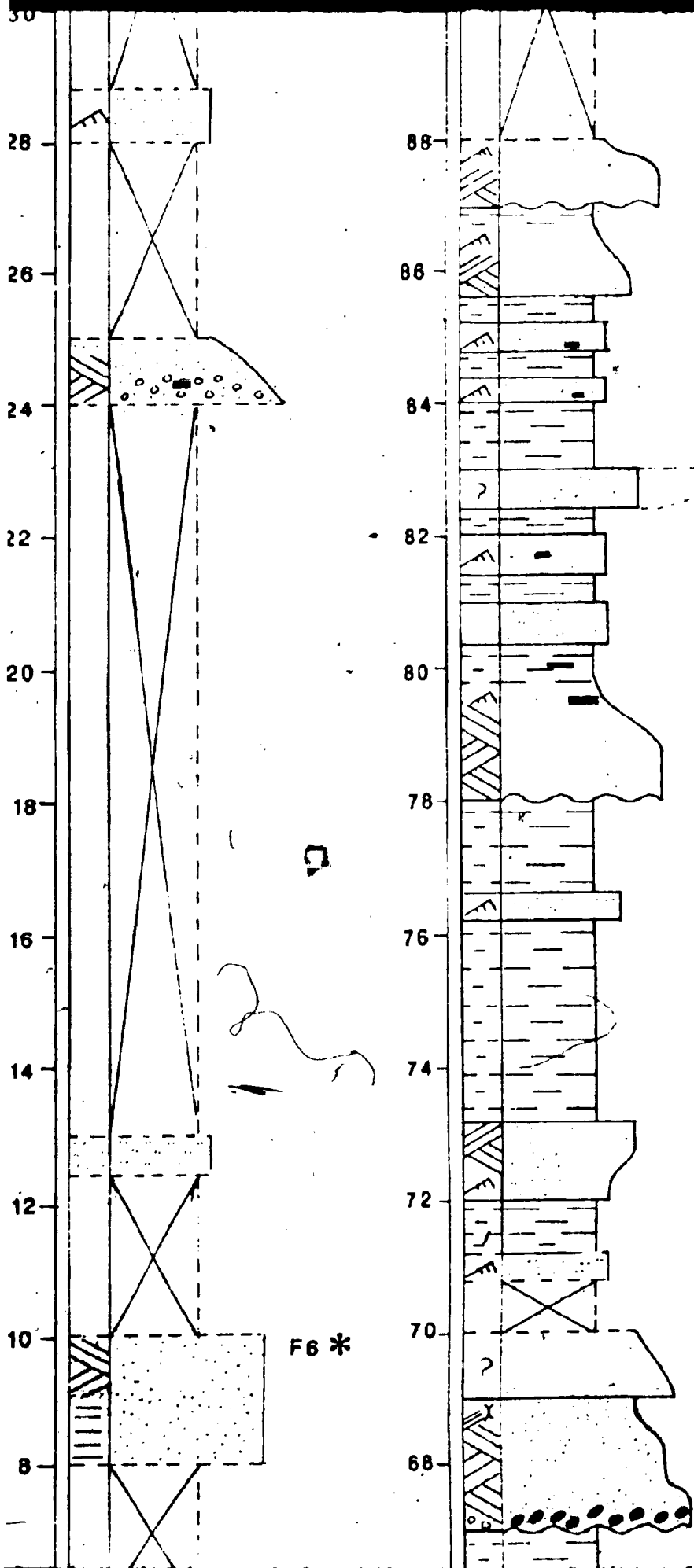
76

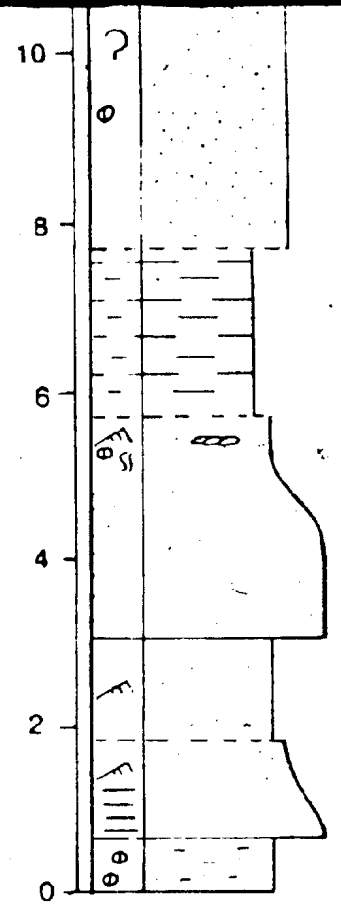
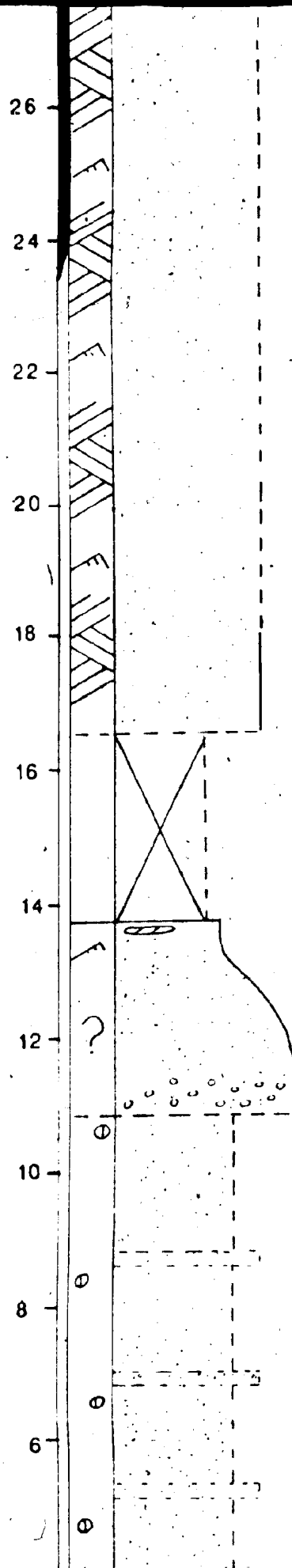
74

72

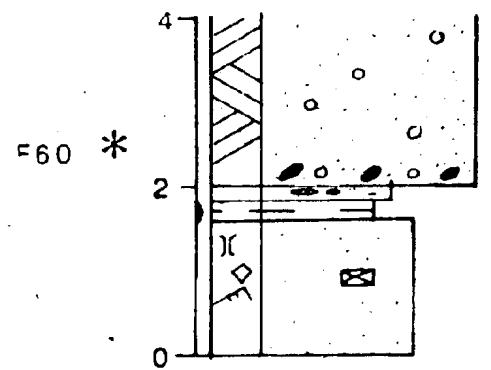
70

68



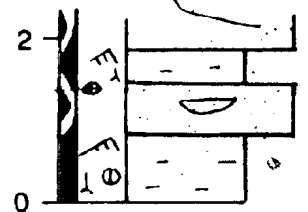


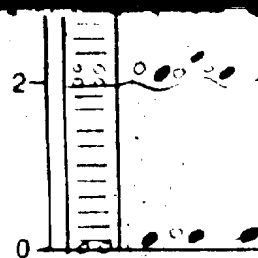
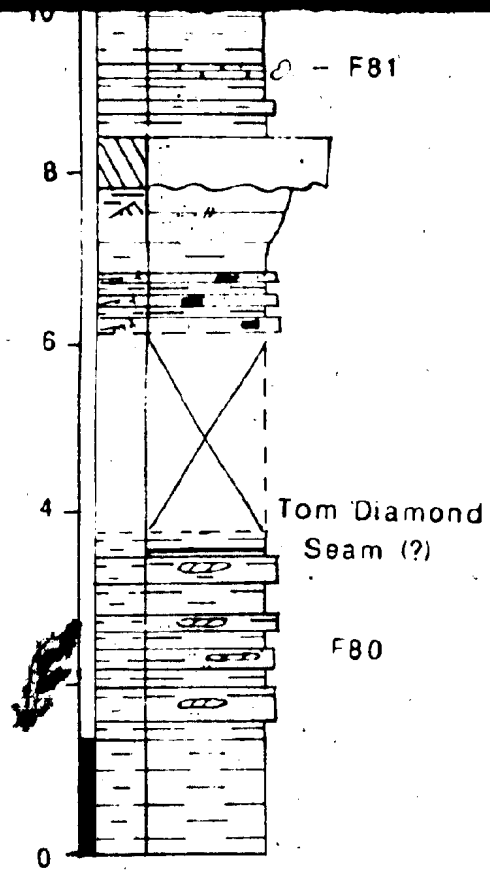
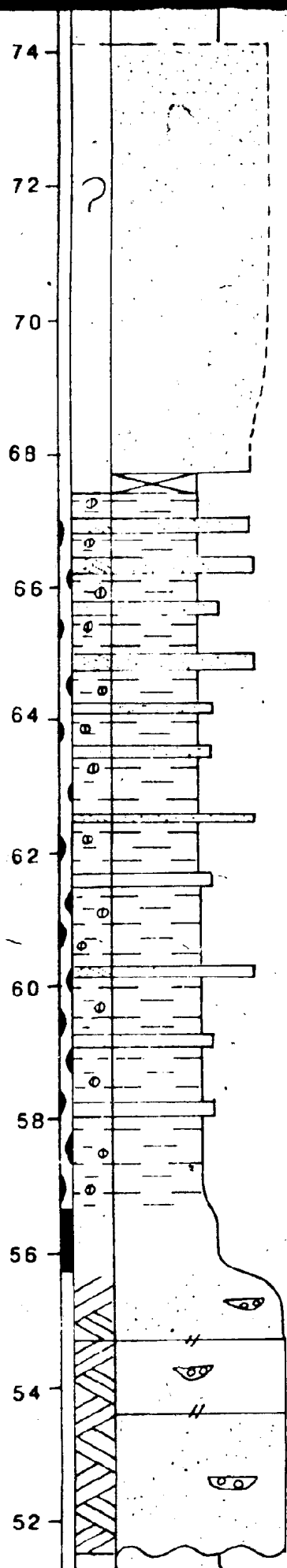
OUTCROP 61



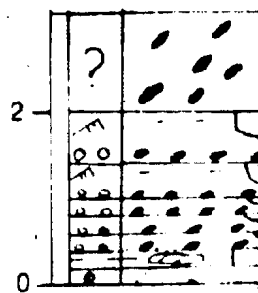
F60 *

OUTCROP 54

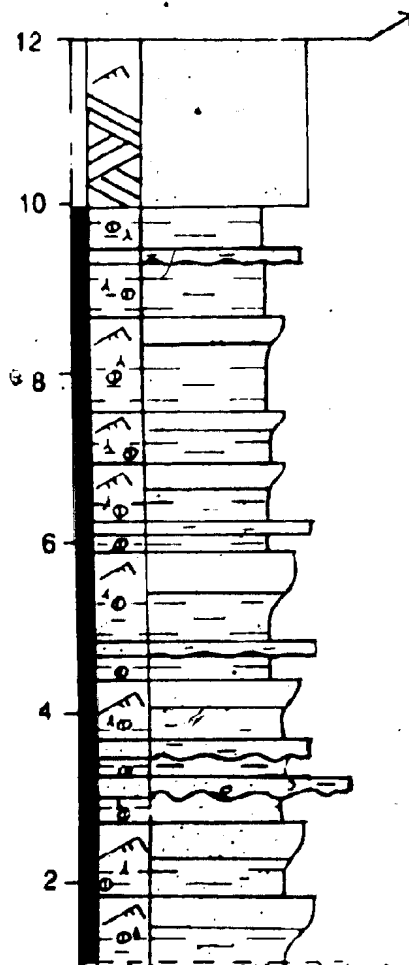




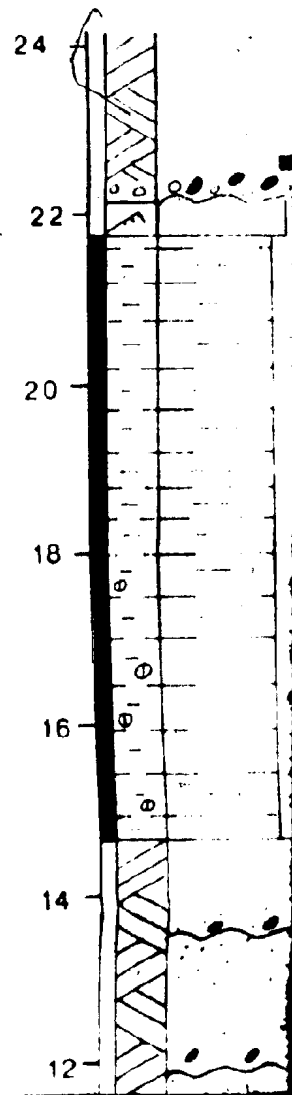
OUTCROP



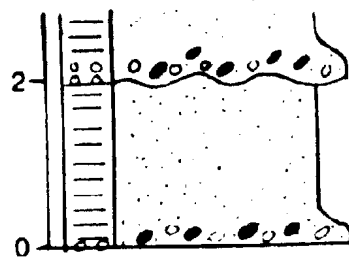
OUTCROP 51b



OUTCROP



OUTCROP 93



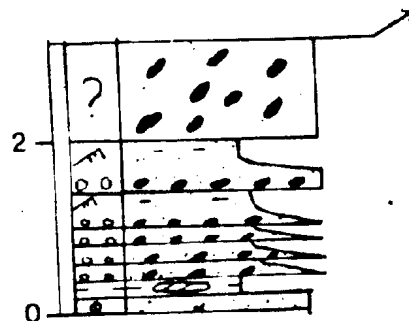
4

2

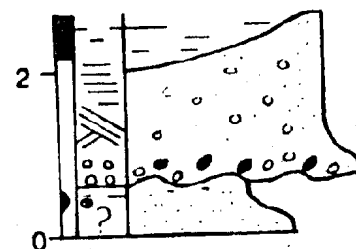
0

cross-strata

OUTCROP 92

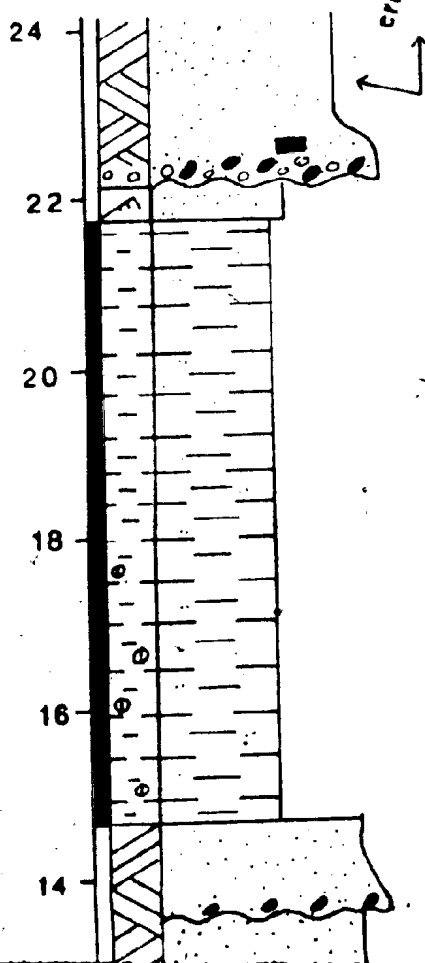


OUTCROP 82

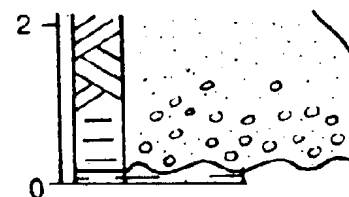


F73 *

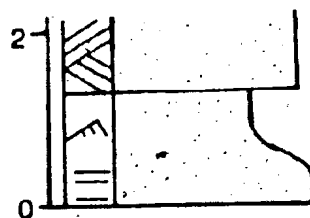
OUTCROP 90



OUTCROP 73b

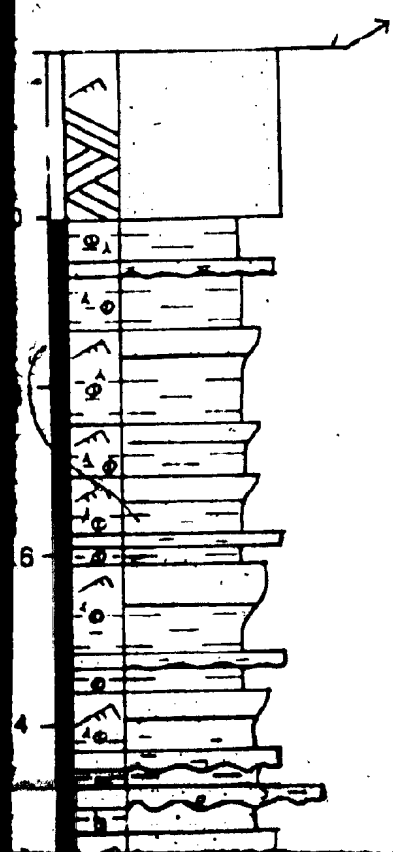


OUTCROP 73



OUTCROP 72

OUTCROP 51b

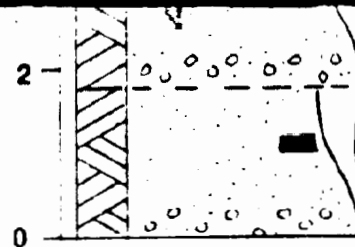
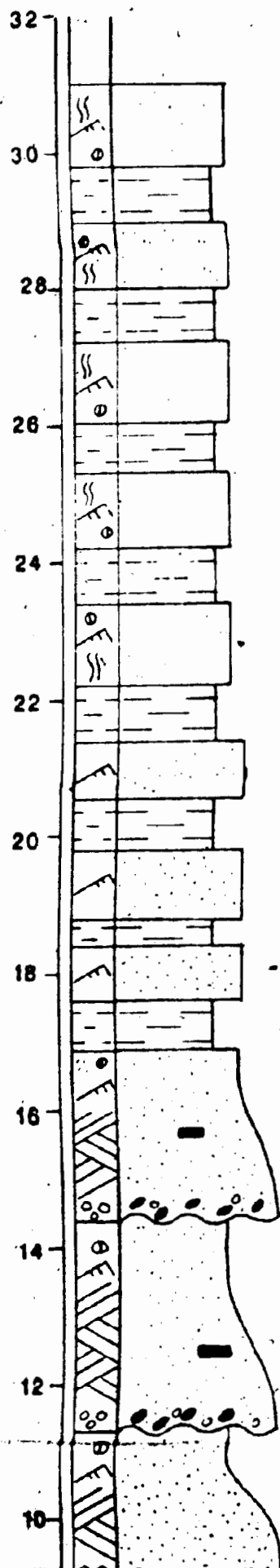


Tom Diamond Seam (?)

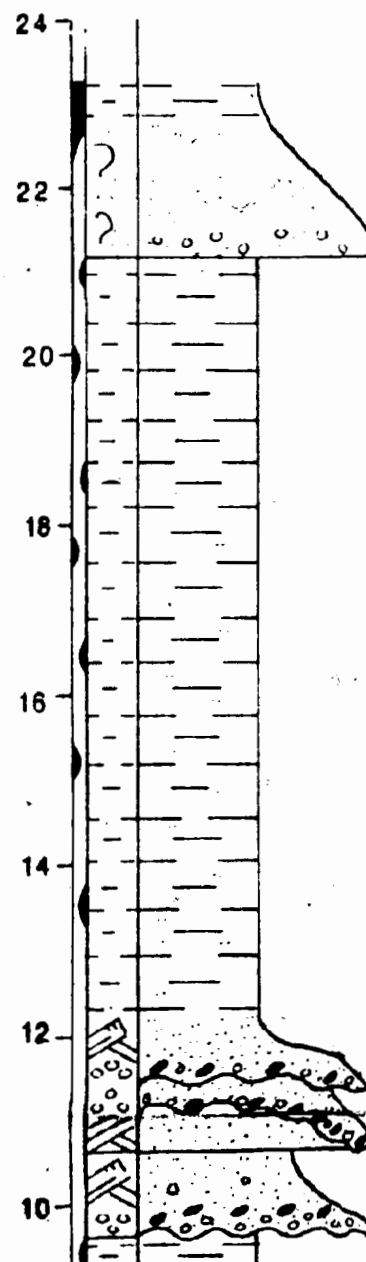
F80

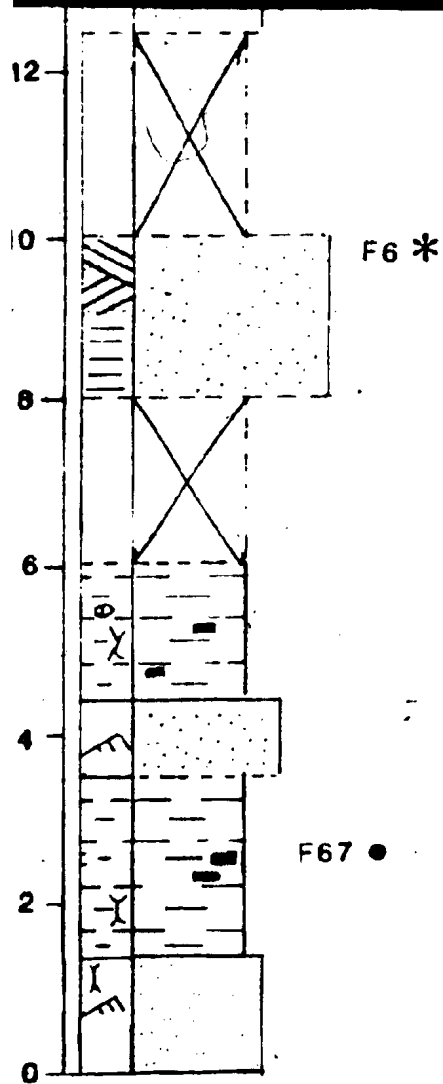
F81

OUTCROP 28/29

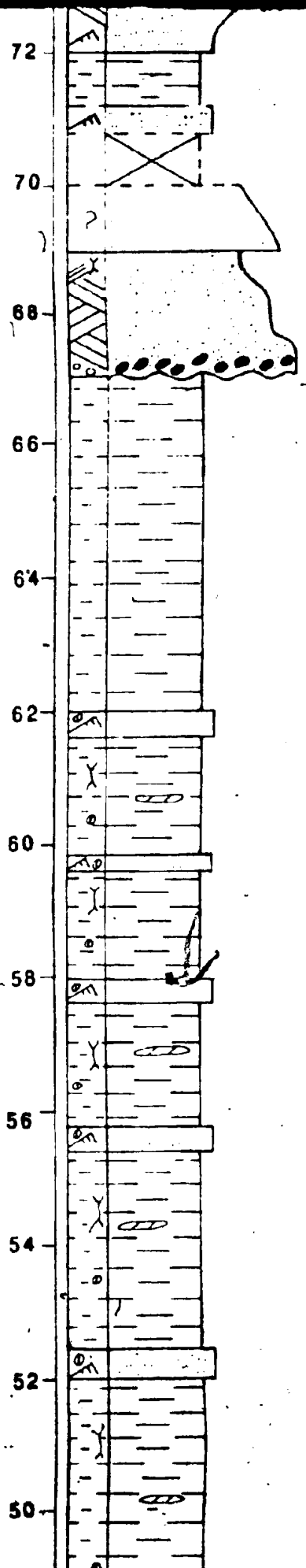
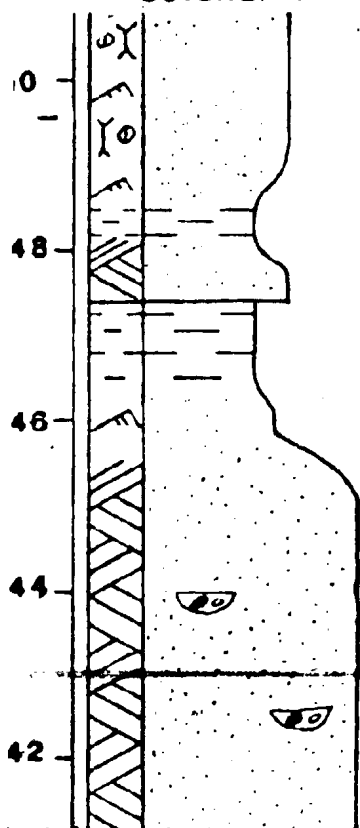


OUTCROP 33

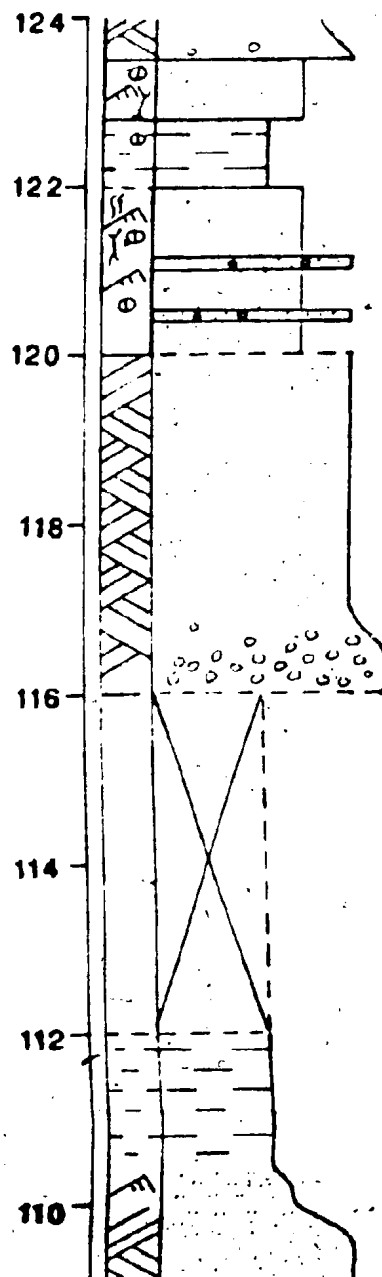




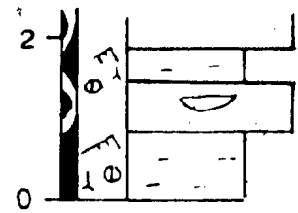
7 m COVERED
OUTCROP 1



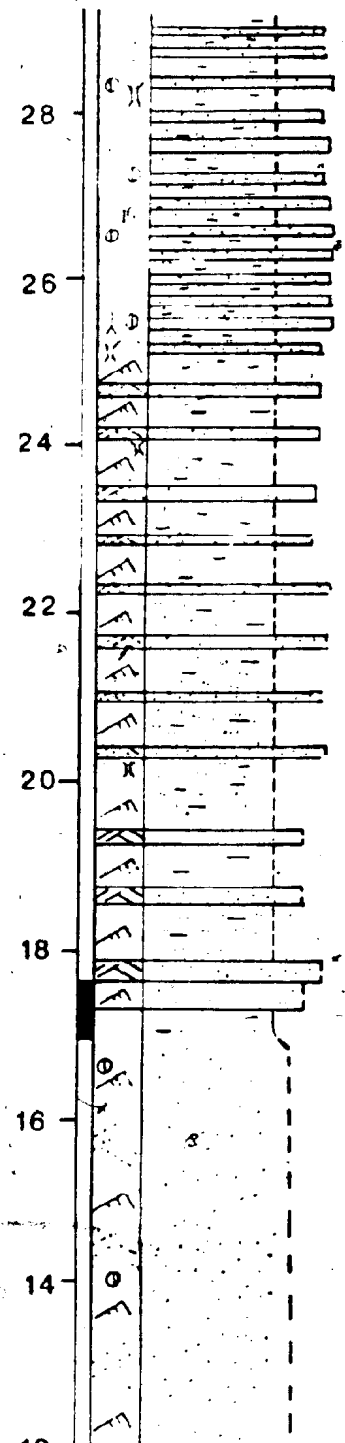
OUTCROPS 2-7



OUTCROP 54

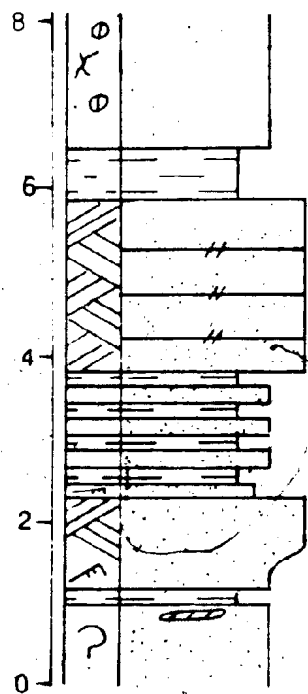


OUTCROP 52



F56

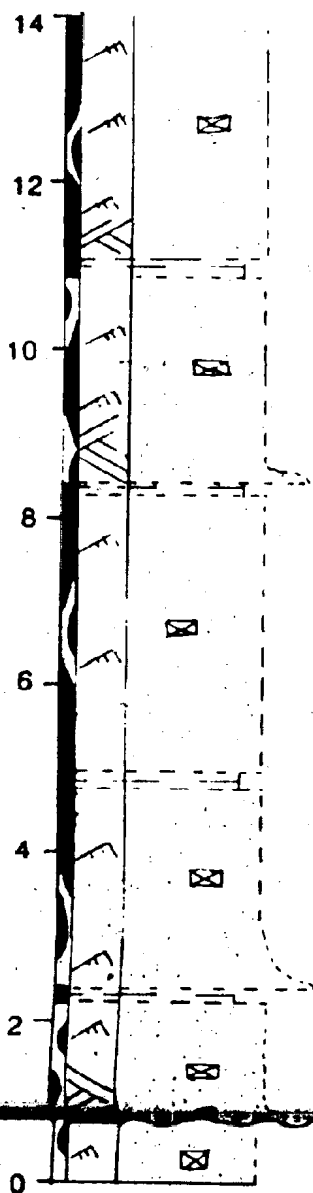
OUTCROP 63

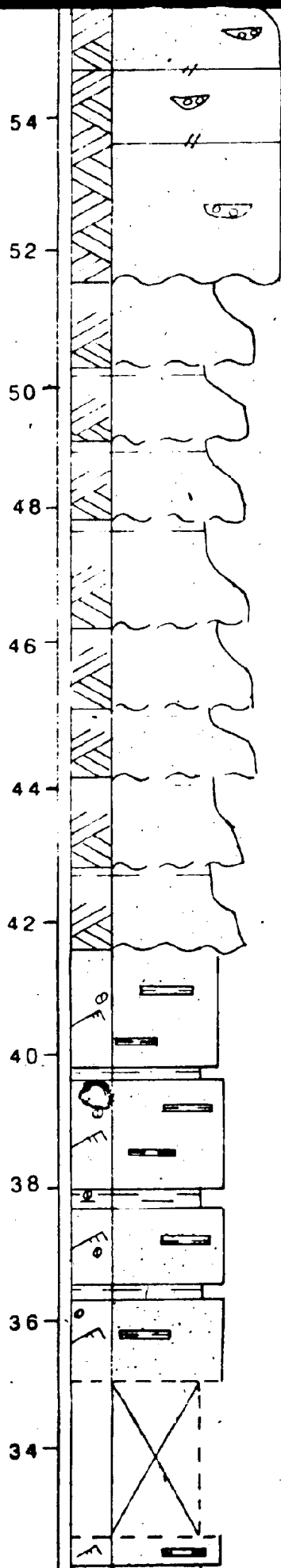


OUTCROP 62a

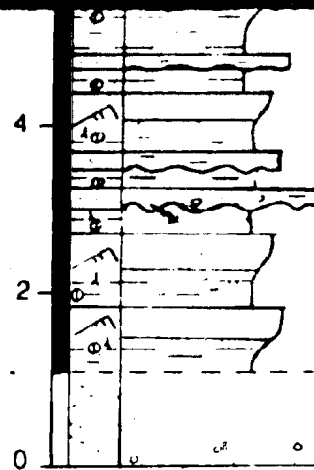


OUTCROP 65a

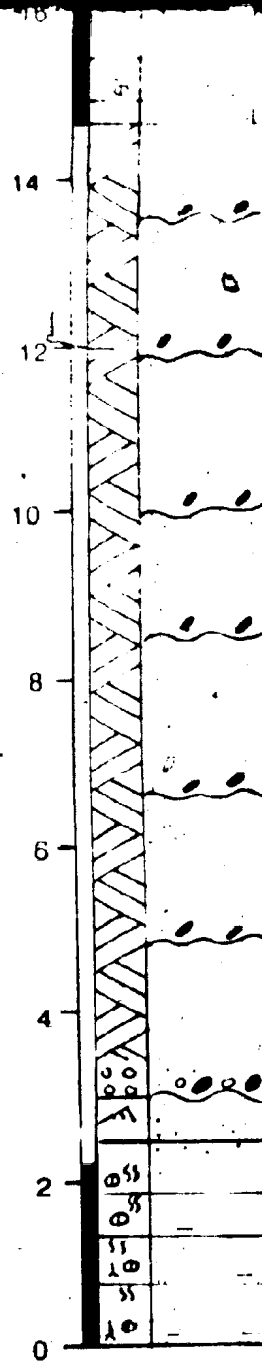
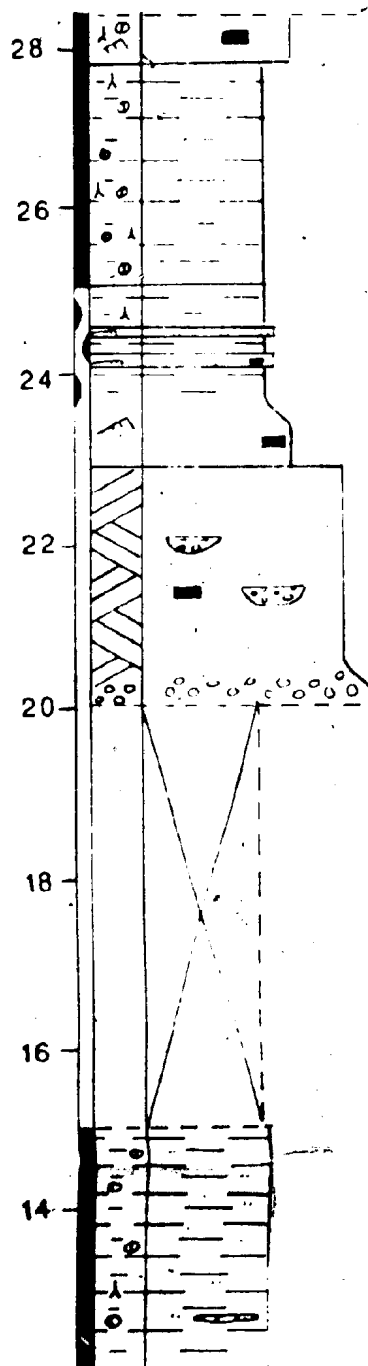




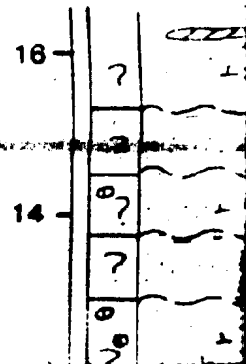
F56 *

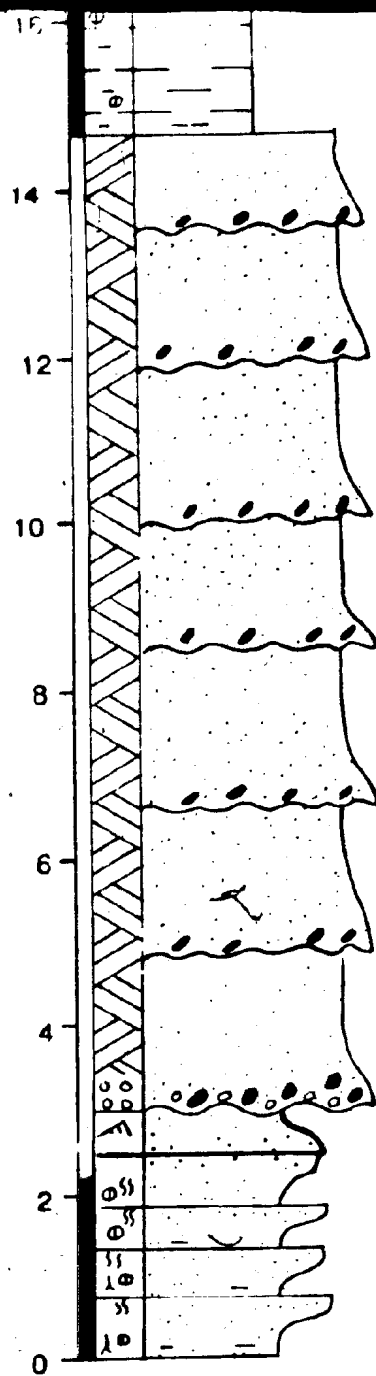


OUTCROP 51a

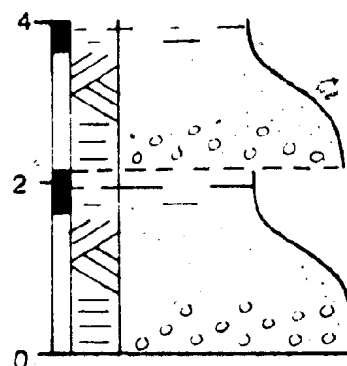


OUTCROP

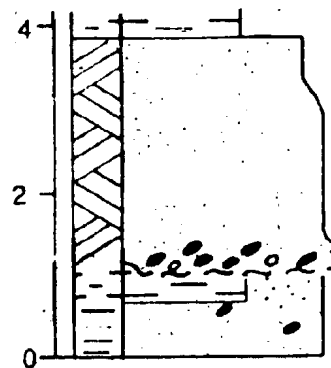




OUTCROP 72

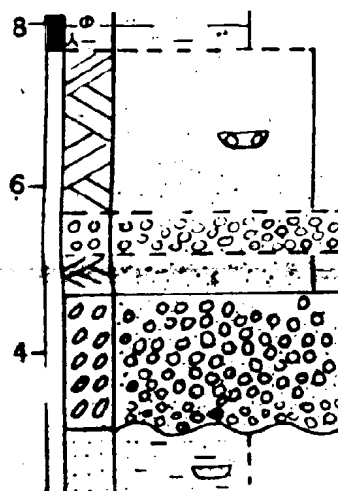


OUTCROP 70

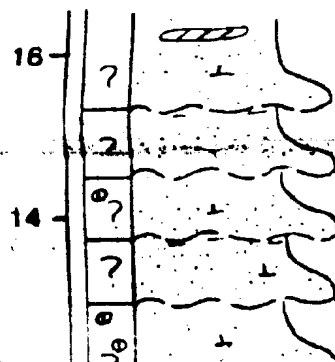


P20 ● ✓

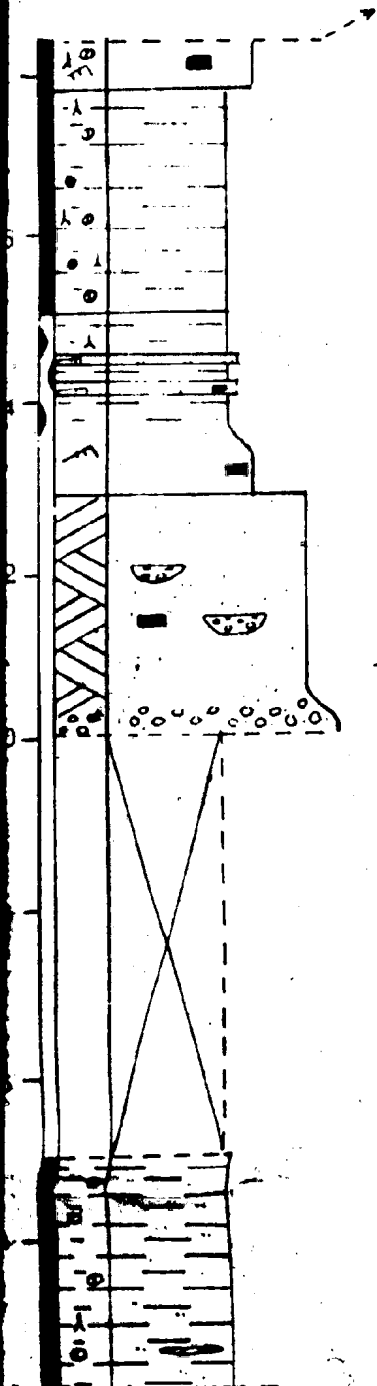
OUTCROP 68a/b

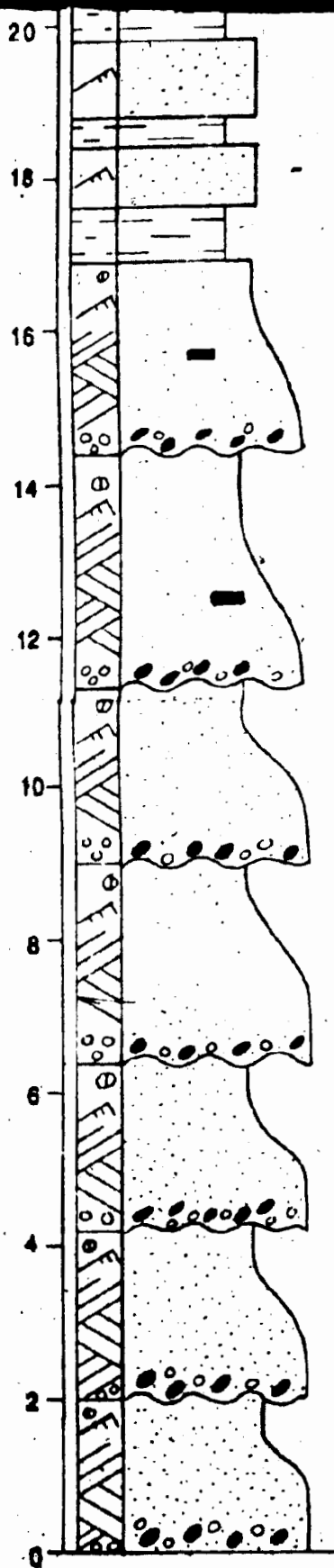


OUTCROP 89

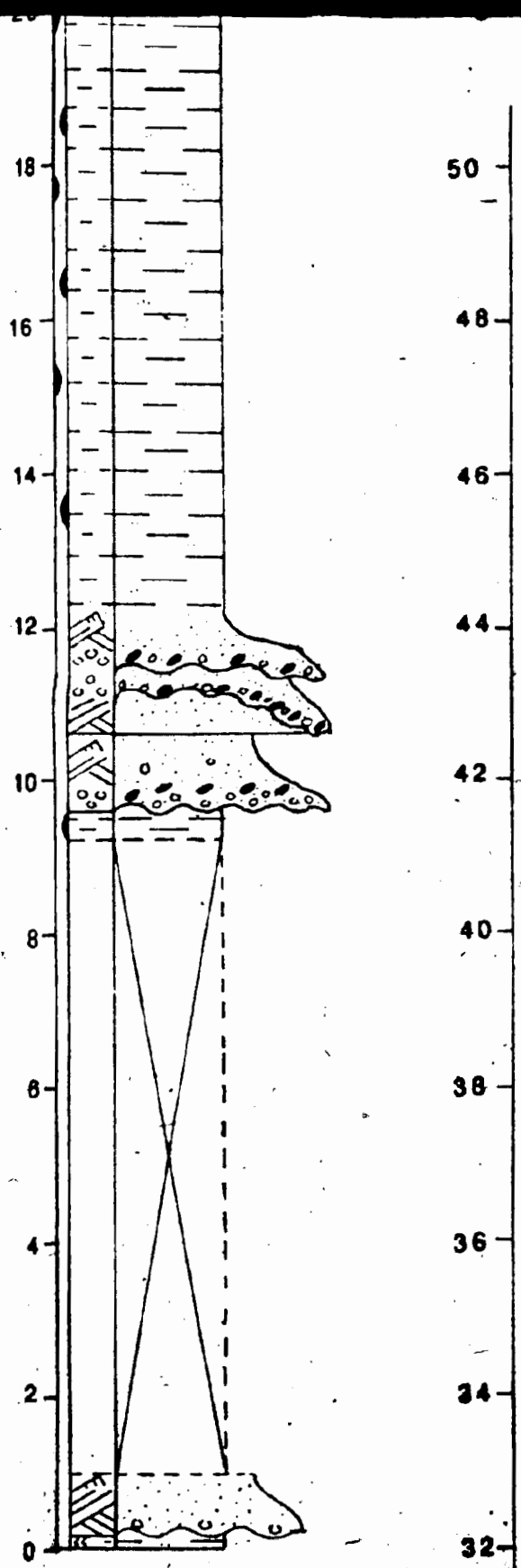


OUTCROP 51a

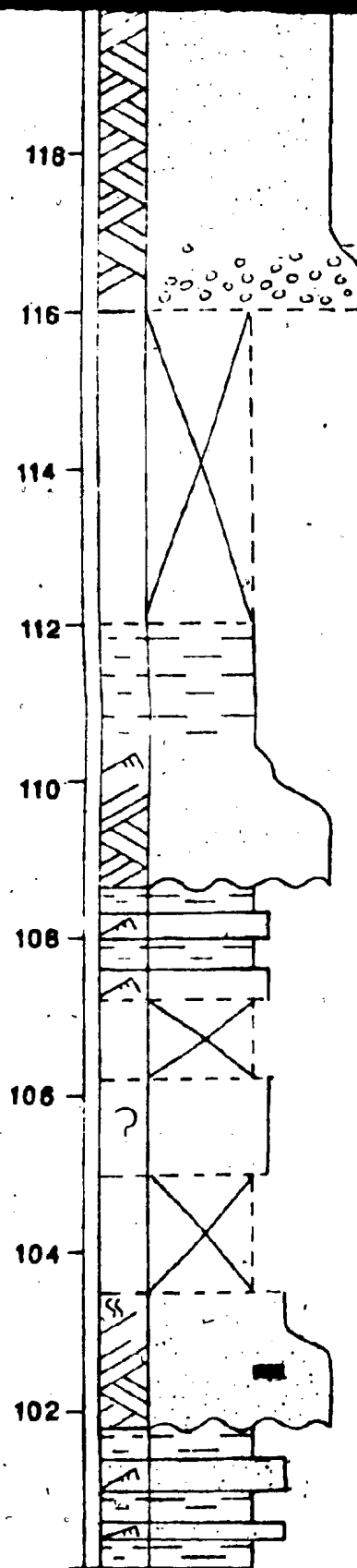
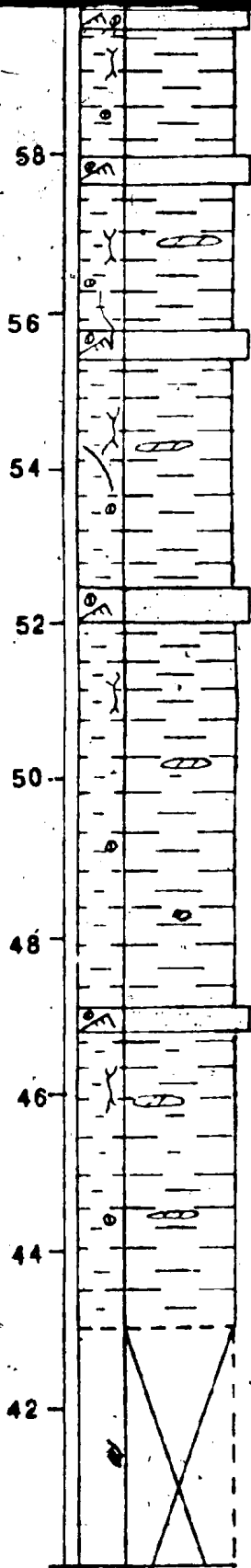
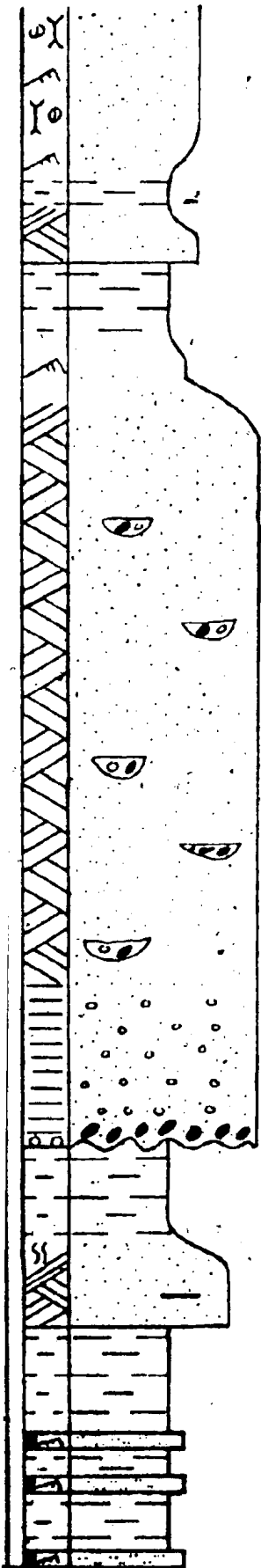




F63 *



7 m COVERED
OUTCROP 1



118

116

114

112

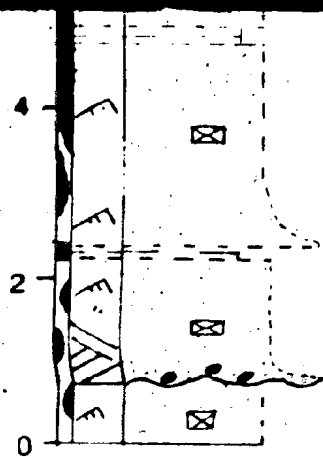
110

108

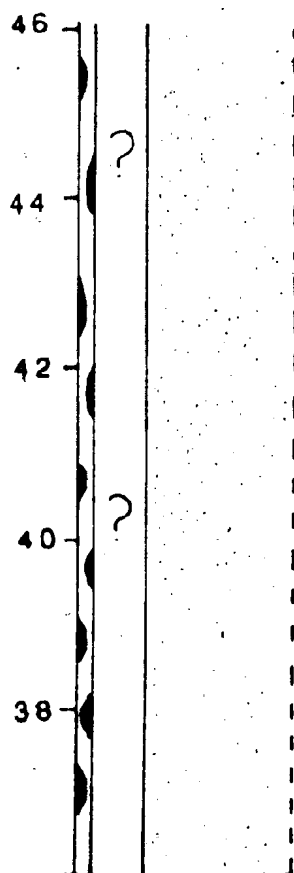
106

104

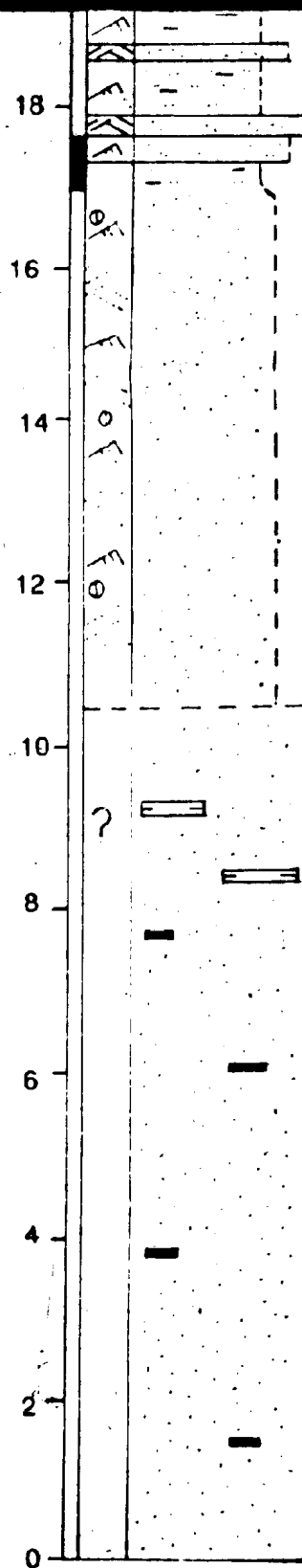
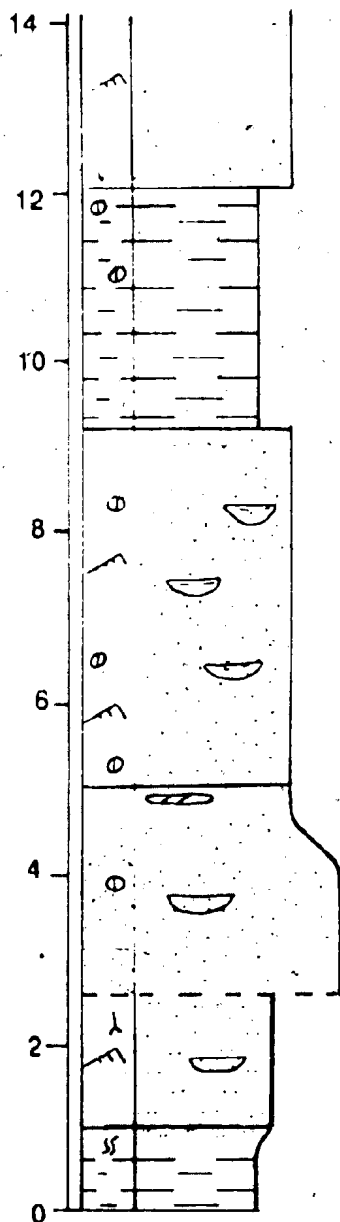
102

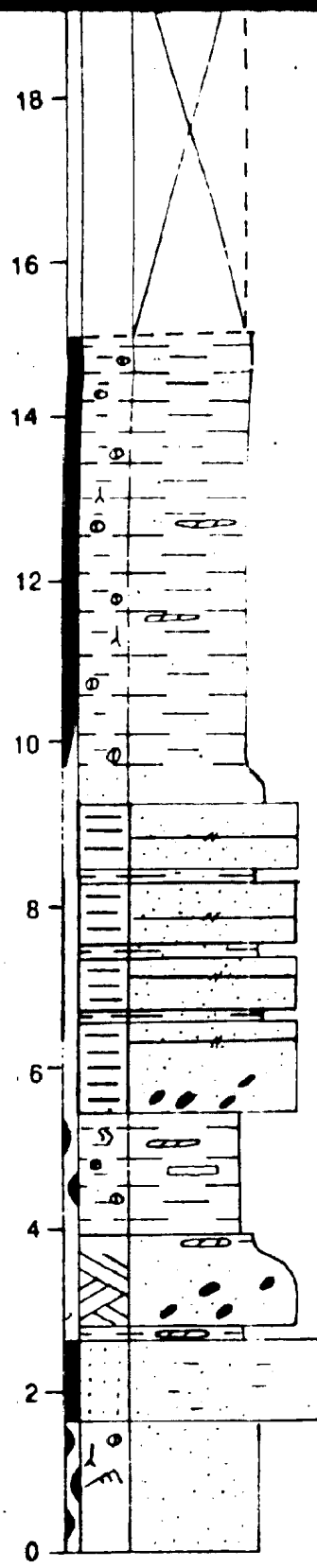
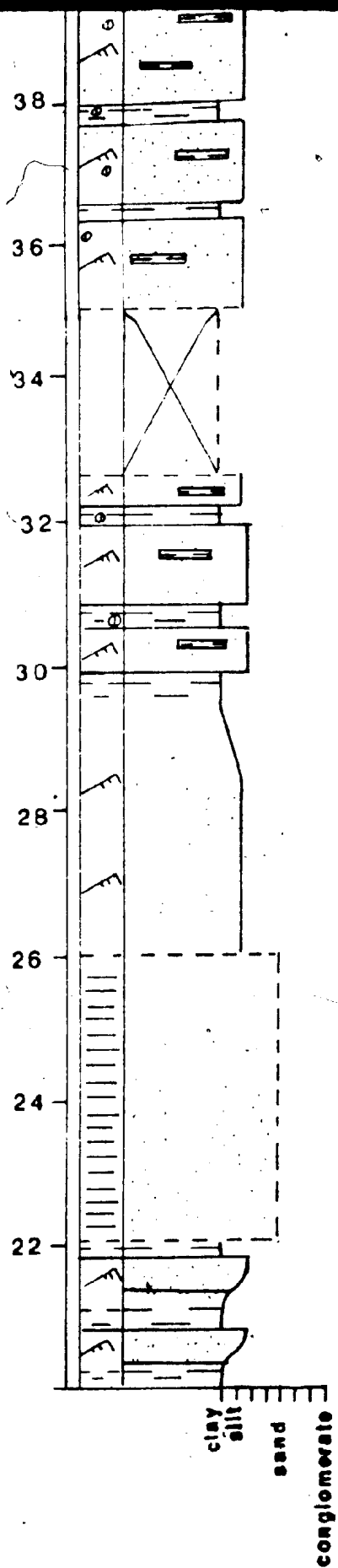


OUTCROP 64



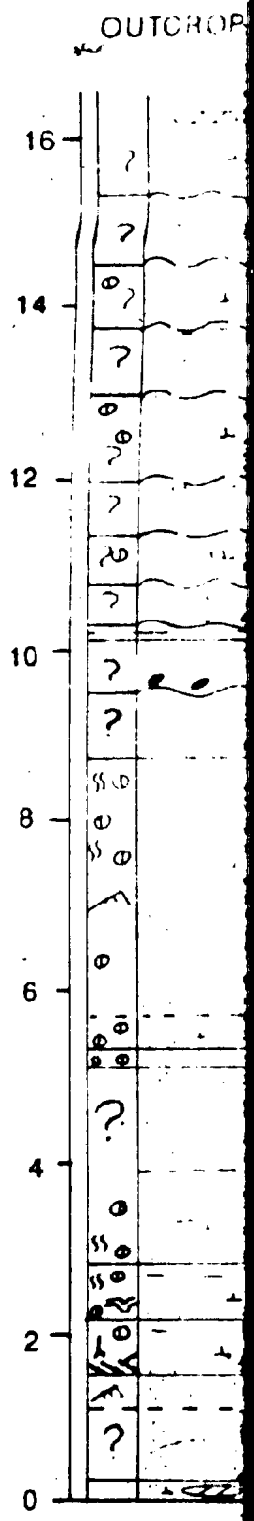
OUTCROP 62a

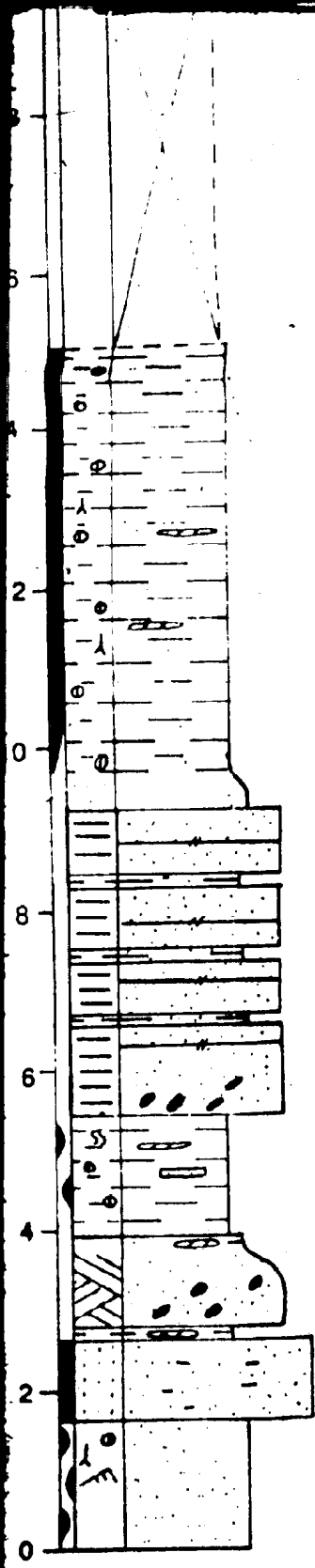




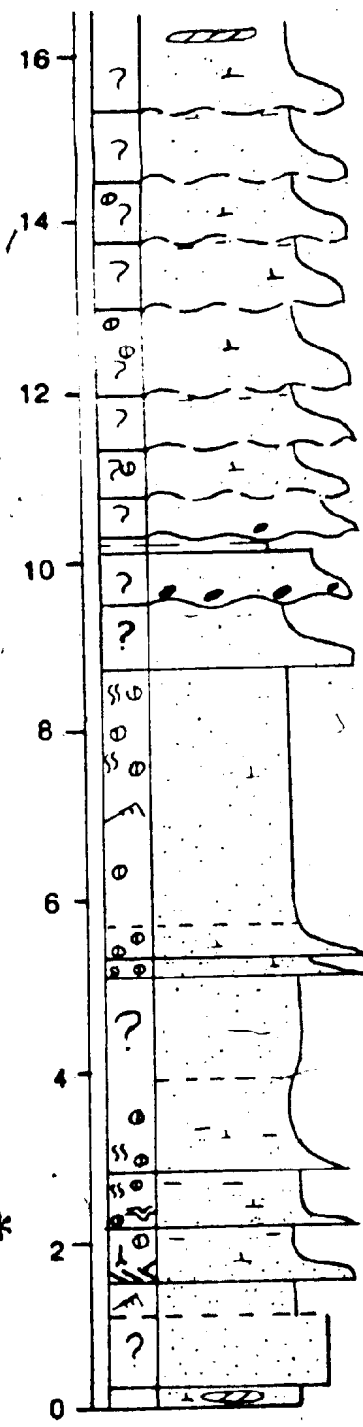
F54 *

F78 *





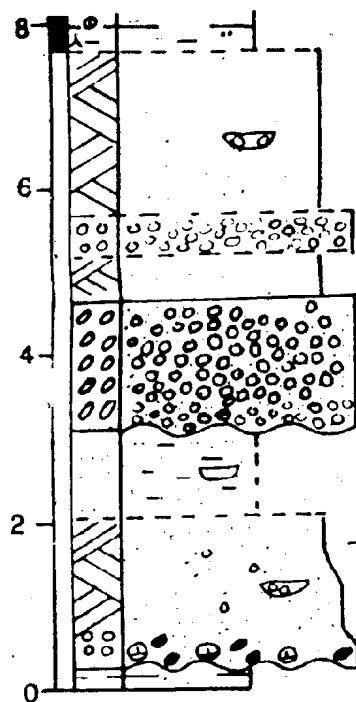
OUTCROP 89



F54 *

F78 *

OUTCROP 68a/b



F70 *

cross-section

OUTCROP 68

